UNIVERSITY OF SOUTHAMPTON

FACULTY OF SCIENCE

School of Physics and Astronomy

Southampton High Energy Physics Group

A Fuller Flavour Treatment of Leptogenesis

by

David Andrew Jones

Presented for the degree of

Doctor of Philosophy

UNIVERSITY OF SOUTHAMPTON

ABSTRACT

FACULTY OF SCIENCE

SCHOOL OF PHYSICS AND ASTRONOMY

SOUTHAMPTON HIGH ENERGY PHYSICS GROUP

DOCTOR OF PHILOSOPHY

A Fuller Flavour Treatment of Leptogenesis

by David Andrew Jones

The theoretical foundations of the seesaw mechanism and baryogenesis are developed, prior to a discussion of leptogenesis - the idea that the baryon asymmetry of the universe (BAU) originates in the physics of the seesaw mechanism. Particular emphasis is placed upon several novel lepton flavour effects arising from decays of the next–to–lightest right–handed neutrino (RHN), N_2. Two new effects are identified: the "flavour swap scenario" and "phantom leptogenesis", either of which can give local order–of–magnitude enhancements to a BAU generated via leptogenesis. Leptogenesis is next reformulated in terms of the density matrix, where decoherence and gauge boson themalisation are taken into account and flavour–basis–independent expressions for the BAU are derived and subsequently specialised to the two RHN model in a two–flavoured basis. This model is then studied extensively, for both standard model and supersymmetric realisations, with N_2 decays fully taken into account. In both cases new N_2–dominated regions are identified, corresponding to models with light sequential dominance. It is shown that these regions get enlarged upon consistent inclusion of the "phantom terms". Results are altered in the supersymmetric case where $\tan\beta$ becomes large and it is shown that new allowed regions emerge, strikingly so for the case of an inverted hierarchy.

Contents

List of Figures

List of Tables

Declaration of Authorship

I, David Andrew Jones, declare that this thesis, entitled "A Fuller Flavour Treatment of Leptogenesis" and the work presented in it are my own. I confirm that

- This work was done wholly or mainly while in candidature for a research degree at this university.
- Where any part of this thesis has previously been submitted for a degree or any other qualification at this university or any other institution, this has been clearly stated.
- Where I have consulted the published work of others, this is always clearly attributed.
- Where I have quoted the work of others, the source is always given. With the exception of such quotations, this thesis is entirely my own work.
- I have acknowledged all main sources of help.
- Where the thesis is based on work done by myself jointly with others, I have made clear exactly what was done by others and what I have contributed myself.
- Work contained in this thesis has previously been published in references [6–8] and also presented at the conferences [9, 10].

Signed:

Date:

Acknowledgements

Many people have in many ways provided encouragement and inspiration over the years and it would be impossible to thank them all here; but I shall try to acknowledge here those to whom I am particularly grateful. First, to my supervisor Pasquale Di Bari, whom I thank for all his guidance during the PhD and especially for the opportunity to work on such a diverse range of interesting projects. For the bulk of the research comprising this thesis I am indebted to, as well as my supervisor, Steve King and Stefan Antusch for many enjoyable and enlightening discussions via skype during our weekly research meetings. I also wish to thank Steve Blanchet and Luca Marzola for our collaboration and discussions (and coffee and biscuits!) during the writing of a further paper.

Whilst at Southampton, I have enjoyed many conversations on on physics and life in general with my fellow PhD students as part of our sociable theory group and I thank them all; but particularly Maria Magou, Iain Cooper and Duncan Cameron (of the astrophysics group) for their friendship (and also to the last two, for putting up with me as a housemate for three years!). I am grateful also to the UK science and technologies funding council, for providing the financial support to make the PhD possible. Lastly, I acknowledge the support of my entire family; without their love, guidance and belief in me over the years I could not have completed the present work.

—DAJ

Overview

Writing at the turn of the previous century, Albert A. Michelson declared that:

"The more important fundamental laws and facts of physical science have all been discovered, and these are now so firmly established that the possibility of their ever being supplanted in consequence of new discoveries is exceedingly remote... our future discoveries must be looked for in the sixth place of decimals." [1]

At that time, there was a widespread sense that all the fundamental problems were now solved, with only a few "loose ends" remaining to tie up. Ambitious young men wishing to make new discoveries were advised to specialise in a more promising field; for example Munich professor Philipp von Jolly advised a young Max Planck against going into physics, warning him that *"in this field, almost everything is already discovered, and all that remains is to fill a few holes."* [2]. As we know today, with the benefit of hindsight, and with apologies to Mark Twain, *"reports of the death of theoretical physics had been greatly exaggerated"*. The twin revolutions of relativity and quantum mechanics shortly followed Michelson's epitaph for fundamental science and the rest is history.

We may be on the verge of a similar revolution going into the 21st century; whilst the Standard Model of particle physics is a fantastically successful theory that seems to have almost every observation of the past century tied up, it leaves several empirical and theoretical problems hanging - such as the hierarchy, flavour and strong CP problems - as intriguing "loose ends" for us to tug upon and see if the model unravels. Out of all these "loose ends" surrounding the Standard Model today, probably the two most glaring empirical ones are the origin of neutrino mass and the

matter–energy content of the universe. If one believes the "standard cosmological model" of ΛCDM (for Lambda Cold Dark Matter - cold dark matter plus a cosmological constant) then the latter comprises of baryons ($\sim 4\%$) dark-matter ($\sim 20\%$) and dark-energy ($\sim 75\%$). Today, rather embarrasingly, we understand the origin of none of these! This work centers around the hypothesis that the origin of primordial matter–anti–matter–asymmetry - a.k.a. **baryogenesis** - lies in the new physics of the neutrino sector - an idea proposed by Fukugita and Yanagida [3] and known as **leptogenesis**.

In recent years there have been many developments around leptogenesis, resulting in an increasingly sophisticated theoretical description. In particular, the importance of lepton **flavour effects** has been appreciated and it has been understood that a consistent treatment of these can alter the final baryon asymmetry produced via leptogenesis by orders of magnitude. Taking full account of all relevant flavour effects is an ongoing project and it will ultimately be necessary to do so if we wish to get the theoretical errors on leptogenesis predictions under control, so as to enter into a "precision era" in which leptogenesis might serve as a relevant constraint on a wide range of interesting particle theories and cosmological models (e.g. inflationary scenarios and Grand Unification, to name two prominent examples). The present work outlines some of my modest contributions towards, as well as my attempts to understand, this ongoing challenge, over the past three years.

The thesis is organised into broadly two halves. The first half comprises mainly a review of the state of play prior to my beginning this project and is organised as follows: in chapter 1 I shall introduce the relevant physics of the neutrino sector, in particular the **seesaw mechanism** [4], an hypothesis which can elegantly account for the anomalously light neutrino sector by postulating the existence of a very heavy right handed neutrino sector. In chapter 2 I consider baryogenesis in general and in particular Andrei Sakharov's original suggestion [5] of a baryon asymmetry originating in the decay of a heavy particle species. In chapter 3 I identify this species as the RHNs of chapter 1 and discuss leptogenesis proper, beginning in Einstein's words *"as simple as possible, but no simpler"* with the so-called "vanilla leptogenesis" scenario before building towards a more sophisticated treatment, gradually taking the lepton

flavour sector more and more fully into account.

The second half details the research I participated in during my PhD studies, comprising mainly of three papers. The first of these papers *"A Fuller Flavour Treatment of N_2–Dominated Leptogenesis"* [6] is the subject of chapter 4. The N_2 dominated scenario serves as a nice application of the theoretical machinery developed in the prior introductory chapters and introduces two novel effects - the "flavour swap scenario" and "phantom leptogenesis", either one of which can modify a predicted final baryon asymmetry by orders of magnitude in relevant regions of parameter space. Chapter 5 is based principally upon the paper *"Leptogenesis With Heavy Neutrino Flavours: From Density Matrix to Boltzmann Equations"* [7] and considers the impact of decoherence effects upon leptogenesis. In particular I include the impact of gauge boson thermalisation of the leptons, which modifies the expression for the "phantom terms" derived in the previous chapter. In chapter 6 I apply the final results of the previous chapter and "revisit" leptogenesis in the two right handed neutrino (2RHN) model, following the paper *"Leptogenesis in the Two Right Handed Neutrino Model Revisited"* [8]. New results are also given, including the "phantom terms" (which were not included in [8]). These enlarge the N_2–dominated regions discovered in that paper, lowering the bound on the lightest RHN mass M_1 in these key regions of parameter space by around an order of magnitude. Finally, in chapter 7, I extend this treatment to supersymmetric 2RHN models, for which there is a "gravitino problem" to worry about. However, it is shown in the final section that upon taking the "phantom terms" consistently into account it may be possible to just avoid this problem within the N_2–dominated regions, which one fails to do in their absence. I then bring these results together for the final Discussion.

Introduction

The matter–anti–matter puzzle

The existence of anti–matter – particles with opposite quantum numbers to their matter counterparts – was first predicted by Paul Dirac on theoretical grounds from 1928–1931 [11–13]. The consistent solution of Dirac's equation for the electron required the existence of a new particle with opposite quantum numbers (here its electric charge) to the electron – the positron (where Dirac referred to it as the "anti–electron" in 1931 [13]). Dirac's "anti–electrons" were soon observed in 1932 in the cloud chamber experiments carried out by Carl Anderson to detect cosmic ray showers in the upper atmosphere [14]. Cosmic rays are high energy particles of extra–solar origin [1]. If the centre of mass energy of a cosmic ray is sufficiently high then it is able to produce the rest mass energy of new particles – for example a cosmic ray with an energy greater than twice the electron's rest mass may produce an electron–positron pair.

Most cosmic rays are high–energy protons, however a much lower flux of anti–protons are observed (cf. fig. I-1). The energy spectrum and fluxes of these anti–proton cosmic rays are consistent with an anti–proton production mechanism of collisions between primary high energy protons in the inter–stellar medium producing secondary anti–proton cosmic rays [15]. This implies that the source of the initial high energy particles – the milky way galaxy – is made almost exclusively of matter rather than anti–matter. It appears too that other galaxies are made of matter, since for anti–matter galaxies situated within our observable universe there would

[1] Victor Hess, who discovered cosmic rays, also proved they were not from the sun by carrying out a balloon flight during a solar eclipse and measuring the same flux of cosmic ray interactions

have to be matter–anti–matter boundaries in the inter–galactic medium, at which pair–annihilations would occur at a non–negligible rates. Since the characteristic gamma radiation signals from such pair–annihilation boundary regions are **not** observed (see [16]), we can conclude that the all galaxies in our observable universe are made predominantly of matter.

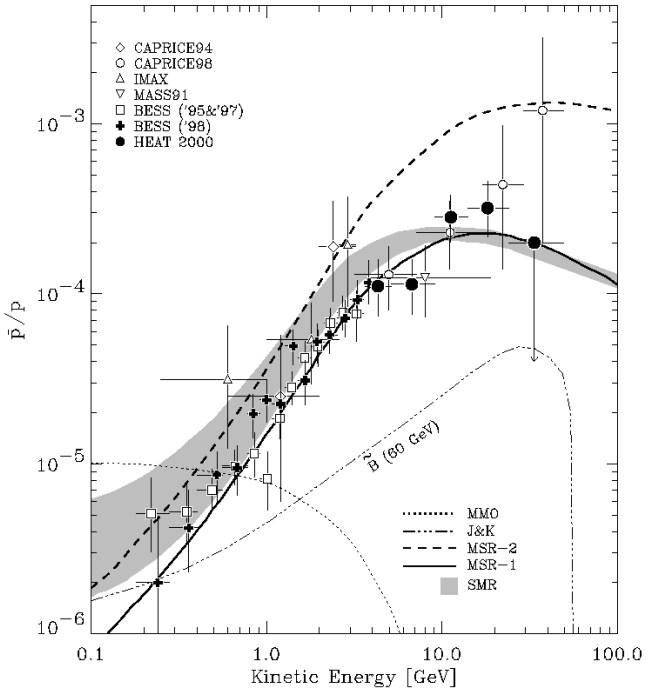

Figure I-1: The anti–proton to proton ratio for cosmic rays [15].

We can now state the matter–antimatter puzzle as follows: why is it that our universe is made almost exclusively of matter? Before trying to give a theoretical answer to this question, I begin by asking the simpler question of how large the observed excess of matter over–anti–matter is. One way to quantify this excess is the baryon number to photon number ratio, defined as

$$\eta_B \equiv \frac{n_B - n_{\bar{B}}}{n_\gamma} \approx 6 \times 10^{-10} \tag{I-1}$$

where n_s refers to the number–density of a species s.

The predicted freeze–out abundance of a symmetric distribution of baryons and anti–baryons is many orders of magnitude lower, since the proton, anti–proton annihilation cross section is quite large compared to the Hubble rate during the relevant

epochs, and so baryons get ample opportunity to annihilate with anti–baryons within the lifetime of the universe. This is sometimes referred to as the "baryon disaster", in contrast to the "WIMP miracle"[2] – the proton, anti–proton annihilation cross section is larger than the weak annihilation cross section by a factor of $\sim \left(\frac{m_W}{m_\pi}\right)^2 \sim 10^6$.

Historically, the ratio η_B was first measured from big bang nucleosynthesis (BBN), given that the primordial abundances of the light elements are sensitive to the baryon density (for a review of BBN, see [17]). This is shown in fig. I-2 below, where boxes denote the allowed regions. One obtains $5.1 \times 10^{-10} \leq \eta_B \leq 6.5 \times 10^{-10}$ $(95\%\, CL)$ [17]. Notice that there is some tension between η_B as determined from primordial lithium abundance versus the other light elements. More recently, a more accurate measurement of η_B has been obtainied from the Cosmic–Microwave–Background (CMB) anisotropy data. The amplitudes of the acousitc peaks which develop during structure formation in the early universe are quite sensitive to η_B (given that more baryons seed larger temperature perturbations – as is shown in fig. I-3). The observed CMB spectrum is consistent with $\eta_B = (6.19 \pm 0.15) \times 10^{-10}$ [19].

Baryogenesis and Sakharov's conditions

In paper written in 1967 [5] Andrei Sakharov first argued that the baryon asymmetry of the universe, quantified as $\eta_B \approx 6 \times 10^{-10}$GeV (cf. eq. (I-1)), may have a dynamical origin. Modern inflationary cosmology gives extra impetus to this suggestion, since an inflationary epoch would erase any baryon asymmetry existing prior to inflation. It then becomes necessary to explain how an excess of baryons over anti–baryons may be generated after (or right at the end of) inflation within an initially "baryon number neutral" universe. Sakharov identified three non–trivial conditions for the dynamical generation of a baryon asymmetry:

1. Baryon number violating processes

2. C and CP violating processes

[2] This refers to the weak interaction cross section naturally predicting the correct freeze–out abundance of dark matter remaining after co–annihilations of a weakly interacting, massive particle (WIMP).

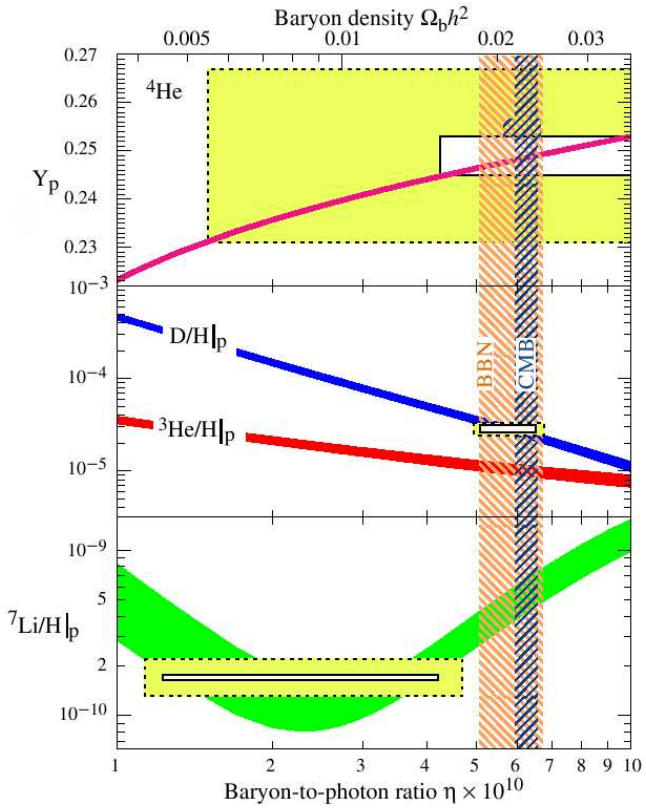

Figure I-2: The determination of η_B from BBN [17].

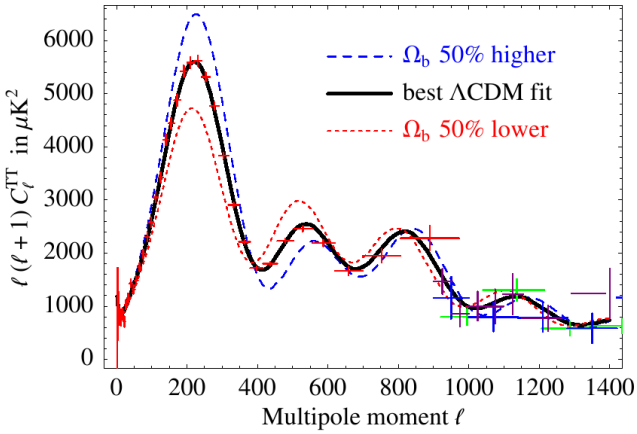

Figure I-3: Sensitivity of CMB anisotropies to η_B [18].

3. A departure from thermal equilibrium

The first condition is quite obvious – in order to have $\dot{B} \neq 0$ (for an overall baryon number B) there must be some B–violating process with a non–zero rate $\Gamma_B \neq 0$.

The second condition is more subtle. Say for instance that $\Gamma_B = \Gamma(X \to Y + B)$ where X, Y are arbitrary non–baryonic initial and final states and B is a baryonic final state. Clearly in order to generate an asymmetry between baryons and anti–

baryons there must be a difference between baryon and anti–baryon production rates. Explicitly, we must have

$$\Gamma(X \to Y + B) \; - \; \Gamma(X^C \to Y^C + B^C) \; \neq \; 0 \tag{I-2}$$

where C denotes charge–conjugation. The above may be written, using an obvious short–hand, as $\Gamma_B \neq C\,\Gamma_B$. However this condition alone is not enough – if the initial state X can also decay into the parity conjugated final state $Y^P + B^P$ then one also require CP violation to have a non–zero net baryon production rate. To see this, consider what happens if CP is conserved. Then one has $\Gamma_B = (CP)\,\Gamma_B$ and hence also that $P\,\Gamma_B = C\,\Gamma_B$. Adding these two conditions, one has

$$\Gamma_B + P\,\Gamma_B = C\;(\Gamma_B + P\,\Gamma_B) \qquad\qquad \text{(if CP is conserved)} \tag{I-3}$$

Hence without both C and CP violation there can be no overall (left plus right–handed) baryon asymmetry generated.

Finally, the third Sakharov condition is also quite obvious – without a departure from equilibrium process like $X \to Y + B$ will be cancelled by an equal inverse process $Y + B \to X$. This departure from thermal equilibrium can be due to either the decay of a heavy particle or a first–order phase transition.

In practice many hypothetical models can realise Sakharov's three conditions. A few of the most popular models are:

1. **GUT baryogenesis**, in which a baryon asymmetry is produced during the decays of a heavy particle at the unification scale. In the original, minimal $SU(5)$ GUT scenario [20] this particle was the $SU(5)$ gauge boson, which decayed into quarks and leptons to produce a $B + L$ asymmetry. We now understand that this scenario is ruled out, given that $B + L$ is **not** conserved at the non–perturbative level, but is instead violated by processes called sphalerons active within the early universe [21]. But non–minimal GUT baryogenesis scenarios remain viable (i.e. those which generate a non–zero $B - L$ asymmetry – $B - L$ is fully conserved by SM processes, including sphalerons.)

2. **Electro–weak baryogenesis**, in which a baryon asymmetry is produced during a first–order electro–weak phase transition (EWPT). B–violation occurs via sphalerons processes. However, sources of CP violation beyond the standard model are required (the physics of the CKM–matrix falls short here by many orders of magnitude [22]). For a review of EWBG, see for example [23].

3. **Affleck–Dine baryogenesis**, in which a baryon asymmetry is produced when the inflaton field(s) oscillating about a flat direction in the supersymmetric field space decays into the super–symmetric scalar partners of SM quarks and leptons. For a review, see [24].

4. **Thermal Leptogenesis**, in which the CP violating decays of thermally produced heavy right–handed neutrinos produce a lepton asymmetry, which is subsequently partially transferred into a baryon asymmetry via sphaleron processes. For a review, see [25].

Each of the above scenarios have their own set of advantages and problems, summarised in table I-1, some of which will be subsequently explored. In this thesis I will almost exclusively consider leptogenesis. Leptogenesis [3] aims to account for the baryon asymmetry of the universe (BAU) (as quantified in eq. (I-1)) using the physics of the seesaw mechanism [4] – a class of neutrino mass models that gives a theoretical explanation for the anomalously light neutrino mass scale measured in neutrino oscillation experiments. I lay the foundations for leptogenesis in the two subsequent chapters, first considering neutrino physics and the seesaw mechanism in chapter 1 and then in developing a fuller description of early universe cosmology and each of Sakharov's conditions in chapter 2. The remaining chapters go on to develop an increasingly sophisticated treatment of the leptogenesis mechanism – culminating in the "fuller flavour treatment of leptogenesis" promised at the outset.

Table I-1: A summary of various baryogenesis scenarios

scenario	pros	cons
GUT baryogenesis	well motivated (GUTs unify strong & EW forces, explain why atoms are electrically neutral etc.)	high reheat temp. can lead to over–production of light, weakly coupled states (e.g. gravitinos); difficult to explicitly falsify.
electro–weak baryogenesis	testable at colliders; requires only minimal extensions to SM physics.	difficult to realise a strongly first–order EWPT – several scenarios already ruled out.
Affleck–Dine baryogenesis	well motivated, given evidence supporting inflation.	SUSY is not yet verified.
thermal leptogenesis	well motivated – neutrinos have mass, at a scale naturally realising leptogenesis (the "leptogenesis conspiracy").	see GUT baryogenesis.

Chapter 1

Neutrino Physics

1.1 The Standard Model and its Symmetries

1.1.1 Space-time Symmetries: Weyl, Dirac and Majorana Spinors

"No one fully understands spinors. Their algebra is formally understood but their general significance is mysterious. In some sense they describe the "square root" of geometry and, just as understanding the square root of -1 took centuries, the same might be true of spinors." – Michael Atiyah [26]

To formally understand the algebra of spinors, we begin by considering the algebra of the Poincare group - of "geometry". The Poincare group is the set of space-time rotations and translations, whose respective generators $M^{\mu\nu}$ and P^{μ} satisfy the Poincare Algebra [27]

$$\begin{aligned} [M^{\mu\nu}, M^{\rho\sigma}] &= i\left(M^{\mu\nu}\eta^{\rho\sigma} + M^{\mu\rho}\eta^{\rho\sigma} - M^{\nu\rho}\eta^{\nu\sigma} - M^{\nu\sigma}\eta^{\mu\rho}\right) \\ [P^{\mu},\, P^{\nu}] &= 0 \\ [M^{\mu\nu},\, P^{\sigma}] &= i\left(P^{\mu}\eta^{\nu\sigma} - P^{\nu}\eta^{\mu\sigma}\right) \end{aligned} \tag{1.1}$$

where $\eta = diag(1, -1, -1, -1)$ is the metric of Minkowski space-time. From the generator of space-time rotations $M^{\mu\nu}$ we can extract three (hermitian) generators of rotations as $J_i \equiv \frac{1}{2}\epsilon_{ijk}\, M_{jk}$ and three (anti-hermitian) generators of boosts $K_i \equiv M_{0i}$.

These are generators of the Lorentz group $SO(3,1)$ and satisfy a Lorentz Algebra [29]

$$\begin{aligned} [J_i, J_j] &= i\epsilon_{ijk} J_k \\ [K_i, K_j] &= -i\epsilon_{ijk} J_k \\ [J_i, K_j] &= i\epsilon_{ijk} K_k \end{aligned} \tag{1.2}$$

The Lorentz group is defined by the set of orthogonal transformations Λ preserving the metric η (and hence the norm $x^T \eta x$ of a four-vector $x \mapsto \Lambda\, x$) according to

$$\eta = \Lambda \eta \Lambda^T \tag{1.3}$$

where Λ is given as some arbitrary combination of the Λ_{J_j} and Λ_{K_j} 4×4 matrices formed by exponentiating the generators of boosts and rotations

$$\Lambda_{J_j} \equiv exp\,[i\,\theta_j J_j] \qquad\qquad \Lambda_{K_j} \equiv exp\,[-i\,\eta_j K_j] \tag{1.4}$$

for angles θ_j in the plane defined by a direction $\hat{x}_j$ in 3-space and boost parameters $v_j \equiv \tan \eta_j$ for a velocity v_j in the $\hat{x}_j$ direction. Explicitly the 4×4 generators of rotations are given by

$$J_1 = \begin{pmatrix} 0 & 0 & 0 & 0 \\ 0 & 0 & 0 & 0 \\ 0 & 0 & 0 & -i \\ 0 & 0 & i & 0 \end{pmatrix} \quad J_2 = \begin{pmatrix} 0 & 0 & 0 & 0 \\ 0 & 0 & 0 & -i \\ 0 & 0 & 0 & 0 \\ 0 & i & 0 & 0 \end{pmatrix} \quad J_3 = \begin{pmatrix} 0 & 0 & 0 & 0 \\ 0 & 0 & -i & 0 \\ 0 & i & 0 & 0 \\ 0 & 0 & 0 & 0 \end{pmatrix} \tag{1.5}$$

and the generators of boosts by

$$K_1 = \begin{pmatrix} 0 & -i & 0 & 0 \\ -i & 0 & 0 & 0 \\ 0 & 0 & 0 & 0 \\ 0 & 0 & 0 & 0 \end{pmatrix} \quad K_2 = \begin{pmatrix} 0 & 0 & -i & 0 \\ 0 & 0 & 0 & 0 \\ -i & 0 & 0 & 0 \\ 0 & 0 & 0 & 0 \end{pmatrix} \quad K_3 = \begin{pmatrix} 0 & 0 & 0 & -i \\ 0 & 0 & 0 & 0 \\ 0 & 0 & 0 & 0 \\ -i & 0 & 0 & 0 \end{pmatrix} \tag{1.6}$$

If we next define two hermitian generators as

$$L_i = \frac{1}{2}(J_i + iK_i) \qquad\qquad R_i = \frac{1}{2}(J_i - iK_i) \tag{1.7}$$

then the Lorentz algebra of eq. (1.2) decouples into two separate algebras

$$\begin{aligned} [L_i, L_j] &= i\varepsilon_{ijk} L_k \\ [R_i, R_j] &= i\varepsilon_{ijk} R_k \\ [L_i, R_j] &= 0 \end{aligned} \tag{1.8}$$

where the generators L_i and R_i belong to two separate $SU(2)$ algebras $SU(2)_L$ and $SU(2)_R$. This would suggest that the Lorentz group $SO(3,1)$ can be represented by the group $SU(2)_L \otimes SU(2)_R$. In practice there is a subtlety to representing $SO(3,1)$ in this way. The complexified lie algebra of $SU(2)_L \otimes SU(2)_R$ is the group $SL(2,\mathcal{C})$ and the mapping from $SL(2,\mathcal{C})$ to $SO(3,1)$ is **two-to-one** rather than one-to-one. So we can write $SO(3,1) \cong SL(2,\mathcal{C}) \,/\, \mathcal{Z}_2$. To see this, compare x^μ, a four vector representation of $SO(3,1)$, with $\hat{x}$, a complex 2×2 matrix representation of $SL(2,\mathcal{C})$. Both can contain the same component information

$$x^\mu = x^\mu e_\mu = \left(x^0,\, x^1,\, x^2,\, x^3\right)^T \tag{1.9}$$

$$\hat{x} = x_\mu \sigma^\mu = \begin{pmatrix} x_0 + x_3 & x_1 - ix_2 \\ x_1 + ix_2 & x_0 - x_3 \end{pmatrix} \tag{1.10}$$

where e_μ are a set of basis 4-vectors and σ^μ are the Pauli matrices

$$\sigma^0 = \begin{pmatrix} 1 & 0 \\ 0 & 1 \end{pmatrix} \quad \sigma^1 = \begin{pmatrix} 0 & 1 \\ 1 & 0 \end{pmatrix} \quad \sigma^2 = \begin{pmatrix} 0 & i \\ -i & 0 \end{pmatrix} \quad \sigma^3 = \begin{pmatrix} 1 & 0 \\ 0 & -1 \end{pmatrix} \tag{1.11}$$

Under an $SO(3,1)$ transformation $x^\mu \mapsto \Lambda^\mu_\nu x^\nu$ the interval $x_\mu\, x^\mu = x_0^2 - x_1^2 - x_2^2 - x_3^2$ is preserved. Under an $SL(2,\,\mathcal{C})$ transformation $\hat{x} \mapsto N^{-1}\hat{x}N$ the interval $\det[\hat{x}] = x_0^2 - x_1^2 - x_2^2 - x_3^2$ is preserved. However in the $SL(2,\mathcal{C})$ case the interval is also preserved for $N \mapsto -N$ and hence the the mapping from $SL(2,\mathcal{C})$ to $SO(3,1)$ is two-to-one.

What all this means is that the information of $SO(3,1)$ can be encoded in the representation of $SL(2,\mathcal{C})$ (but not necessarily vice-versa [1]). $SL(2,\mathcal{C})$ is thus referred to as the **universal cover group** of $SO(3,1)$ [28] and representations of $SO(3,1)$ can be denoted by the (spinor) representations of $SL(2,\mathcal{C})$ - or, equivalently, by representations of the two $SU(2)$ groups that build it. We can label the fundamental representation of $SU(2)_L$, a left-handed (LH) Weyl spinor ξ, by $(\frac{1}{2}, 0)$ and the fundamental representation of $SU(2)_R$, a right-handed (RH) Weyl spinor $\bar{\chi}$, by $(0, \frac{1}{2})$. The bar in $\bar{\chi}$ is **not an operator** but merely denotes that the field $\bar{\chi}$ is a RH Weyl spinor, belonging to $(0, \frac{1}{2})$. From this $(\frac{1}{2}, 0) \oplus (0, \frac{1}{2}) \equiv (\frac{1}{2}, \frac{1}{2})$ corresponds to a Dirac or Majorana spinor and $(\frac{1}{2}, 0) \otimes (0, \frac{1}{2}) \equiv (0,1) \oplus (1,0) \oplus (0,0)$ correspond to covariant vectors $(0,1)$ contravariant vectors $(1,0)$ and scalars $(0,0)$. This is summarised in the table 1.1

Table 1.1: SM spinor reps of SO(3,1)

field name	field label	spinor rep	# DOF
LH Weyl spinor	ξ	$(\frac{1}{2}, 0)$	2
RH Weyl spinor	$\bar{\chi}$	$(0, \frac{1}{2})$	2
Dirac spinor	Ψ_D	$(\frac{1}{2}, \frac{1}{2})$	4
Majorana spinor	Ψ_M	$(\frac{1}{2}, \frac{1}{2})$	2
Covariant 4-vector	A^μ	$(0, 1)$	4
Contravariant 4-vector	A_μ	$(1, 0)$	4
Complex Scalar	ϕ	$(0, 0)$	2

We first consider a LH Weyl spinor ξ. This is a two-component object transforming under rotations and boosts respectively as [29]

$$\xi \mapsto \xi\, e^{-\frac{i}{2}\theta\cdot\sigma} \qquad\qquad \xi \mapsto \xi\, e^{-\frac{i}{2}\eta\cdot\sigma} \tag{1.12}$$

The transformation law eq. (1.12) implies that $\epsilon_{\alpha\beta}\xi^\alpha\xi^\beta$ forms a Lorentz invariant scalar product, where ϵ is the 2×2 anti-symmetric tensor - the Weyl spinor analogue to the 4-vector metric $\eta = diag(1, -1, -1, -1)$. A Lorentz invariant **Majorana**

[1] It works for bosons, but not for fermions. This quirk of group theory is related to the fact that whilst a boson field maps to itself when rotated through an angle of 2π a fermion field maps to minus itself - it must be rotated through 4π to map to itself. This can be seen from eq. (1.12)

mass term $\mathcal{L}_M$ may then be constructed from ξ as

$$\mathcal{L}_M = \frac{1}{2} m_M \left(\xi^T \epsilon \xi\right) + \text{h.c.} \tag{1.13}$$

However, if the field ξ also transforms under a unitary symmetry group U then the above Majorana mass term is not invariant under $\xi \mapsto U\,\xi$ (except for the special case $U = U^\star$). To write an allowed mass term for a general (complex) U, we must define a second LH Weyl spinor, χ, one transforming under the conjugate representation of U

$$\xi \mapsto U\xi \qquad\qquad \chi \mapsto U^\star \chi \tag{1.14}$$

such that χ is effectively an anti-particle of ξ. It is then possible to write the Lorentz invariant **Dirac mass term**

$$\mathcal{L}_D = m\,\chi^T \epsilon \xi + \text{h.c.} \tag{1.15}$$

which is invariant under $\xi \mapsto U\xi$ and $\chi \mapsto U^\star \chi$.

From our two independent LH Weyl 2-spinors ξ, χ we now define the Majorana and Dirac four-spinors [2] (each belonging to a $(\frac{1}{2}, 0) \oplus (0, \frac{1}{2})$ representation of the Lorentz group)

$$\Psi_M \equiv \begin{pmatrix} \xi \\ \epsilon\,\xi^\star \end{pmatrix} \qquad\qquad \Psi_D \equiv \begin{pmatrix} \xi \\ \epsilon\,\chi^\star \end{pmatrix} \tag{1.16}$$

in the **Weyl basis** for the Dirac gamma matrices, given by

$$\gamma^0 = \begin{pmatrix} 0 & I \\ I & 0 \end{pmatrix} \quad \gamma^i = \begin{pmatrix} 0 & \sigma^i \\ -\sigma^i & 0 \end{pmatrix} \qquad \gamma^5 \equiv i\gamma^0\gamma^1\gamma^2\gamma^3 = \begin{pmatrix} -I & 0 \\ 0 & I \end{pmatrix} \tag{1.17}$$

where I denotes the 2×2 identity matrix. In this basis the projector $P_L \equiv \frac{1}{2}(1 - \gamma^5)$ projects a four-spinor $\Psi \equiv (\psi_L,\, \psi_R)^T$ into its pure $(\frac{1}{2},\, 0)$ part $\psi_L = \xi$, while the projector $P_L = \frac{1}{2}(1 + \gamma^5)$ projects Ψ into its pure $(0,\, \frac{1}{2})$ part $\psi_R = \varepsilon\chi^\star \equiv \bar{\chi}$ There are ways to relate the upper and lower halves of Ψ. We can define a charge conjugation

[2] Just to be clear, I am reserving upper case Ψ for the four-spinor (Dirac or Majorana) and lower case ψ for its component 2-spinors (Weyl).

operator (in the Weyl basis) as

$$\Psi^c \equiv C\gamma^0\Psi^\star \qquad\qquad C = \begin{pmatrix} -\epsilon & 0 \\ 0 & -\epsilon \end{pmatrix} \tag{1.18}$$

Applied to Ψ_M this gives the Majorana condition $\Psi^c_M = \Psi_M$. Applied to Ψ_D it swaps $\xi \leftrightarrow \chi$ in eq. (1.16). Hence (given eq. (1.14)) it swaps which of the fields ξ, χ transforms under U and which transforms under $U^\star$ - it swaps particle and anti-particle, just as a charge conjugation operator should. It is also useful to define an operator

$$\bar{\Psi} \equiv \Psi^\dagger\gamma^0 \tag{1.19}$$

such that $m_D\bar{\Psi}_D\Psi_D$ gives a Dirac mass term and $m_D\bar{\Psi}_M\Psi_M$ a Majorana mass term [3].

A Lagrangian can be written either in terms of 4-spinors Ψ, $\bar{\Psi}$ and projectors P_L, P_R or in terms of 2-spinors $\bar{\xi}$, χ (plus their hermitian conjugates). The simplest way to specify the SM Lagrangian is in terms of Weyl spinors ξ, $\bar{\chi}$ - the irreducible representations (irreps) of the Lorentz group - and not in terms of the Dirac and Majorana spinors, which are reducible to pairs of Weyl spinors. For example, an electron field can be specified by the Weyl spinors e and $\bar{e}$, with e corresponding to e_L and $\bar{e}$ to e_R in the 4-spinor $\Psi_e \equiv (e_L, e_R)^T$. This is how the SM fields are given in table 1.2.

1.1.2 Internal Symmetries: Gauge, Flavour and Global $B - L$

The standard model gauge group is [4] $SU(3)_C \otimes SU(2)_I \otimes U(1)_Y$ where C denotes quark colour charges, I denotes weak isospin charges and Y denotes hyper-charge. Each SM representation of this group may be labeled by the notation (c, i, y), where c denotes the representation of $SU(3)_C$, i the representation of $SU(2)_I$ and Y the

[3] The **4-spinor** $\bar{\Psi}$, with the bar denoting an operator acting on Ψ, should not be confused with the **2-spinor** spinor $\bar{\chi}$, with the bar merely denoting $\bar{\chi}$ as a $(0, \frac{1}{2})$ representation of the Lorentz group.

[4] I prefer to label the weak isospin group by the label "I" rather than the conventional label "L", in order to avoid confusing an $SU(2)$ gauge symmetry with the $\left(\frac{1}{2}, 0\right)$ representations of the Lorentz group that happen to be charged under it. The two groups are distinct and so I prefer to reserve distinct labels for them. For example, the Higgs field ϕ is an $SU(2)_I$ doublet, but is a $(0, 0)$ scalar representation of the Lorentz group and so is not "left-handed".

representation of $U(1)_Y$. For example $\left(3,\, 2,\, \frac{1}{3}\right)$ denotes a left-handed quark with hyper-charge $Y = +\frac{1}{3}$.

There are three generations of fermion flavours, which can be denoted by a generation index $i, j = 1, 2, 3$. The gauge bosons - the vector representation of the Lorentz group - couple in exactly the same way to all three generations. Only the scalar higgs field ϕ distinguishes them through its Yukawa couplings. When these Yukawa couplings are negligible, flavour symmetry is unbroken and there is an extra $U(3)$ symmetry for each of the five fermionic fields in table - an extra global $[U(1)]^5$ SM flavour symmetry group. Explicitly we can define five unique unitary transformations in flavour space as [29]

$$\begin{aligned} Q_i &\mapsto U^Q_{ij}\, Q_i \\ \bar{u}_i &\mapsto U^{\bar{u}}_{ij}\, \bar{u}_i \\ \bar{d}_i &\mapsto U^{\bar{d}}_{ij}\, \bar{d}_i \\ L_i &\mapsto U^L_{ij}\, L_i \\ \bar{e}_i &\mapsto U^{\bar{e}}_{ij}\, \bar{e}_i \end{aligned} \tag{1.20}$$

where $Q_i \equiv (u_i,\, d_i)^T$ and $L_i \equiv (\nu_i,\, e_i)^T$ - the LH fermions are grouped into doublets of $SU(2)_I$ (see table 1.2). When the above flavour symmetries are partially broken by $\bar{\chi}\,\phi\,\xi$ couplings, only a small subgroup of $[U(1)]^5$ remains unbroken, corresponding to baryon number

$$\begin{aligned} Q_i &\mapsto e^{i\theta_B/3}\, Q_i \\ \bar{u}_i &\mapsto e^{i\theta_B/3}\, \bar{u}_i \\ \bar{d}_i &\mapsto e^{i\theta_B/3}\, \bar{d}_i \end{aligned} \tag{1.21}$$

and lepton number

$$\begin{aligned} L_i &\mapsto e^{i\theta_L}\, L_i \\ \bar{e}_i &\mapsto e^{i\theta_L}\, \bar{e}_i \end{aligned} \tag{1.22}$$

and so SM particles carry conserved charges B (for baryons) and L (for leptons). In fact, as we shall see in section 2.3.1, both baryon number and lepton number are violated anomalously in the SM. Only the anti-symmetric component $B - L$ is a globally conserved charge. This will turn out to be very important for leptogenesis. In the SM, $B - L$ is an accidental global symmetry. The word "accidental" refers to the fact that there is no local symmetry group explicitly forbidding $B - L$ violation - it just so happens that all the renormalisable terms one is allowed to write down that conserve Lorentz and gauge symmetry also ("accidentally") conserve global $B - L$ number [5].

Table 1.2: Symmetries of Standard Model fields

field	gauge rep	Lorentz rep	B	L
$\begin{pmatrix} u \\ d \end{pmatrix}$ $\begin{pmatrix} c \\ s \end{pmatrix}$ $\begin{pmatrix} t \\ b \end{pmatrix}$	$(3,\, 2,\, \frac{1}{3})$	$(\frac{1}{2},\, 0)$	$\frac{1}{3}$	0
$\bar{u}$ $\bar{c}$ $\bar{t}$	$(\bar{3},\, 1,\, -\frac{4}{3})$	$(0,\, \frac{1}{2})$	$-\frac{1}{3}$	0
$\bar{d}$ $\bar{s}$ $\bar{b}$	$(\bar{3},\, 1,\, \frac{2}{3})$	$(0,\, \frac{1}{2})$	$-\frac{1}{3}$	0
$\begin{pmatrix} \nu_e \\ e \end{pmatrix}$ $\begin{pmatrix} \nu_\mu \\ \mu \end{pmatrix}$ $\begin{pmatrix} \nu_\tau \\ \tau \end{pmatrix}$	$(1,\, 2,\, -1)$	$(\frac{1}{2},\, 0)$	0	1
$\bar{e}$ $\bar{\mu}$ $\bar{\tau}$	$(1,\, 1,\, 2)$	$(0,\, \frac{1}{2})$	0	-1
g^μ (gluons)	$(8, 1, 0)$	$(0,\, 1)$	0	0
W^μ (weak isospin triplet)	$(1,\, 3,\, 0)$	$(0,\, 1)$	0	0
B^μ (weak isospin singlet)	$(1,\, 1,\, 0)$	$(0,\, 1)$	0	0
$\begin{pmatrix} \phi_u^+ \\ \phi_u^0 \end{pmatrix}$ (higgs isospin doublet)	$(1,\, 2,\, 1)$	$(0,\, 0)$	0	0
$\begin{pmatrix} \phi_d^0 \\ \phi_d^- \end{pmatrix}$ (higgs isospin doublet)	$(1,\, 2,\, -1)$	$(0,\, 0)$	0	0

The results of this section are summarised in table 1.2. All terms in the SM Lagrangian $\mathcal{L}_{SM}$ are built from these field operators, which create a SM particle

[5] This is no longer the case when an extra $(0,\, \frac{1}{2})$ spinor charged as $(1,\, 1,\, 0)$ is added to the SM - a RH neutrino $\bar{N}$. As we'll see in section 1.4 this allows L violating terms to be written down.

with gauge and B, L charges specified above, and their hermitian conjugates, which annihilate the same SM particle. In table 1.2 I have identified the field $\phi \equiv (\phi_u^+,\, \phi_u^0)^T$ as the higgs field belonging to the (1, 2, 1) SM gauge representation. The "+" and "0" labels in the components of ϕ denote its electric charge $Q \equiv Y/2 + I_3$ after electro-weak symmetry breaking [6]. The "u" label denotes that ϕ gives mass to the upper components of fermion $SU(2)_I$ doublets and so the term $Y_{ij}^u\, \bar{u}_i\, \phi\, Q_j$ + h.c. in $\mathcal{L}_{SM}$ can give mass to up-type quarks [7]. Notice that in the SM there is no right-handed neutrino $\bar{N}$ and so the term $Y_{ij}^\nu\, \bar{N}_i\, \phi\, L_j$ + h.c. does not exist - in the SM neutrinos are strictly massless.

In the SM it is actually not necessary to have a second higgs field give mass to down type-quarks and leptons, as the table might imply. If we define the field $\widetilde{\phi} \equiv \varepsilon \phi^\star$ then if ϕ belongs to (1, 2, 1) it follows that $\widetilde{\phi}$ belongs to $(1, 2, 1)^c = (1, 2, -1)$ - it is a "quirk" of the $SU(2)$ group that $2 \equiv \bar{2}$. So we can identify $\widetilde{\phi} \equiv (\phi_d^0\,,\, \phi_d^{-1})^T$ and write mass terms $Y_{ij}^d\, \bar{d}_i\, \widetilde{\phi}\, Q_j$ + h.c. and $Y_{ij}^e\, \bar{e}_i\, \widetilde{\phi}\, L_j$ + h.c. where $L_j \equiv (\nu_j,\, e_j)^T$. In the SM one higgs boson goes a long way - it gives mass to all the SM field representations and also breaks the electro–weak symmetry $SU(2)_I \times U(1)_Y \mapsto U(1)_Q$ - higgs sectors for extensions to the SM are typically not quite so economical.

1.2 Neutrino Oscillations: Experiment

1.2.1 The Story So Far

Neutrinos (neutrino meaning "little neutral one" in Italian) were first proposed by Wolfgang Pauli in 1930 as a "desperate remedy" [8] to account for missing energy in β decay experiments. Pauli thought he had "committed the ultimate sin" of proposing a particle that could not be measured and bet a case of champagne that his "neutrinos" would never be discovered. He eventually lost the bet in 1956 when Clyde Cowan and

[6] in the standard parametrisation this happens when the neutral component of ϕ acquires a vacuum expectation value (vev) of $\langle \phi_u^0 \rangle$

[7] Lorentz and gauge indices have been suppressed - appropriate contraction over these indices, leading to a Lorentz and gauge invariant Lagrangian, is implicitly assumed whenever writing terms in $\mathcal{L}_{SM}$

[8] Pauli's famous "Dear Radioactive Ladies and Gentlemen" letter, proposing the "neutron" (later renamed "neutrino" by Fermi), can be read at *http://www.pp.rhul.ac.uk/~ptd/TEACHING/PH2510/pauli-letter.html*.

Fred Reines detected anti-neutrinos produced by the Savanna River nuclear reactor in South Carolina, USA [30].

The sun produces electron neutrinos by nuclear fusion in its core, through the reaction $4p^+ \mapsto 4He + 2e^+ + 2\nu_e$. These solar neutrinos were first observed directly at the homestake mine in South Dakota during the 1960s by Ray Davis. In his experiment, solar neutrinos were detected when captured by radioactive chlorine isotopes, with the capture occurring via an inverse beta decay, $\nu_e + {}^{37}Cl \rightarrow e^- + {}^{37}Ar$. Davis observed a ν_e flux of only around $\frac{1}{3}$ of that predicted by the Standard Solar Model, as pioneered by John Bachall [31]. This missing ν_e flux became know as the **solar neutrino problem**. Neutrino oscillation had first been proposed as a both a theoretical possibility and possible resolution of the solar neutrino problem by Bruno Pontecorvo [32] and Mikeyev, Smirnov and Wolfenstein proposed what came to be known as the MSW mechanism [33], which finally resolved the problem.

In the MSW mechanism the solar neutrino deficit is explained by solar matter effects which resonantly enhance the $|\nu_{2m}\rangle$ mass eigenstate. The electron neutrinos states $|\nu_e\rangle$ produced by nuclear fusion reactions in the sun's core can be written as a mixture of two mass eigenstates $|\nu_{1m}\rangle$ and $|\nu_{2m}\rangle$.

$$\begin{pmatrix} |\nu_e\rangle \\ |\nu_e^\perp\rangle \end{pmatrix} = \begin{pmatrix} \cos\theta_m & \sin\theta_m \\ -\sin\theta_m & \cos\theta_m \end{pmatrix} \begin{pmatrix} |\nu_{1m}\rangle \\ |\nu_{2m}\rangle \end{pmatrix} \tag{1.23}$$

where θ_m is a matter mixing angle and $|\nu_e^\perp\rangle$ is a "non-electron" flavour eigenstate orthogonal to e - in Ray Davis' experiment the $|\nu_e^\perp\rangle$ would not interact with the ^{37}Cl isotopes, resulting in a ν_e deficit. Inverting eq. (1.23) above we obtain

$$\begin{pmatrix} |\nu_{1m}\rangle \\ |\nu_{2m}\rangle \end{pmatrix} = \begin{pmatrix} \cos\theta_m & -\sin\theta_m \\ \sin\theta_m & \cos\theta_m \end{pmatrix} \begin{pmatrix} |\nu_e\rangle \\ |\nu_e^\perp\rangle \end{pmatrix} \tag{1.24}$$

and the probability of observing an electron neutrino is predicted as $|\langle\nu_e|\nu_{2m}\rangle|^2 = \sin^2\theta_m \approx \frac{1}{3}$, thus explaining the solar neutrino deficit.

In 1987 the Supernova 1987A produced a burst of neutrinos detected at the Superkamiokande (SKK) detector in Tokyo, Japan. The observation of differences

in arrival times between neutrino flavours would have given evidence that neutrinos have mass (since strictly massless neutrinos would travel at the speed of light and hence arrive simultaneously). Unfortunately the detector was not calibrated to detect supernova neutrinos and too few events were measures with insufficiently precise timing equipment to draw firm conclusions. Direct confirmation of neutrino oscillations at SKK had to wait another decade until 1998, when the disappearance of atmospheric ν_μ was first observed [34] - a deficit of muon neutrinos arriving from below the detector (traveling through the diameter of the earth) versus those arriving from above the detector, which had traveled a far shorter distance through the atmosphere alone. The solar neutrino deficit was finally resolved once and for all in 2003 when the Sudbury Neutrino Observatory (SNO) in Canada confirmed the existence of solar neutrino oscillations [35] which could be accounted for by the MSW effect and standard solar physics.

The so-called atmospheric and solar mixing angles θ_{23} and θ_{12} and mass-splittings Δm^2_{12}, Δm^2_{23} have been known for around a decade (though measured with increasing precision during that time). Non-zero θ_{13} has been very recently confirmed (2011) by the Daya Bay and Reno experiments [36], [37]. Excitingly, these non zero measured values of θ_{13} open the door to the measurement of leptonic CP violation in the coming years, if the Dirac phase δ is found to be a non-integer multiple of π. The experimental situation today is summarised in the table below, where upper (lower) figures in a given row refer to NH (IH) best fits.

1.2.2 The Future

As table 1.3 indicates, we have thus far measured two mass splittings, three non-zero mixing angles and are beginning to get a handle on δ, the Dirac CP violating phase of neutrino oscillations, which currently has a best fit value of $\delta \approx \pi$, though with large errors. It is also known from solar matter effects that $m_2 > m_1$ although we do not know whether $m_3 > m_2$ or $m_3 < m_1$. These two possible mass patterns are referred to as "normal" and "inverted" ordering and are summarised in fig. 1.1.

The mass of the lightest neutrino, establishing the overall light neutrino mass

Table 1.3: Oscillation experiments circa 2012 - data from [38]

parameter	best fit	1σ range	2σ range	3σ range
$\Delta m^2_{21}[10^{-5}eV]$	7.62	$7.43 - 7.81$	$7.27 - 8.01$	$7.12 - 8.20$
$\Delta m^2_{31}[10^{-3}eV]$	2.55 2.43	$2.46 - 2.61$ $2.37 - 2.50$	$2.38 - 2.68$ $2.29 - 2.58$	$2.31 - 2.74$ $2.21 - 2.64$
$\sin^2\theta_{12}$	0.320	$0.303 - 0.336$	$0.29 - 0.35$	$0.27 - 0.37$
$\sin^2\theta_{23}$	0.613 0.600	$0.573 - 0.635$ $0.569 - 0.626$	$0.38 - 0.66$ $0.39 - 0.65$	$0.36 - 0.68$ $0.37 - 0.67$
$\sin^2\theta_{13}$	0.0246 0.0250	$0.0218 - 0.0275$ $0.0223 - 0.0276$	$0.019 - 0.030$ $0.020 - 0.030$	$0.017 - 0.033$

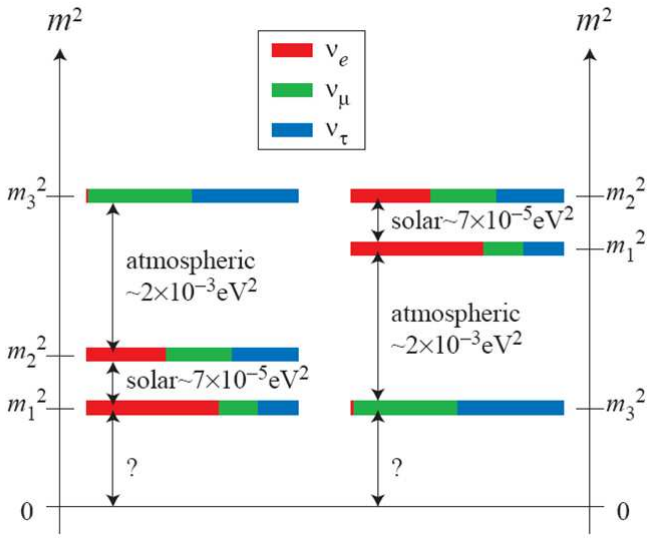

Figure 1.1: The two possible ν_L mass spectra - image from [41]

scale, is also not known (as the "?" in fig. 1.1 indicates). There is currently an indirect bound of $m_{cosmo} \equiv m_1 + m_2 + m_3 \lesssim 0.2$eV from the CMB data [39] while the Katrin experiment (which measures neutrino mass from nuclear recoil momentum in βdecays) has a sensitivity down to $m_{\nu_e} \lesssim 0.35$ev [40]. Experiments like Katrin may also resolve the ordering in future, since if the absolute mass scale is low enough the so-called "normal" and "inverted" orderings can be distinguished. Prospects for measuring the absolute neutrino mass scale and/or resolving the ordering using the various nuclear decay experiments are summarised in fig. 1.2.

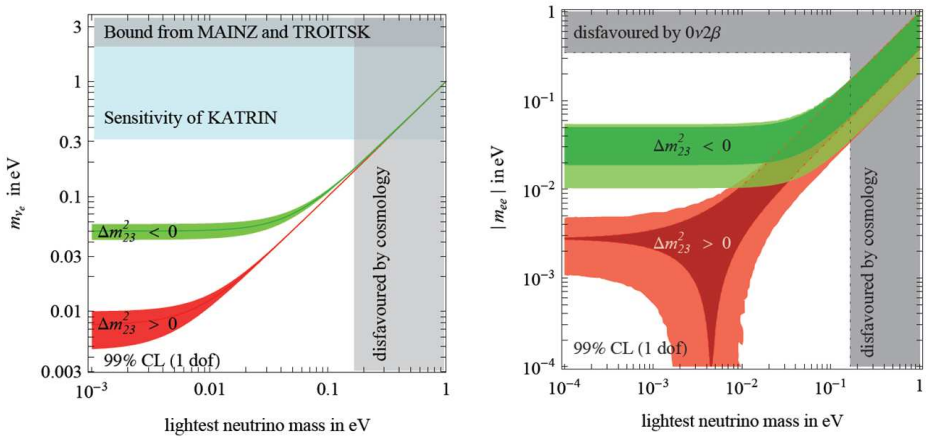

Figure 1.2: Prospecs for resolving the hierarchy. Lines show 99% confidence limits on m_{ν_e} measured in β-decay experiments (left panel) and m_{ee} measured in $0\nu\beta\beta$ experiments (right panel). Taken from [18]

Also unknown is whether neutrinos are Majorana or Dirac particles. If neutrinos are Majorana then the interaction shown below in fig. 1.3 –known as neutrinoless double beta decay – is allowed. If ν_L are instead Dirac then $0\nu\beta\beta$ is disallowed, since then lepton number remains unbroken. Several experiments are currently searching for $0\nu\beta\beta$ decay, but without success thus far. The observation of $0\nu\beta\beta$ decay would also give support to the idea of leptogenesis, since $0\nu\beta\beta$ decay confirms that lepton number symmetry is broken in neutrino interactions, a key requirement of the leptogenesis mechanism for baryogenesis, as we shall see in chapter 2.

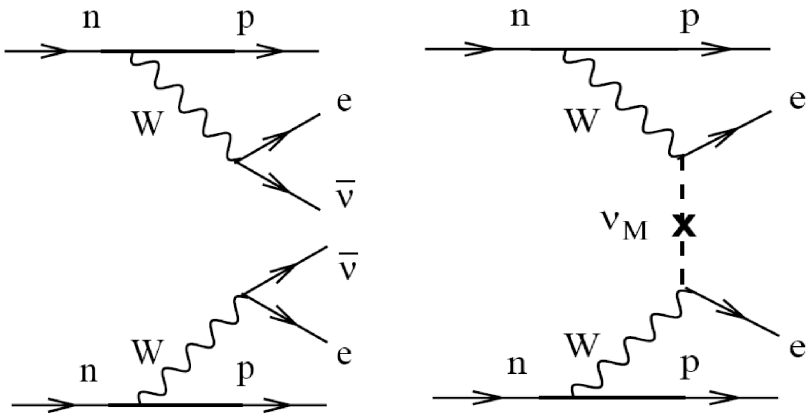

Figure 1.3: Standard (left) versus neutrinoless (right) double beta decay. From [42]

1.3 Neutrino Oscillations: Theory

Neutrino oscillations can be understood from ordinary non-relativistic quantum mechanics [43]. A flavour eigenstate may be written as a sum over mass eigenstates

$$|\nu_\alpha\rangle \equiv \sum_j \langle \nu_j | \nu_\alpha \rangle \, |\nu_j\rangle \equiv \sum_j U^\star_{\alpha j} \, |\nu_j\rangle \tag{1.25}$$

where we have defined $U_{\alpha j} \equiv \langle \nu_\alpha | \nu_j \rangle$ as the matrix which rotates between the mass and flavour basis. The initial state $|\nu_\alpha\rangle$ above will evolve after a time t into the state

$$|\nu_\alpha(t)\rangle = \sum_j e^{iE_j t} \, U^*_{\alpha j} \, |\nu_j\rangle \tag{1.26}$$

given that $\mathcal{H}|\nu_j\rangle = E_j|\nu_j\rangle$ because $|\nu_j\rangle$ is a mass/energy eigenstate of $\mathcal{H}$. The energies E_i of the neutrinos in the beam are given in terms of their momentum and masses as

$$E_i = \sqrt{m_i^2 + \mathbf{p}_i^2} \approx |\mathbf{p}| + \frac{m_i^2}{2|\mathbf{p}|} \tag{1.27}$$

where the final approximation is made using a binomial expansion with $\mathbf{p}_i^2 >> m_i^2$ and replacing $\mathbf{p}_1 \approx \mathbf{p}_2 \approx \mathbf{p}_3$ by a common momentum $|\mathbf{p}|$, given that the ν_i are all highly relativistic. A ν-beam velocity $v_\nu \approx c = 1$ also implies that an oscillation time, t, may be exchanged directly for an oscillation length, x. Making these approximations, one obtains an oscillation probability of

$$\begin{aligned} P_{\nu_\alpha \to \nu_{\alpha'}} \equiv |\langle \nu_\alpha | \nu_{\alpha'} \rangle|^2 \approx \delta_{\alpha\alpha'} - 4 \sum_{i>j} Re[U^\star_{\alpha i} \, U_{\alpha' i} \, U_{\alpha j} \, U^\star_{\alpha' j}] \sin^2 \left(\frac{\Delta m^2_{ij}}{4E} \, x \right) \\ + 2 \sum_{i>j} Im[U^\star_{\alpha i} \, U_{\alpha' i} \, U_{\alpha j} \, U^\star_{\alpha' j}] \, \sin \left(\frac{\Delta m^2_{ij}}{4E} \, x \right) \end{aligned} \tag{1.28}$$

where $\Delta m^2_{ij} \equiv m_i^2 - m_j^2$ and $E \approx |\mathbf{P}|$ is the beam energy. The U-matrix of eq. (1.32) is the mixing matrix rotating between mass and flavour basis for neutrinos. We can similarly define a V-matrix as the mixing matrix rotating between mass and flavour

basis for the charged leptons. Together they give

$$\begin{aligned} |\nu_\alpha\rangle &\equiv \sum_j \langle \nu_i|\nu_\alpha\rangle\, |\nu_i\rangle \equiv \sum_j U^\star_{\alpha j}\, |\nu_j\rangle \\ |e_\alpha\rangle &\equiv \sum_j \langle e_i|e_\alpha\rangle\, |e_i\rangle \equiv \sum_j V^\star_{\alpha j}\, |e_j\rangle \end{aligned} \tag{1.29}$$

and hence matrices $U_{\alpha i} \equiv \langle \nu_\alpha|\nu_i\rangle$ and $V_{\alpha i} \equiv \langle e_\alpha|e_i\rangle$ will diagonalise the mass-matrices m_ν and m_e. These mass-matrices appear as the Lagrangian terms below

$$\mathcal{L}_{m_\nu} = (m_\nu)_{\alpha\beta}\, \bar{\nu}_{L\alpha}(\nu_{L\beta})^c \tag{1.30}$$

$$\mathcal{L}_{m_e} = (m_e)_{\alpha\beta}\, \bar{e}_{L\alpha} e_{L\beta} \tag{1.31}$$

where I have assumed a Dirac mass term for charged leptons and a Majorana mass term for neutrinos. The above mass matrices are diagonalised as

$$\begin{aligned} U^\dagger m_\nu U^\star &\equiv diag(m_1, m_2, m_3) \\ V^\dagger m_e V &\equiv diag(m_{e_1}, m_{e_2}, m_{e_3}) \end{aligned} \tag{1.32}$$

From the above we can now define the Pontecorvo–Maki–Nakagawa–Sakata (PMNS) matrix as

$$U^{PMNS}_{\alpha\beta} \equiv \sum_i V_{\alpha i}\, (U_{\beta i})^T \tag{1.33}$$

which is exactly analogous to the matrix V^{CKM} of the quark sector. It is convenient to work in a basis for which $V = I$ is fixed by redefining the phases of the $|e_\alpha\rangle$ states (since they belong to a $U(1)_Y$ group we have the freedom to rephase each particle separately). In such a basis we have that $U^{PMNS} = U$.

As with V^{CKM}, many of the phases in $U^{PMNS} = U$ are not physical. In the quark sector the story goes like this: a general $N \times N$ complex matrix for N generations of quarks has $2N^2$ (real) parameters. A general **unitary** $N \times N$ matrix such as V^{CKM} only has N^2 given that there are N^2 unitarity constraints $U^\dagger U = I$. Of these N^2 parameters $2N - 1$ of them are not physical, because $2N - 1$ phase differences between $2N$ particles (N d_R and N u_R) can be eliminated by rephasing [9].

[9] Each of the 2N fields can be separately rephased given that they belong to complex representa-

This leaves $N^2 - (2N-1) = (N-1)^2$ physical parameters. Of these there will be $\frac{1}{2}N(N-1)$ mixing angles, leaving $(N-1)^2 - \frac{1}{2}N(N-1) = \frac{1}{2}(N-1)(N-2)$ CP violating phases. As such, one needs at least $N = 3$ generations of quarks to have a non-zero number of physical CP violating phases.

The lepton sector comes with a twist, however. If the neutrinos are Majorana representation of $U(1)_Y$ then it is no longer possible to eliminate a further $N-1$ parameters by rephasing these fields. This means only N unphysical phases can be removed rather than the $2N-1$ that could be removed with Dirac neutrinos. The additional $N-1$ physical phases are known as Majorana phases. Adding them back to the $\frac{1}{2}(N-1)(N-2)$ Dirac phases gives a total of $\frac{1}{2}N(N-1)$ phases for Majorana lepton sector - unlike the quark sector it is possible to have CP violation with $N = 2$ generations only [10] The standard way to parametrise the PMNS matrix is to separate out these Majorana phases α_i from the "quark–like" mixing angles and Dirac phase, as below (for N=3)

$$U = \begin{pmatrix} c_{12}\, c_{13} & s_{12}\, c_{13} & s_{13}\, e^{-\mathrm{i}\,\delta} \\ -s_{12}\, c_{23} - c_{12}\, s_{23}\, s_{13}\, e^{\mathrm{i}\,\delta} & c_{12}\, c_{23} - s_{12}\, s_{23}\, s_{13}\, e^{\mathrm{i}\,\delta} & s_{23}\, c_{13} \\ s_{12}\, s_{23} - c_{12}\, c_{23}\, s_{13}\, e^{\mathrm{i}\,\delta} & -c_{12}\, s_{23} - s_{12}\, c_{23}\, s_{13}\, e^{\mathrm{i}\,\delta} & c_{23}\, c_{13} \end{pmatrix} \times \mathrm{diag}\left(e^{i\,\frac{\alpha_1}{2}},\, e^{i\,\frac{\alpha_2}{2}},\, 1\right) \quad (1.34)$$

where $c_{ij} \equiv \cos\theta_{ij}$, $s_{ij} \equiv \sin\theta_{ij}$ and the θ_{ij} and δ of course will differ from those of the CKM matrix for quark mixing.

1.4 Neutrino Mass Models: the Seesaw Mechanism

We now consider a class of models that have been proposed to "naturally" account for the neutrino masses and mixings just described - "the seesaw mechanism" [4]. In a quantum field theory, the "philosophy" when constructing a Lagrangian is that "terms not forbidden by any symmetries are mandatory". A right handed neutrino

tions of a $U(1)_Y$ gauge group.

[10] You might say "so what" given that we know there are three generations of neutrinos. However, it was not clear until quite recently that all of them mixed with one another. $\theta_{13} = 0$ would have ruled out Dirac CP violation, but still allowed Majorana CP violation.

is a singlet under the standard model gauge group $SU(3)_C \times SU(2)_L \times U(1)_Y$. Upon adding a right-handed neutrino field $\bar{N}$ to the standard model fields, two new terms can be added to the standard model Lagrangian $\mathcal{L}_{SM}$ as follows [11]

$$\mathcal{L}_{Seesaw} = \mathcal{L}_{SM} - Y^{\nu}_{i\alpha}\, \bar{N}_i\, \phi\, L_\alpha - \frac{1}{2} M_{ij} \bar{N}_i \bar{N}_j + \text{h.c.} \qquad i = 1,\, 2,\, 3 \quad \alpha = e,\, \mu,\, \tau \quad (1.35)$$

where I have suppressed spinor and gauge indices. These should be suitably contracted to obtain an invariant Lagrangian - for example $\bar{N}_i \bar{N}_j$ implies a contraction over RH Weyl spinor indices $\varepsilon_{\dot{\alpha}\dot{\beta}}\, \bar{N}_i^{\dot{\alpha}} \bar{N}^{\dot{\beta}}$ is made. Notice that the final term in $\mathcal{L}_{Seesaw}$ is a **Majorana mass term** for $\bar{N}_i$ - allowed given that this is a **real representation** of the standard model gauge group (in contrast to the SM fermion fields, which have non-zero gauge charges). The above Lagrangian $\mathcal{L}_{Seesaw}$ is for a **type 1 seesaw mechanism** [4]. Type 1 refers to the fact that the standard model is extended by adding an isospin singlet fermion (called $\bar{N}$). It could also have been extended by adding an isospin triplet boson (this is called "type 2" [44]) or an isospin triplet fermion (this is called "type 3" [45]). This is summarised in the table below

Table 1.4: Adding seesaw fields to the SM

seesaw		field	gauge rep	Lorentz rep	B	L
type 1	$\bar{N}$	(RH neutrino)	(1, 1, 0)	$(0, \frac{1}{2})$	0	?
type 2	$\hat{\Delta}$	(scalar triplet)	(1, 3, 0)	(0, 0)	0	?
type 3	$\hat{\rho}$	(fermion triplet)	(1, 3, 0)	$(0, \frac{1}{2})$	0	?

I have put a "?" for the lepton number of the new "seesaw" fields - as we shall soon see for the type 1 case, extending the SM with extra fields that couple to SM leptons breaks the "accidental" global lepton number symmetry of section 1.1.2. Once lepton number violating terms exist, lepton number cannot be uniquely assigned. I won't consider type 2 or type 3 seesaws in this thesis, so whenever I subsequently refer to "the seesaw mechanism" I am referring to the minimal extension of the SM made by adding an extra $\bar{N}$ field row to table 1.2.

Why is this called "the seesaw mechanism" then? Consider the neutrino mass

[11] For now I will assume three generations of $\bar{N}$, as with the SM fields. However this is not a requirement, as it is possible to account for the date described in section 1.2 with only two $\bar{N}$ (a possibility I consider in chapter 6) or with more than three $\bar{N}$.

matrix we derive from eq. (1.35), which can be written in the $\{\nu, \bar{N}\}$ basis as

$$m^{\nu} = \begin{pmatrix} 0 & m_D \\ m_D^T & M_M \end{pmatrix} \tag{1.36}$$

where the Dirac mass-matrix $m_D \equiv v\, Y^{\nu}$ mixes ν and $\bar{N}$ fields and the Majorana mass matrix M_N can gives mass exclusively to the $\bar{N}$ field. If we assume that $M_N \gg \Lambda_{EW}$ then we can diagonalise the above to obtain an effective neutrino mass matrix

$$m^{\nu}_{eff} = \begin{pmatrix} m_d^T\, M_M^{-1}\, m_D & 0 \\ 0 & M_M \end{pmatrix} (1 \,+\, \mathcal{O}(\Lambda_{EW}/M_N)) \tag{1.37}$$

where we can identify

$$(m_{\nu})_{\alpha\beta} \equiv \left(m_D^T\, M^{-1}\, m_D\right)_{\alpha\beta} \tag{1.38}$$

as a light Majorana mass matrix mixing $\nu_{\alpha} \leftrightarrow \nu_{\beta}$ flavour eigenstates. This explains the name "seesaw" - to derive $(m_{\nu})_{\alpha\beta}$ above we assumed $M_N \gg \Lambda_{EW}$ and as we have just shown, the more the scale M_N is raised, the more the scale m_{ν} will be lowered. Using the effective mass, we can next write an effective Lagrangian for the seesaw mechanism as

$$\mathcal{L}^{\nu}_{eff} = (m_{\nu})_{\alpha\beta}\, \bar{\nu}_{\alpha} \nu^{c}_{\beta}\, (1 + \mathcal{O}(\Lambda_{EW}/M_N) + ...) \tag{1.39}$$

The above describes the low energy physics contained in $\mathcal{L}_{seesaw}$. Notice that we have got back to eq. (1.30) of section 1.3 and so we can once again identify the U-matrix by

$$\text{diag}\,(m_1,\, m_2\, m_3) \;=\; U^{\dagger} m_{\nu}\, U^{\star} \tag{1.40}$$

where m_1, m_2, m_3 are the light neutrino mass matrices. Recall from section 1.2 that we have measured the mass splittings $\Delta m^2_{21} \sim 7.6 \times 10^{-5}\,\text{eV}^2$ and $\Delta m^2_{31} \sim 2.5 \times 10^{-3}\,\text{eV}^2$ in oscillation experiments and we know that $m_2 > m_1$ from solar neutrino matter effects. We also have a bound on the light neutrino mass scale $m_{\nu} \lesssim 0.2ev$ from cosmology, which according to eq. (1.38) should be given by $m_{\nu} \sim (v\, Y^{\nu})^2 \;/\, M_N$. The seesaw mechanism thus works for quite a range of Y^{ν}, from "natural" values $\mathcal{O}(1)$ with $M_N \sim \Lambda_{GUT}$ all the way down to $\mathcal{O}(10^{-6})$ with $M_N \sim \Lambda_{EW}$, where there is

potential scope to test the seesaw mechanism at the LHC (see for example [46], [47])

It is particularly interesting to speculate that the origin of neutrino mass is associated with GUT scale physics. This is "natural" for reasons other than just the $Y^{\nu} \sim 1$ it allows in $\mathcal{L}_{seesaw}$. Considering $SO(10)$ unification (for a nice introduction see [48]), the SM fields plus three $\bar{N}$s fit perfectly into three 16 representations of $SO(10)$ (one for each generation). One might then claim that $SO(10)$ unification "predicts" an $\bar{N}$ field with mass $M_N \sim 10^{16} GeV$ and hence an observed neutrino mass scale of $m_{\nu} \sim 0.1$ev. To me, this is rather reminiscent of some theoretical physicists' claims that string theory "predicts" gravity [12].

1.5 Sequential Dominance

As already mentioned, the presence of a Majorana mass term allows the theoretical possibility of large differences between the inter-generational mixing angles for the quark and lepton sector, as turns out to be the case experimentally. Order of magnitude wise, experiments measure

$$V^{CKM} \sim \begin{pmatrix} 0.1 & 0.01 & 0.001 \\ 0.01 & 0.1 & 0.001 \\ 0.001 & 0.01 & 0.1 \end{pmatrix} \qquad U^{PMNS} \sim \begin{pmatrix} 1 & 1 & 0.1 \\ 1 & 1 & 1 \\ 1 & 1 & 1 \end{pmatrix} \tag{1.41}$$

The idea of **Sequential Dominance** [49–52] (SD) is to develop a parametrisation of the neutrino Yukawa matrix Y^{ν} whereby the large neutrino mixing angles above are realised naturally for hierarchical light neutrino masses. We begin by parametrising Y^{ν} and M_N in eq. (1.35) for $\mathcal{L}_{seesaw}$ as

$$Y^{\nu} \equiv \begin{pmatrix} A_1 & B_1 & C_1 \\ A_2 & B_2 & C_2 \\ A_3 & B_3 & C_3 \end{pmatrix} \qquad M_{\rm RR} = \begin{pmatrix} M_A & 0 & 0 \\ 0 & M_B & 0 \\ 0 & 0 & M_C \end{pmatrix} \tag{1.42}$$

[12] Or at least string theory "postdicts" it, to use Ed Witten's terminology. With $SO(10)$ we can potentially claim "prediction" as opposed to "postdiction", since $SO(10)$ and the seesaw mechanism came decades before evidence for $m_{\nu} \sim 0.1ev$.

In terms of this parametrisation eq. (1.39) for $\mathcal{L}^{\nu}_{eff}$ is given as

$$\mathcal{L}^{m_\nu}_{eff} = \frac{(\nu_i^T A_i)(A_j^T \nu_j)v^2}{M_A} + \frac{(\nu_i^T B_i)(B_j^T \nu_j)v^2}{M_B} + \frac{(\nu_i^T C_i)(C_j^T \nu_j)v^2}{M_C} \tag{1.43}$$

One can see above that the contributions of a given N_R to ν_L mixing depend upon a given column of the Dirac Mass matrix. In SD one then makes the following ansatz

$$\frac{A_i A_j}{M_A} \gg \frac{B_i B_j}{M_B} \gg \frac{C_i C_j}{M_C}\,. \tag{1.44}$$

Though ad hoc in this context, the above ansatz can be realised in models containing a discrete flavour symmetry [53], through choosing specific alignments of flavon vevs [13] The SD ansatz eq. (1.44) ensures that the three N_R contribute hierarchically to ν_L mixing, one dominantly (A), one sub–dominantly (B) and a final one effectively decouples from the seesaw (C). Thus SD realises an effective two RHN scenario – this observation will have applications in chapter 6. Eq. (1.44) implies a fully hierarchical mass spectrum $m_1 \ll m_2 \ll m_3$, where explicitly one obtains

$$\begin{aligned} m_3 &\approx \frac{(|A_2|^2 + |A_3|^2)v^2}{M_A} \\ m_2 &\approx \frac{|B_1|^2 v^2}{s_{12}^2 M_B} \\ m_1 &\approx \mathcal{O}(|C|^2 v^2/M_C) \end{aligned} \tag{1.45}$$

Also, two large mixing angles θ_{12} and θ_{23} are naturally realised, where explicitly one obtains

$$\begin{aligned} \tan\theta_{23} &\approx \frac{|A_2|}{|A_3|} \\ \tan\theta_{12} &\approx \frac{|B_1|}{c_{23}|B_2|\cos\tilde{\phi}_2 - s_{23}|B_3|\sin\tilde{\phi}_3} \\ \theta_{13} &\approx e^{i\tilde{\phi}_4}\frac{|B_1|(A_2^* B_2 + A_3^* B_3)}{[|A_2|^2 + |A_3|^2]^{3/2}}\frac{M_A}{M_B} + \frac{e^{i\tilde{\phi}_5}|A_1|}{\sqrt{|A_2|^2 + |A_3|^2}} \end{aligned} \tag{1.46}$$

[13] Flavons are higgs-like fields carrying some charge under a discrete flavour symmetry group. The breaking of this discrete symmetry group proceeds via the flavon fields acquiring vevs and hence alignment in a given direction of this discrete flavour space. Such a broken symmetry may explain the observed lepton mixing pattern and why this is so different to the quark mixing pattern. Although such models will not be considered in this thesis, it is worth mentioning here that they exist: they are both popular within the literature and have relevant implications for leptogenesis.

where further setting $A_1 \ll A_2$, A_3 above, one naturally realises $\theta_{13} \ll \theta_{12}$, θ_{23}. The phases ϕ_i are not important here for considering the natural scale of the parameters.

There are then $3! = 6$ different possibilities for realising SD:

1. **Light Sequential Dominance** (LSD), where the lightest N_R contributes dominantly to mixing (A=1)

$$\begin{array}{cccc} & \frac{A_iA_j}{M_1} & \gg & \frac{B_iB_j}{M_2} \gg \frac{C_iC_j}{M_3} \\ \text{or} & \frac{A_iA_j}{M_1} & \gg & \frac{B_iB_j}{M_3} \gg \frac{C_iC_j}{M_2} \end{array} \tag{1.47}$$

2. **Medium Sequential Dominance** (MSD), where the intermediate mass N_R contributes dominantly to mixing (A=2)

$$\begin{array}{cccc} & \frac{A_iA_j}{M_2} & \gg & \frac{B_iB_j}{M_1} \gg \frac{C_iC_j}{M_3} \\ \text{or} & \frac{A_iA_j}{M_2} & \gg & \frac{B_iB_j}{M_3} \gg \frac{C_iC_j}{M_1} \end{array} \tag{1.48}$$

3. **Heavy Sequential Dominance** (HSD), where the heaviest N_R contributes dominantly to mixing (A=3)

$$\begin{array}{cccc} & \frac{A_iA_j}{M_3} & \gg & \frac{B_iB_j}{M_1} \gg \frac{C_iC_j}{M_2} \\ \text{or} & \frac{A_iA_j}{M_3} & \gg & \frac{B_iB_j}{M_2} \gg \frac{C_iC_j}{M_1} \end{array} \tag{1.49}$$

The first possibility (an LSD with $M_A < M_B < M_C$) is considered later, in the context of two-right handed neutrino models.

Chapter 2

Cosmology and Baryogenesis

2.1 The Friedmann Robertson Walker Metric

The **cosmological principle** is the idea that the part of the universe in which we find ourselves is not "special". More formally, we can say that on cosmological scales our universe becomes **homogeneous** - it looks the same in each place - and **isotropic** - it looks the same in all directions from a given place. The homogeneity and isotropy of an $n+1$ dimensional space-time imply a metric of the form

$$ds^2 = c^2dt^2 - R^2(t)d\sigma^2 \tag{2.1}$$

In the above t is the time co-ordinate of an observer whose word-line is a geodesic of the above metric. If R(t) increases with t, this corresponds to a co-moving observer in an expanding universe. Homogeneity and isotropy also imply that the spatial part of the metric $d\sigma^2$ describes an n dimensional surface σ of constant curvature - this is the Friedmann–Robertson–Walker (FRW) metric, given explicitly by [56]

$$d\sigma^2 = \frac{1}{1-kr^2}\,dr^2 + r^2 d\Omega^2 \tag{2.2}$$

Here $r(t)$ is the co-moving distance between events and Ω the solid angle between events, as measured by a co-moving observer living on the surface σ described by the above metric. To show where the metric $d\sigma^2$ comes from and the meaning of the

co-ordinates $R(t)$, r, Ω, consider the $2+1$ dimensional universe of fig. 2.1 for which $d\Omega^2 = d\theta^2$, the circles of radius $r^{'} < R$ give lines of latitude parametrising the surface of a 2-sphere of radius $R(t)$ and the normalised parameter $r \equiv \frac{r^{'}}{R}$ may be defined for convenience as a co-moving distance between events A and B below.

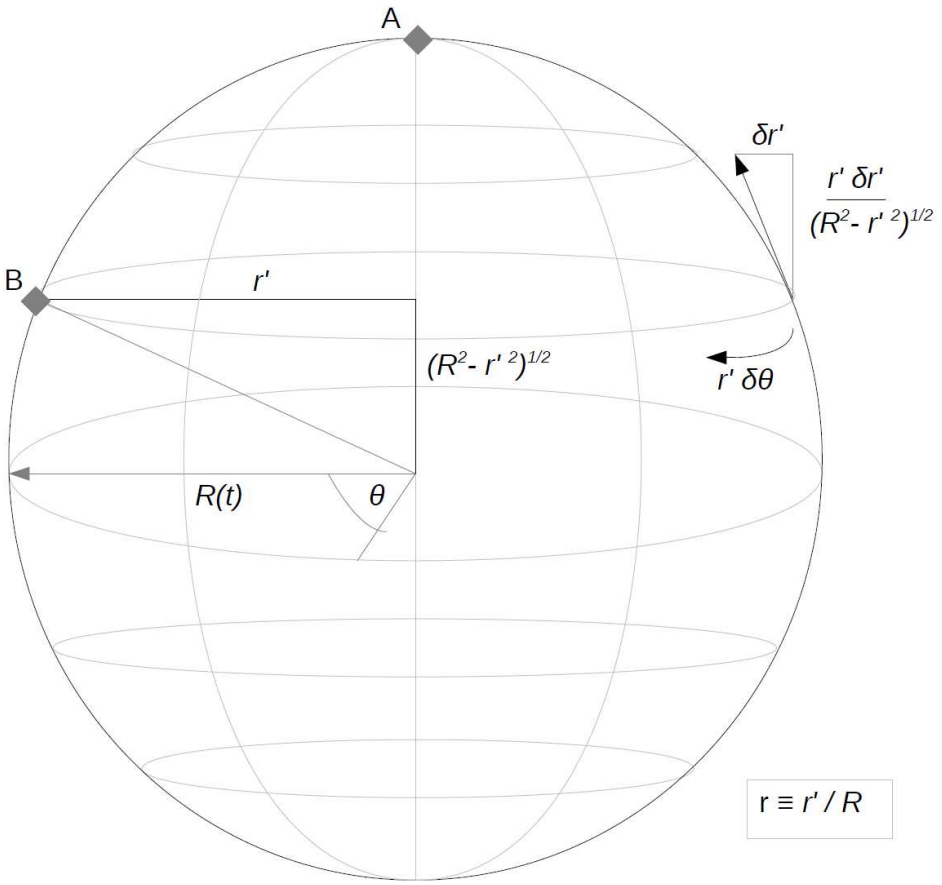

Figure 2.1: The parametrisation of a 2-sphere universe ($k = +1$). Observers on the sphere's surface travel in the orthogonal directions indicated by arrows

The $2+1$ dimensional universe of fig. 2.1 is closed and has the finite area $4\pi R^2$. An observer located at point A could discover that this universe is positively curved by counting galaxies within a circle of radius $r^{'}$ and noticing that as the circle is made bigger the number of galaxies per unit area within it increases, with galaxies bunching up more and more at the edges of the circle. To describe our $3+1$ dimensional universe, we simply replace $d\Omega^2 = d\theta^2$ with $d\Omega^2 = d\theta^2 + sin^2\theta\, d\phi^2$. Hence the full FRW metric for our $3+1$-dimensional universe is

$$ds^2_{FRW} = c^2dt^2 - R^2(t)\left[\frac{1}{1-kr^2}\,dr^2 + r^2\,d\theta^2 + r^2\,\sin^2\theta\,d\phi^2\right] \qquad (2.3)$$

$k = 1$ describes a closed 3-sphere universe of finite volume $16\pi^2 R^3$. $k = -1$ describes an open hyperbolic universe. $k = 0$ describes an infinite Euclidean 3-plane or "flat" universe (an infinite cubic lattice). The latest WMAP 7-year results constrain the geometry of our universe as flat to within $\lesssim 1\%$ [39]. To go from the metric of the universe to its dynamical evolution (i.e. to find $R(t)$ explicitly) we must solve Einstein's equation:

$$R_{\mu\nu} - \frac{1}{2} R\, g_{\mu\nu} = 8\pi G\, T_{\mu\nu} \tag{2.4}$$

The left-hand side of Einstein's equation is a function of the metric tensor $g_{\mu\nu}$, defined in terms of interval ds^2 as

$$ds^2 = g_{\mu\nu} dx^\mu dx^\nu \tag{2.5}$$

applying the above to eq. (2.3) obtains the FRW metric

$$g_{FRW} = \mathrm{diag}\left(c^2,\, \frac{R^2}{1 - kr^2},\, r^2,\, r^2 \sin^2\theta\right) \tag{2.6}$$

The right-hand side describes the matter-energy content of the universe; in other words "*Matter tells space how to curve, space tells matter how to move*" (Wheeler). A good approximate description of the right-hand side is to assume a stress–energy tensor of the form

$$T = \mathrm{diag}\,(\rho,\, p,\, p,\, p) \tag{2.7}$$

which describes a so-called 'perfect fluid' of energy density ρ and pressure p. Putting eq. (2.3) for $g_{\mu\nu}$ and eq. (2.7) for $T_{\mu\nu}$ into Einstein's equation and solving obtains two independent equations for the expansion parameter, $R(t)$:

$$\left(\frac{d}{dt}R\right)^2 = \frac{8\pi G}{3}\rho(R)\; R^2 \;-\; k \tag{2.8}$$

$$\frac{d^2}{dt^2}R = -\frac{4\pi G}{3}(\rho(R) + 3p(R))\; R \tag{2.9}$$

The equation for dR/dt is the **Friedmann equation**, describing the spatial expansion of the universe given its matter-energy content. The second for d^2R/dt^2 is the **acceleration equation** describing the ultimate fate of the universe. To solve the Friedmann equation, we must derive an expression for ρ as a function of $R(t)$. This

is done by noting that the behaviour of the energy-density in expanding space is constrained by matter-energy conservation. In the language of General relativity, there is a constraint is on the co-variant derivative of the stress-energy tensor

$$T^{\mu}_{\nu;\mu} = 0 \tag{2.10}$$

Taking the zero-zero component, one arrives at the more familiar first law of thermodynamics

$$d\left(\rho R^3\right) + p\, d\left(R^3\right) = 0 \tag{2.11}$$

To solve this equation, we must assume an **equation of state** relating p to ρ. We assume them to be proportional, with constant of proportionality w.

$$p = w\rho \tag{2.12}$$

Applying the above ansatz to eq. (2.11), one first finds that

$$\frac{d\rho}{\rho} = -(1+w)\frac{d\left(R^3\right)}{R^3} \tag{2.13}$$

and upon integrating the above one obtains

$$\rho(R) \propto R^{-3(1+w)} \tag{2.14}$$

This expression can now be substituted into the Friedmann equation (2.8), which for $k = 0$ (our flat universe) becomes

$$\frac{dR}{dt} \propto R^{-\frac{1}{2}(1+3w)} \tag{2.15}$$

In a radiation dominated universe $w = \frac{1}{3}$ and the above is solved by $R(t) \propto t^{\frac{1}{2}}$, as may be verified by substitution. The proportionality can be made into an equality by dividing through by a reference value $R(t_0)$ of R at time t_0, the present age of the universe. This obtains

$$a(t) \equiv \frac{R(t)}{R(t_0)} = \left(\frac{t}{t_0}\right)^{\frac{1}{2}} \tag{2.16}$$

where I have introduced $a(t) \equiv \frac{R(t)}{R(t_0)}$ as a normalised scale factor, such that at the current age of the universe t_0 we have $a(t_0) = 1$. Similarly, for $w = 0$ - a matter dominated, flat universe - we find the solution

$$a(t) = \left(\frac{t}{t_0}\right)^{\frac{2}{3}} \tag{2.17}$$

and for $w = -1$ - a dark-energy dominated, flat universe

$$a(t) = \exp\left(\frac{t}{t_0}\right) \tag{2.18}$$

The early universe is populated by the set of SM particle species $\{s\}$ with number densities n_s and energy densities ρ_s given by

$$\rho_s = \frac{g}{2\pi^3}\int d^{(3)}k\, f_s(k,t)\, E_s \quad = \quad \begin{array}{ll} \frac{\pi^2}{30}\, gT_s^4 & \text{(bosons)} \\ \left(\frac{7}{8}\right)\frac{\pi^2}{30}\, gT_s^4 & \text{(fermions)} \end{array} \tag{2.19}$$

$$n_s = \frac{g}{2\pi^3}\int d^{(3)}k\, f_s(k,t) \quad = \quad \begin{array}{ll} \frac{\zeta(3)}{\pi^2}\, gT_s^3 & \text{(bosons)} \\ \left(\frac{7}{8}\right)\frac{\zeta(3)}{\pi^2}\, gT_s^3 & \text{(fermions)} \end{array} \tag{2.20}$$

where the last equality applies in the ultra-relativistic limit. From the above we can define a total plasma energy density ρ and a total plasma number density n as

$$\begin{aligned} \rho &= \sigma\, g^\star\, T^4 \\ n &= \frac{\zeta(3)}{\pi^2}\, g^{\star\, s}\, T^3 \end{aligned} \tag{2.21}$$

where $\sigma \equiv \frac{\pi^2}{30}$ is the Stefan-Boltzmann constant and

$$g^\star \equiv \sum_{bosons} g_s \left(\frac{T_s}{T}\right)^4 + \left(\frac{7}{8}\right)\sum_{fermions} g_s \left(\frac{T_s}{T}\right)^4 \tag{2.22}$$

$$g^{\star\, s} \equiv \sum_{bosons} g_s \left(\frac{T_s}{T}\right)^3 + \left(\frac{7}{8}\right)\sum_{fermions} g_s \left(\frac{T_s}{T}\right)^3 \tag{2.23}$$

where T is a common plasma temperature and factors of $\left(\frac{T_s}{T}\right)$ account for particle species' s which have decoupled from the plasma. For $T >> TeV$ all the SM particles species are coupled to the plasma in ultra-relativistic equilibrium and $g^\star_{SM} = g^{\star\, s}_{SM} =$

106.75. The **Hubble Parameter** is defined as

$$H(t) \equiv \frac{\dot{a}}{a} = \frac{1}{2t} \tag{2.24}$$

where the last equality applies for $w = \frac{1}{3}$ only, having substituted eq. (2.16). $H(t)$ is an important quantity - it is the constant of proportionality relating the recessional velocities of galaxies $\propto \dot{a}$ to their distances $\propto a$, as measured on cosmological scales by a co-moving observer. Substituting eq. (2.21) we may re-express eq. (2.8) for a flat ($k = 0$) radiation dominated universe as

$$H(T) = \sqrt{\left(\frac{8\pi^3 g^\star}{90}\right)} \frac{T^2}{M_{pl}} \tag{2.25}$$

where $M_{pl} = \frac{1}{\sqrt{G}} \sim 10^{19}$GeV is the Planck mass and T is the plasma temperature.

As the universe expands and cools, more and more massive species go non-relativistic and "freeze out" to final abundances $n_{\text{matter}} \ll n_{\text{radiation}}$. The light neutrinos are unique insofar as they decouple from the plasma whilst still relativistic. At $T_{dec} \sim MeV$ the 3 generations of light neutrinos decouple from the plasma of electrons-positron pairs (with $g_{e^-} + g_{e^+} = 4$) and photons (with $g_\gamma = 2$). Shortly after neutrino decoupling the electron-positron pairs co-annihilate, transferring their heat energy to the photons, but not to the decoupled neutrinos. The photon number density after this energy transfer must be equal to the photon plus electron number density before it. Equating these using eq. (2.20) for n_s one obtains

$$\left(\frac{T_\nu}{T_\gamma}\right) = \left(\frac{g_\gamma}{g_\gamma + \left(\frac{7}{8}\right) g_{e^-} + \left(\frac{7}{8}\right) g_{e^+}}\right)^{\frac{1}{3}} = \left(\frac{4}{11}\right)^{\frac{1}{3}} \tag{2.26}$$

where T_ν is the neutrino temperature - equal to the plasma temperature before electron-positron co-annihilation - and T_γ is the plasma temperature after electron-positron co-annihilation, into photons.

Today a relic neutrino "sea" with a temperature $T_\nu = T_{CMB}\left(\frac{4}{11}\right)^{\frac{1}{3}} \approx 1.9K$ is predicted to be observed. Note that it is possible for part of the matter anti-matter asymmetry to end up "stored" in this relic neutrino sea. In fact, one of the

predictions of leptogenesis is that there is an excess of anti-neutrinos over neutrinos approximately twice the excess of baryons over anti-baryons (this will be shown later, in section 3.3). Given that the relic neutrinos have not even been detected yet, it will probably take a long time to confirm this prediction - the relic photons were first measured in 1964 [54] but it wasn't until the COBE measurements in 1992 [55] that anisotropies in the CMB spectrum, of order $\frac{\Delta T}{T} \sim 10^{-6}$ were first probed. Still, neutrino telescopes have started to be developed [1], so perhaps one day this direct test of a prediction of leptogenesis will be possible?

2.2 Boltzmann Equations

The Boltzmann equation describing the collisions of a particle species ψ, with statistical distribution $f_\psi(E_\psi, t)$, is [56]

$$\hat{L}\left[f_\psi\right] = \hat{C}\left[f_\psi\right] \tag{2.27}$$

Notice that we are assuming that f_ψ depends only upon $|\mathbf{p}_\psi| = E_\psi$, the modulus of the ψ particle's three-momentum vector, and not upon its direction. This is merely as a consequence of assuming an isotropic universe, as we did beginning section 3.1. The covariant Liouville operator $\hat{L}$ is in general given by

$$\hat{L} = p^\mu \frac{\partial}{\partial x^\mu} \; - \; \Gamma^\mu_{\nu\sigma}\, p^\nu p^\sigma \frac{\partial}{\partial x^\mu} \tag{2.28}$$

For the FRW metric (c.f. eq. (2.3)), the above operator becomes

$$\hat{L}\left[f(E_\psi, t)\right] = E\,\frac{\partial f}{\partial t} - H(t)\,E_\psi \frac{\partial f}{\partial E_\psi} \tag{2.29}$$

[1] For example Icecube: *http://www.icecube.com/* and Antares: *http://antares.in2p3.fr/*

To obtain the RHS, we consider a collision operator $\hat{C}$ applying to a process $\psi + a + b + ... \leftrightarrow i + j + ...$

$$\begin{aligned}\hat{C}[f_\psi] &= -\int d\Pi_a d\Pi_b ... d\Pi_i d\Pi_j ... (2\pi)^4 \delta^{(4)}(p_\psi + p_a + p_b + ... - p_i - p_j - ...) \\ &\times \{|\mathcal{M}|^2_{\psi\, a\, b\, ... \to i\, j\, ...} f_a f_b ... f_\psi (1 \pm f_i)(1 \pm f_j) ... \\ &- |\mathcal{M}|^2_{i\, j\, ... \to \psi\, a\, b\, ...} f_i f_j ... (1 \pm f_a)(1 \pm f_b) ... (1 \pm f_\psi)\} \end{aligned} \tag{2.30}$$

where for $\pm$ the sign $+$ applies to bosons and the sign $-$ to fermions and $d\Pi_s$ denotes an integral over phase space for particle species s

$$d\Pi_s \equiv \frac{g_s}{(2\pi)^3} \frac{d^{(3)}\mathbf{p}_s}{2E_s} \tag{2.31}$$

The number density of species s, n_s, is defined in terms of f_s as

$$n_s = \frac{g_s}{(2\pi)^3} \int d^{(3)}\mathbf{p}_s f_s(E_s,\, \mathbf{p}_s) \tag{2.32}$$

We would now like to go from an equation in terms of $f_\psi(E_\psi, t)$ to one in terms of $n_\psi(t)$. This is managed straightforwardly by applying the operator $\int d\Pi_\psi$ to both sides of eq. (2.27). Using integration by parts, one obtains that

$$\int d\Pi_\psi \hat{L}[f] = \frac{dn_\psi}{dt} + 3Hn_\psi \tag{2.33}$$

and for the RHS that

$$\begin{aligned}\int d\Pi_\psi \hat{C}[f_\psi] &= -\int d\Pi_\psi d\Pi_a d\Pi_b ... d\Pi_i d\Pi_j (2\pi)^4 \delta^{(4)}(p_\psi + p_a + p_b + ... - p_i - p_j - ...) \\ &\times \{f_\psi f_a f_b ... |\mathcal{M}|^2_{\psi\, a\, b\, ... \to i\, j\, ...} - f_i f_j ... |\mathcal{M}|^2_{i\, j\, ... \to \psi\, a\, b\, ...}\} \end{aligned} \tag{2.34}$$

where we have assumed above that factors $(1 \pm f_s) \approx 1$ i.e. we **ignore quantum statistical effects** of stimulated emission and Pauli blocking. We have also assumed that upon applying $\int d\Pi_\psi$ to obtain an equation in terms of n_ψ, important information is not lost from the original Boltzmann equation by **thermal averaging** over $p_\psi \equiv (E_\psi, \mathbf{p}_\psi)$. The validity of both assumptions is discussed at the end of the

section. Putting both sides together, one obtains a general Boltzmann equation as

$$\begin{aligned}\frac{dn_\psi}{dt} + 3Hn_\psi &= -\int d\Pi_\psi d\Pi_a d\Pi_b ... d\Pi_i d\Pi_j ... (2\pi)^4 \delta^{(4)}(p_\psi + p_a + p_b + ... - p_i - p_j - ...) \\ &\times \{f_\psi f_a f_b ... |\mathcal{M}|^2_{\psi\, a\, b\, ... \to i\, j\, ...} - f_i f_j ... |\mathcal{M}|^2_{i\, j\, ... \to \psi\, a\, b\, ...}\} \end{aligned} \tag{2.35}$$

The above can be simplified by factoring out the expansion of the universe. This is achieved by defining the **co-moving number density** N_s of a particle species s, according to

$$N_s \equiv a^3 n_s \tag{2.36}$$

The chain rule then implies that

$$\frac{dn_s}{dt} = a^{-3}\frac{dN_s}{dt} - 3a^{-2}\dot{a}\, N_s = a^{-3}\left(\frac{dN_s}{dt} - 3HN_s\right) \tag{2.37}$$

where the final step uses $H \equiv \frac{\dot{a}}{a}$. Hence the Hubble parameter will cancel out of eq. (2.35) when reformulated in terms of N_ψ as

$$\begin{aligned}\frac{dN_\psi}{dt} &= -\int d\Pi_\psi d\Pi_a d\Pi_b ... d\Pi_i d\Pi_j ... (2\pi)^4 \delta^{(4)}(p_\psi + p_a + p_b + ... - p_i - p_j - ...) \\ &\times \{f_\psi f_a f_b ... |\mathcal{M}|^2_{\psi\, a\, b\, ... \to i\, j\, ...} - f_i f_j ... |\mathcal{M}|^2_{i\, j\, ... \to \psi\, a\, b\, ...}\} \end{aligned} \tag{2.38}$$

If we now assume **kinetic equilibrium** for all species, we can take $\frac{f_s}{f_s^{eq}} \approx \frac{N_s}{N_s^{eq}}$ above and hence replace f_s by its equilibrium density, pulling a factor of $\frac{N_s}{N_s^{eq}}$ out to the front of the integral for each species. If we furthermore identify γ^{eq}, the space-time density (i.e. # per unit volume per unit time) of various equilibrium processes as

$$\begin{aligned}\gamma^{eq}(\psi ab ... \to ij ...) &= \int d\Pi_\psi d\Pi_a d\Pi_b ... f^{eq}_\psi f^{eq}_a f^{eq}_b ... \int d\Pi_i d\Pi_j ... (2\pi)^4 \\ &\times \delta^{(4)}(p_\psi + p_a + p_b + ... - p_i - p_j - ...)\ |\mathcal{M}|^2_{\psi ab ... \to ij ...} \end{aligned} \tag{2.39}$$

then the eq. (2.38) can be recast as

$$\frac{dN_\psi}{dt} = -\gamma^{eq}(\psi ab ... \to ij ...)\ \frac{N_\psi N_a N_b ...}{N^{eq}_\psi N^{eq}_a N^{eq}_b ...} + \gamma^{eq}(ij ... \to \psi ab ...)\ \frac{N_i N_j ...}{N^{eq}_i N^{eq}_j ...} \tag{2.40}$$

Strictly speaking eq. (2.40) should be called a rate equation rather than Boltzmann equation (a strict Boltzmann equation is given in terms of f_ψ rather than n_ψ or N_ψ). However, equations like eq. (2.40) for δN_ψ are referred to as a Boltzmann equations throughout the literature and so I shall do the same, having noted this possible objection. Now recall that to derive eq. (2.40) we made some simplifying assumptions:

1. We performed thermal averaging over the statistical distribution of ψ by applying the operator $\int \frac{d^{(3)}p_\psi}{(2\pi)^2 2E_\psi}$ to both sides of eq. (2.27)
2. We ignored quantum statistical factors by taking $(1 \pm f_s) \approx s$ for $\{s\}$ and assumed Boltzmann statistics, taking $f_s^{eq} = \exp\left[\frac{E_s}{T}\right]$.
3. We assumed kinetic equilibrium, taking $\frac{f_s}{f_s^{eq}} \approx \frac{N_s}{N_s^{eq}}$.

A recent study [57] has investigated the impact of relaxing some of the above assumptions. A relevant result from their paper is shown below in fig. 2.2. The four curves in each of the panels refer to which assumptions the authors relaxed to obtain the curve. D1 assumes both Boltzmann statistics and Kinetic equilibrium. D2 relaxes the assumption of kinetic equilibrium but keeps the assumption of Boltzmann statistics - and vice versa for D3. D4 relaxes all assumptions to study the full collision integrals without simplifying assumptions. The classical Boltzmann equations of the D1 curves eq. (2.40) appear to give a good approximation to the full quantum mechanical Boltzmann equations of the D4 curves. The authors of [59] similarly report $15-30\%$ corrections due to quantum mechanical effects in the relevant regions of parameter space and so the classical Boltzmann equation (cf. eq. 2.40) can be regarded as a reliable approximation.

However, thermal averaging was still taken in fig. 2.2. Other recent studies [58], [61] have looked at the effects of further relaxing this simplification and undertaken to study the full **Kadanoff–Baym equations** [60] - including thermal corrections and the so-called "memory effects" - comparing them with the simplified Boltzmann of eq. (2.40) and "quantum Boltzmann equations" of the D4 curves in fig 2.2. No large (i.e. greater than $\sim 50\%$) corrections have yet been discovered in the physically relevant regions of the parameter space I shall consider for this thesis. Hence it will

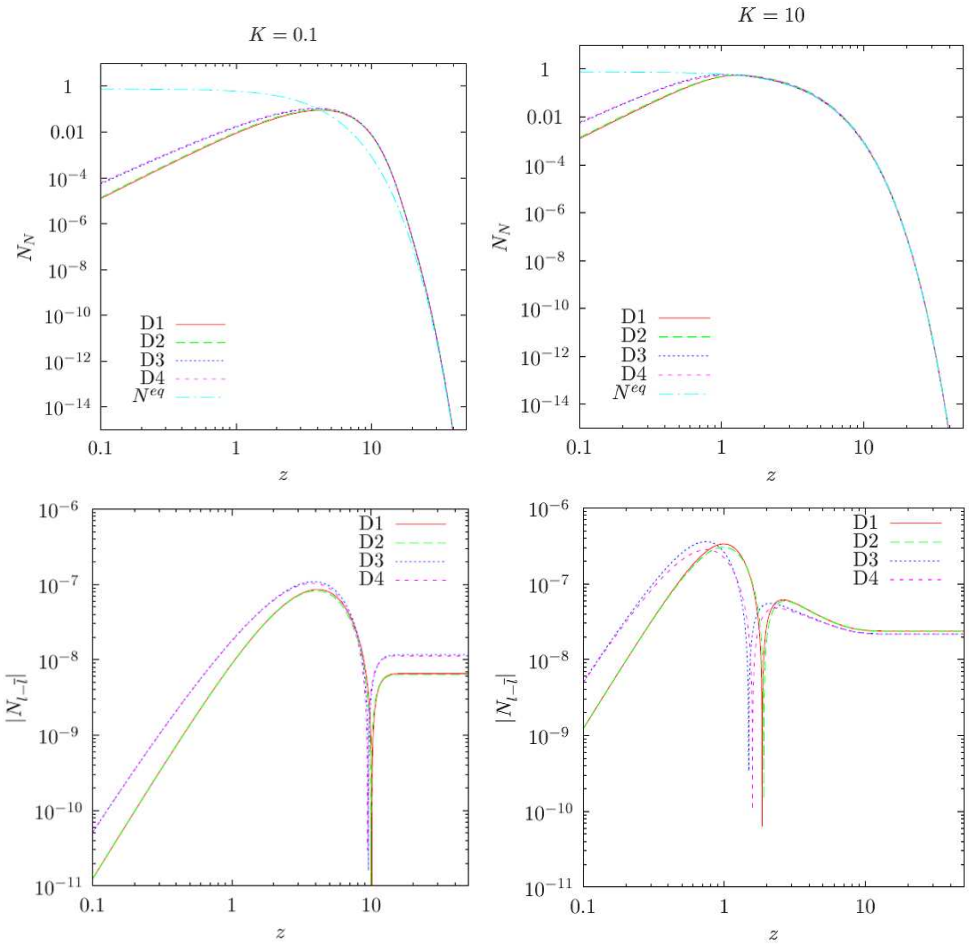

Figure 2.2: Plots from [57] comparing classical with quantum Boltzmann equations. Upper panels (lower panels) show evolution of RHNs (lepton asymmetries) as the universe expands and cools. Left panels (right panels) are for weak (strong) washout.

be acceptable to make all the simplifying assumptions discussed in this section and use eq. (2.40) in subsequent sections to study the evolution of a baryon asymmetry.

2.3 Sakharov's Condition #1: B Violation

Recall from the Introduction section that three **Sakharov conditions** must be satisfied to dynamically generate the baryon asymmetry. These are:

1. Baryon number (B) violating processes

2. C and CP violating processes

3. A departure from thermal equilibrium

For the remainder of this chapter, we shall consider the SM and BSM physics which can satisfy each of the three Sakharov conditions, beginning with #1, baryon number violating processes.

2.3.1 Instantons and B-violation

The (classically) conserved current $J^{\mu\alpha} = \bar{\Psi}\gamma^{\mu}T_{\alpha}\Psi$ for a chiral fermion field $\Psi = (\xi, \bar{\chi})^{T}$ will have an (anomalous) non-zero divergence associated with the gauge 3-vertex, arising from the diagram below

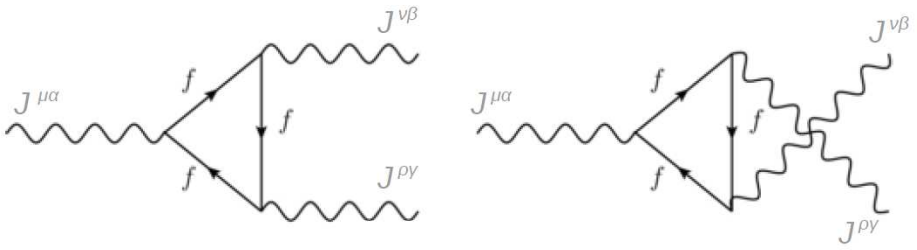

Figure 2.3: Triangle diagrams responsible for anomalous $J^{\mu\alpha}$

The divergence of the current can be evaluated explicitly from the above Feynman graphs as (see [62] chapter 22.3)

$$[\partial_{\mu}J^{\mu\alpha}]_{anom} = -\frac{1}{32\pi^2}\, D_{\alpha\beta\gamma}\epsilon^{\mu\nu\rho\sigma}F^{\beta}_{\mu\nu}F^{\gamma}_{\rho\sigma} \tag{2.41}$$

where $F^{\alpha}_{\mu\nu}$ is the field operator associated with the covariant derivative of the gauge field A^{α}_{μ} belonging to the adjoint rep T^{α} for $\alpha = 1, 2, ...N^2 - 1$ of a gauge group $SU(N)$ and the symmetric quantity $D_{\alpha\beta\gamma}$ is given by

$$D_{\alpha\beta\gamma} = \frac{1}{2}Tr[\{T_{\alpha}, T_{\beta}\}T_{\gamma}] \tag{2.42}$$

In the SM all gauge anomalies cancel generation by generation when we sum over all irreducible representations (irreps) (see [62] chapter 22.4) - $\sum_{irreps}[\partial_{\mu}J^{\mu\alpha}]_{anom} = 0$. However, recall from section 1.1.2 that the SM also has an "accidental" global $U(1)_B$ symmetry and so a baryon number current also "goes along for the ride" whenever a baryon decays into two gauge boson in fig. 2.3. To see what happens to a classically conserved global $U(1)_B$ symmetry, we now take $t^a \mapsto B = \frac{1}{3}$ for a quark doublet

decaying into two gauge bosons. This gives a baryon current of

$$J_B^\mu = B\,\bar{\Psi}\gamma^\mu\left(\frac{1+\gamma^5}{2}\right)\Psi \tag{2.43}$$

When the baryon decays into two $SU(3)_c$ gauge bosons we still obtain $D_{\alpha\beta\gamma} = 0$. However when it decays into $SU(2)_I$ we take $T_{\beta,\gamma} \mapsto \sigma_{i,j}$ and obtain $D_{\alpha\beta\gamma} = \delta^{ij}Tr[B] \neq 0$ (using $\left\{\sigma^i,\,\sigma^j\right\} = 2\delta^{ij}\,I_{2\times 2}$) and when it decays into two $U(1)_Y$ gauge bosons we take $T_{\beta,\gamma} \mapsto Y$ and obtain $D_{\alpha\beta\gamma} = \frac{1}{2}Tr[BY^2] \neq 0$. Taking the traces over all SM irreps and generations results in total $SU(2)_I \times U(1)$ anomalous baryon current of

$$[\partial_\mu J_B^\mu]_{anom} = \frac{N_g}{16\pi^2}\epsilon^{\mu\nu\rho\sigma}\left(B_{\mu\nu}B_{\rho\sigma} - \frac{N_2}{2}W^i_{\mu\nu}W^i_{\rho\sigma}\right) \tag{2.44}$$

where $N_2 = \frac{1}{2}$ for $SU(2)$ and $N_g = 3$ is the number of SM generations, with each generation contributing equally to $[\partial_\mu J_B^\mu]_{anom} \neq 0$ and where B^μ and W^i_μ are gauge fields belonging to the adjoint representations of $U(1)_Y$ and $SU(2)_I$. Repeating the same steps for the leptons we find that a lepton current

$$J_L^\mu = L\,\bar{\Psi}\gamma^\mu\left(\frac{1+\gamma^5}{2}\right)\Psi \tag{2.45}$$

satisfies $[\partial_\mu J_L^\mu]_{anom} = [\partial_\mu J_B^\mu]_{anom}$. As such the quantum number $B+L$ is anomalously non-conserved ($J_B^\mu + J_L^\mu \neq 0$) while the quantum number $B-L$ is fully conserved at the non-perturbative level ($J_B^\mu - J_L^\mu = 0$). What are the implications for baryogenesis? If we write the baryon asymmetry as a sum of its symmetric and anti-symmetric parts in Δ_B and Δ_L then

$$\Delta_B \equiv \frac{1}{2}\Delta_{B+L} - \frac{1}{2}\Delta_{B-L} \neq 0 \tag{2.46}$$

and we see that the second component is protected, whereas the first component may be washed out via non-perturbative $B+L$-violating interactions. This turns out to be the fate of the original minimal $SU(5)$ GUT baryogenesis scenario (see [48] chapter VII.5 for an introduction), which being $B-L$ conserving cannot account for the baryon asymmetry.

To work out $[\partial_\mu J_B^\mu]_{anom}$ explicitly, we now consider the change in macroscopic

charge $B \equiv \int J_0^B d^3x$ associated with the non-conservation of J_B^μ

$$\partial_o B = \int d^3x \left(\partial_0 J_B^0\right) = \int d^3x [\partial_\mu J_B^\mu]_{anom} \tag{2.47}$$

If we integrate the above with respect to time, defining the change $\Delta B = B(t_f) - B(t_i)$ in B between times $t_i = 0$ and $t_f \to \infty$ and substituting eq. (2.44) for $[\partial_\mu J_B^\mu]_{anom}$, we obtain

$$\Delta B = \frac{N_g}{16\pi^2}\epsilon^{\alpha\beta\mu\nu} \int d^4x \left(F_{1\alpha\beta}F_{1\mu\nu} - \frac{N_2}{2}F^\rho_{2\alpha\beta}F^\rho_{2\mu\nu}\right) \tag{2.48}$$

To progress further with the above integral we can introduce the Chern–Simons 3-form. In the mathematician's notation of forms, the Chern–Simons 3-form is given by $J_{CS} = Tr[F \wedge A - \frac{1}{3}A \wedge A \wedge A]$. This important quantity can be written in the physicist's index notation as the current

$$J^i_{CS} = \epsilon_{ijkl}\frac{2}{N_g}Tr\left[A_j F_{kl} + \frac{2i}{3}A_j A_k A_l\right] \tag{2.49}$$

where we have just performed a Wick rotation, to go from Minkowski to Euclidina space. Note that the sum runs only over the spatial components $\{i, j, k, l = 1, 2, 3\}$ of the vector fields A_μ and that $J^0_{CS} = 0$. This is because we can gauge-fix to set $A_0 = 0$, simplifying the calculation. The current J^μ_{CS} has the key property that its divergence is the dual product of F with itself. In form notation $dJ_{CS} = F \wedge F$, or in index notation

$$\partial_\mu J^\mu_{CS} = \frac{1}{2}\epsilon_{ijkl}F^{\alpha ij}F^{\alpha kl} \tag{2.50}$$

The above property allows us to replace the 4-volume integral in eq. (2.48) by a 3-surface integral over J^{CS}. Using the 4D analogue of Gauss' theorem - recalling that we have Wick rotated to Euclidian 4-space - obtains

$$\Delta B = \int d^4x \partial_\mu J^\mu_{CS} = \int_{S^3} \hat{x}_i \, J^i_{CS} \tag{2.51}$$

where the unit 3-vector $\hat{\mathbf{x}}$ points radially outward from the origin. As well as the gauge condition $A_0 = 0$ over S^3, the field strength F_{jk} must vanish over S^3, such

that the energy of a given field configuration will be finite. Substituting eq. (2.49) for J^i_{CS} with this simplification obtains

$$\Delta B = -\frac{iN_g}{24\pi^2}\epsilon_{ijk}\int_{S^3} Tr\left[A_i A_j A_k\right] \tag{2.52}$$

Theoretical physicists are used to the vector fields A doing "strange" things - the Aharanov–Bohm effect [63] being one famous example. Here is another example - there are configurations for which the A^α_i do not vanish at infinity despite having an associated zero field strength F^{ij}. One such configuration was found by Belavin et al [64] and is know as the instanton

$$iA_j(x) = \left(\frac{r^2}{r^2+R^2}\right) g^{-1}(\hat{x}\partial_j g(\hat{x}) \tag{2.53}$$

$$g(\hat{x}) = \left(\frac{x_0 + 2i\sigma\cdot x}{r}\right) \tag{2.54}$$

where $r \equiv \sqrt{\mathbf{x}^2}$ and R is a characteristic size for the above instanton field configuration. Substituting the instanton field configuration into eq. (2.52) we may perform the integral over S^3 by parametrising the surface using co-ordinates $\{\theta_1, \theta_2, \theta_3\}$ according to

$$\Delta B = \frac{N_g}{24\pi^2}\mathcal{I} \tag{2.55}$$

where

$$\begin{aligned}\mathcal{I} &= -i\lim_{r\to\infty} r^3 \int d\theta^1 d\theta^2 d\theta^3 \epsilon^{abc}\frac{\partial\hat{x}_i}{\partial\theta_a}\frac{\partial\hat{x}_j}{\partial\theta_b}\frac{\partial\hat{x}_k}{\partial\theta_c} Tr[A_i A_j A_k] \\ &= \int d\theta^1 d\theta^2 d\theta^3 \epsilon^{abc} Tr\left[g^{-1}(\theta)\frac{\partial g(\theta)}{\partial\theta^a}g^{-1}(\theta)\frac{\partial g(\theta)}{\partial\theta^b}g^{-1}(\theta)\frac{\partial g(\theta)}{\partial\theta^c}\right]\end{aligned} \tag{2.56}$$

Mathematicians are familiar with the integral $\mathcal{I}$ above - they call it a Cartan-Maurer Form. It is a manifestly topological object, since any local perturbation to $g(\theta)$ leaves $\mathcal{I}[g(\theta)]$ invariant. It can be computed explicitly (see [62], chapter 23.4) and is given as

$$\mathcal{I} = 24\pi^2 N_{CS} \tag{2.57}$$

where N_{CS} is an integer known as the Chern-Simons or winding number. The integer value of N_{CS} (and hence of $\mathcal{I}$ itself) depends only upon the topology of the instanton's

gauge field configuration - it corresponds to the number of times these are wound around S^3. In topological notation we can say that $\Pi_3(S^3) = Z$ - meaning that the mapping of S^3 onto S^3 gives the group Z, the integers. This statement can be generalised to $\Pi_N(S^N) = Z$ for a positive integer N. The $N = 1$ case of a circle mapping to a circle is illustrated below, where a "rubber band" is shown wound around a "post" $N_{CS} = 1, 2, 3, ...$ times (having been given $N_{CS} = 1, 2, 3, ...$ half-twists).

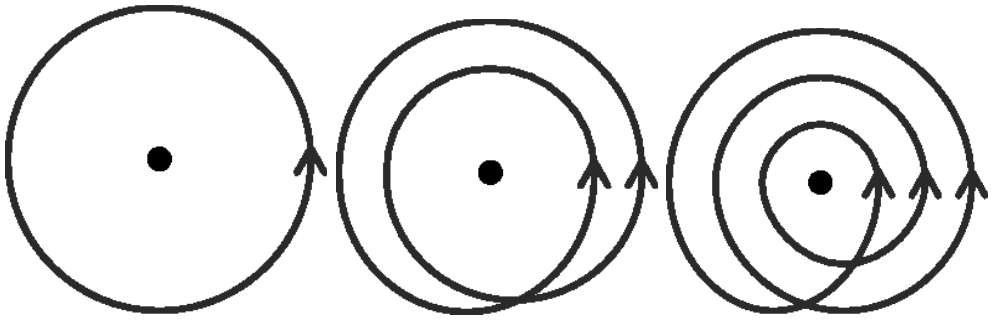

Figure 2.4: A rubber band can be wound $\pm N_{CS}$ times around a post. Image from *http://en.wikipedia.org/wiki/Winding_number*

Are instanton effects important? For an instanton action

$$S_{ins} = n_g \, \mathfrak{I} \, N_{CS} = \frac{8\pi^2}{g^2} \, N_{CS} \tag{2.58}$$

an instanton tunneling rate [2] goes like $exp[-S_{ins}]$. For example, the $B + L$ violating decay $He^3 \to e^+ + \mu^+ + \bar{\nu}_\tau$ can proceed via instanton processes (see [62], chapter 23.6), with a probability estimated by $\exp\left(-8\,|N_{CS}|\,\pi^2/g^2\right) \approx \exp(-373)$, so instanton processes such as this decay are very unlikely to be observed. However, in the early universe instanton-like processes can be important as the potential barrier separating vacua with distinct winding numbers can be surpassed via thermal fluctuations (as opposed to quantum tunneling). We now turn to this possibility.

[2] This tunneling between vacuum states with distinct values of N_{CS} is a fully non-perturbative effect, since the function $\exp\left(-8\,|N_{CS}|\,\pi^2/g^2\right)$ is a power series in $\frac{1}{g^2}$, which can never be written as a power series in g. As Tony Zee says [48] "*you could draw Feynman diagrams until you were blue in the face*" and never discover instantons.

2.3.2 Sphalerons and B-violation

In the previous section we considered the pure Yang-Mills theory. The inclusion of matter and Higgs fields can change things significantly - a new instanton-like solution appears, known as the **Sphaleron**. Sphalerons are saddle points solutions of the Weinberg-Salam theory [65]. They are the solutions to the classical equations of motion for the electro-weak fields where energy density is minimised in all directions of field configuration space except one, and hence the field configuration is unstable - "sphaleron" means "ready to fall" in Greek. Hence passing through the sphaleron configuration can allow a transition between two topologically distinct vacuum states separated by an energy "ridge" in field configuration space - a journey which can end with anomalous $B + L$ violation. The exact sphaleron solution cannot be given in general, but in the limit $\sin\theta_W \to 0$ it takes the following analytic form

$$A_i = \frac{i}{g}\frac{\epsilon_{ijk}x_j\tau_k}{r^2}f(\xi) \tag{2.59}$$

$$\phi = \frac{iv}{\sqrt{2}}\frac{x_i\tau_i}{r}\begin{pmatrix} 0 \\ 1 \end{pmatrix}h(\xi) \tag{2.60}$$

where $\tau_i \equiv \frac{1}{2}\sigma_i$ are the normalised Pauli matrices. For $\xi \equiv \frac{r}{r_0} = rgv$ - a radial parameter, normalised by the characteristic sphaleron size $r_0 = \frac{1}{gv}$ - the functions $f(\xi)$, $h(\xi)$ have the asymptotic behaviour

$$f(\xi) \to \sim \xi^2,\ \xi \to 0 \tag{2.61}$$

$$h(\xi) \to \sim \xi,\ \xi \to 0 \tag{2.62}$$

The sphaleron solution interpolates between a vacuum state for $\xi \to \infty$ and the maximum of the Higgs potential for $\xi \to 0$. One can estimate the characteristic sphaleron energy and temperature (T) dependent B violation rate via sphalerons as,

respectively [21]

$$E_{sph} \sim \frac{8\pi v}{g} \sim 10\,\mathrm{TeV} \tag{2.63}$$

$$\dot{B} \sim B\,T \exp\left(-\frac{E_{sph}}{T}\right) \tag{2.64}$$

Sphaleron processes are active where their rates are greater than the Hubble rate $H \sim \sqrt{g^{\star}_{SM}} T^2/M_{pl}$ (c.f. eq. (2.25)), which occurs for temperatures $T_{sph} \gtrsim 100\mathrm{GeV}$ and are a key component of the leptogenesis mechanism. They violate baryon number per unit co-moving volume at a rate $\dot{B} \propto B\,\Gamma_{sph}$ [56] , thereby partially converting an initial lepton asymmetry into final baryon asymmetry. The baryon number B will "freeze out" to its final value at $T \lesssim T_{sph}$. Sphalerons put $\approx 1/3$ of the $B-L$ asymmetry generated by N_R decays (which are the only processes violating $B-L$) and initially stored in lepton and higgs doublets, into a final baryon asymmetry. The exact fraction is derived later, in section 3.3

Since electro-weak gauge field configurations can't carry colour or flavour charges, sphalerons can only couple to a flavour and colour singlet combination of the left-handed fermions. We can write the allowed $B+L$ violating (and $B-L$ conserving) sphaleron-fermion interactions as an effective dimension 18 operator, given by

$$\widehat{\mathcal{O}}_{B+L} = \prod_{i,\alpha} \left(Q^i_r\, Q^i_g\, Q^i_b\, L_\alpha\right) \qquad i = 1,\, 2,\, 3 \quad \alpha = e,\, \mu,\, \tau \tag{2.65}$$

which violates $B+L$ by six units. The above operator can be represented schematically by pictures such as fig. 2.5.

2.4 Sakharov's Condition #2: CP Violation

There is both C and CP violation in the SM, so Sakharov's second condition is also satisfied. C is violated maximally in the weak interaction and CP is violated through quark mixing, parametrised by a V_{CKM} matrix accounting for the mismatch between weak eigenstates and mass eigenstates in quark mixing. In terms of V_{CKM} mixing angles θ_{ij} and Dirac phase δ it can be shown that the magnitude of CP violation

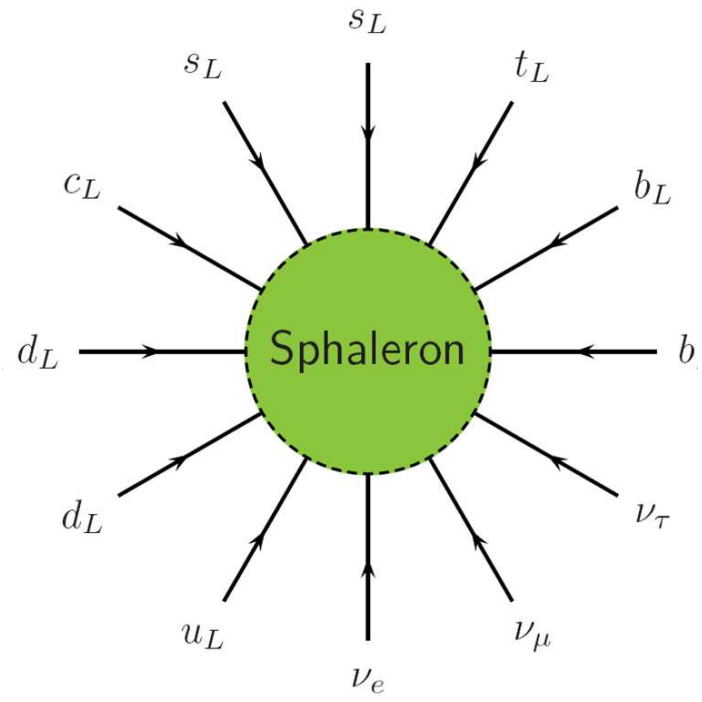

Figure 2.5: One of the sphaleron processes coupling a colour and flavour singlet combination of left-handed quarks and leptons. $B - L$ is conserved. $B + L$ violated by 6 units. Image from [67]

goes like [66]

$$J_{CP} = s_{12}\, s_{12}\, s_{13}\, s_{23}\, c_{12}\, c_{23}\, c_{13}^2\, \sin\delta \tag{2.66}$$

The above parameter is equal to twice the area of each of the six triangles in the complex plane defined by unitarity constraints $\left(V^\dagger V\right)_{ij} = \delta_{ij}$ for $i \neq j$. One of these triangles - known as "the unitarity triangle" - has three sides of similar length and is illustrated in fig. 2.6, which summarises experimental measurements of SM CP violation in quark mixing. However, it can be shown that the for the CKM matrix as the only source of CP violation, one fails to account for the BAU by many orders of magnitude [22]. A new source of CP violation is required, such as from additional CP violating phases in Higgs doublets, super-symmetric particles, or, in the context of leptogenesis, neutrinos. For a thermal leptogenesis, occurring at a scale $\Lambda \gtrsim 10^9 GeV$, the decay $N_i \to l_i + \phi$ may violate CP directly. For the rest of this section, we shall consider this potential new source of CP violation explicitly.

One has direct CP violation in the decay $N_i \to l_i + \phi$ if there is a difference between decay rates $\Gamma_i \equiv \Gamma_{N_i \to l_i + \phi}$ and $\bar{\Gamma}_i \equiv \Gamma_{N_i \to \bar{l}_i + \phi^\dagger}$. It is convenient to normalise this difference, dividing by the total decay rate to define a dimensionless **CP**

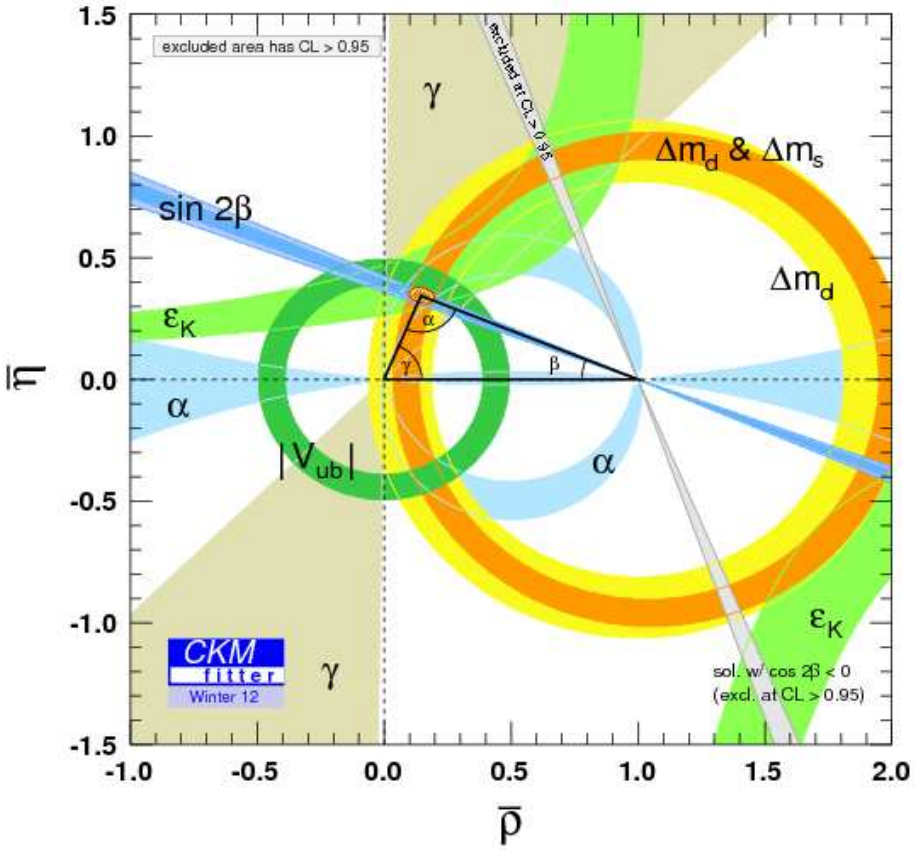

Figure 2.6: The unitarity triangle, circa 2012. Note some tension between $\sin 2\beta$ and $|V_{ub}|$ measurements.

violating parameter ε_i as [3]

$$\varepsilon_i \equiv -\frac{\Gamma_{N_i\to l_i+\phi} - \Gamma_{N_i\to \bar{l}_i+\phi^\dagger}}{\Gamma_{N_i\to l_i+\phi} + \Gamma_{N_i\to \bar{l}_i+\phi^\dagger}} \equiv -\frac{\Gamma_i - \bar{\Gamma}_i}{\Gamma_i + \bar{\Gamma}_i} \tag{2.67}$$

where the decay rates Γ_i and $\bar{\Gamma}$ can be written as phase space integrals involving the square modulus matrix elements $|\mathcal{M}|^2$ for the decay $N_i \to l_i + \phi$ and $|\bar{\mathcal{M}}|^2$ for the decay $N_i \to \bar{l}_i + \phi^\dagger$ respectively. The difference $\Gamma_i - \bar{\Gamma}$ can be obtained from the interferences between the tree–level and loop–level wavefunction and vertex graphs of fig. 2.7.

The total CP violating parameter ε_i may be calculated explicitly (from the

[3] I have chosen to define ε_i with an explicit minus sign, such that a negative lepton asymmetry implies a positive baryon asymmetry (recall from section 2.3.2 that $B-L$ is conserved by sphalerons). Since the baryon asymmetry of the universe is indeed positive, the above definition makes $\varepsilon_{i\alpha} > 0$ the "physical" result and avoids the need to carry around any extra minus signs in expressions for a final $B - L$ asymmetry produced via leptogenesis.

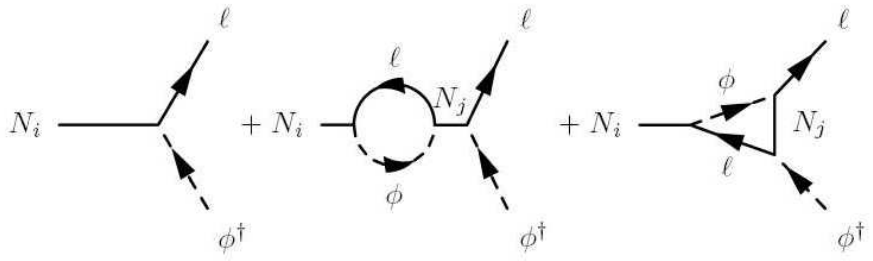

Figure 2.7: The interference of the tree diagram (left) with wavefunction (middle) and vertex (right) diagram results in CP violating decays in leptogenesis scenarios [68]

sum of its tree-wavefunction and tree-vertex interference terms) as [68]

$$\varepsilon_i = \frac{3}{16\pi} \sum_{k \neq i} \frac{Im\left[\left(Y^{\nu\dagger}Y^{\nu}\right)^2_{ik}\right]}{\left(Y^{\nu\dagger}Y^{\nu}\right)_{ii}} \frac{\xi\left(x_{ki}\right)}{\sqrt{x_{ki}}} \tag{2.68}$$

where I have defined the kinematic functions $\xi(x) \equiv \frac{2}{3}x\left[(1+x)\ ln\left(\frac{1+x}{x}\right) - \frac{2-x}{1-x}\right]$ and $x_{ki} \equiv \left(\frac{M_k}{M_i}\right)^2$. In the hierarchical limit $M_k \gg M_i$ one finds $\xi(\infty) = 1$ and an upper bound on ε_i may be derived as [69]

$$|\varepsilon_i| \leq \bar{\varepsilon}_i \equiv \frac{3 M_i m_{atm}}{16\pi v^2} \tag{2.69}$$

known as the Davidson–Ibarra bound for hierarchical neutrinos [4].

2.5 Sakharov's Condition #3: Departure From Equilibrium

There are two generic ways to produce baryon asymmetry during a departure from equilibrium:

1. A first order phase transition
2. The decay of a heavy particle species

Electroweak baryogenesis is an example of the first idea. In electroweak baryogenesis a strongly first order electroweak phase transition may produce sufficient

[4] In their original paper, Davidson and Ibarra derived the supersymmetric version of this bound, which is relaxed by a factor of two compared to the SM case.

baryon asymmetry to account for cosmological observations. Whether the phase transition is first or second order depends upon the one loop, finite temperature effective higgs potential $V_{eff}^{(1)}$, given explicitly in the SM by [23]

$$V_{eff}^{(1)}(\Phi;T) = \left(\frac{3}{32}g^2 + \frac{\lambda}{4} + \frac{m_{top}^2}{4v^2}\right)(T^2 - T_\star^2)\Phi^2 - \frac{3g^2}{32\pi}T\Phi^3 + \frac{\lambda}{4}\Phi^4 \qquad (2.70)$$

where $\Phi \equiv \sqrt{\phi^\dagger\phi}$ and $T_\star$ is a critical temperature. For $T > T_\star$ there is a potential barrier separating a local minimum of $V_{eff}^{(1)}$ at $\Phi = 0$ from the global minimum of $V_{eff}^{(1)}$. For $T < T_\star$ this potential barrier disappears and the transition becomes second order. In the SM the phase transition is only strongly first order for $m_\phi \lesssim 80GeV$ [70] ruling out SM electroweak baryogenesis. The presence of additional light particles, such as light stops in the MSSM, can increase the effect of the Φ^2 term in eq. (2.70), making the phase transition more strongly first order and thereby rescuing electroweak baryogenesis. These new particles may also provide the additional CP violating phases required for successful electroweak baryogenesis.

During a first order phase transition, bubbles of "true vacuum" $\langle\phi\rangle = v$ form inside regions of "false vacuum" $\langle\phi\rangle = 0$ due to tunneling through the potential barrier separating the two vacuum states. Above a critical size, a bubble of "true vacuum" will grow to fill the universe. If more quarks than anti-quarks are reflected by the bubble wall as it sweeps through the quark-gluon plasma then a baryon excess will be generated inside the bubble. Baryon number violating processes partially erase the anti-baryon excess outside the bubble, but these processes are suppressed inside the bubble and so the baryon excess here is entirely preserved.

The second idea - baryogenesis through the CP and B (or L) violating decays of a heavy particle - was Sakharov's original suggestion (of "maximons") and also how minimal $SU(5)$ GUT baryogenesis worked. It was later realised that sphaleron processes rule out the latter, by washing out the pure $B + L$ asymmetry generated by the decays of the $SU(5)$ gauge bosons. However, non-minimal versions of GUT baryogenesis which generate a non-zero $B-L$ component of baryon asymmetry (which sphalerons, being $B - L$ conserving, cannot touch) are still viable. In leptogenesis the heavy particle is of course the RHN.

To consider the decay of a heavy particle species quantitatively, we return to eq. (2.40) derived in section 2.2 and consider the special case $\mathrm{x} \leftrightarrow i + j$ where $\psi \mapsto \mathrm{x}$ is a particle species with mass M_{x} much greater than that of its decay products i and j. Eq. (2.40) then becomes

$$\frac{dN_{\mathrm{x}}}{dt} = -\gamma^{eq}(x \to ij)\,\frac{N_{\mathrm{x}}}{N_{\mathrm{x}}^{eq}} + \gamma^{eq}(ij \to x)\,\frac{N_i N_j}{N_i^{eq} N_j^{eq}} \tag{2.71}$$

One further approximation that can be made is to take Boltzmann statistics $f_s^{eq} = \exp\left[\frac{-E_s}{T}\right]$ for $s = x,\, i,\, j$ above and hence by energy conservation one has that $f_x^{eq} = f_i^{eq} f_j^{eq}$ and can therefore take $\gamma^{eq}\ (x \to ij) = \gamma^{eq}\ (ij \to x)$ given eq. (2.39). We can further assume that, being much heavier, only x departs from equilibrium whereas $N_i \approx N_i^{eq}$ and $N_j \approx N_j^{eq}$. Applying these consideration, eq. (2.71) reduces to

$$\frac{dN_{\mathrm{x}}}{dt} = -\gamma^{eq}(x \to ij)\,\left(\frac{N_{\mathrm{x}}}{N_{\mathrm{x}}^{eq}} - 1\right) \tag{2.72}$$

The spacetime density integral $\gamma^{eq}(x \to ij)$ can be evaluated as

$$\gamma^{eq}(x \to ij) = N_{\mathrm{x}}^{eq}\,\Gamma_{\mathrm{x}}\left\langle \frac{1}{\gamma} \right\rangle \tag{2.73}$$

where Γ_{x} is the vacuum decay rate in the rest frame of the x particle

$$\Gamma_{\mathrm{x}} = \int d\Pi_i d\Pi_j (2\pi)^4 \delta^{(4)}(p_x - p_i - p_j) |\mathcal{M}|^2_{x \to ij} \tag{2.74}$$

and $\left\langle \frac{1}{\gamma} \right\rangle$ is a thermal averaging dilation factor of

$$\left\langle \frac{1}{\gamma} \right\rangle = \frac{1}{N_{\mathrm{x}}^{eq}} \int d\Pi_{\mathrm{x}} \exp\left[-\frac{E_{\mathrm{x}}}{T}\right] \tag{2.75}$$

Substituting these relations back into eq. (2.72) then obtains

$$\frac{dN_{\mathrm{x}}}{dt} = -\Gamma_{\mathrm{x}} \left\langle \frac{1}{\gamma} \right\rangle (\, N_{\mathrm{x}} \,-\, N_{\mathrm{x}}^{eq}) \tag{2.76}$$

The parameter $z \equiv \frac{M_{\mathrm{x}}}{T}$ is a more natural parametrisation for the x dynamics, which are governed by how relativistic the x particles are (with $z = 0$ being fully relativistic,

$z \to \infty$ fully non-relativistic). Using eq. (2.24) for $H(t) = \frac{1}{2t}$ and eq. (2.25) for $H(z) = H(z=1)\,/\,z^2$ (given $T \equiv M_{\rm x}\,/\,z$) we may derive that $z(t) = \sqrt{2t\,H(z=1)}$ and hence that $\frac{dN_{\rm x}}{dt} = \frac{dN_{\rm x}}{dz}\,\frac{dz}{dt} = Hz\,\frac{dN_{\rm x}}{dz}$. Eq. (2.76) then becomes

$$\frac{dN_{\rm x}}{dz} = -\frac{\Gamma_{\rm x}}{Hz}\left\langle\frac{1}{\gamma}\right\rangle\,(N_{\rm x} - N_{\rm x}^{eq}) \tag{2.77}$$

Performing the integral eq. (2.75) explicitly obtains [57]

$$\left\langle\frac{1}{\gamma}\right\rangle \equiv \frac{\mathcal{K}_1(z)}{\mathcal{K}_2(z)} \tag{2.78}$$

where $\mathcal{K}_1$ and $\mathcal{K}_2$ are the first and second modified Bessel functions. One can make accurate interpolating approximations to the Bessel functions $\mathcal{K}_1$ and $\mathcal{K}_2$, valid for all z, as [71]

$$\begin{aligned}\mathcal{K}_2(z) &\approx (\frac{15}{8}+z)\mathcal{K}_1(z)\\ &\approx \frac{1}{z^2}(\frac{15}{8}+z)\left(1+\frac{\pi}{2}z\right)^{\frac{1}{2}}\,e^{-z}\end{aligned} \tag{2.79}$$

It is useful to introduce a so-called **washout parameter** K as

$$K \equiv \frac{\Gamma_{\rm x}}{H(z=1)} \tag{2.80}$$

Given that $H(z) \propto \frac{1}{z^2}$ we have $H(z=1) = z^2 H(z)$ and hence eq. (2.77) may be expressed in terms of K above as

$$\frac{dN_{\rm x}}{dz} = -zK\,\frac{\mathcal{K}_1}{\mathcal{K}_2}\,(N_{\rm x} - N_{\rm x}^{eq}) \tag{2.81}$$

where a thermally averaged equilibrium abundance of a heavy species x is given explicitly by

$$N_{\rm x}^{eq}(z) = \frac{1}{2}N_{\rm x}^{eq}(z=0)\,z^2\mathcal{K}_2(z) \tag{2.82}$$

The relevant case for thermal leptogenesis will be for ${\rm x} \mapsto N$, a RHN with a mass M_N of order at least $10^9 GeV$ (considering the bound eq. (2.69)). I have chosen to adopt a normalisation convention where $N_N^{eq}(z=0) = 1$ i.e. there is one ultra-relativistic

RHN per unit of co-moving volume. This in turn implies a photon number density of $\frac{4}{3}$ at $T \sim M_N$. Calculating $\Gamma_D \equiv \Gamma_{N_i \mapsto l_i \phi}$ from the Feynman diagrams read off from eq. (1.35) of section 1.4 and $H(z=1)$ from eq. (2.25), one finds explicitly

$$\Gamma_D = \frac{3M_i}{8\pi} \left(Y^{\nu\,\dagger} Y^{\nu}\right)_{ii} \qquad \text{and} \qquad H(z=1) = \sqrt{\frac{8\pi^3 g_\star}{90}} \frac{M_1^2}{M_{pl}} \tag{2.83}$$

and hence for the washout parameter eq. (2.80) for RHNs one finds

$$K_i = \frac{\tilde{m}_i}{m_\star} \qquad \text{for} \qquad \tilde{m}_i \equiv \frac{(m_D^\dagger m_D)_{ii}}{M_i} \quad m_\star \equiv \frac{16\,\pi^{5/2}\sqrt{g_\star}}{3\sqrt{45}} \frac{v^2}{M_{\rm Pl}} \tag{2.84}$$

where $m_D \equiv v\,Y^\nu$ is the Dirac neutrino mass-matrix and $m_\star \approx 1.08 \times 10^{-3}$ in the SM. The eq. (2.81) for x $\mapsto N_i$ can be integrated either numerically or analytically to obtain $N_{N_i}(z)$.

Fig. 2.8 compares analytic and numerical estimates for $N_{N_i}(z)$ (for $i = 1$). From an initial equilibrium population of RHNs their number falls after $z \sim 1$ due to Boltzmann suppression of the inverse decay rate by a factor of $\exp[-z]$. At $K = 10^{-4}$ it takes longer for the RHN population to re-equilibrate than at $K = 10^{-2}$, given that the decay and inverse decay rates are proportional to K. Notice that $N_{N_1}^{eq}(z=0) \neq 1$ in fig. 2.8since the authors of [71] adopted the normalisation convention $N_{N_1}^{eq}(z = 0) = \frac{3}{4}$ (i.e. one photon per unit co-moving volume at $T \sim M_{N_1}$) as opposed to my convention of $N_{N_1}^{eq}(z=0) = 1$ (i.e. one ultra–relativistic RHN per unit co-moving volume).

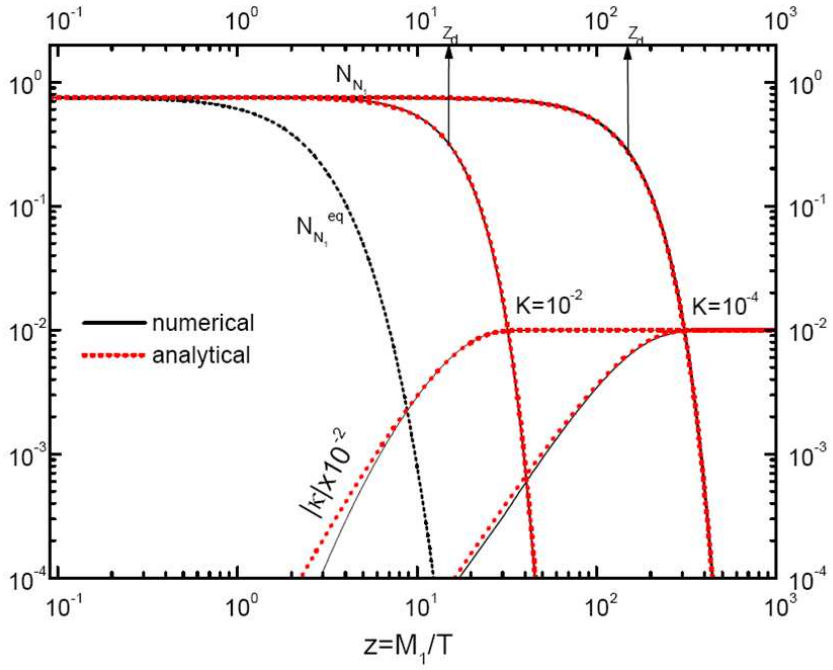

Figure 2.8: N_1 decays for $K = 10^{-2}$ and $K = 10^{-4}$. Plot from [71]

Chapter 3

From Vanilla to Flavoured Leptogenesis

3.1 Vanilla Leptogenesis

Now we are ready to put the results of the previous section together and consider an explicit example of baryogenesis via leptogenesis. We consider first the simplest possible viable scenario for generating the BAU via leptogenesis, often referred to in the literature as "vanilla leptogenesis". The "vanilla" case is that for which BAU is generated by the decays $N \mapsto l + \phi$ of lightest RH neutrinos $N \equiv N_1$ and flavour effects do not play a role, so we consider only the evolution of leptons $l \equiv l_1$ and anti-leptons $\bar{l} \equiv \bar{l}_1$ number. To obtain a Boltzmann equation for the **difference** between leptons and anti–leptons one must include higher order terms in Y^ν and so the derivation is more involved than that for the RHN abundance (cf. section 2.5). A thorough derivation is given in chapter 6 of [25] resulting in a final Boltzmann equation for Δ_{l_1} (neglecting $2 \leftrightarrow 2$ scattering terms) of

$$\frac{dN_{\Delta_{l_1}}}{dz} = -D_1\,\varepsilon_1\left(N_{N_1} - N_{N_1}^{eq}\right) - W_1\left(N_{\Delta_{l_1}} + N_{\Delta_\phi}\right) + \mathcal{O}(\Delta^2) \tag{3.1}$$

where **CP violating parameter** [1] ε_1 is defined as

$$\varepsilon_1 \equiv -\frac{\Gamma_1 - \bar{\Gamma}_1}{\Gamma_1 + \bar{\Gamma}_1} \tag{3.2}$$

for decay rates defined by

$$\left\langle \frac{1}{\gamma} \right\rangle \Gamma_1 = \frac{\gamma(N_1 \to l_1 \phi)}{N_{N_1}^{eq}} \qquad \text{and} \qquad \left\langle \frac{1}{\gamma} \right\rangle \bar{\Gamma}_1 = \frac{\gamma(N_1 \to \bar{l_1} \phi^\dagger)}{N_{N_1}^{eq}} \tag{3.3}$$

and the **decay** and **washout** functions $D_1(z)$ and $W_1(z)$ are defined as

$$D_1(z) \equiv \left\langle \frac{1}{\gamma} \right\rangle \frac{\Gamma_1 + \bar{\Gamma}_1}{Hz} \tag{3.4}$$

$$W_1(z) \equiv \left\langle \frac{1}{\gamma} \right\rangle \frac{1}{2} \frac{\Gamma_1^{ID} + \bar{\Gamma}_1^{ID}}{Hz} \tag{3.5}$$

for inverse decay rates defined by equilibrium conditions

$$N_{N_1}^{eq} \Gamma_1 = N_{l_1}^{eq} N_\phi^{eq} \Gamma_1^{ID} \qquad \text{and} \qquad N_{N_1}^{eq} \bar{\Gamma}_1 = N_{\bar{l}_1}^{eq} N_{\phi^\dagger}^{eq} \bar{\Gamma}_1^{ID} \tag{3.6}$$

Next, recall that the only processes violating $B - L$ are the RHN processes. We will assume for now that $N_{\Delta_{l_1}} + N_{\Delta_\phi} = -N_{\Delta_{B-L}}$ - in other words we assume for now that all of the $B - L$ asymmetry initially stored in lepton and Higgs doublets after $N_1 \mapsto l_1 + \phi$ remains there and is not shared out amongst other SM species [2]. Making this further simplifications (and neglecting $\mathcal{O}(\Delta^2)$ terms) allows us to write a final set of Boltzmann equation for the evolution of $d\Delta_{B-L} = -d\Delta_{l_1}$ as

$$\frac{dN_{N_1}}{dz} = D_1 \left(N_{N_1} - N_{N_1}^{eq} \right) \tag{3.7}$$

$$\frac{dN_{\Delta_{B-L}}}{dz} = D_1 \, \varepsilon_1 \left(N_{N_1} - N_{N_1}^{eq} \right) - W_1 \, N_{\Delta_{B-L}} \tag{3.8}$$

One can see each of Sakharov's conditions implicit in the first term of eq. (3.8) - D_1 contains Γ_1, a $B-L$ violating decay, ε_1 parametrises CP violation and $N_{N_1} - N_{N_1}^{eq} \neq 0$ implies a departure from equilibrium. There is a kind of "competition" going on

[1] I have chosen to define ε_1 with an overall minus sign such that for positive ε_1 the final $B - L$ asymmetry is positive (as required for a positive final baryon asymmetry after sphaleron conversion).

[2] This simplifying assumption will be relaxed in for section 3.3, where it is shown how to calculate the fraction of $B - L$ asymmetry redistributed amongst all of the various SM particle species comprising the relativistic plasma filling the early universe.

between this first term, which produces $B-L$ asymmetry and the second term, which washes it out. But since the inverse decay rate is Boltzmann suppressed by a factor of $\exp[-z]$ when $z > 1$ and this is precisely the moment when the departure from equilibrium is largest, it is the production term that "wins" this competition, in the sense that some final $B-L$ asymmetry will survive the washout. Why does asymmetry production go like the decay rate and asymmetry washout like the inverse decay rate? Say there is some initial excess of leptons over anti-leptons. The inverse decay $l_1 + \phi \to N_1$ is then more likely to happen than $\bar{l}_1 + \phi^\dagger \to N_1$. When there is no CP violating decay $N_1 \to l_1 + \phi,\ \bar{l}_1 + \phi^\dagger$ to compensate this effect, more leptons than anti-leptons will be annihilated per unit time, whereas the same number of each are produced per unit time. So over time an initial lepton excess will be erased [3].

Integrating eq. (3.8) obtains the solution

$$N_{\Delta_{B-L}}(z, z_{in}) = N_{\Delta_{B-L}}(z = z_{in})\, e^{-\int_{z_{in}}^{z} dz^{'} W(z^{'})} - \varepsilon_1\, \kappa(z_{in}, z) \tag{3.9}$$

where the efficiency factor $\kappa(z_{in}, z)$ is defined by the integral

$$\kappa(z_{in}, z) = \int_{z_{in}}^{z} dz^{'}\, D(N_N - N_N^{eq})\, e^{-\int_{z^{'}}^{z} dz^{''} W(z^{''})} \tag{3.10}$$

and so the final efficiency factor $\kappa^f \equiv \kappa(0, \infty)$ gives the final Δ_{B-L} asymmetry produced from $z_{in} \mapsto 0$ [4] until after all the RHNs have frozen out at $z \mapsto \infty$

$$N^f_{\Delta_{B-L}} = N^{in}_{\Delta_{B-L}}\, e^{-\int_0^\infty dz^{'} W(z^{'})} - \varepsilon_1 \kappa^f \qquad\qquad \kappa^f \equiv \kappa(0, \infty) \tag{3.11}$$

where we have defined $N^{in}_{\Delta_{B-L}} \equiv N_{\Delta_{B-L}}(z = z_{in} \mapsto 0)$ above as a potential Δ_{B-L} asymmetry present prior to leptogenesis. To evaluate the above integrals we must give $D(z)$ and $W(z)$ of eq. (3.5) explicitly in terms of z. Recalling eq. (3.5) and

[3] As an analogy to this "competition" between production and washout, I like to imagine lining up a row of coins which can be "heads" or "tails" - the production term tries to turn over more heads than tails and the washout term tries to flip the coins. Without the continued action of the production term, one would soon arrive back to a 50% heads 50% tails situation.

[4] In taking $z_{in} \mapsto 0$ to simplify the calculation of $N^f_{\Delta_{B-L}}$ we are assuming a reheat temperature of the universe $T_{RH} > M_N$ such that the baryon asymmetry starts being produced when $z \ll 1$.

eq. (2.78) one obtains

$$D(z) = K\, z \left\langle \frac{1}{\gamma} \right\rangle = K\, z\, \frac{\mathcal{K}_1(z)}{\mathcal{K}_2(z)} \tag{3.12}$$

and recalling eq. (3.6) we may relate $W(z)$ to $D(z)$ as

$$W(z) = \frac{1}{2} \frac{N_N^{eq}}{N_l^{eq} N_\phi^{eq}} D(z) = \frac{3}{16} K z^3 \mathcal{K}_1(z) N_{N_1}^{eq}(z = \infty) \tag{3.13}$$

where the second equality follows from eq. (3.12) for $D(z)$ and

$$\begin{aligned} N_{N_1}^{eq}(z) &= \frac{1}{2} z^2 \mathcal{K}_2(z) N_{N_1}^{eq}(z = \infty) \\ N_{l_1}^{eq} &= N_{N_1}^{eq}(z = \infty) \\ N_\phi^{eq} &= \frac{4}{3} N_{N_1}^{eq}(z = \infty) \end{aligned} \tag{3.14}$$

Henceforth I will adopt the convention that $N_{N_1}^{eq}(z = \infty) = 1$ - that there is one ultra-relativistic RHN per unit of co-moving volume.

From eq. (2.79) it can be seen explicitly that eq. (3.13) for $W(z) \propto \mathcal{K}_1$ is Boltzmann suppressed by $\exp[-z]$ when $z > 1$ whereas $D(z) \propto \frac{\mathcal{K}_1}{\mathcal{K}_2}$ is unsuppressed. Eq. (3.13) now allows the first term of eq. (3.11) to be integrated exactly - using properties of the first modified Bessel function $\mathcal{K}_1$ it can be shown that $\int_0^\infty dx\, x^3\, \mathcal{K}_1(x) = 2\pi$ and hence

$$\int_0^\infty dz^{'} W(z^{'}) = \frac{3}{16} K \int_0^\infty dz^{'} z^{'3}\, \mathcal{K}_1(z^{'}) = \frac{3\pi}{8}\, K \tag{3.15}$$

Substituting the above result back into eq. (3.11) the final $B-L$ asymmetry becomes, for $z_{in} \mapsto 0$

$$N_{\Delta_{B-L}}^f = N_{\Delta_{B-L}}^{in}\, e^{-\frac{3\pi}{8} K} - \varepsilon_1 \kappa^f \tag{3.16}$$

Various analytic approximations exist for the final efficiency factor. If we define the function $\psi(z^{'}, z)$ by

$$\kappa(z_{in}, z) \equiv \int_{z_{in}}^{z} dz^{'} e^{-\psi(z^{'}, z)} \tag{3.17}$$

then the above integral is dominated by the region of $z^{'}$ where $\psi(z^{'}, z)$ is a minimum. If we define z_B as the value of $z^{'}$ which minimises ψ over the interval $\{z_{in}, z\}$ then

$\kappa(z_{in}, z)$ can be evaluated using the method of steepest descent. For $N_N^{in} = 1$ or a thermal initial abundance of RHNs an accurate analytic approximation for $\kappa^f \equiv \kappa(0, \infty)$ is given by

$$\kappa^f(K) \approx \frac{2}{KZ_B(K)} \left(1 - \exp\left[-\frac{1}{2} KZ_B(K)\right]\right) \tag{3.18}$$

where $z_B(K)$ is approximated by

$$z_B(K) \approx 2 + 4K^{0.13} \exp\left[-\frac{2.5}{K}\right] \tag{3.19}$$

while for $N_N^{in} = 0$ or a vanishing initial abundance of RHNs an accurate analytic approximation is given by

$$\kappa^f(K) \approx \frac{2}{KZ_B(K)} \left(1 - \exp\left[-\frac{1}{2} Kz_B(K)\, N_N^{eq}(K)\right]\right) \tag{3.20}$$

where $z_B(K)$ was already given and

$$N_N^{eq}(K) = \frac{\frac{3\pi K}{4}}{\left(1 + \sqrt{\frac{3\pi K}{4}}\right)^2} \tag{3.21}$$

is the equilibrium RHN abundance in terms of the washout parameter K. One can see that in the limit $K \mapsto \infty$ one obtains $N_N^{eq}(\infty) = 1$ and hence eq. (3.18) and eq. (6.81) become the same as required - strong washout eliminates all dependence on initial conditions.

Fig. 3.1 compares analytic and numerical approximation for strong and weak washout, showing how the $B - L$ asymmetry evolves from z_{in} to $z \mapsto \infty$. Notice that the RHNs begin from zero initial abundance in these plots, so at first a $B - L$ asymmetry of the "wrong" sign (i.e. negative) is produced because the inverse decay rate of RHNs is larger than its decay rate. These rates equalise at $z = z_{eq}$ after which decays dominate inverse decays to produce a final positive $B - L$ asymmetry. Note that since the negative $B-L$ asymmetry produced during $z < z_{eq}$ is washed out more than the positive $B-L$ asymmetry produced during $z > z_{eq}$ the final $B-L$ asymmetry after all the RHNs have decayed will be net positive. However, one gets close to a

cancellation in the upper panel plot, because $K \ll 1$ here making the $z < z_{eq}$ and $z > z_{eq}$ phases almost symmetric. The analytic approximations for κ^f used to obtain fig. 3.1 are accurate to within $\sim 1\%$ [71]. This is more than good enough for our purposes, given there are theoretical uncertainties of probably $\sim 50\%$ on $N^f_{\Delta_{B-L}} \neq 0$ in most regions of leptogenesis parameter space [5]. As emphasised in section 2.2 this uncertainty arises from approximating the full quantum kinetic treatment [57] to a Boltzmann equation treatment and from non-equilibrium thermal corrections [58,61].

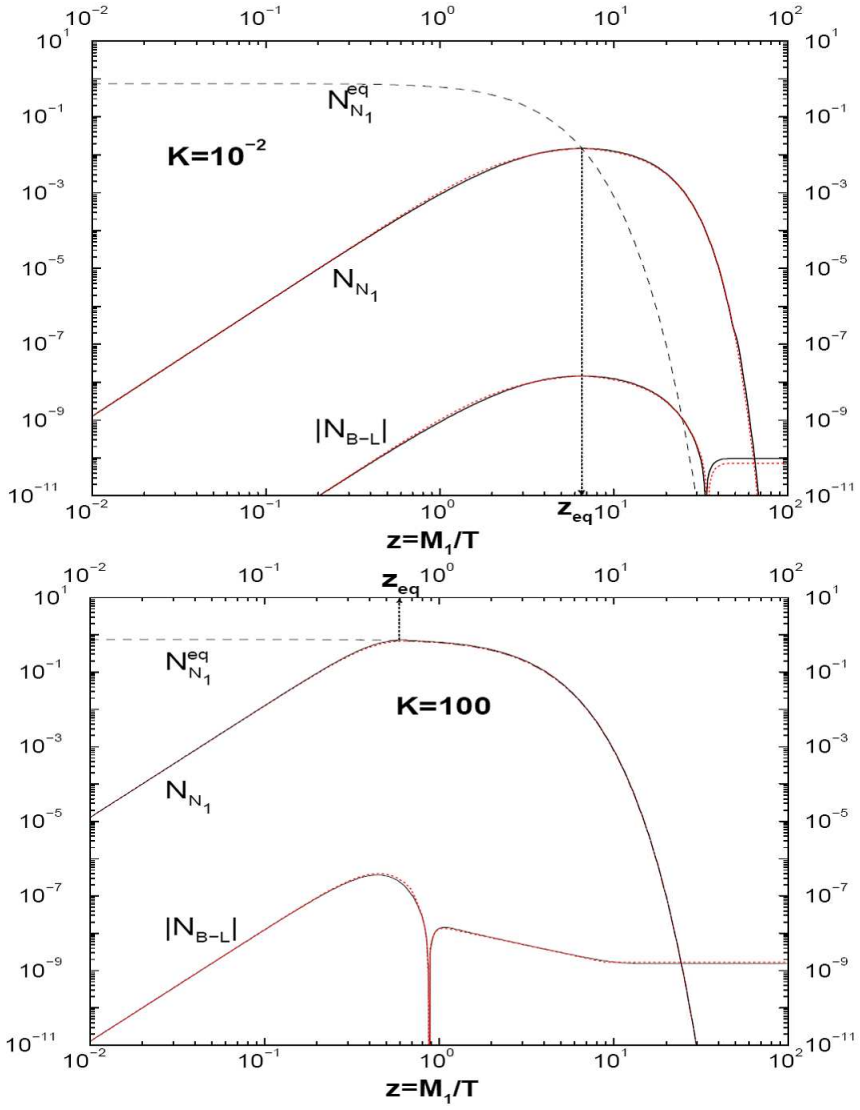

Figure 3.1: Final Δ_{B-L} asymmetry for $K = 10^{-2}$ (upper panel) and $K = 100$ (lower panel). Plot from [71].

[5] and perhaps significantly higher than this in the resonant regime, where two RHNs have almost degenerate masses or in the weak washout regime, where thermal and quantum corrections can be large.

A final Baryon to photon ratio is obtained from the final $B-L$ asymmetry as

$$\eta_B \equiv \frac{N^f_{\Delta_B}}{N^{\rm rec}_\gamma} = a_{\rm sph}\,\frac{N^{\rm f}_{\Delta_{B-L}}}{N^{\rm rec}_\gamma} \simeq 0.01\,N^{\rm f}_{B-L} \tag{3.22}$$

$a_{\rm sph} = \frac{28}{79} \approx \frac{1}{3}$ is a factor accounting for the partial redistribution, via sphalerons, of a final $B-L$ asymmetry into a final B asymmetry [6] (the result will be derived in section 3.3). $N^{\rm rec}_\gamma \approx 36$ is the photon co-moving number density after "re"combination - the epoch where electrons first combine with nuclei to form atoms. This can be calculated using a normalisation convention where $N_{N_1}(z=0)=1$ implying that $N_\gamma = \frac{4}{3}$ when all SM species are still relativistic. By "re"combination all SM species have co-annihilated into photons and the three light neutrino species, conserving total co-moving number densities before and after co-annihilation, hence

$$N^{rec}_\gamma = \frac{4}{3}\frac{g^{\star s}_{SM}}{g^{\star s}_{rec}} \approx 36 \tag{3.23}$$

where $g^{\star s}_{SM} = g^\star_{SM} = 106.75$ and $g^{\star s}_{rec} = 2 + \frac{7}{8}\times 2\times 3\times\left(\frac{4}{11}\right) \approx 3.91$ was calculated using eq. (2.23) and eq. (2.26) from section 2.1. If leptogenesis is really the mechanism by which the BAU is generated then eq. (3.22) for η_B should equal the observed CMB baryon-to-photon abundance [19]

$$\eta^{\rm CMB}_B = (6.19 \pm 0.15)\times 10^{-10} \tag{3.24}$$

3.2 The Importance of Flavour Effects

Flavour effects are quite important within leptogenesis scenarios, where they can give order–of–magnitude wise enhancements to the final baryon–to–photon ratio [72, 73] and so in this section I show how to incorporate them. The decays $N_i \mapsto l_i + \phi$ and $N_i \mapsto \bar{l}_i + \phi^\dagger$ produce the respective lepton states $|l_i\rangle$ and $|l_i\rangle$, which are coherent

[6] Notice here that $N^f_{\Delta_B} \approx \frac{1}{3}N^f_{\Delta_{B-L}}$ implies a final lepton asymmetry of $N^f_{\Delta_L} \approx -\frac{2}{3}N^f_{\Delta_L}$ stored in the ν_e, ν_μ, ν_τ cosmic neutrino "seas", as was discussed at the end of section 2.1, where it was noted that there are no immediate prospects to test this prediction of leptogenesis using neutrino telescopes.

states in lepton flavour space

$$\begin{aligned} |l_i\rangle &\equiv \sum_\alpha \langle l_\alpha|l_i\rangle\, |l_\alpha\rangle \equiv \sum_\alpha \mathcal{C}_{i\alpha}|l_\alpha\rangle \\ |\bar{l}_i\rangle &\equiv \sum_\alpha \langle \bar{l}_\alpha|\bar{l}_i\rangle\, |\bar{l}_\alpha\rangle \equiv \sum_\alpha \bar{\mathcal{C}}_{i\alpha}|\bar{l}_\alpha\rangle \end{aligned} \tag{3.25}$$

where $\{\alpha\}$ gives a complete basis in flavour space - for example $\alpha = e, \mu, \tau$

The coherences of $|l_i\rangle$, $|\bar{l}_i\rangle$ above are broken by leptonic Yukawa interactions which "measure" flavour, thus projecting into a given flavour α with probability

$$\begin{aligned} p_{i\alpha} &= |\langle l_\alpha|l_i\rangle|^2 \equiv |\mathcal{C}_{i\alpha}|^2 \\ \bar{p}_{i\alpha} &= |\langle \bar{l}_\alpha|\bar{l}_i\rangle|^2 \equiv |\bar{\mathcal{C}}_{i\alpha}|^2 \end{aligned} \tag{3.26}$$

The above probabilities can be identified as the branching ratios for the flavoured decay rates

$$\begin{aligned} \Gamma_{i\alpha} &\equiv p_{i\alpha}\,\Gamma_i \qquad \text{for} \qquad \Gamma_i \equiv \Gamma_{N_i \mapsto l_i + \phi} \quad \Gamma_{i\alpha} \equiv \Gamma_{N_i \mapsto l_\alpha + \phi} \\ \bar{\Gamma}_{i\alpha} &\equiv \bar{p}_{i\alpha}\,\bar{\Gamma}_i \qquad \text{for} \qquad \bar{\Gamma}_i \equiv \Gamma_{N_i \mapsto \bar{l}_i + \phi^\dagger} \quad \bar{\Gamma}_{i\alpha} \equiv \Gamma_{N_i \mapsto \bar{l}_\alpha + \phi^\dagger} \end{aligned} \tag{3.27}$$

It is also convenient to define $p_{i\alpha}$ and $\bar{p}_{i\alpha}$ in terms of their symmetric and anti-symmetric parts

$$\begin{aligned} p_{i\alpha} &\equiv p^0_{i\alpha} + \frac{1}{2}\Delta p_{i\alpha} \\ \bar{p}_{i\alpha} &\equiv p^0_{i\alpha} - \frac{1}{2}\Delta p_{i\alpha} \end{aligned} \tag{3.28}$$

where $p^0_{i\alpha} \equiv \frac{1}{2}(p_{i\alpha} + \bar{p}_{i\alpha})$ and $\Delta p_{i\alpha} \equiv p_{i\alpha} - \bar{p}_{i\alpha}$. We can next define a flavoured washout parameter as

$$K_{i\alpha} \equiv p^0_{i\alpha} K_i \tag{3.29}$$

and a flavoured CP asymmetry as

$$\varepsilon_{i\alpha} \equiv -\frac{p_{i\alpha}\,\Gamma_i - \bar{p}_{i\alpha}\,\overline{\Gamma}_i}{\Gamma_i + \overline{\Gamma}_i} \equiv\ p^0_{i\alpha}\varepsilon_i\ -\ \frac{\Delta p_{i\alpha}}{2} \tag{3.30}$$

where the final identity follows from eq. (3.28) and $\varepsilon_i \equiv -\frac{\Gamma_i - \bar{\Gamma}_i}{\Gamma_i + \bar{\Gamma}_i}$. Hence the flavoured

CP asymmetry may be obtained from the unflavoured symmetry of section 2.4, provided we can calculate $p^0_{i\alpha}$ and $\Delta p_{i\alpha}$ explicitly. Recall from eq. (3.28) that these are given in terms of coefficients $\mathcal{C}_{i\alpha} \equiv \langle l_i | l_\alpha \rangle$ and $\bar{\mathcal{C}}_{i\alpha} \equiv \langle \bar{l}_i | \bar{l}_\alpha \rangle$ as

$$p^0_{i\alpha} = \frac{1}{2}\left(|\mathcal{C}_{i\alpha}|^2 + |\bar{\mathcal{C}}_{i\alpha}|^2\right) \qquad \text{and} \qquad \Delta p_{i\alpha} = |\mathcal{C}_{i\alpha}|^2 - |\bar{\mathcal{C}}_{i\alpha}|^2 \tag{3.31}$$

The $\mathcal{C}_{i\alpha}$ are given in terms of the neutrino Yukawa matrix Y^ν and N_i masses M_i. At tree level one has

$$\mathcal{C}^0_{i\alpha} = \frac{Y^\nu_{\alpha i}}{\sqrt{(Y^\nu\, Y^\nu)_{ii}}} \qquad \text{and} \qquad \bar{\mathcal{C}}^0_{i\alpha} = \frac{Y^{\nu\star}_{\alpha i}}{\sqrt{(Y^\nu\, Y^\nu)_{ii}}} \tag{3.32}$$

and at one loop order [7] [74]

$$\begin{aligned} \mathcal{C}_{i\alpha} &= \frac{1}{\sqrt{(Y^{\nu\dagger}\, Y^\nu)_{ii} - 2\,\mathrm{Re}(Y^{\nu\dagger}\, Y^\nu\, \xi_u)_{ii}}}\,(Y^\nu_{\alpha i} - (Y^\nu\, \xi_u)_{\alpha i}) \\ \bar{\mathcal{C}}_{\bar{i}\bar{\alpha}} &= \frac{1}{\sqrt{(Y^{\nu\dagger}\, Y^\nu)_{ii} - 2\,\mathrm{Re}(Y^{\nu\dagger}\, Y^\nu\, \xi^\star_v)_{ii}}}\,(Y^{\nu\star}_{\alpha i} - (Y^{\nu\star}\, \xi_v)_{\alpha i}) \end{aligned} \tag{3.33}$$

where ξ_u and ξ_v are loop-level kinematic functions given by

$$\begin{aligned} \left[\xi_u(M_i^2)\right]_{ki} &\equiv \left[u^T(M_i^2) + Mb(M_i^2)(Y^{\nu\dagger}\, Y^\nu)^T M\right]_{ki} \\ \left[\xi_v(M_i^2)\right]_{ki} &\equiv \left[v^T(M_i^2) + Mb(M_i^2)(Y^{\nu\dagger}\, Y^\nu) M\right]_{ki} \end{aligned} \tag{3.34}$$

and u and v terms above are given by

$$\begin{aligned} u_{ki}(M_i^2) &= \omega_{ki}(M_i^2)\left[M_i \Sigma_{N,ik}(M_i^2) + M_k \Sigma_{N,ki}(M_i^2)\right] \\ v_{ki}(M_i^2) &= \omega_{ki}(M_i^2)\left[M_i \Sigma_{N,ki}(M_i^2) + M_k \Sigma_{N,ik}(M_i^2)\right] \end{aligned} \tag{3.35}$$

which depend on the N_i self-energy Σ_N

$$\Sigma_{N,ki}(M_i^2) = a(M_i^2)(Y^{\nu\dagger} Y^\nu)_{ki} \tag{3.36}$$

for which the loop factor a is evaluated on mass-shell for the RH neutrino N_i.

[7] It might seem like "overkill" to give the $\mathcal{C}_{i\alpha}$ explicitly like this, rather than just stating a final result for $\varepsilon_{i\alpha}$ as was done for ε_i. The reason I introduce these explicit expressions is that they will also turn out to be useful in chapter 6, in a different context.

Substituting these explicit expressions back into eq. (3.31) we obtain

$$
\begin{aligned}
p^0_{i\alpha} &= \frac{|Y^\nu_{\alpha i}|^2}{(Y^{\nu\dagger}\,Y^\nu)_{ii}} + \mathcal{O}(Y^2) && (3.37)\\
\Delta p_{i\alpha} &= -\frac{2}{(Y^{\nu\dagger}\,Y^\nu)_{ii}} \sum_{k\neq i} \mathrm{Re}\left[Y^{\nu\star}_{\alpha i}\, Y^\nu_{\alpha k}\, (\xi_U - \xi^\star_V)_{ki}\right] \\
&+ \frac{2\,|Y^\nu_{\alpha i}|^2}{(Y^{\nu\dagger}Y^\nu)^2_{ii}} \sum_{k\neq i} \mathrm{Re}\left[\left(Y^{\nu\dagger}\,Y^\nu\right)_{ik} (\xi_U - \xi^\star_V)_{ki}\right] + \mathcal{O}(Y^4) && (3.38)
\end{aligned}
$$

where the first term comes from the loop level terms in the numerator of eq. (3.33) and the second term from the loop level terms in the denominator (which may be evaluated using the binomial theorem). The kinematic parts are given explicitly by

$$
\begin{aligned}
\frac{1}{2i}(\xi_U - \xi^\star_V)_{ki} &= \mathrm{Re}\left[\omega_{ki}(M_i^2)\right]\, \left[M_i (Y^{\nu\dagger}\,Y^\nu)_{ki} + M_k (Y^{\nu\dagger} Y^\nu)_{ik}\right]\, \mathrm{Im}\left[a_i\right] \\
&+ M_i M_k (Y^{\nu\dagger} Y^\nu)_{ik}\, \mathrm{Im}\left[b_{ki}\right] && (3.39)
\end{aligned}
$$

Since a decaying N_i contains real intermediate states the imaginary parts of a_i and b_{ki} are indeed non-zero (by the optical theorem) and are given explicitly (in limit of hierarchical M_i) as

$$
\begin{aligned}
Im[a(M_i)] &= -\frac{1}{16\pi} \\
Im[b(x_{ki})] &= \frac{1}{16\pi M_i M_k} \sqrt{x}_{ki} \left(1 - (1+x_{ki}) log\left(\frac{1+x_{ki}}{x_{ki}}\right)\right) && (3.40)
\end{aligned}
$$

where $x_{ki} \equiv \left(\frac{M_k}{M_i}\right)^2$. Finally, the real part of ω_{ki}, also evaluated on shell, is given by

$$
\mathrm{Re}\left[\omega_{ki}(M_i^2)\right] = \frac{M_i (M_k^2 - M_i^2)}{(M_k^2 - M_i^2)^2 + (M_k \Gamma_i - M_i \Gamma_k)^2} \qquad (3.41)
$$

which in the hierarchical mass limit reduces to $\mathrm{Re}\left[\omega_{ki}(M_i^2)\right] = \frac{M_i}{M_k^2 - M_i^2}$. Putting all

the previous expressions together, we finally obtain for $\Delta p_{i\alpha}$

$$\begin{aligned}\Delta p_{i\alpha} &= -\frac{3}{8\pi}\sum_{k\neq i}\{\frac{\mathrm{Im}\left[Y^{\nu\star}_{\alpha i}Y^{\nu}_{\alpha k}(Y^{\nu\dagger}Y^{\nu})_{ik}\right]}{(Y^{\nu\dagger}Y^{\nu})_{ii}}\frac{\xi(x_{ki})}{\sqrt{x_{ki}}} \\ &+ \frac{2}{3(x_{ki}-1)}\frac{\mathrm{Im}\left[Y^{\nu\star}_{\alpha i}Y^{\nu}_{\alpha k}(Y^{\nu\dagger}Y^{\nu})_{ki}\right]}{(Y^{\nu\dagger}Y^{\nu})_{ii}}\} \\ &+ \frac{2\left|Y^{\nu}_{\alpha i}\right|^2}{(Y^{\nu\dagger}Y^{\nu})_{ii}}\frac{3}{16\pi}\sum_{k\neq i}\frac{Im\left[\left(Y^{\nu\dagger}Y^{\nu}\right)^2_{ik}\right]}{(Y^{\nu\dagger}Y^{\nu})_{ii}}\frac{\xi\left(x_{ki}\right)}{\sqrt{x_{ki}}}\end{aligned} \tag{3.42}$$

where $\xi(x)\equiv\frac{2}{3}x\left[(1+x)\;ln\left(\frac{1+x}{x}\right)-\frac{2-x}{1-x}\right]$ and $x_{ki}\equiv\left(\frac{M_k}{M_i}\right)^2$. One may also verify explicitly that $\sum_\alpha\Delta p_{i\alpha}=0$. The final term in $\Delta p_{i\alpha}$ can be identified as $2p^0_{i\alpha}\varepsilon_i$ (by recalling eq. (2.68) for ε_i from section 2.4 and noting that $p^0_{i\alpha}=\frac{\left|Y^{\nu}_{\alpha i}\right|^2}{\left(Y^{\nu\dagger}Y^{\nu}\right)_{ii}}$) and so by eq. (3.43) the remaining terms can be identified as $-2\varepsilon_{i\alpha}$. Multiplying these by $-\frac{1}{2}$ we obtain the flavoured CP asymmetry

$$\begin{aligned}\varepsilon_{i\alpha}=\frac{3}{16\pi}\sum_{k\neq i}\;\{\;&\frac{\mathrm{Im}\left[Y^{\nu\star}_{\alpha i}Y^{\nu}_{\alpha k}(Y^{\nu\dagger}Y^{\nu})_{ik}\right]}{(Y^{\nu\dagger}Y^{\nu})_{ii}}\frac{\xi(x_{ki})}{\sqrt{x_{ki}}} \\ &+\frac{2}{3(x_{ki}-1)}\frac{\mathrm{Im}\left[Y^{\nu\star}_{\alpha i}Y^{\nu}_{\alpha k}(Y^{\nu\dagger}Y^{\nu})_{ki}\right]}{(Y^{\nu\dagger}Y^{\nu})_{ii}}\;\}\end{aligned} \tag{3.43}$$

A similar bound to the Davidson-Ibarra bound $\varepsilon_1\leq\bar{\varepsilon}_1$ (cf. eq. (2.69)) also exists for the flavoured CP asymmetries, for which it can be shown that [8] [8]

$$\varepsilon_{1\alpha}\lesssim\sqrt{p^0_{1\alpha}}\,\bar{\varepsilon}_1 \tag{3.44}$$

Flavoured Boltzmann equations for the evolution of a Δ_{l_α} asymmetry may now be derived in exactly the same way as eq. (3.1) for a Δ_{l_1} asymmetry. Following exactly the same steps only for $l_1\mapsto l_\alpha$ the final result is

$$\begin{aligned}\frac{dN_{N_i}}{dz} &= D_i\left(N_{N_i}-N^{eq}_{N_i}\right), \\ \frac{dN_{\Delta_{l_\alpha}}}{dz} &= -\varepsilon_{i\alpha}D_i\left(N_{N_i}-N^{eq}_{N_i}\right)-p^0_{i\alpha}W_i\left(N_{\Delta_{l_\alpha}}+N_{\Delta_\phi}\right)\end{aligned} \tag{3.45}$$

We would like to recast the above equation in terms of a $\Delta_\alpha\equiv\Delta_{B/3-L_\alpha}$ asymmetry, since this is the quantity conserved by SM interactions and not Δ_{l_α}. In the

[8] I reproduce the derivation of the exact bound from [8] in section 6.4.3.

unflavoured case we simplified using $\Delta_{l_i} + \Delta_{\phi_i} = -\Delta_{B-L}$. For the flavoured case we need to define a matrix which converts between the Δ_α and $\Delta_{l_\alpha} + \Delta_\phi$ bases [9] as

$$N_{\Delta_{l_\alpha}} + N_{\Delta_\phi} \equiv -\sum_\beta C_{\alpha\beta} N_{\Delta_\beta} \tag{3.46}$$

which allows us to rewrite eq. (3.45) in the $\{\Delta_\alpha\}$ basis as

$$\begin{aligned} \frac{dN_{N_i}}{dz} &= D_i \left(N_{N_i} - N_{N_i}^{eq}\right) \\ \frac{dN_{\Delta_\alpha}}{dz} &= \varepsilon_{i\alpha} D_i \left(N_{N_i} - N_{N_i}^{eq}\right) - p_{i\alpha}^0 W_i \sum_\beta C_{\alpha\beta} N_{\Delta_\beta} \end{aligned} \tag{3.47}$$

Taking again that $C_{\alpha\beta} \approx \delta_{\alpha\beta}$ the above can be integrated to obtain

$$N_{\Delta_{B-L}}^f = \sum_\alpha \varepsilon_{i\alpha} \kappa^f(K_{i\alpha}) \tag{3.48}$$

where flavoured efficiency factors $k^f(K_{i\alpha})$ are defined in an analagous way to eq. (3.10) by simply replacing an integral over W_i by an integral over $W_{i\alpha} \equiv P_{i\alpha}^0 W_i$.

Recall from eq. (3.44) that $\varepsilon_{i\alpha} \propto \sqrt{p_{i\alpha}^0}$. Given a flavoured washout of $K_{i\alpha} = p_{i\alpha}^0 K_i$ it can also be shown that for $K_{1\alpha} \gtrsim 1$ the efficiency factor goes roughly like $\kappa^f(K_{1\alpha}) \propto K_{1\alpha}^{-1.1}$ [71] and so it follows that $N_{\Delta_\alpha} = \varepsilon_{1\alpha}\kappa^f(K_{1\alpha}) \propto \frac{1}{\sqrt{p_{1\alpha}^0}}$, approximately - the flavoured efficiency is enhanced by a factor of $p_{i\alpha}$ (for $K_{1\alpha} \gtrsim 1$) whilst the flavoured CP asymmetry is only suppressed by a factor of $\sqrt{p_{i\alpha}^0}$ versus the unflavoured asymmetry. It follows that when $K_1 \gg 1$ a far larger final asymmetry can be produced versus the unflavoured case, by "storing" $B-L$ asymmetry in a flavour α that is "optimally" washed out as $K_{1\alpha} \sim 1$. In this way the final flavoured $B-L$ asymmetry can receive an enhancement by a factor of $\approx \frac{1}{\sqrt{p_{i\alpha}^0}} \gg 1$ versus the unflavoured case.

I now give a concrete example where the final flavoured $B-L$ asymmetry is far larger than the final unflavoured $B-L$ asymmetry, showing that flavour effects may give order-of-magnitude-wise enhancements to the final asymmetry. Consider

[9] What has been called the "A-matrix" in the literature [75] is not this matrix, but refers only to the lepton doublets, vis $N_{\Delta_{l_\alpha}} \equiv \sum_\beta A_{\alpha\beta} N_{\Delta_\beta}$. It is not really correct to treat this as the leptogenesis flavour coupling matrix, since the rate of Δ_α washout goes like $\Delta_{l_\alpha} + \Delta_\phi$ and not solely Δ_{l_α}.

the asymmetry produced by N_1 decays ($i = 1$) into a two-flavour basis $\{\alpha\} = \tau_1^\perp, \tau$, which obtains in cases where the τ flavour alone has been "measured" whilst the other flavours remain in a partially coherent state $|\tau_1^\perp\rangle \equiv \langle e|l_1\rangle\,|e\rangle + \langle \mu|l_1\rangle\,|\mu\rangle$. To simplify matters further we will also ignore coupling between distinct flavours $\alpha \neq \beta$ by assuming $C_{\alpha\beta} = \delta_{\alpha\beta}$ (this assumption is relaxed for the next sections). The set of Boltzmann equations for $\Delta_{\tau_1^\perp}$ and Δ_τ then simplify down to

$$\begin{aligned} \frac{dN_{\Delta_{\tau_1^\perp}}}{dz} &= \varepsilon_{1\alpha}\, D_1 \left(N_{N_1} - N_{N_1}^{eq}\right) - p^0_{1\tau_1^\perp}\, W_1\, N_{\Delta_{\tau_1^\perp}} \\ \frac{dN_{\Delta_\tau}}{dz} &= \varepsilon_{1\tau}\, D_1 \left(N_{N_1} - N_{N_1}^{eq}\right) - p^0_{1\alpha}\, W_1\, N_{\Delta_\tau} \end{aligned} \tag{3.49}$$

Integrating the above set of equations and making use of eq. (3.30) obtains a final asymmetry $N^{\rm f}_{\Delta_{B-L}} = N^{\rm f}_{\Delta_{\tau_1^\perp}} + N^{\rm f}_{\Delta_\tau}$ of

$$N^{\rm f}_{B-L} \simeq 2\,\varepsilon_1\,\kappa(K_1) + \frac{\Delta p_{1\tau}}{2}\,\left[\kappa(K_{1\tau_1^\perp}) - \kappa(K_{1\tau})\right] \tag{3.50}$$

where we have also used that $\Delta p_{1\tau_1^\perp} + \Delta p_{1\tau} = 0$ to simplify the result. The above can be can be compared to the unflavoured case $N^{\rm f}_{B-L} = \varepsilon_1\,\kappa(K_1)$.

The above equation shows the importance of flavour effects when there is an asymmetry between flavoured washouts - when $\kappa(K_{\tau_1^\perp}) \neq \kappa(K_{1\tau})$. In such cases the second term may introduce order–of–magnitude–wise corrections to the final asymmetry when compared to the un-flavoured case. For example, in the case where $K_1 \gg 1$ but $K_{1\tau} \sim 1$ an un-flavoured asymmetry would be strongly washed out, whereas a flavoured Δ_τ asymmetry is only weakly washed out. Without the second term in eq. (3.50) (without $\Delta p_{1\tau} \neq 0$) there could be only $\mathcal{O}(1)$ corrections due to flavour effects. Non-zero $\Delta p_{1\tau} \equiv |\langle l_\tau|l_1\rangle|^2 - |\langle \bar{l}_\tau|\bar{l}_1\rangle|^2$ implies **differences in flavour composition** between lepton and anti–lepton states. This effect is the key to the potentially large impact of flavour effects in leptogenesis. It also has a further relevant impact (so-called "phantom leptogenesis") which is explored in section 3.5.

Strictly speaking, it remains to be shown that $K_{1\alpha} \ll K_1$ and $\Delta p_{1\alpha} \lesssim \bar{\varepsilon}_i$ can be generically realised within the seesaw model's sub-space space of experimentally allowed parameters. The authors of [76] have shown that this is true, by fixing the

low-energy seesaw model parameters to within their experimentally allowed values (cf. table 1.3) and scanning over remaining "free" parameters. In fig. 3.2 below each point denotes a region in the (K_1, M_1) plane found by the scan which is able to reproduce both the experimentally observed baryon asymmetry and neutrino oscillation data. Green points denote a "vanilla" calculation of $N^f_{\Delta_{B-L}}$ and red points the (correct) flavoured calculation. One sees that correctly including flavour effects allows successful leptogenesis for lower values of M_1. The bound on M_1 can be lowered by 1–2 orders of magnitude, demonstrating the strong impact of flavour effects. Notice however that the impact of flavour effects is lessened for larger values of the ratio $\frac{M_1}{M_k}$ where $k = 2, 3$. One can see from eq. (3.42) that $\Delta p_{1\alpha}$ is sensitive to the ratio $\left(\frac{M_k}{M_1}\right)$ for $k = 2, 3$ and from fig. 3.2 the sensitivity appears to increase when $M_1 \ll M_2,\, M_3$. We will see an explicit example of this behaviour in chapter 6.

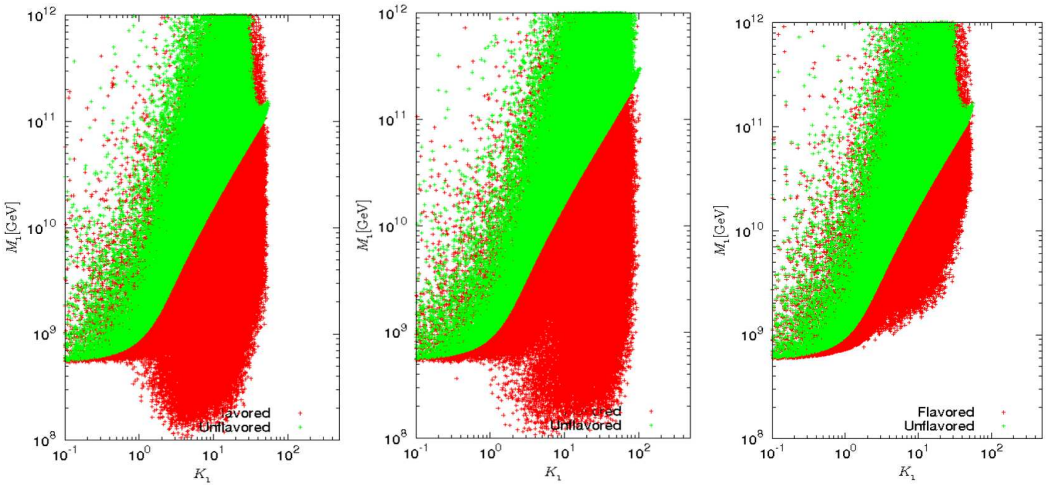

Figure 3.2: Three plots from [76] showing maximal impact of flavour effects. Red crosses (green crosses) denote successful flavoured (unflavoured) leptogenesis in the $(K_1,\, M_1)$ plane, for fixed PMNS matrix paramaters and scanning over free parameters. Left and center panels: normal and inverted hierarchy, respectively, and $M_2 = M_3 = 3M_1$. Right panel: normal hierarchy and $M_2 = M_3 = 30M_1$. All panels for $N^{in}_{N_1} = 1$ (thermal initial abundance) and $m_1 = 0$ (a massless lightest neutrino).

3.3 Spectator Processes and Flavour Coupling

Having defined a C–matrix in eq. (3.46) we now wish to relax the assumption $C_{\alpha\beta} = \delta_{\alpha\beta}$ and consider the effects of coupled flavour dynamics. This will require that we calculate all coefficients of $C_{\alpha\beta}$ explicitly - I now show how to do this (further details are given in an appendix).

What are these coefficients, physically? Following the decay $N_i \to l_\alpha + \phi$ an asymmetry initially "stored" within lepton and Higgs doublets does not remain in these doublets. SM interactions collectively redistribute the initial lepton and Higgs asymmetry amongst all particles in chemical equilibrium with the thermal bath. For example, the sphaleron interactions discussed in section 2.3.2 redistribute some fraction of initial lepton asymmetry into quark asymmetry (cf. fig 2.5). The coefficients $C_{\alpha\beta}$ of eq. (3.46) say what fraction of an initial $\Delta_{l_\alpha} + \Delta_\phi$ asymmetry is put into each of the Δ_α asymmetries.

To find the coefficients $C_{\alpha\beta}$ we solve the set of constraints on the number densities n_s of the set of all particle species $\{s\}$ in equilibrium with the thermal bath. Each equilibrium n_s is given as the integral over all modes of the Fermi-Dirac (+1 for fermions, f) or Bose-Einstein (−1 for bosons, b) distributions

$$\begin{aligned} n_s^{eq} &= \frac{g_s}{(2\pi)^3}\int d^3k f_s^{eq}(k) \\ f_s^{eq}(k) &= \frac{1}{exp(\frac{E_s-\mu_s}{T}) \pm 1} \end{aligned} \tag{3.51}$$

An expansion in the chemical potential can be performed for relativistic particles $m_s \ll T$ resulting in number density asymmetries of

$$\begin{aligned} n_f - \bar{n}_f &= \frac{T^3}{6} g_f \mu_f \\ n_b - \bar{n}_b &= \frac{T^3}{3} g_b \mu_b \end{aligned} \tag{3.52}$$

The above number densities $n_s - \bar{n}_s \equiv n_{\Delta_s}$ can be made into **co–moving** number density asymmetries $N_{\Delta_s} = a^3\, n_{\Delta_s}$. In a radiation dominated universe $a \propto \frac{1}{T}$ and so $a = \frac{k}{T}$ for a constant of proportionality k with dimensions of mass. Substituting $n_{\Delta_s} = kT^3 N_{\Delta_s}$ into eq. (3.52), one obtains

$$\begin{aligned} N_{\Delta_s} &= k^3 \frac{1}{6} g_s \mu_s \qquad \text{(fermions)} \\ N_{\Delta_s} &= k^3 \frac{1}{3} g_s \mu_s \qquad \text{(bosons)} \end{aligned} \tag{3.53}$$

The value of k is unimportant, since to determine the $C_{\alpha\beta}$ we need only know the

ratios between the various co–moving number density asymmetries. For a particle species s, the interpretation of its chemical potential μ_s is as follows: μ_s is the change in the plasma's internal energy U for a given change in the number density of that particle species n_s, fixing entropy (s), volume (V) and the asymmetries of the remaining particle species $\{s^{'} \neq s\}$

$$\mu_s \equiv \left(\frac{\partial U}{\partial n_s}\right)_{s,V,n_{s^{'}\neq s}} \tag{3.54}$$

Strictly speaking, chemical potentials cannot be defined in an expanding universe, since the volume and entropy of a patch of universe can't be fixed. Provided the Hubble rate is much smaller than particle species s's rate of interaction this point is not important - the particles then don't experience an expanding universe on timescales relevant to their dynamics. However, this does imply that we cannot sensibly define a chemical potential for the RHNs whose decay rates are of the order of the Hubble rate.

Any and all particle interactions must conserve the total energy of the plasma, U - assuming this to be a homogeneous perfect fluid, which is an excellent approximation at the relevant cosmological scales. Each such interaction translates into a constraint on chemical potentials of the following form:

$$\delta U = \sum_s \mu_s \delta n_s = 0 \tag{3.55}$$

For example, take the leptonic Yukawa interaction , which could redistribute an initial pure l_α asymmetry into a mixture of l_α, α_R and Higgs asymmetries via $l_\alpha \leftrightarrow \tilde{\phi} + \alpha_R$. Given that $\delta n_{\tilde{\phi}} = \delta n_{\alpha_R} = -\delta n_{l_\alpha}$ one obtains the constraint

$$\mu_{\tilde{\phi}} + \mu_{\alpha_R} - \mu_{l_\alpha} = 0\,. \tag{3.56}$$

Similar constraints obtain for the remaining SM particle interactions. The full set of SM constraints are given in eqs. (3.57–3.64) below, where $i = 1, 2, 3$, $\alpha = e, \mu, \tau$, $\beta = u, c, t$ and $\gamma = d, s, b$. The first three constraints eqs. (3.57–3.59) are for the Yukawa couplings. The next two constraints eqs. (3.60, 3.61) are for

electroweak sphalerons [10] and eq. 3.62 is for the QCD sphalerons. The penultimate constraint eq. (3.63) ensures the overall hypercharge neutrality of the plasma [11], by fixing $\sum_s n_{\Delta_s} Y_s = 0$. The final constraint eq. (3.64) fixes $N_{\Delta_\phi} = -N_{\Delta_{\tilde{\phi}}}$ in the SM, which makes sense given that $\tilde{\phi}$ is the conjugate of ϕ in table 1.2. If this final constraint is dropped then eqs. (3.57–3.64) also apply to the super–fields of supersymmetric leptogenesis within the co-called super–equilibration regime [77].

$$0 = \mu_{l_i} + \mu_{\phi_d} - \mu_{\alpha_R} \tag{3.57}$$

$$0 = \mu_{q_i} + \mu_{\phi_u} - \mu_{\beta_R} \tag{3.58}$$

$$0 = \mu_{q_i} + \mu_{\phi_d} - \mu_{\gamma_R} \tag{3.59}$$

$$0 = \sum_i \mu_{l_i} + 3\sum_i \mu_{q_i} \tag{3.60}$$

$$2\mu_{Q_3} + \mu_{t_R} + \mu_{b_R} = 2\mu_{Q_2} + \mu_{c_R} + \mu_{s_R} = 2\mu_{Q_1} + \mu_{u_R} + \mu_{d_R} \tag{3.61}$$

$$0 = 2\sum_i \mu_{q_i} - \sum_\beta \mu_{\beta_R} - \sum_\gamma \mu_{\gamma_R} \tag{3.62}$$

$$0 = \sum_i \mu_{q_i} + 2\sum_\beta \mu_{\beta_R} - \sum_\gamma \mu_{\gamma_R} - \sum_i \mu_{l_i} - \sum_\alpha \mu_{\alpha_R} + \mu_{\phi_u} + \mu_{\phi_d} \tag{3.63}$$

$$0 = \mu_{\phi_u} + \mu_{\phi_d} \tag{3.64}$$

Gauge boson interactions are implicitly taken into account by the above constraints – the effect of gauge bosons is to equilibrate the different colour and isospin components of each SM particle. For example, the interaction $q_r + g_{\bar{r}b} \leftrightarrow q_b$ (a red quark becoming a blue quark via gluon exchange) will imply the constraint $\mu_{q_r} = \mu_{q_b}$ (where I have used that $\mu_g = 0$, given that gauge bosons are in the adjoint representation). As such, it is not necessary to label colour or isospin components separately, since the same constraint applies whatever the isospin or colour.

As one goes to higher temperatures T, some constraints become redundant as the particles they "constrain" are no longer produced within a Hubble time. When this happens a constraint can be replaced by an initial condition - for example $N_{\Delta_B} =$

[10] Because the electroweak sphalerons populate all three generations equally (cf. fig. 2.5) the total baryon asymmetry in each generation is equal and so $\Delta_{B_i} = \frac{B}{3}$ is an initial condition – which is equivalent to eq. (3.63).

[11] The universe must be electrically neutral to an extremely high degree of precision - just a tiny net charge would upset galaxy formation given how much stronger the electromagnetic force is compared to gravity.

0 before electroweak sphalerons come into equilibrium. As a rough "rule of thumb" constraints apply to all processes with rates at least equal to the Hubble rate (which falls as the universe expands and cools). Hence as the universe expands and cools, more and more SM interactions come into chemical equilibrium and develop non-zero abundances N_{Δ_s}. Equilibrium temperatures for various processes were given in [25] and I reproduce their results in the table 3.1.

Table 3.1: Processes in equilibrium at various temperatures

T [GeV]	processes in equilibrium
$\gg 10^{13}$GeV	top Yukawa
$\sim 10^{13}$GeV	+ QCD sphalerons
$10^{12,13}$	+ bottom, tau Yukawas
$10^{11,12}$	+ EW sphalerons, charm Yukawa
$10^{8,9,10}$	+ strange, mu Yukawas
$\ll 10^{8} GeV$	+ all remaining Yukawas

Solving the full set of relevant constraint equations allows one to express all the μ_s (and hence all the N_{Δ_s}) in terms of the basis $\{N_{\Delta_\alpha}\}$, which serves to define the coefficients $C_{\alpha\beta}$. Further details on how to do this, at various temperatures, are provided in an appendix.

Here are the $C_{\alpha\beta}$ for three relevant temperature regimes:

$$C^{(1)} = \begin{pmatrix} 4/3 & 1/3 & 1/3 \\ 1/3 & 4/3 & 1/3 \\ 1/3 & 1/3 & 4/3 \end{pmatrix} \mapsto 2 \tag{3.65}$$

$$C^{(2)} = \begin{pmatrix} 585/589 & -4/589 & 52/589 \\ -4/589 & 585/589 & 52/589 \\ 52/589 & 52/589 & 502/589 \end{pmatrix} \mapsto \begin{pmatrix} 581/589 & 104/589 \\ 52/589 & 502/589 \end{pmatrix} \tag{3.66}$$

$$C^{(3)} = \begin{pmatrix} 339/358 & 6/179 & 6/179 \\ 6/179 & 422/537 & 64/537 \\ 6/179 & 64/537 & 422/537 \end{pmatrix} \tag{3.67}$$

where the arrows show a map from the $\{e, \mu, \tau\}$ basis in which the constaint equa-

tions are solved, to the flavour basis relevant to the given temperature regime. The mappings $3 \times 3 \mapsto 1 \times 1$ and $3 \times 3 \mapsto 2 \times 2$ are obtained by averaging across the rows and summing down the columns of those flavours that cannot be distinguished. The labels (1), (2), (3) correspond to three different flavour bases:

1. An un-flavoured or "vanilla" regime for $T \gg 10^{12}$GeV, in which no $|l_\alpha\rangle$ states are "measured" because no leptonic Yukawas are in equilibrium.

2. A two-flavoured regime for $10^9\text{GeV} \ll T \ll 10^{12}\text{GeV}$ in which $|l_\tau\rangle$ states are "measured" because the tau Yukawa is in equilibrium, but not $|l_e\rangle$ or $|l_\mu\rangle$ states.

3. A three or "fully flavoured" regime for $T \ll 10^9$GeV in which $|l_\tau\rangle$ and $|l_\mu\rangle$ states - and hence by default $|l_e\rangle$ also - are "measured" because both tauon and muon Yukawas are in equilibrium.

Another important quantity obtained by solving eqs.(3.57-3.64) is the ratio of $B-L$ to B asymmetry, giving the fraction of initial Lepton asymmetry redistributed into quark asymmetry by Sphaleron processes as

$$a_{sph} \equiv \frac{N_{\Delta_B}}{N_{\Delta_{B-L}}} = \frac{\frac{1}{3}\sum_q g_q\,\mu_q}{\frac{1}{3}\sum_q g_q\,\mu_q \;-\; \sum_l g_l\,\mu_l} = \frac{28}{79} \tag{3.68}$$

Sometimes one sees instead $\frac{22}{31}$ in the literature. The answer depends upon whether one assumes the sphalerons drop out of equilibrium before or after the electroweak phase transition, as is explained in [78]. The difference, of order a few percent, is not important. Hence I have assumed sphalerons drop out of equilibrium after EWPT, as this is the more straightforward of the two cases to calculate.

A common approximation made in the literature is to set $C_{\alpha\beta} = \delta_{\alpha\beta}$, which looks initially plausible given that the off-diagonal elements are order 1/5. This procedure - that of "throwing away" the flavour coupling dynamics - indeed gives a correct order of magnitude estimate of the final Baryon asymmetry $N^f_{\Delta_B}$ over much of the leptogenesis parameter space. In [79] the authors consider N_1 dominated leptogenesis and find correction no larger than $\sim \pm 40\%$ due to flavour coupling. However, as I will show in chapter 4, regions of parameter space do exist for which this procedure can underestimate $N^f_{\Delta_B}$ by orders of magnitude.

In a general j-flavour regime an N_i-dominated leptogenesis is described by a system of $j+1$ coupled Boltzmann equations

$$\begin{aligned}\frac{dN_{N_i}}{dz} &= D_i\left(N_{N_i}-N_{N_i}^{eq}\right)\\ \frac{dN_{\Delta_\alpha}}{dz} &= \varepsilon_{i\alpha}\,D_i\,\left(N_{N_i}-N_{N_i}^{eq}\right)-P_{i\alpha}^{0}\,W_i\sum_{\beta}C_{\alpha\beta}^{(j)}\,N_{\Delta_\beta}\end{aligned}\tag{3.69}$$

For the $j=1$ or "vanilla" case one simply re-obtains eqs. (3.8) from section 3.1. For the $j=2$ or two-flavour case one reobtains the $\alpha=\{\tau,\,\tau^{\perp_1}\}$ 2-flavour example considered in section 3.2. For the $j=3$ or three-flavour case $\alpha=\{e,\mu,\tau\}$ given that both tauon and muon (and hence, by default, electron) flavours are "measured". In chapter 4 I will develop an example of the above coupled equations in some detail and we will see that order–of–magnitude–wise enhancements to $N_{\Delta_{B-L}}^{f}$ are possible. But first we consider leptogenesis with more that one RHN and how this differs from the N_1–dominated scenarios considered thus far.

3.4 The Importance of N_2 Leptogenesis

This section takes its name from the paper [80] where the impact of the **projection effect** upon N_2 leptogenesis was considered. Thus far we have been considering, for simplicity, that $B-L$ asymmetry has been dominantly produced by the lightest RH neutrino N_1. It will turn out that adding the decays of heavier RHNs introduces many novel flavour effects to leptogenesis scenarios which are absent from the N_1-dominated case. The first new effect we shall consider are the so-called **heavy flavour effects**. What are these? Consider hierarchical masses $M_1 \ll M_2 \ll M_3$ for three RHNs N_1, N_2 and N_3. These RHNs will decay into coherent states $|l_i\rangle$ where in general $|l_i\rangle \neq |l_k\rangle$. However N_i can only washout an asymmetry along the $|l_i\rangle$ direction in $\{e,\,\mu,\,\tau\}$ flavour space, so in general part of the asymmetry produced by N_k along the $|l_k\rangle \equiv \mathcal{C}_{ki}\,|l_i\rangle + \mathcal{C}_{ki_\perp}\,|l_i^{\perp}\rangle$ direction will be left unwashed by N_i (i.e. the part that is stored along the $|l_i^{\perp}\rangle$ direction, given $\langle l_i|l_i^{\perp}\rangle = 0$ by definition). This **heavy flavoured scenario** is shown in fig. 3.3.

Heavy flavour effects have relevance concerning the predictiveness of leptogene-

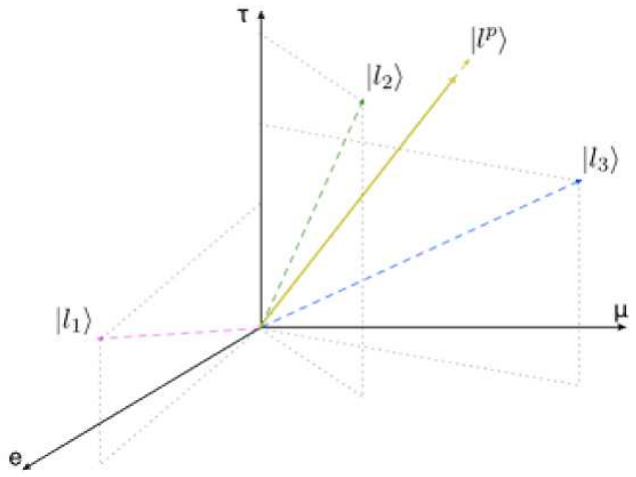

Figure 3.3: The heavy flavoured scenario. Projections of $|l_1\rangle$, $|l_2\rangle$ and $|l_3\rangle$ are shown in $\{e, \mu, \tau\}$ flavour space. Also shown is a possible pre-existing lepton asymmetry aligned along $|l^P\rangle$. Image from [81]

sis. In most leptogenesis scenarios there will be a non-zero component of pre-existing asymmetry that can survive washout by all three RHNs due to the survival of an orthogonal component at each stage of washout. However the authors of [81] have identified a specific scenario - the tauon N_2-dominated scenario - where it is still possible to fully washout a preexisting asymmetry. They refer to this condition as **strong thermal leptogenesis**. For now I am not so much concerned with the dependence on initial conditions as describing heavy flavour effects in general. In the paper these effects were studied exhaustively and two relevant scenarios identified:

1. A heavy flavoured scenario, where $M_i \gg 10^{12} GeV$ for $i = 1, 2, 3$. Light flavour effects play no role.

2. Light flavoured scenarios, where $M_i \ll 10^{12} GeV$ for at least one RHN. Various light flavoured effects play a role depending upon which leptonic Yukawa couplings are in equilibrium.

The ten possible mass patterns for 3RHNs are illustrated in fig. 3.4, where the top left picture shows the heavy flavour scenario and the other nine panels various light flavoured scenarios in which the $|l_i\rangle$ have been partially or fully been projected into their $|l_e\rangle$, $|l_\mu\rangle$ and $|l_\tau\rangle$ components by leptonic Yukawa interactions - the light flavour effects discussed in section 3.2. The grey bands at $T \sim 10^{12}$GeV and $T \sim 10^9$GeV in fig. 3.4 represent transitions from the $1 \mapsto 2$ light flavoured regime and the

$2 \mapsto 3$ light flavoured regime, respectively. Where RHN masses fall between these transition regimes the leptogenesis can be well described by the classical Boltzmann equations developed in section 2.2 [12]. However, where RHN masses fall within the transition regimes a more general treatment, to be developed in chapter 5, is required. I shall now consider the heavy flavour scenario in detail, to illustrate the impact of

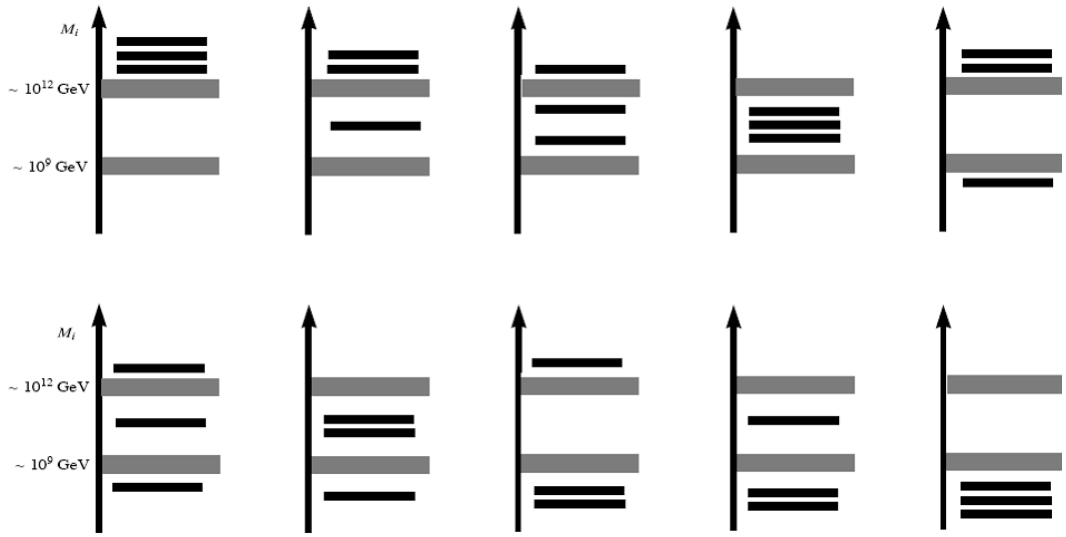

Figure 3.4: The ten different three RH neutrino mass patterns requiring 10 different sets of Boltzmann equations for the calculation of the asymmetry. Grey bands denote transitions between distinct light flavour regimes. Image from [7].

projection effects and heavy flavour effects.

3.5 Phantom Leptogenesis in Heavy Flavoured Scenario

"Every act of creation is first an act of destruction" – Pablo Picasso

If there is more than one RHN involved in the generation of $N^f_{\Delta_{B-L}} \neq 0$ a new flavour effect - **phantom leptogenesis** [6], [7] - becomes possible. Phantom leptogenesis involves the creation of some final asymmetry by destroying the perfect cancellation between a pair of initially equal and opposite asymmetries (called "phantom terms"). To illustrate phantom leptogenesis, we consider a simplified heavy flavoured scenario where just two RHNs N_1 and N_2 both decay in an "unflavoured"

[12] A different set of Boltzmann equations obtains for each of the spectra shown in fig. 3.4. I develop some examples later - in chapter 4 the lower left panel for $M_3 \gg 10^{14}$GeV (N_2 dominated scenario) will be studied in detail and in chapter 6 the upper centre panel for $M_3 \gg 10^{14}$GeV (2RHN model) will be studied in detail.

regime $T \gg 10^{12} GeV$. This leptogenesis happens in two stages:

1. The N_2 decay at temperature $T \sim M_2$. They finish decaying at a temperature $T_{N_2} > M_1$, having produced an asymmetry $N^{N_2}_{\Delta_{l_2}} = \varepsilon_2 \kappa(K_2)$.

2. Next, the N_1 decay at a temperature $T \sim M_1$ and partially washout the $N^{T_2}_{\Delta_{l_2}}$ asymmetry. They also produce their own asymmetry $N^{N_1}_{\Delta_{l_1}} = \varepsilon_1 \kappa(K_1)$.

To asses the effect of N_1 washout on the N_2 generated asymmetry $N^{N_2}_{\Delta_{l_2}}$ we begin by writing the $|l_2\rangle$ states in the $\{|l_1\rangle, |l_1^\perp\rangle\}$ basis

$$\begin{aligned} |l_2\rangle &= \langle l_1\,|l_2\rangle |l_1\rangle + \langle l_1^\perp\,|l_2\rangle |l_1^\perp\rangle \\ |\bar{l}_2\rangle &= \langle \bar{l}_1\,|\bar{l}_2\rangle |\bar{l}_1\rangle + \langle \bar{l}_1^\perp\,|\bar{l}_2\rangle |\bar{l}_\tau^\perp\rangle \end{aligned} \tag{3.70}$$

The N_{l_2} and $N_{\bar{l}_2}$ number densities can be projected into their $N_{\Delta_{l_1}}$ and $N_{\Delta_{l_1^\perp}}$ components as

$$\begin{aligned} N^{N_2}_{l_1} &= p_{12}\, N^{N_2}_{l_2} \\ N^{N_2}_{\bar{l}_1} &= \bar{p}_{12}\, N^{N_2}_{\bar{l}_2} \\ N^{N_2}_{l_1^\perp} &= (1 - p_{12})\, N^{N_2}_{l_2} \\ N^{N_2}_{\bar{l}_1^\perp} &= (1 - \bar{p}_{12})\, N^{N_2}_{\bar{l}_2} \end{aligned} \tag{3.71}$$

where $p_{12} \equiv |\langle l_1 | l_2 \rangle|^2$ and $\bar{p}_{12} \equiv |\langle \bar{l}_1 | \bar{l}_2 \rangle|^2$

The next step is to write these total lepton numbers as a sum of their symmetric and anti-symmetric parts as

$$\begin{aligned} N^{N_2}_{l_2} &\equiv \frac{1}{2}\left(N^{N_2}_{l_2} + N^{N_2}_{\bar{l}_2}\right) + N^{N_2}_{\Delta_{l_2}} = \frac{1}{2} N^{in}_{N_2} + \frac{1}{2} N^{N_2}_{\Delta_{l_2}} \\ N^{N_2}_{\bar{l}_2} &\equiv \frac{1}{2}\left(N^{T_2}_{l_2} + N^{N_2}_{\bar{l}_2}\right) - N^{N_2}_{\Delta_{l_2}} = \frac{1}{2} N^{in}_{N_2} - \frac{1}{2} N^{N_2}_{\Delta_{l_2}} \end{aligned} \tag{3.72}$$

where the final equalities follow from the fact that all the N_2 have decayed into either l_2 or $\bar{l}_2$ and so the total number of these is just $N^{in}_{N_2}$, the initial abundance of N_2s. We can also write the projectors p_{12} and $\bar{p}_{12}$ in terms of their symmetric and

anti-symmetric parts as

$$\begin{aligned} p_{12} &\equiv p^0_{12} + \frac{1}{2}\Delta p_{12} \\ \bar{p}_{12} &\equiv p^0_{12} - \frac{1}{2}\Delta p_{12} \end{aligned} \tag{3.73}$$

where $p^0_{12} \equiv \frac{1}{2}\left(p_{12} + \bar{p}_{12}\right)$ and $\Delta p_{12} \equiv p_{12} - \bar{p}_{12}$.

The final step is substitute eqs. (3.72, 3.73) into eqs. (3.71) and take differences between the lepton and anti-lepton numbers. This obtains equations for the projection of $N^{N_2}_{\Delta_{l_2}}$ into its $N^{N_2}_{\Delta_{l_1}}$ and $N^{N_2}_{\Delta_{l_1^\perp}}$ components as

$$\begin{aligned} N^{N_2}_{\Delta_{l_1}} &= p^0_{12} N^{N_2}_{\Delta_{l_2}} + \Delta p_{12} N^{in}_{N_2} \\ N^{N_2}_{\Delta_{l_1^\perp}} &= (1 - p^0_{12}) N^{N_2}_{\Delta_{l_2}} - \Delta p_{12} N^{in}_{N_2} \end{aligned} \tag{3.74}$$

The final two terms in the above pair of equations are known as **phantom terms** and give a contribution to $N^{N_2}_{\Delta_{B-L}} = N^{N_2}_{\Delta_{l_1}} + N^{N_2}_{\Delta_{l_1^\perp}}$ summing to zero. However, this is no longer the case after N_1 washout, whereupon the asymmetries become

$$\begin{aligned} N^f_{\Delta_{l_1}} &= \varepsilon_1 \kappa(K_1) + \left(p^0_{12} \varepsilon_2\, \kappa(K_2) + \Delta p_{12} N^{in}_{N_2}\right) e^{-\frac{3\pi}{8} K_1} \\ N^f_{\Delta_{l_1^\perp}} &= (1 - p^0_{12}) \varepsilon_2\, \kappa(K_2) - \Delta p_{12} N^{in}_{N_2} \end{aligned} \tag{3.75}$$

where I substituted $N^{N_2}_{\Delta_{l_2}} = \varepsilon_2\, \kappa(K_2)$ and added the additional asymmetry $\varepsilon_1\, \kappa(K_2)$ produced by N_1 decays. The $N^{N_2}_{\Delta_{l_1}}$ component of $N^{N_2}_{\Delta_{l_2}}$ is very strongly washed out for $K_1 \gg 1$, whereas the $N^{N_2}_{\Delta_{l_1^\perp}}$ component is not washed out at all by the N_1 [13]. Taking the sum of final flavoured asymmetries, the final Δ_{B-L} asymmetry becomes

$$N_{\Delta_{B-L}} = \varepsilon_1 \kappa(K_1) + \varepsilon_2 \kappa(K_2) - \Delta p_{12} N^{in}_{N_2} \left(1 - e^{-\frac{3\pi}{8} K_1}\right) \tag{3.76}$$

Notice the similarity of the above to eq. (3.50). In fact, phantom terms are closely analogous to the more well-known light flavour effects discussed in section 3.2. Notice again that phantom leptogenesis requires both $\Delta p_{2\tau} \neq 0$ - a difference in flavour

[13] We shall see in chapter 5 that there is in fact some washout of the component of Δ_{B-L} along the $|l_1^\perp\rangle$ direction in flavour space due to gauge boson interactions, and that these washout the phantom terms by exactly **half as much** as N_1 inverse decays washout the component of Δ_{B-L} along the $|l_1\rangle$ direction.

composition between lepton and anti-leptons quantum states - and $K_{1\tau} \neq K_{1\tau_1^{\perp}}$ - an asymmetry in washouts.

The scenario is illustrated pictorially in fig. 3.5. In the figure, the length of the coloured "bars" denote the number density of a given particle species and show how the initially equal and opposite asymmetries produced by N_2 decays and stored in the flavours gamma and tau are revealed by a lighter neutrino N_1, which first "measures" this difference in flavour composition, then washes it out asymmetrically with respect to each flavour. The vertical dashed line shows how the "phantom" effect will vanish in cases where there is no difference in flavour composition between leptons and anti–leptons.

From this specific example of the 2RHN heavy flavoured scenario we can make several more general comments about "phantom leptogenesis" [14]:

1. Phantom leptogenesis requires that an asymmetry produced in a given basis by a given RHN gets asymmetrically washed out in a distinct basis by a lighter RHN.

2. Before asymmetric washout in this distinct basis, the phantom terms cancel from the final $B - L$ asymmetry (given that the differences in flavour composition summed over all flavours give zero), but after this asymmetric washout they do not.

3. Phantom leptogenesis requires a non–zero difference in flavour composition between leptons and anti-leptons (as measured in the flavour basis in which the produced asymmetry is partially washed out).

4. Phantom leptogenesis is not viable within N_1-dominated leptogenesis - here the $B - L$ asymmetry is produced and washed out in the same basis, at a common temperature $T \sim M_1$.

5. Lastly, phantom leptogenesis cannot apply to any asymmetry generated below a temperature $T \sim 10^9$GeV, given that all states $|l_i\rangle$ have been projected into

[14] The name "phantom" was meant to suggest the manner in which an asymmetry is at first hidden and later "pops out" due to the N_1 interactions which measure it. With hindsight we might have picked a more descriptive name – "phantom" is not meant to imply that this flavour effect is not physically real! It is just as "real" as the standard "light flavoured" effects discussed in section 3.1.

the same $\{e, \mu, \tau\}$ basis, so condition #1 above is unrealisable.

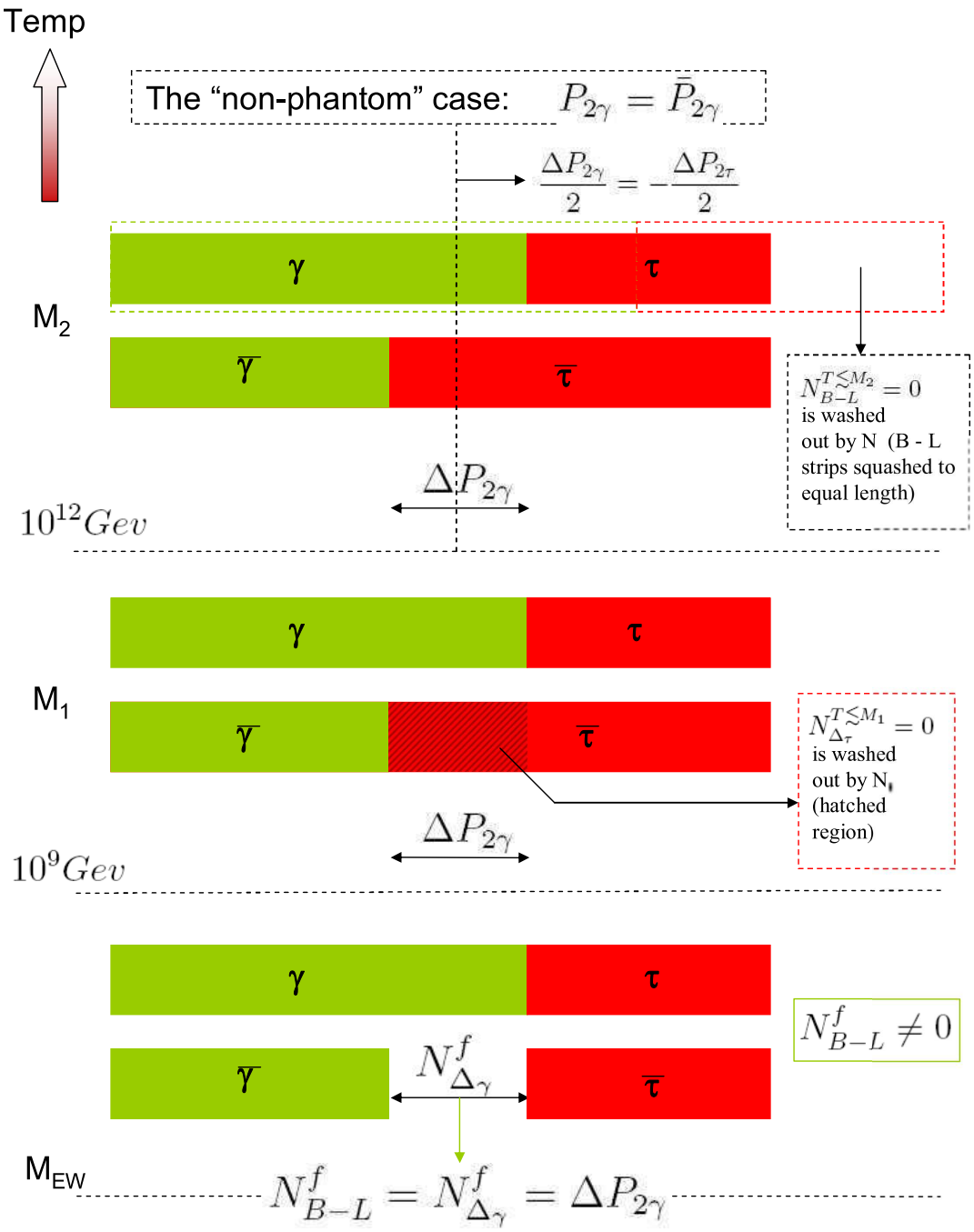

Figure 3.5: Phantom leptogenesis in the heavy flavoured scenario.

Chapter 4

A Fuller Flavour Treatment of N_2 Dominated Leptogenesis

4.1 The N_2 Dominated Scenario

The N_2-dominated scenario will serve as a good example of all the various flavour effects discussed in the previous chapter. This chapter is based largely upon the paper [6], in which the N_2–dominated scenario was studied extensively. We begin by assuming the following mass spectrum for the heavy neutrinos:

$$M_1 \ll 10^9 \text{GeV} \ll M_2 \ll 10^{12} \text{GeV} \ll M_3 \tag{4.1}$$

i.e. the top center panel of fig. 3.4. Having assumed this spectrum there are two independent regimes relevant to the generation of a final $B - L$ asymmetry. These are:

1. An N_2 production stage: production of $\Delta_\alpha \neq 0$ in a $j = 2$-flavoured regime, for $\alpha = \gamma, \tau$ (where $\gamma \equiv \tau_2^\perp$ denotes the component of $|l_2\rangle$ projected along the direction orthogonal to $|\tau\rangle$ in flavour space) and its partial washout by $N_2 \leftrightarrow l_\alpha + \phi$ processes.

2. An N_1 washout stage: partial washout of the $\Delta_\alpha \neq 0$ produced by N_2 decay, by $N_1 \leftrightarrow l_\alpha + \phi$ processes in a $j = 3$-flavoured regime with $\alpha = e, \mu, \tau$.

The N_2 production stage at $T \sim M_2$ is described by the set of 3 coupled equations

$$\begin{aligned}
\frac{dN_{N_2}}{dz} &= D_2 \left(N_{N_2} - N_{N_2}^{eq} \right) \\
\frac{dN_{\Delta_\gamma}}{dz} &= \varepsilon_{2\gamma} D_2 \left(N_{N_2} - N_{N_2}^{eq} \right) - P_{2\gamma}^0 W_2 \sum_{\beta=\gamma,\tau} C_{\gamma\beta}^{(2)} N_{\Delta_\beta} \\
\frac{dN_{\Delta_\tau}}{dz} &= \varepsilon_{2\tau} D_2 \left(N_{N_2} - N_{N_2}^{eq} \right) - P_{2\tau}^0 W_2 \sum_{\beta=\gamma,\tau} C_{\tau\beta}^{(2)} N_{\Delta_\beta}
\end{aligned} \tag{4.2}$$

where the quantities $\varepsilon_{i\alpha}$, D_i, W_i and $p_{i\alpha}^0$ were defined in sections 3.1, 3.2 and in section 3.3 we calculated $C^{(2)}$ as

$$C^{(2)} \equiv \begin{pmatrix} C_{\gamma\gamma}^{(2)} & C_{\gamma\tau}^{(2)} \\ C_{\tau\gamma}^{(2)} & C_{\tau\tau}^{(2)} \end{pmatrix} = \begin{pmatrix} 581/589 & 104/589 \\ 52/589 & 502/589 \end{pmatrix} \tag{4.3}$$

The N_1 washout stage at $T \sim M_1$ is described by a set of 4 coupled equations

$$\begin{aligned}
\frac{dN_{N_1}}{dz} &= D_1 \left(N_{N_1} - N_{N_1}^{eq} \right) \\
\frac{dN_{\Delta_e}}{dz} &= -P_{1e}^0 W_1 \sum_{\beta=e,\mu,\tau} C_{e\beta}^{(3)} N_{\Delta_\beta} \\
\frac{dN_{\Delta_\mu}}{dz} &= -P_{1\mu}^0 W_1 \sum_{\beta=e,\mu,\tau} C_{\mu\beta}^{(3)} N_{\Delta_\beta} \\
\frac{dN_{\Delta_\tau}}{dz} &= -P_{1\tau}^0 W_1 \sum_{\beta=e,\mu,\tau} C_{\tau\beta}^{(3)} N_{\Delta_\beta}
\end{aligned} \tag{4.4}$$

where the $\varepsilon_{1\alpha}$ term is neglected above, given that $M_1 << 10^9 GeV$ (cf. eq. (4.1)) and in section 3.3 we calculated $C^{(3)}$ as

$$C^{(3)} \equiv \begin{pmatrix} C_{ee}^{(3)} & C_{e\mu}^{(3)} & C_{e\tau}^{(3)} \\ C_{\mu e}^{(3)} & C_{\mu\mu}^{(3)} & C_{\mu\tau}^{(3)} \\ C_{\tau e}^{(3)} & C_{\tau\mu}^{(3)} & C_{\tau\tau}^{(3)} \end{pmatrix} = \begin{pmatrix} 339/358 & 6/179 & 6/179 \\ 6/179 & 422/537 & 64/537 \\ 6/179 & 64/537 & 422/537 \end{pmatrix} \tag{4.5}$$

4.2 The N_2 Production Stage

The first step is to calculate the asymmetry produced in $N_2 \leftrightarrow l_\alpha + \phi$ processes only. The strategy will be to rotate eqs. (4.2) into a flavour basis in which they decouple, integrate the equations within this basis using the results of section 3.1, then rotate

the final asymmetry in this diagonal basis back into the physical basis $\{\gamma, \tau\}$, thus obtaining the final Δ_γ and Δ_τ asymmetries. We first define a (unitary) U-matrix as that rotating the $\{\gamma, \tau\}$ basis into a diagonal basis $\{\gamma', \tau'\}$, according to

$$\begin{pmatrix} N_{\Delta_{\gamma'}} \\ N_{\Delta_{\tau'}} \end{pmatrix} = U \begin{pmatrix} N_{\Delta_\gamma} \\ N_{\Delta_\tau} \end{pmatrix}, \quad \text{where} \quad U \equiv \begin{pmatrix} U_{\gamma'\gamma} & U_{\gamma'\tau} \\ U_{\tau'\gamma} & U_{\tau'\tau} \end{pmatrix} \tag{4.6}$$

is the matrix that diagonalizes

$$P_2^0 \equiv \begin{pmatrix} P_{2\gamma}^0 \, C_{\gamma\gamma}^{(2)} & P_{2\gamma}^0 \, C_{\gamma\tau}^{(2)} \\ P_{2\tau}^0 \, C_{\tau\gamma}^{(2)} & P_{2\tau}^0 \, C_{\tau\tau}^{(2)} \end{pmatrix} \tag{4.7}$$

i.e. $U \, P_2^0 \, U^{-1} = \mathrm{diag}(P_{2\gamma'}^0, P_{2\tau'}^0)$. In the new primed basis eqs. (4.2) decouple as

$$\begin{aligned} \frac{dN_{\Delta_{\gamma'}}}{dz_2} &= \varepsilon_{2\gamma'} \, D_2 \, (N_{N_2} - N_{N_2}^{\mathrm{eq}}) - P_{2\gamma'}^0 \, W_2 \, N_{\Delta_{\gamma'}} \\ \frac{dN_{\Delta_{\tau'}}}{dz_2} &= \varepsilon_{2\tau'} \, D_2 \, (N_{N_2} - N_{N_2}^{\mathrm{eq}}) - P_{2\tau'}^0 \, W_2 \, N_{\Delta_{\tau'}} \end{aligned} \tag{4.8}$$

where we defined

$$\begin{pmatrix} \varepsilon_{2\gamma'} \\ \varepsilon_{2\tau'} \end{pmatrix} \equiv U \begin{pmatrix} \varepsilon_{2\gamma} \\ \varepsilon_{2\tau} \end{pmatrix} \tag{4.9}$$

Integrating the decoupled equations gives

$$\begin{aligned} N_{\Delta_{\gamma'}}^{T\sim T_L} &= \varepsilon_{2\gamma'} \kappa \left(K_{2\gamma'} \right) \\ N_{\Delta_{\tau'}}^{T\sim T_L} &= \varepsilon_{2\tau'} \kappa \left(K_{2\tau'} \right) \end{aligned} \tag{4.10}$$

Finally, the above $\{\Delta_{\gamma'} \Delta_{\tau'}\}$ can be rotated back into the physical $\{\Delta_\gamma, \Delta_\tau\}$ basis

$$\begin{pmatrix} N_{\Delta_\gamma}^{T\sim T_L} \\ N_{\Delta_\tau}^{T\sim T_L} \end{pmatrix} = U^{-1} \begin{pmatrix} N_{\Delta_{\gamma'}}^{T\sim T_L} \\ N_{\Delta_{\tau'}}^{T\sim T_L} \end{pmatrix}, \quad \text{where} \quad U^{-1} \equiv \begin{pmatrix} U_{\gamma\gamma'}^{-1} & U_{\gamma\tau'}^{-1} \\ U_{\tau\gamma'}^{-1} & U_{\tau\tau'}^{-1} \end{pmatrix}. \tag{4.11}$$

We would like to compare the case $C \neq I$ with $C = I$ (corresponding to $U = I$ above). In making this comparison it is useful to define a ratio R, where

$$R \equiv \left| \frac{N_{B-L}}{N_{B-L}|_{C=I}} \right| \tag{4.12}$$

If we want to calculate the value of R at the end of the N_2 production stage, we have to express $N_{B-L}^{T\sim T_L}$ in terms of the 'unprimed' quantities in eq. (4.10). This is quite easy for the $K_{2\alpha'}$, since one has simply to find the eigenvalues of the matrix P_2^0. Taking for simplicity the approximation $C_{\gamma\gamma}^{(2)} \simeq C_{\tau\tau}^{(2)} \simeq 1$, and remembering that $P_{2\gamma}^0 + P_{2\tau}^0 = 1$, one obtains

$$\begin{aligned} P_{2\gamma'}^0 &\simeq \frac{1}{2}\left(1 + \sqrt{(P_{2\gamma}^0 - P_{2\tau}^0)^2 + 4\, C_{\gamma\tau}^{(2)}\, C_{\tau\gamma}^{(2)}\, P_{2\gamma}^0\, P_{2\tau}^0}\right) \\ P_{2\tau'}^0 &\simeq \frac{1}{2}\left(1 - \sqrt{(P_{2\gamma}^0 - P_{2\tau}^0)^2 + 4\, C_{\gamma\tau}^{(2)}\, C_{\tau\gamma}^{(2)}\, P_{2\gamma}^0\, P_{2\tau}^0}\right) \end{aligned} \tag{4.13}$$

Notice that, both for $\alpha = \tau$ and $\alpha = \gamma$, one has $P_{2\alpha'}^0 \simeq P_{2\alpha}^0 + \mathcal{O}(\sqrt{C_{\gamma\tau}^{(2)}\, C_{\tau\gamma}^{(2)}})$ if $P_{2\tau} \simeq P_{2\gamma}^0 \simeq 1/2$ and $P_{2\alpha'}^0 \simeq P_{2\alpha}^0 + \mathcal{O}(C_{\gamma\tau}^{(2)}\, C_{\tau\gamma}^{(2)})$ if $P_{2\tau} \ll P_{2\gamma}^0$ or vice-versa. Considering moreover that, if $K_{2\alpha} \gg 1$, one has approximately $\kappa(K_{2\alpha}) \sim 1/K_{2\alpha}^{1.2}$ [71], one can write

$$\begin{aligned} N_{\Delta_{\gamma'}}^{T\sim T_L} &\simeq \varepsilon_{2\gamma'}\, \kappa(K_{2\gamma}) \\ N_{\Delta_{\tau'}}^{T\sim T_L} &\simeq \varepsilon_{2\tau'}\, \kappa(K_{2\tau}) \end{aligned} \tag{4.14}$$

We have now to consider the effect of flavour coupling encoded in the primed *CP* asymmetries. If these are re-expressed in terms of the unprimed *CP* asymmetries we can obtain explicitly the flavour composition of the asymmetry generated at $T \simeq T_L$ plugging eqs. (4.14) and eq. (4.9) into eqs. (4.11),

$$\begin{aligned} N_{\Delta_\gamma}^{T\sim T_L} &= U_{\gamma\gamma'}^{-1}\left[U_{\gamma'\gamma}\,\varepsilon_{2\gamma} + U_{\gamma'\tau}\,\varepsilon_{2\tau}\right]\,\kappa(K_{2\gamma}) + U_{\gamma\tau'}^{-1}\left[U_{\tau'\gamma}\,\varepsilon_{2\gamma} + U_{\tau'\tau}\,\varepsilon_{2\tau}\right]\,\kappa(K_{2\tau}) \\ N_{\Delta_\tau}^{T\sim T_L} &= U_{\tau\gamma'}^{-1}\left[U_{\gamma'\gamma}\,\varepsilon_{2\gamma} + U_{\gamma'\tau}\,\varepsilon_{2\tau}\right]\,\kappa(K_{2\gamma}) + U_{\tau\tau'}^{-1}\left[U_{\tau'\gamma}\,\varepsilon_{2\gamma} + U_{\tau'\tau}\,\varepsilon_{2\tau}\right]\,\kappa(K_{2\tau}) \\ N_{\Delta_{B-L}}^{T\sim T_L} &= N_{\Delta_\gamma}^{T\sim T_L} + N_{\Delta_\tau}^{T\sim T_L} \end{aligned} \tag{4.15}$$

We can distinguish two different cases. The first one is for $P_{2\tau}^0 \simeq P_{2\gamma}^0 \simeq 1/2$, implying $K_{2\tau} = K_{2\gamma} = K_2/2$ and therefore $\kappa(K_{2\gamma}) = \kappa(K_{2\tau}) = \kappa(K_2/2)$. In this situation one can see immediately that

$$N_{\Delta_\gamma}^{T\sim T_L} \simeq \varepsilon_{2\gamma}\,\kappa(K_2/2) \qquad \text{and} \qquad N_{\Delta_\tau}^{T\sim T_L} \simeq \varepsilon_{2\tau}\,\kappa(K_2/2) \tag{4.16}$$

Therefore, barring the case $\varepsilon_{2\gamma} = -\varepsilon_{2\tau}$, one has not only $N_{\Delta_{B-L}}^{T\sim T_L} \simeq N_{\Delta_{B-L}}^{T\sim T_L}\Big|_{C=I}$, implying $R^{T\sim T_L} = 1$, but even that the flavour composition is the same compared to a usual calculation where flavour coupling is neglected. However, if $\varepsilon_{2\gamma} = -\varepsilon_{2\tau}$, a more careful treatment is necessary. From the eqs. (4.13) one finds $P^0_{2\gamma'} = (1 + \sqrt{C^{(2)}_{\gamma\tau}\, C^{(2)}_{\tau\gamma}})/2 \neq P^0_{2\tau'} = (1 - \sqrt{C^{(2)}_{\gamma\tau}\, C^{(2)}_{\tau\gamma}})/2$. This difference induced by the off-diagonal terms of the $C^{(2)}$ matrix prevents an exact cancellation or at least it changes the condition where it is realized, an effect that occurs also within N_1 leptogenesis [79].

Let us now see what happens on the other hand when either $P^0_{2\tau}$ or $P^0_{2\gamma}$ is much smaller than the other. This situation has not to be regarded as fine tuned, since it occurs quite naturally for a random choice of the parameters. At the first order in the $C^{(2)}$ off-diagonal terms, one has

$$U \simeq \begin{pmatrix} 1 & C^{(2)}_{\gamma\tau}\, \frac{P^0_{2\gamma}}{P^0_{2\gamma}-P^0_{2\tau}} \\ C^{(2)}_{\tau\gamma}\, \frac{P^0_{2\tau}}{P^0_{2\tau}-P^0_{2\gamma}} & 1 \end{pmatrix} \quad U^{-1} \simeq \begin{pmatrix} 1 & -C^{(2)}_{\gamma\tau}\, \frac{P^0_{2\gamma}}{P^0_{2\gamma}-P^0_{2\tau}} \\ -C^{(2)}_{\tau\gamma}\, \frac{P^0_{2\tau}}{P^0_{2\tau}-P^0_{2\gamma}} & 1 \end{pmatrix} \tag{4.17}$$

Let us for definiteness assume that $P^0_{2\tau} \ll P^0_{2\gamma}$ and that $K_2 \gg 1$ (this second condition also occurs for natural choices of the parameters). In this case one has necessarily $\kappa(K_{2\tau}) \gg \kappa(K_{2\gamma})$. We can therefore specify eqs. (4.15) writing approximately for the flavour asymmetries in the two flavours,

$$N_{\Delta_\gamma}^{T\sim T_L} \simeq \varepsilon_{2\gamma}\, \kappa(K_{2\gamma}) - C^{(2)}_{\gamma\tau}\, \varepsilon_{2\tau}\, \kappa(K_{2\tau}) \tag{4.18}$$

$$N_{\Delta_\tau}^{T\sim T_L} \simeq \varepsilon_{2\tau}\, \kappa(K_{2\tau}) \tag{4.19}$$

where we neglected all terms containing products either of two off-diagonal terms of $C^{(2)}$, or of one off-diagonal term times $\kappa(K_{2\gamma})$. We can therefore see that the total final asymmetry cannot differ much from the standard calculation,

$$N_{\Delta_{B-L}}^{T\sim T_L} \simeq \varepsilon_{2\gamma}\, \kappa(K_{2\gamma}) + \varepsilon_{2\tau}\, \kappa(K_{2\tau}) - C^{(2)}_{\gamma\tau}\, \varepsilon_{2\tau}\, \kappa(K_{2\tau}) \tag{4.20}$$

implying

$$R^{T\sim T_L} \simeq 1 - C^{(2)}_{\gamma\tau}\, \frac{\varepsilon_{2\tau}\, \kappa(K_{2\tau})}{\varepsilon_{2\gamma}\, \kappa(K_{2\gamma}) + \varepsilon_{2\tau}\, \kappa(K_{2\tau})} \tag{4.21}$$

This holds because the dominant contribution comes from the tauonic flavour asymmetry that is not changed at first order. Notice by the way that since $C^{(2)}_{\gamma\tau} > 0$ and necessarily $\varepsilon_{2\tau} > 0$, the effect of flavour coupling even produces a reduction of the total asymmetry at $T \sim T_L$ [1].

On the other hand the asymmetry in the sub-dominant flavour γ can be greatly enhanced since the quantity

$$R^{T\sim T_L}_{\Delta_\gamma} \equiv \left| \frac{N^{T\sim T_L}_{\Delta_\gamma}}{N^{T\sim T_L}_{\Delta_\gamma}\Big|_{C=I}} \right| \simeq \left| 1 - C^{(2)}_{\gamma\tau} \frac{\varepsilon_{2\tau}\,\kappa(K_{2\tau})}{\varepsilon_{2\gamma}\,\kappa(K_{2\gamma})} \right| \tag{4.22}$$

can be in general much higher than unity. In this respect it is important to notice that the assumption $P^0_{2\tau} \ll P^0_{2\gamma}$ does not necessarily imply $\varepsilon_{2\tau} \ll \varepsilon_{2\gamma}$ since $\varepsilon_{2\alpha} \lesssim 10^{-6}\,(M_2/10^{10}\,\mathrm{GeV})\,\sqrt{P^0_{2\alpha}}$ [8]. Notice also that if vice versa $P^0_{2\gamma} \ll P^0_{2\tau}$, then the τ flavour asymmetry is sub-dominant and can be strongly enhanced.

There is a simple physical interpretation to the enhancement of the sub–dominant flavoured asymmetry. This can be given in terms of the effect of tau flavour coupling on the final γ asymmetry that is described by the off-diagonal terms of the $C^{(2)}$ matrix. The dominant contribution to these terms comes from the Higgs asymmetry produced in $N_2 \mapsto l_\alpha + \phi^\dagger$ decays. Let us still assume for definiteness that $P^0_{2\tau} \ll P^0_{2\gamma}$ and that $K_2 \gg 1$. This implies that the γ asymmetry is efficiently washed-out and there is a substantial equilibrium between decays and inverse processes.

On the other hand the τ asymmetry is weakly washed-out and for simplicity we can think to the extreme case when is not washed-out at all (true for $K_{2\tau} \ll 1$). An excess of tau over γ asymmetry results in an excess of Higgs over γ asymmetry. This excess Higgs asymmetry increases the inverse decays of ℓ_γ over the $\bar{\ell}_\gamma$ states (or vice versa, depending on its sign) and 'soaks up' either more particle or more anti-particle states generating an imbalance. Hence one can have $R^{T\sim T_L}_{\Delta\gamma} \gg 1$ thanks to the dominant effect of the extra inverse decay processes that 'switch on' when

[1] This result differs from the one of [79] where, within N_1 leptogenesis, the authors find an enhancement instead of a reduction. This is simply explained by the fact that we are also accounting for the Higgs asymmetry that determines the (correct) positive sign for $C^{(2)}_{\gamma\tau}$.

$C \neq I$.

This effect had been already discussed within N_1-dominated leptogenesis [79], where the authors found $\sim \pm 40\%$ corrections upon inclusion of coupling terms. Our results, for the asymmetry at the production stage, are qualitatively similar though we also took into account the dominant contribution to flavour coupling coming from the Higgs asymmetry and we solved analytically the kinetic equations including flavour coupling without any approximation. As we already noticed, quantitatively, the account of the Higgs asymmetry produces important effects. For instance, when the Higgs asymmetry is included, the results are quite symmetric under the interchange of $P^0_{2\gamma}$ and $P^0_{2\tau}$ since the total matrix $C^{(2)}$ is much more symmetrical than $C^{l(2)}$.

There is however a much more important difference in this respect between N_2-dominated and N_1-dominated leptogenesis. While in the latter case a strong enhancement of the sub-dominant flavoured asymmetry does not translate into a strong enhancement of the final asymmetry, in the case of the N_2-dominated scenario this becomes possible, thanks to the presence of the additional stage of lightest RH neutrino wash-out - as we shall see presently.

4.3 The $2 \mapsto 3$ flavour projection stage

Immediately after the N_2 production stage there will be an asymmetry $N^{T\sim T_L}_{\Delta_\alpha} = \left(N^{T\sim T_L}_{\Delta_\gamma}, N^{T\sim T_L}_{\Delta_\tau}\right)$. At $T \sim T' = 10^9\,\mathrm{GeV}$ this asymmetry is projected from the $\{\gamma, \tau\}$ into the $\{e, \mu, \tau\}$ basis obtaining $N^{T\sim T'}_{\Delta_\alpha} = \left(N^{T\sim T'}_{\Delta_e}, N^{T\sim T'}_{\Delta_\mu}, N^{T\sim T'}_{\Delta_\tau}\right)$. Following the notation and method of section 3.5 this can be written explicitly as

$$\begin{aligned} N^{T\sim T'}_{\Delta_e} &= p^0_{e\gamma}\, N^{T\sim T_L}_{\Delta_\gamma} + \Delta p_{e\gamma}\, p^0_{2\gamma}\, N^{in}_{N_2} \\ N^{T\sim T'}_{\Delta_\mu} &= (1 - p^0_{e\gamma})\, N^{T\sim T_L}_{\Delta_\gamma} - \frac{\Delta p_{e\gamma}}{2}\, p^0_{2\gamma}\, N^{in}_{N_2} \\ N^{T\sim T'}_{\Delta_\tau} &= N^{T\sim T_L}_{\Delta_\tau} \end{aligned} \tag{4.23}$$

where notice there is an extra factor of $p^0_{2\gamma}$ versus eqs. (3.75) since in the 2-flavoured regime only a fraction $p^0_{2\gamma} \leq 1$ of the initial N_2 number density is transferred into the l_γ doublets after these decay. The tree-level projector $p^0_{e\gamma}$ is just the tree level

branching ratio for $l_\gamma \mapsto l_e$ and hence may be written directly as

$$p^0_{e\gamma} = \frac{p^0_{2e}}{p^0_{ee} + p^0_{2\mu}} \tag{4.24}$$

The loop-level projector $\Delta p_{e\gamma} \equiv |\langle l_e | l_\gamma \rangle|^2 - |\langle \bar{l}_e | \bar{l}_\gamma \rangle|^2$ involves a little more work to derive in terms of known quantities. We begin its derivation by writing it in terms the loop level branching ratios, as

$$\Delta p_{e\gamma} = p_{e\gamma} - \bar{p}_{e\gamma} = \frac{p_{2e}}{p_{2e} + p_{2\mu}} \; - \; \frac{\bar{p}_{2e}}{p_{2e} + p_{2\mu}} \tag{4.25}$$

The above expression can be given in terms of the flavoured CP asymmetries $\varepsilon_{2\gamma}$ and ε_{2e}. Recall from eq. (3.43) in section 3.1 that we may write

$$\varepsilon_{i\alpha} = p^0_{i\alpha} \varepsilon_i \; - \; \frac{\Delta p_{i\alpha}}{2} \tag{4.26}$$

Applying the above to eq. (4.25) it is possible to derive the relation

$$\Delta p_{e\gamma} = \frac{1}{p^0_{2\gamma}} \left(\varepsilon_{2e} - \frac{p^0_{2e}}{p^0_{2\gamma}} \, \varepsilon_{2\gamma} \right) + \mathcal{O}\left(\Delta^2\right) \tag{4.27}$$

as may be verified upon direct substitution of eq. (4.26) for $\alpha = e, \gamma$ into the above. If we now identify the "phantom terms" in eqs. (4.23) as given by

$$p_\delta \equiv \Delta p_{e\gamma} \, p^0_{2\gamma} \, N^{in}_{N_2} \tag{4.28}$$

then an explicit expression for phantom terms (neglecting $\mathcal{O}(\Delta^2)$ contributions) is

$$p_\delta = \left(\varepsilon_{2e} - \frac{p^0_{2e}}{p^0_{2\gamma}} \, \varepsilon_{2\gamma} \right) \, N^{in}_{N_2} \tag{4.29}$$

and the final asymmetries after projection at $T \sim T'$ are given by

$$\begin{aligned} N^{T\sim T'}_{\Delta_\delta} &= p_\delta + \frac{p^0_{2\delta}}{p^0_{2\gamma}} \, N^{T\sim T_L}_{\Delta_\gamma} \qquad \text{for} \quad \delta = e, \, \mu \\ N^{T\sim T'}_{\Delta_\tau} &= N^{T\sim T_L}_{\Delta_\tau} \end{aligned} \tag{4.30}$$

where $p^0_{2\gamma} = p^0_{2e} + p^0_{2\mu}$, p_δ is given by eq. (4.29) and $N^{T\sim T_L}_{\Delta_\gamma}$ was given explicitly in eqs. (4.15).

4.4 The N_1 Washout Stage

We next consider how the asymmetries produced by N_2 decays and subsequently projected into a three flavour basis - the $N^{T\sim T'}_{\Delta_\alpha}$ given in eqs. (4.30) - get modified by N_1 washout, including coupling effects due to $C^{(3)} \neq I$. We first re-write eqs. (4.4) in the compact form

$$\frac{d\vec{N}_\Delta}{dz_1} = -W_1\, P^0_1\, \vec{N}_\Delta \tag{4.31}$$

where $\vec{N}_\Delta \equiv (N_{\Delta_e}, N_{\Delta_\mu}, N_{\Delta_\tau})$ and I have defined the matrix P^0_1 as

$$P^0_1 \equiv \begin{pmatrix} p^0_{1e}\, C^{(3)}_{ee} & p^0_{1e}\, C^{(3)}_{e\mu} & p^0_{1e}\, C^{(3)}_{e\tau} \\ p^0_{1\mu}\, C^{(3)}_{\mu e} & p^0_{1\mu}\, C^{(3)}_{\mu\mu} & p^0_{1\mu}\, C^{(3)}_{\mu\tau} \\ p^0_{1\tau}\, C^{(3)}_{\tau e} & p^0_{1\tau}\, C^{(3)}_{\tau\mu} & p^0_{1\tau}\, C^{(3)}_{\tau\tau} \end{pmatrix} \tag{4.32}$$

Applying the same procedure as for the N_2 production stage, we begin by rotating the initial asymmetries into a new basis

$$\vec{N}_{\Delta''} = V\, \vec{N}_\Delta\,, \qquad \text{where} \qquad V \equiv \begin{pmatrix} V_{e''e} & V_{e''\mu} & V_{e''\tau} \\ V_{\mu''e} & V_{\mu''\mu} & V_{\mu''\tau} \\ V_{\tau''e} & V_{\tau''\mu} & V_{\tau''\tau} \end{pmatrix} \tag{4.33}$$

is the matrix that diagonalizes P^0_1, i.e. $V\, P^0_1\, V^{-1} = P^0_{1''} \equiv \mathrm{diag}(p^0_{1e''}, p^0_{1\mu''}, p^0_{1\tau''})$ and $\vec{N}_{\Delta''} \equiv (N_{\Delta_{e''}}, N_{\Delta_{\mu''}}, N_{\Delta_{\tau''}})$. Eqs. (4.31) will now decouple when written in this new "double primed" basis, as

$$\frac{d\vec{N}_{\Delta''}}{dz_1} = -W_1\, P^0_{1''}\, \vec{N}_{\Delta''} \tag{4.34}$$

and integrating the above decoupled equations, one gets

$$\vec{N}^{\rm f}_{\Delta''} = \left(N^{T\sim T'}_{\Delta_{e''}}\, e^{-\frac{3\,\pi}{8}\, K_{1e''}}\,, N^{T\sim T'}_{\Delta_{\mu''}}\, e^{-\frac{3\,\pi}{8}\, K_{1\mu''}}\,, N^{T\sim T'}_{\Delta_{\tau''}}\, e^{-\frac{3\,\pi}{8}\, K_{1\tau''}} \right) \tag{4.35}$$

where $K_{1\alpha''} \equiv p^0_{1\alpha''} K_1$. Applying the inverse transformation, we can then finally obtain final flavoured asymmetries of

$$\vec{N}^{\rm f}_{\Delta} = V^{-1}\, \vec{N}^{\rm f}_{\Delta''} \quad \text{for} \quad V^{-1} \equiv \begin{pmatrix} V^{-1}_{ee''} & V^{-1}_{\mu e''} & V^{-1}_{\tau e''} \\ V^{-1}_{e\mu''} & V^{-1}_{\mu\mu''} & V^{-1}_{\tau\mu''} \\ V^{-1}_{e\tau''} & V^{-1}_{\mu\tau''} & V^{-1}_{\tau\tau''} \end{pmatrix} \tag{4.36}$$

or explicitly for the single components

$$\begin{aligned} N^{\rm f}_{\Delta_\alpha} &= \sum_{\alpha''} V^{-1}_{\alpha\alpha''} \left[N^{T\sim T'}_{\alpha''}\, e^{-\frac{3\pi}{8} K_{1\alpha''}} \right] \\ &= \sum_{\alpha''} V^{-1}_{\alpha\alpha''}\, e^{-\frac{3\pi}{8} K_{1\alpha''}} \left[\sum_{\beta} V_{\alpha''\beta}\, N^{T\sim T'}_{\Delta_\beta} \right] \end{aligned} \tag{4.37}$$

where the $N^{T\sim T'}_{\Delta_\beta}$'s are given by eqs. (4.30). This equation is the general analytical solution and should be regarded as the "master equation" for flavour coupling in N_2-dominated leptogenesis. It was first given in the paper [6]. Expanding the sums over $\alpha'' = e'', \mu'', \tau''$ and $\beta = e, \mu, \tau$ it can be written more explicitly as

$$\begin{aligned} N^{\rm f}_{\Delta_\alpha} \simeq\ & V^{-1}_{\alpha e''} \left[V_{e''e}\, N^{T\sim T'}_{\Delta_e} + V_{e''\mu}\, N^{T\sim T'}_{\Delta_\mu} + V_{e''\tau}\, N^{T\sim T'}_{\Delta_\tau} \right] e^{-\frac{3\pi}{8} K_{1e}} \\ +\ & V^{-1}_{\alpha\mu''} \left[V_{\mu''e}\, N^{T\sim T'}_{\Delta_e} + V_{\mu''\mu}\, N^{T\sim T'}_{\Delta_\mu} + V_{\mu''\tau}\, N^{T\sim T'}_{\Delta_\tau} \right] e^{-\frac{3\pi}{8} K_{1\mu}} \\ +\ & V^{-1}_{\alpha\tau''} \left[V_{\tau''e}\, N^{T\sim T'}_{\Delta_e} + V_{\tau''\mu}\, N^{T\sim T'}_{\Delta_\mu} + V_{\tau''\tau}\, N^{T\sim T'}_{\Delta_\tau} \right] e^{-\frac{3\pi}{8} K_{1\tau}} \end{aligned} \tag{4.38}$$

4.5 The Flavour Swap Scenario

In the "flavour swap scenario" the inclusion of flavour coupling effects from the off-diagonal terms of the $C^{(2)}$ and $C^{(3)}$ matrices (plus the phantom terms) can result in order-of-magnitude-wise enhancements to the final $B - L$ asymmetry. In this scenario, the flavour τ which is dominant at the N_2 production stage gets strongly washed out at the N_1 washout stage - however a fraction of this large asymmetry gets transferred into a δ flavour by the $\delta \leftrightarrow \tau$ coupling introducing a large departure from thermal equilibrium to the δ flavour via the higgs asymmetry (recall the discussion at the end of section 4.2). As a result, the dominant flavour is swapped from the τ

flavour at $T \sim T_L$ to the δ flavour at $T \sim M_1$ and hence the final $B-L$ asymmetry can be much larger upon inclusion of coupling effects. This "story" is shown in the "cartoon" below [2].

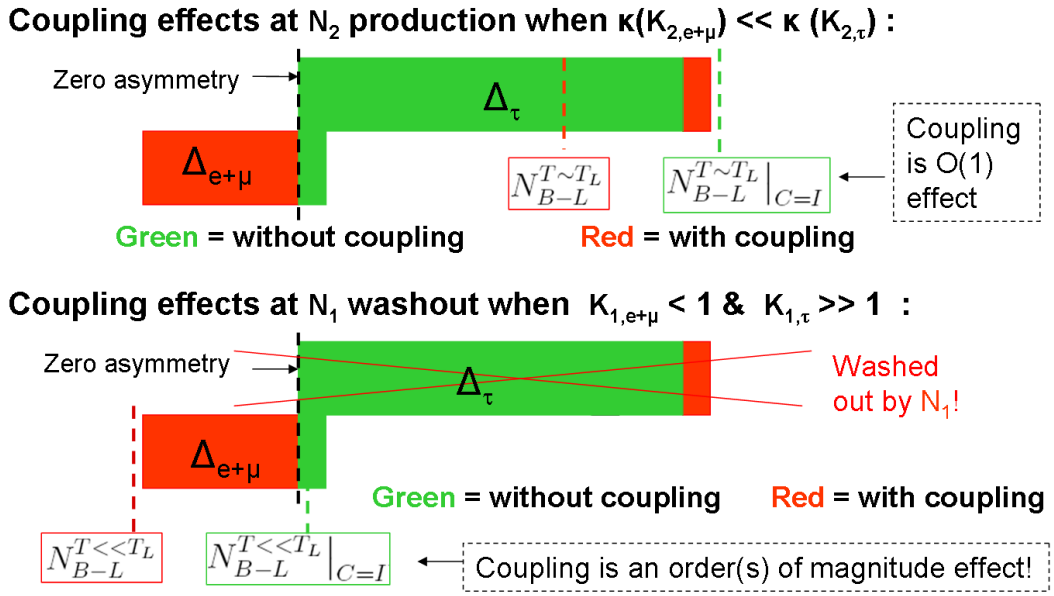

Figure 4.1: Flavour swap scenario (case A).

The flavour swap scenario implies for the washout parameters that out of the two flavours e and μ, one has $K_{1\delta} \lesssim 1$ (where δ can be either e or μ). The other flavour will be denoted by β, so if $\delta = e$ then $\beta = \mu$ or vice versa. For $K_{1\beta}$ we will assume that $K_{1\beta} \sim K_{1\tau} \sim K_1 \gg 1$, such that asymmetries in the β'' as well as in the τ'' flavours will be (almost) completely erased by the exponential N_1 washout. The only asymmetry relevant after N_1 washout will be the one in the flavour δ''.

Obviously, this already simplifies eq. (4.37) significantly. Now one has, similarly to what happened before with the $K_{1\alpha'}$, that $K_{1\delta''} = K_{1\delta}\,(1+\mathcal{O}(C^{(3)}_{\alpha\neq\beta})^3) \simeq K_{1\delta}$. At the same time $K_{1\beta\tau''} = K_{1\beta\tau}\,(1+\mathcal{O}(C^{(3)}_{\alpha\neq\beta}))$ and therefore $K_{1\beta\tau''} \sim K_1 \gg 1$. This implies that in eq. (4.37) only the terms with $\alpha'' = \delta''$ survive, while the terms with $\alpha'' = \beta'', \tau''$ undergo a strong wash-out from the lightest RH neutrino inverse processes and can be neglected. Therefore, if we calculate the final flavoured asymmetries and make the approximation $\exp(-3\pi\, K_{1\delta}/8) \simeq 1$, from the general eq. (4.38) we can

[2]The figure shows a "case A" flavour swap in which the $C^{(2)}$–matrix couplings at N_2 production introduce a large enhancement to the final asymmetry. There may also be a "case B" with enhancement due to the $C^{(3)}$–matrix and described later.

write

$$N^{\rm f}_{\Delta_\beta} \simeq V^{-1}_{\beta\delta''}\, V_{\delta''\beta}\, N^{T\sim T'}_{\Delta_\beta} + V^{-1}_{\beta\delta''}\, V_{\delta''\delta}\, N^{T\sim T'}_{\Delta_\delta} + V^{-1}_{\beta\delta''}\, V_{\delta''\tau}\, N^{T\sim T'}_{\Delta_\tau} \quad (4.39)$$

$$N^{\rm f}_{\Delta_\delta} \simeq V^{-1}_{\delta\delta''}\, V_{\delta''\beta}\, N^{T\sim T'}_{\Delta_\beta} + V^{-1}_{\delta\delta''}\, V_{\delta''\delta}\, N^{T\sim T'}_{\Delta_\delta} + V^{-1}_{\delta\delta''}\, V_{\delta''\tau}\, N^{T\sim T'}_{\Delta_\tau} \quad (4.40)$$

$$N^{\rm f}_{\Delta_\tau} \simeq V^{-1}_{\tau\delta''}\, V_{\delta''\beta}\, N^{T\sim T'}_{\Delta_\beta} + V^{-1}_{\tau\delta''}\, V_{\delta''\delta}\, N^{T\sim T'}_{\Delta_\delta} + V^{-1}_{\tau\delta''}\, V_{\delta''\tau}\, N^{T\sim T'}_{\Delta_\tau} \quad (4.41)$$

At the production, for the three $N^{T\sim T'}_{\Delta_\alpha}$'s, we assume the conditions that led to the eqs. (4.18) and (4.19), i.e. $p^0_{2\tau} \ll p^0_{2\gamma}$ (notice again that one could also analogously consider the opposite case $p^0_{2\tau} \ll p^0_{2\gamma}$) and $K_2 \gg 1$, implying $\kappa(K_{2\gamma}) \ll 1$. The matrices V and V^{-1}, whose entries are defined by the eqs. (4.33) and (4.36) respectively, at the first order in the $C^{(3)}$ off-diagonal terms, are given by

$$V \simeq \begin{pmatrix} 1 & C^{(3)}_{e\mu} & -C^{(3)}_{e\tau}\,\frac{p^0_{1e}}{p^0_{1\tau}} \\ -C^{(3)}_{\mu e}\,\frac{p^0_{1\mu}}{p^0_{1e}} & 1 & -C^{(3)}_{\mu\tau}\,\frac{p^0_{1\mu}}{p^0_{1\tau}} \\ C^{(3)}_{\tau e} & C^{(3)}_{\tau\mu} & 1 \end{pmatrix} \quad V^{-1} \simeq \begin{pmatrix} 1 & -C^{(3)}_{e\mu} & C^{(3)}_{e\tau}\,\frac{p^0_{1e}}{p^0_{1\tau}} \\ C^{(3)}_{\mu e}\,\frac{p^0_{1\mu}}{p^0_{1e}} & 1 & C^{(3)}_{\mu\tau}\,\frac{p^0_{1\mu}}{p^0_{1\tau}} \\ -C^{(3)}_{\tau e} & -C^{(3)}_{\tau\mu} & 1 \end{pmatrix} \quad (4.42)$$

Therefore, we find for the three $N^{\rm f}_{\Delta_\alpha}$'s

$$N^{\rm f}_{\Delta_\beta} \simeq -C^{(3)}_{\beta\delta}\, C^{(3)}_{\delta\beta}\, \frac{p^0_{1\delta}}{p^0_{1\beta}}\, N^{T\sim T'}_{\Delta_\beta} - C^{(3)}_{\beta\delta}\, N^{T\sim T'}_{\Delta_\delta} + C^{(3)}_{\beta\delta}\, C^{(3)}_{\delta\tau}\, \frac{p^0_{1\delta}}{p^0_{1\tau}}\, N^{T\sim T'}_{\Delta_\tau} \quad (4.43)$$

$$\simeq -C^{(3)}_{\beta\delta} \left\{ p_\delta + \frac{p^0_{2\delta}}{p^0_{2\gamma}} \left[\varepsilon_{2\gamma} \kappa(K_{2\gamma}) - C^{(2)}_{\gamma\tau}\, \varepsilon_{2\tau}\, \kappa(K_{2\tau}) \right] \right\}$$

$$N^{\rm f}_{\Delta_\delta} \simeq -C^{(3)}_{\delta\beta}\, \frac{p^0_{1\delta}}{p^0_{1\beta}}\, N^{T\sim T'}_{\Delta_\beta} + N^{T\sim T'}_{\Delta_\delta} - C^{(3)}_{\delta\tau}\, \frac{p^0_{1\delta}}{p^0_{1\tau}}\, N^{T\sim T'}_{\Delta_\tau} \quad (4.44)$$

$$\simeq p_\delta + \frac{p^0_{2\delta}}{p^0_{2\gamma}} \left[\varepsilon_{2\gamma} \kappa(K_{2\gamma}) - C^{(2)}_{\gamma\tau}\, \varepsilon_{2\tau}\, \kappa(K_{2\tau}) \right] - C^{(3)}_{\delta\tau}\, \frac{p^0_{1\delta}}{p^0_{1\tau}}\, \varepsilon_{2\tau}\, \kappa(K_{2\tau}) \,,$$

$$N^{\rm f}_{\Delta_\tau} \simeq C^{(3)}_{\tau\delta}\, C^{(3)}_{\delta\beta}\, \frac{p^0_{1\delta}}{p^0_{1\beta}}\, N^{T\sim T'}_{\Delta_\beta} - C^{(3)}_{\tau\delta}\, N^{T\sim T'}_{\Delta_\delta} - C^{(3)}_{\tau\delta}\, C^{(3)}_{\delta\tau}\, \frac{p^0_{1\delta}}{p^0_{1\tau}}\, N^{T\sim T'}_{\Delta_\tau} \quad (4.45)$$

$$\simeq -C^{(3)}_{\tau\delta} \left\{ p_\delta + \frac{p^0_{2\delta}}{p^0_{2\gamma}} \left[\varepsilon_{2\gamma} \kappa(K_{2\gamma}) - C^{(2)}_{\gamma\tau}\, \varepsilon_{2\tau}\, \kappa(K_{2\tau}) \right] \right\}$$

The total final asymmetry is then given by the sum of the flavoured asymmetries. It can be checked that if flavour coupling is neglected ($C^{(2)} = C^{(3)} = I$), then one

obtains the expected result

$$N^{\rm f}_{\Delta_{B-L}} \simeq N^{T\sim T'}_{\Delta_\delta} = p_\delta + \frac{p^0_{2\delta}}{p^0_{2\gamma}}\,\varepsilon_{2\gamma}\kappa(K_{2\gamma}) \tag{4.46}$$

corresponding to an asymmetry produced in the flavour δ, i.e. in the only flavour that survives washout by the lightest RH neutrino.

However, taking into account flavour coupling, new terms arise and the final asymmetry can be considerably enhanced. More explicitly, we have approximately

$$N^{\rm f}_{\Delta_{B-L}} \simeq \left(1 - C^{(3)}_{\beta\delta} - C^{(3)}_{\tau\delta}\right)\left\{p_\delta + \frac{p^0_{2\delta}}{p^0_{2\gamma}}\,\left[\varepsilon_{2\gamma}\kappa(K_{2\gamma}) - C^{(2)}_{\gamma\tau}\,\varepsilon_{2\tau}\,\kappa(K_{2\tau})\right]\right\} - C^{(3)}_{\delta\tau}\,\frac{p^0_{1\delta}}{p^0_{1\tau}}\,\varepsilon_{2\tau}\,\kappa(K_{2\tau}) \tag{4.47}$$

where we have neglected all terms that contain the product either of two or more off-diagonal terms of the coupling matrix, or of one or more off-diagonal term with $\kappa(K_{2\gamma}) \ll 1$. From eq. (4.47) one can readily see examples for strong enhancement of the asymmetries due to flavour coupling, i.e. conditions under which $R^{\rm f} \gg 1$. There are two generic cases for which $R^{\rm f} \gg 1$, referred to henceforth as "case A" and "case B":

- **Case A: Enhancement from flavour coupling at N_2 decay**

  Let us assume $\kappa(K_{2\gamma}) \ll \kappa(K_{2\tau})$ and in addition $P^0_{1\delta}/P^0_{1\tau} = K_{1\delta}/K_{1\tau} \ll 1$. Then the first and third terms in eq. (4.47) dominate and we can estimate

  $$N^{\rm f}_{\Delta_{B-L}} \simeq p_\delta - C^{(2)}_{\gamma\tau}\,\frac{P^0_{2\delta}}{P^0_{2\gamma}}\,\varepsilon_{2\tau}\,\kappa(K_{2\tau}) \tag{4.48}$$

  In order to show more clearly the conditions for this case to be realized, we have plotted in the fig. 4.2 the R iso-contour lines (cf. eq (4.12)) in the plane ($K_{2\gamma}$, $K_{2\tau}$). We have fixed $K_{1\mu} \lesssim 1$, K_{1e}, $K_{1\tau} \gg 1$, so that only the muonic asymmetry survives the lightest RH neutrino wash-out. We have also set $\frac{K_{2\mu}}{K_{2\gamma}} = \frac{1}{2} \gg \frac{K_{1\mu}}{K_{1\tau}}$, so that the last term in the eq. (4.47) can be neglected. Concerning the CP asymmetries, in the left panel we have set $\varepsilon_{2\gamma} = \varepsilon^{max}_{2\gamma}$ and $\varepsilon_{2\tau} = \varepsilon^{max}_{2\tau}$. One can see that in this case the enhancement of the asymmetry becomes

relevant when $K_{2\gamma} \gg K_{2\tau}$ but for $K_{2\gamma} \lesssim 100$ (a reasonable maximum value), it cannot be higher than about $R \approx 2.5$. Notice that, since we choose $\frac{\varepsilon_{2\gamma}}{\varepsilon_{2\tau}} > 1$, a reduction is also possible due to a cancellation of the traditional term and of the new term due to flavour coupling. In the right panels we have set $\varepsilon_{2\gamma} = 0.1\,\varepsilon_{2\gamma}^{max}$ and this time one can see how R can be as large as one order of magnitude. This shows that for $\varepsilon_{2\gamma} \mapsto 0$ the enhancement can be arbitrarily large.

- **Case B: Enhancement from flavour coupling at N_1 washout**

  Another interesting case is when $\kappa(K_{2\gamma}) \ll \kappa(K_{2\tau})$ and in addition $P^0_{2\delta}/P^0_{2\gamma} \ll P^0_{1\delta}/P^0_{1\tau}$. In this case the first and fourth terms in eq. (4.47) dominate and we obtain approximately

$$N^{\rm f}_{\Delta_{B-L}} \simeq p_\delta - C^{(3)}_{\delta\tau}\,\frac{P^0_{1\delta}}{P^0_{1\tau}}\,\varepsilon_{2\tau}\,\kappa(K_{2\tau}) \tag{4.49}$$

  Also for this case B, we have plotted, in the fig. 4.3 , the R iso–contour lines (cf. eq. (4.12)) in the plane ($K_{2\gamma}$, $K_{2\tau}$). We have set $K_{1e} \lesssim 1$ while $K_{1\mu}$, $K_{1\tau} \gg 1$, so that now only the electron asymmetry survives the lightest RH neutrino wash-out. Moreover this time we have set $\varepsilon_{2\tau} = \varepsilon_{2\tau}^{max}$ and $\frac{\varepsilon_{2\mu}}{\varepsilon_{2\tau}} > 1$ so that the last term in the eq. (4.47) becomes dominant and case B is realized. For the CP asymmetries, as before, in the left panel we fixed $|\varepsilon_{2\mu}| = \varepsilon_{2\mu}^{max}$ while in the right panel $|\varepsilon_{2\mu}| = 0.1\varepsilon_{2\mu}^{max}$ and in both cases $\varepsilon_{2\tau} = \varepsilon_{2\tau}^{max}$. Now the enhancement of the final asymmetry R is $\gg 1$ in both cases, simply because the traditional term is this time suppressed by $\frac{K_{2e}}{K_{2\gamma}} \ll 1$. This means that after the decoherence of the γ lepton quantum states, there is a negligible asymmetry in the electron flavour. However, at the lightest RHN washout, an electron asymmetry is generated thanks to flavour coupling.

4.6 Examples of Flavour Swap Scenario for Sequential Dominance

Recall from section 1.5 that Sequential Dominance [49–52] is a way of specialising to regions of the seesaw model's parameter space in which neutrino mixing angles are

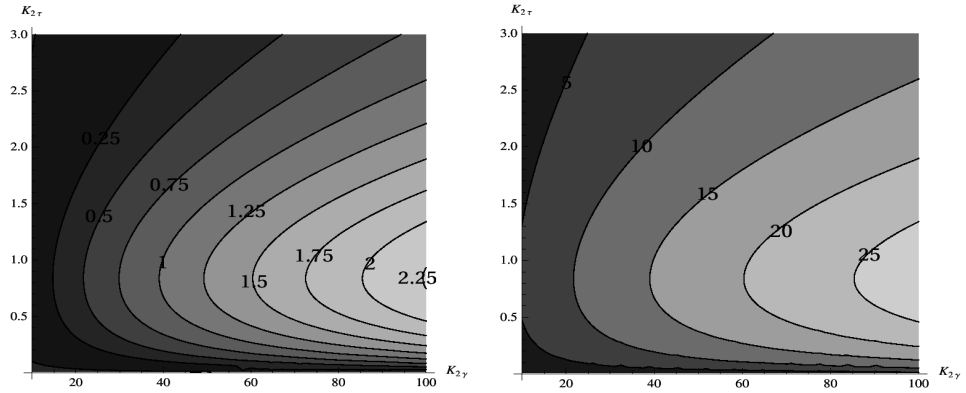

Figure 4.2: Contour plots of R (cf. eq. (4.12)) in the flavour swap scenario for $K_{1\tau}$, $K_{1e} \gg 1$, $K_{1\mu} \lesssim 1$, $K_{2e} = K_{2\mu}$. The latter condition implies that the last term in eq. (4.47) is negligible. Left panel: $|\varepsilon_{2\mu}| = \varepsilon_{2\mu}^{max}$; right panel: $|\varepsilon_{2\mu}| = 0.1\varepsilon_{2\mu}^{max}$ (cf. eq. (4.48)). In both panels $\varepsilon_{2\tau} = \varepsilon_{2\tau}^{max}$ and $\frac{\varepsilon_{2\mu}}{\varepsilon_{2\tau}} > 1$.

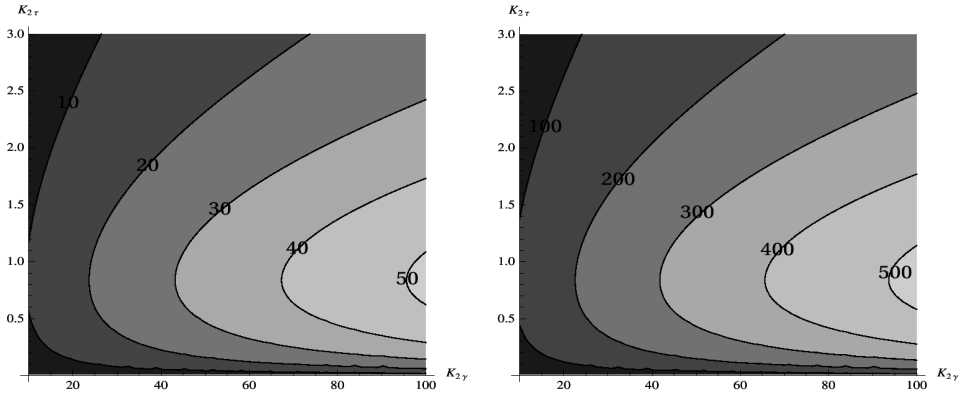

Figure 4.3: Contour plots of R (cf. eq. (4.12)) in the flavour swap scenario for $K_{1\tau}$, $K_{1\mu} \gg 1$, $K_{1e} \lesssim 1$, $\frac{K_{2e}}{K_{2\mu}} \ll \frac{K_{1e}}{K_{1\tau}}$. The last condition implies that the last term in the eq. (4.47) dominates. Left panel: $\varepsilon_{2\mu} = \varepsilon_{2\tau}$; right panel: $\varepsilon_{2\mu} = 0.1\varepsilon_{2\tau}$ (cf. eq. (4.49)). In both panels $\varepsilon_{2\tau} = \varepsilon_{2\tau}^{max}$ and $\frac{\varepsilon_{2\mu}}{\varepsilon_{2\tau}} > 1$.

naturally large - as they are observed to be in oscillation experiments. Recall that for a neutrino Yukawa matrix parametrised as

$$Y^{\nu} = (A,\, B,\, C) = \begin{pmatrix} a_1 & b_1 & c_1 \\ a_2 & b_2 & c_2 \\ a_3 & b_3 & c_3 \end{pmatrix} \tag{4.50}$$

sequential dominance involves making the ansatz

$$\frac{A_i A_j}{M_A} \gg \frac{B_i B_j}{M_B} \gg \frac{C_i C_j}{M_C} \tag{4.51}$$

resulting in two large mixing angles θ_{12} and θ_{23}. In addition, we shall shortly see that small θ_{13} and almost maximal θ_{23} require

$$|A_1| \ll |A_2| \approx |A_2| \tag{4.52}$$

In [6] we found that Case A can be realised within **heavy sequential dominance** and case B can be realised within **light sequential dominance**, as I now explain.

4.6.1 Example for Case A within Heavy Sequential Dominance

To understand how heavy sequential dominance works, we begin by writing the RH neutrino Majorana mass matrix $M_{\rm RR}$ in a diagonal basis as

$$M_{\rm RR} = \begin{pmatrix} M_C & 0 & 0 \\ 0 & M_B & 0 \\ 0 & 0 & M_A \end{pmatrix} \tag{4.53}$$

where we have ordered the columns according to $M_{RR} = \text{diag}(M_1, M_2, M_3)$ where $M_1 < M_2 < M_3$. We identify the dominant RH neutrino and Yukawa couplings as A, the subdominant ones as B, and the almost decoupled (subsubdominant) ones as C i.e. the heaviest RHN is identified as giving the dominant contribution to light neutrino mixing. Working in the mass basis of the charged leptons, we obtain for the lepton mixing angles:

$$\tan\theta_{23} \approx \frac{|A_2|}{|A_3|} \tag{4.54a}$$

$$\tan\theta_{12} \approx \frac{|B_1|}{c_{23}|B_2|\cos\tilde{\phi}_2 - s_{23}|B_3|\sin\tilde{\phi}_3} \tag{4.54b}$$

$$\theta_{13} \approx e^{i\tilde{\phi}_4}\frac{|B_1|(A_2^*B_2 + A_3^*B_3)}{[|A_2|^2+|A_3|^2]^{3/2}}\frac{M_A}{M_B} + \frac{e^{i\tilde{\phi}_5}|A_1|}{\sqrt{|A_2|^2+|A_3|^2}} \tag{4.54c}$$

where the phases do not need to concern us.

The neutrino masses are:

$$m_3 \approx \frac{(|A_2|^2+|A_3|^2)v^2}{M_A} \tag{4.55a}$$

$$m_2 \approx \frac{|B_1|^2 v^2}{s_{12}^2 M_B} \tag{4.55b}$$

$$m_1 \approx \mathcal{O}(|C|^2 v^2/M_C) \tag{4.55c}$$

Tri-bimaximal mixing corresponds to:

$$|A_1| = 0, \tag{4.56}$$

$$|A_2| = |A_3| \tag{4.57}$$

$$|B_1| = |B_2| = |B_3| \tag{4.58}$$

$$A^\dagger B = 0 \tag{4.59}$$

This is called constrained sequential dominance (CSD). For N_2 leptogenesis, the flavour specific decay asymmetries are $\varepsilon_{2\alpha}$ where the leading contribution comes from the heavier RH neutrino of mass $M_A = M_3$ in the loop which may be approximated via eq. (3.43) as:

$$\varepsilon_{2\alpha} \approx -\frac{3}{16\pi v^2}\frac{M_2}{M_3}\frac{1}{B^\dagger B}\mathrm{Im}\left[B_\alpha^*(B^\dagger A)A_\alpha\right] \tag{4.60}$$

Clearly the asymmetry vanishes in the case of CSD due to eq. (6.81) and so in the following we shall consider examples which violate CSD. The mixing angles are given by the following estimates:

$$\tan\theta_{23} \sim \frac{A_2}{A_3} \sim 1, \quad \tan\theta_{12} \sim \frac{\sqrt{2}B_1}{B_2+B_3} \sim \frac{1}{\sqrt{2}}, \quad \theta_{13} \sim \frac{A_1}{\sqrt{2}A_2} \sim \frac{r}{\sqrt{2}} \tag{4.61}$$

Suppose we parametrize the Yukawa couplings consistent with these mixing angles as:

$$A_2 = A_3, \quad A_1 = r\,A_2, \quad B_3 = q\,B_2, \quad B_1 = \frac{1}{2}(1+q)\,B_2 \tag{4.62}$$

where $r < 1$ is related to θ_{13} via eq. (4.61), then we find

$$\varepsilon_{2\mu} \approx -\frac{3}{16\pi v^2}\,M_2 m_3 \qquad \varepsilon_{2\tau} \approx q\,\varepsilon_{2\mu} \qquad \varepsilon_{2e} \approx \frac{r}{2}\,\varepsilon_{2\mu} \tag{4.63}$$

The flavoured effective neutrino masses $\widetilde{m}_{2\alpha}$, $\widetilde{m}_{1\alpha}$ are given by:

$$\widetilde{m}_{2\alpha} = \frac{|B_\alpha|^2 v^2}{M_B} \sim m_2 \qquad \widetilde{m}_{1\alpha} = \frac{|C_\alpha|^2 v^2}{M_C} \sim m_1 \tag{4.64}$$

Neutrino oscillation experiments tell us that $r < 1$ is small (here we shall assume $r \sim 0.2$ as a specific example consistent with current experimental results) and we find

$$K_{2\mu} = \frac{\widetilde{m}_{2\mu}}{m_\star} \sim \frac{m_2}{m_\star} \sim 10, \quad K_{2e} \sim \frac{(1+q)^2}{4} K_{2\mu}, \quad K_{2\tau} \sim q^2 K_{2\mu} \tag{4.65}$$

which allows strong washout for $K_{2\gamma}$ ($\gamma = \mu + e$) with weak washout for $K_{2\tau}$. By assuming that $C_1, C_2 \ll C_3$ we have

$$K_{1\tau} = \frac{\widetilde{m}_{1\tau}}{m_\star} \sim 10 \frac{m_1}{m_2} K_{1e} \qquad K_{1\mu} \ll K_{1\tau} \tag{4.66}$$

which allows for strong washout for $K_{1\tau}$ (at least if $m_1 \sim m_2$) with weak washouts for $K_{1e}, K_{1\mu}$.

Thus, without flavour coupling and phantom terms, we would have strong (exponential) N_1 washout for $K_{1\tau} \sim 10$, with negligible N_1 washout for $K_{1e}, K_{1\mu} < 1$. Since $\varepsilon_{2e} \approx \frac{r}{2}\varepsilon_{2\mu} < 0.1\varepsilon_{2\mu}$ we may neglect ε_{2e} and then we find that the term proportional to $\varepsilon_{2\gamma}\,\kappa(K_{2\gamma})$ is strongly washed out since $K_{2\gamma} \sim 10$. Therefore, without flavour coupling and phantom effects, $N^{\rm f}_{B-L}$ tend to be quite small in this scenario.

While, allowing for the effects of flavour redistribution and including the phantom term, we find (cf. eq. (4.48)),

$$N^{\rm f}_{\Delta_{B-L}} \sim p_\mu + \frac{K_{2\mu}}{K_{2\gamma}}\,\varepsilon_{2\gamma}\,\kappa(K_{2\gamma}) - \frac{K_{2\mu}}{K_{2\gamma}} C^{(2)}_{\gamma\tau}\,\varepsilon_{2\tau}\,\kappa(K_{2\tau}) \tag{4.67}$$

Since $\frac{K_{2\gamma}}{K_{2\mu}} \approx \frac{4}{5+2q}$ and $p_\mu \approx \frac{1+2q}{5+2q}\varepsilon_{2\mu}\,N^{in}_{N_2}$, then we have

$$N^{f}_{\Delta_{B-L}} \sim \frac{1+2q}{5+2q}\,\varepsilon_{2\mu} N^{in}_{N_2} + \frac{4}{4+(1+q)^2}\left[\varepsilon_{2\gamma}\kappa(K_{2\gamma}) - C^{(2)}_{\gamma\tau}\varepsilon_{2\tau}\kappa(K_{2\tau})\right] \tag{4.68}$$

where $K_{2\tau} \sim q^2 K_{2\mu} \sim 10q^2$ leads to only weak wash out with $\varepsilon_{2\mu} \sim -\frac{3}{16\pi^2 v^2} M_2 m_3$

being large. Notice that there is a partial cancellation of the two terms but this is just depending on the particular choice of values for r and q and on $N_{N_2}^{in}$. This is an example, consistent with neutrino data, where $N^f_{\Delta_{B-L}}$ would be very small without flavour coupling and phantom term, but will be quite large including the two effects that both produce a large contribution. If we indeed, for definiteness, assume $N_{N_2}^{in} = 0$ and $q \sim 0.5$ such that $K_{2\tau} \sim 1$ corresponding to $\kappa)K_{2\tau} \approx 0.3$, then we find for R (cf. eq (4.12))

$$R \approx \left| 1 - C^{(2)}_{\gamma\tau} \frac{\kappa(K_{2\tau})}{\kappa(K_{2\gamma})} \frac{\varepsilon_{2\tau}}{\varepsilon_{2\gamma}} \right| \tag{4.69}$$

In fig. 4.4 we plotted R as a function of $q = \frac{\varepsilon_{2\tau}}{\varepsilon_{2\mu}}$. One can see that this example realizes a specific case of the general situation shown in the left panel of fig. 4.2. In particular, one can see that there can be a relevant suppression for positive q and up to a 50% enhancement for negative q. On the other hand, in case of initial thermal abundance, one can easily verify that the presence of the phantom term can yield an enhancement up to three orders of magnitude [3].

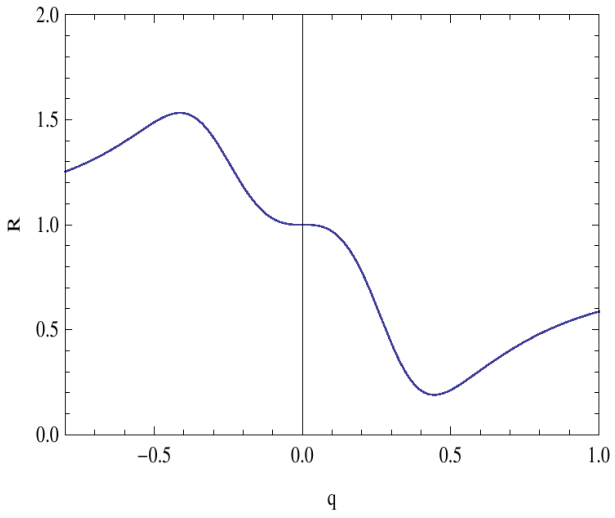

Figure 4.4: Plot of R as a function of q as from the eq. (4.69).

[3] As we shall soon see in chapter 5, the phantom terms are not quite the "free lunch" they are presented as here - they do in fact receive some washout from gauge bosons. Taking this into account, the phantom terms are supressed by an additional factor of $\kappa(\frac{K_{2\gamma}}{2}) \approx \left(\frac{K_{2\gamma}}{2}\right)^{-1.2}$ for $K_{2\gamma} \gg 1$.

4.6.2 Example for Case B within Light Sequential Dominance

To give an example for case B (i.e. an example where $K_{1e} \ll K_{1\mu}, K_{1\tau}$ while $\varepsilon_{2\tau} \gg \varepsilon_{2\mu}, \varepsilon_{2e}$ and $K_{2e} \ll K_{2\gamma}$), we may consider another class of sequential dominance, namely light sequential dominance (LSD). Now, in eq. (4.47) and eq. (4.49) we have to replace $\delta = e$ and $\beta = \mu$.

In the example of LSD we will consider, using the same notation for the dominant, subdominant and subsubdominant RH neutrinos and corresponding couplings, we have:

$$M_{\rm RR} = \begin{pmatrix} M_A & 0 & 0 \\ 0 & M_C & 0 \\ 0 & 0 & M_B \end{pmatrix} \tag{4.70}$$

i.e. the lightest RH neutrino with mass $M_1 = M_A$ dominates the seesaw mechanism. More specifically, let us now consider, within LSD, a variant of CSD called partially constrained sequential dominance (PCSD) [82] where $|A_2| = |A_3| = a$ and $|B_1| = |B_2| = |B_3| = b$, but $A_1 \neq 0$. In addition, we may assume $C = (C_1, C_2, C_3)$ with $C_1 = 0$ and $C_2/C_3 = \zeta \ll 1$ as a specific example. Under these conditions, and using $A_1 = rA_2 = \sqrt{2}\theta_{13}A_2$ defined in the previous section, we can write the neutrino Yukawa matrix as

$$\lambda_\nu = \begin{pmatrix} \sqrt{2}\theta_{13}a & 0 & b \\ a & \zeta c & b \\ -a & c & b \end{pmatrix} \tag{4.71}$$

The flavoured effective neutrino masses $\widetilde{m}_{2\alpha}$, $\widetilde{m}_{1\alpha}$ in this specific LSD scenario are given by:

$$\widetilde{m}_{2\alpha} = \frac{|C_\alpha|^2 v^2}{M_C} \sim m_2 \qquad \widetilde{m}_{1\alpha} = \frac{|A_\alpha|^2 v^2}{M_A} \tag{4.72}$$

For $\widetilde{m}_{1e}$, $\widetilde{m}_{1\mu}$ and $\widetilde{m}_{1\tau}$ we obtain explicitly

$$\widetilde{m}_{1e} = \frac{|\sqrt{2}\,\theta_{13}\,a|^2 v^2}{M_1} = m_3\,\theta_{13}^2 \qquad \widetilde{m}_{1\mu} = \widetilde{m}_{1\tau} = \frac{|a|^2 v^2}{M_1} = \frac{m_3}{2} \tag{4.73}$$

The parameters $K_{i\alpha}$ are related to the $\widetilde{m}_{i\alpha}$'s simply by $K_{i\alpha} = \widetilde{m}_{i\alpha}/m^*$. Since we know from neutrino oscillation experiments that the leptonic mixing angle θ_{13} is small

(at least $< 10^\circ$) we have that $K_{1e} \ll K_{1\mu} = K_{1\tau}$, i.e.

$$K_{1\mu} = K_{1\tau} \sim \frac{m_3}{m^*} \sim 50 \tag{4.74}$$

and

$$\frac{K_{1e}}{K_{1\mu}} = \frac{K_{1e}}{K_{1\tau}} = (\sqrt{2}\theta_{13})^2 \tag{4.75}$$

Consequently, the asymmetries in the τ and in the μ flavours will be almost completely washed out by the N_1 washout related to $K_{1\tau}$ and $K_{1\mu}$. In the e-flavour we have weak N_1-washout. Furthermore, using $\frac{|C_\alpha|^2 v^2}{M_C} \sim m_1$, we obtain at the N_2 decay stage

$$K_{2\tau} \sim \frac{m_1}{m^*}, \quad K_{2\mu} \sim \zeta \frac{m_1}{m^*} \ll K_{2\tau} \quad \text{and} \quad K_{2e} = 0 \tag{4.76}$$

which implies

$$K_{2\gamma} = K_{2\mu} + K_{2e} \ll K_{2\tau} \tag{4.77}$$

The N_2 decay asymmetries, ignoring the contribution with N_1 in the loop which is very small for the considered case that $N_1 \ll N_2$, are given via eq. (3.43) by

$$\varepsilon_{2\alpha} \approx -\frac{3}{16\pi v^2} \frac{M_2}{M_3} \frac{1}{B^\dagger B} \mathrm{Im}\left[B^*_\alpha (B^\dagger C) C_\alpha\right] \tag{4.78}$$

Using B and C as specified above eq. (4.71) and $m_1 \sim \frac{|C_\alpha|^2 v^2}{M_C}$, we obtain for the decay asymmetries $\varepsilon_{2\alpha}$:

$$\varepsilon_{2\tau} \sim -\frac{3}{16\pi v^2} M_2 \, m_2, \quad \varepsilon_{2\mu} = \zeta \varepsilon_{2\tau} \ll \varepsilon_{2\tau}, \quad \varepsilon_{2e} = 0 \tag{4.79}$$

Considering eq. (4.47) and noting that $K_{2e} = 0$ together with $\varepsilon_{2e} = 0$ implies $p_\delta = 0$ we see that all terms apart from the one proportional to $C^{(3)}_{e\tau}$ are strongly suppressed provided that ζ is sufficiently tiny ($\zeta \ll r$). In other words, the considered LSD scenario provides an example for case B, a final asymmetry dominated by flavour coupling effects at the N_1 washout stage, as in eq. (4.49). Explicitly, we obtain for the final asymmetry

$$N^{\mathrm{f}}_{\Delta_{B-L}} \sim -C^{(3)}_{e\tau} \frac{K_{1e}}{K_{1\tau}} \varepsilon_{2\tau} \, \kappa(K_{2\tau}) \sim \frac{3 C^{(3)}_{e\tau}}{16\pi} \frac{M_2 \, m_2}{v^2} (\sqrt{2}\theta_{13})^2 \kappa\left(\frac{m_1}{m^*}\right) \tag{4.80}$$

Here one can see that

$$R \simeq 1 + 0.01\,\zeta^{-1}\left(\frac{\theta_{13}}{10^\circ}\right)^2 \frac{\kappa(m_1/m_\star)}{0.3} \tag{4.81}$$

This case is quite interesting because it shows that, if $\theta_{13} \neq 0$ and $m_1 \gtrsim m_\star$, one can obtain a huge enhancement for $\zeta \to 0$, indicating that accounting for flavour coupling one can have an asymmetry in a situation where one would otherwise obtain basically a zero asymmetry. This happens because part of the tauon asymmetry, thanks to flavour coupling at the lightest RH neutrino wash-out, escapes the wash out from the lightest RH neutrinos.

Chapter 5

Decoherence and the Density Matrix

5.1 The Quantum Theory of Measurement

As Richard Feynman wrote in *Statistical Mechanics, A Set Of Lectures* [83]:

"When we solve a quantum-mechanical problem, what we really do is divide the universe into two parts - the system in which we are interested and the rest of the universe."

I will denote the state of "the system in which we are interested" as $|S\rangle$ and the state of "the rest of the universe" as $|E\rangle$ (the "environment" in which that system is immersed). The total system-environment quantum state $|\Psi_{SE}\rangle$ may be written as a direct product of system and environment states

$$|\Psi_{SE}\rangle = |S\rangle\,|E\rangle \tag{5.1}$$

Given that the initial state of the system (call this $|S^{in}\rangle$) is a coherent state, it may be written as a super-position of the set of basis eigen-kets $\{|s_n\rangle\}$ of an operator $\mathcal{O}_S$ acting upon $|S\rangle$, where n denotes the set of quantum numbers defining the nth eigen-ket in the basis. In a coherent state all $|s_n\rangle$ will have the same phase, which can be eliminated for simplicity by a phase rotation of $|\Psi^{in}_{SE}\rangle$ (the initial state of $|\Psi_{SE}\rangle$).

Hence we may write

$$|S^{in}\rangle = \sum_n \langle s_n|S^{in}\rangle\,|s_n\rangle \tag{5.2}$$

$$|\Psi^{in}_{SE}\rangle = \sum_n \langle s_n|S^{in}\rangle\,|s_n\rangle\,|E\rangle \tag{5.3}$$

In quantum mechanics, the outcomes of physical measurements upon a state Ψ_{SE} can be calculated from the expectation values $\langle\hat{\mathcal{O}}_{SE}\rangle \equiv \langle\Psi_{SE}|\hat{\mathcal{O}}_{SE}|\Psi_{SE}\rangle$ of operators $\hat{\mathcal{O}}_{SE}$. Any measurement of the coherent initial system state $|S^{in}\rangle$ which leaves the state of its environment $|E\rangle$ unperturbed corresponds to an operator of the form $\hat{\mathcal{O}}_{SE} = \hat{\mathcal{O}}_S \otimes \hat{I}_E$, where $\hat{I}_E$ denotes that identity operator leaving $|E\rangle$ invariant. The expectation value of such a measurement can be written as

$$\langle\hat{\mathcal{O}}_{SE}\rangle_{\Psi_{SE}} \equiv \langle\Psi_{SE}|\hat{\mathcal{O}}_{SE}|\Psi_{SE}\rangle = \sum_{nm} \mathcal{C}_n\mathcal{C}^{\star}_m\langle s_n|\hat{\mathcal{O}}_S|s_m\rangle \tag{5.4}$$

For example if $\hat{\mathcal{O}}_S = \hat{\mathcal{H}}_S$, the Hamiltonian of S, then $\langle\hat{\mathcal{O}}_S\rangle$ is the expectation energy of the state $|S\rangle$. The above equation represents an idealised situation whereby an experiment can discover the properties of $|S\rangle$ without any unwanted influences from $|E\rangle$. This idealised situation may not hold in practise - as physicists trying to build a quantum computer know all too well!

An alternative way to formulate quantum mechanics is using the **density matrix** [83]. The density matrix ρ_{SE} corresponding to the state $|\Psi_{SE}\rangle$ is defined as

$$\rho_{SE} \equiv |\Psi_{SE}\rangle\langle\Psi_{SE}| \tag{5.5}$$

One may then define the **reduced density matrix** as the trace of the full density matrix ρ_{SE} over the states of the environment, vis

$$\rho_S \equiv Tr_E\,\rho_{SE} \equiv \langle E|\rho_{SE}|E\rangle \tag{5.6}$$

This tracing procedure amounts to taking a statistical average over the physical impacts of the various system-environment couplings acting upon state $|S\rangle$ between time $t = 0$ and the time at which a property of S is measured. The outcomes of this

measurement (i.e. the expectation values of an operator $\hat{\mathcal{O}}_S$ acting upon $|S\rangle$) may be obtained from ρ_S according to

$$\left\langle \hat{\mathcal{O}}_S \right\rangle = Tr_S \left[\rho_S \hat{\mathcal{O}}_S \right] \equiv \langle S|\rho_S \hat{\mathcal{O}}_S|S\rangle \tag{5.7}$$

The density matrix serves an especially convenient formalism to describe the phenomena of **decoherence**, the subject of the subsequent section (for a nice review on decoherence, see [84]).

Evaluating the expectation values of operators is merely a calculational procedure to obtain the outcomes of quantum measurements, and not a meaningful description of such measurements. What actually happens in "a measurement"? A measurement requires some physical apparatus, A, to become entangled with the system upon which a measurement is being performed. The apparatus state $|A\rangle$ will be the super-position of a set of macroscopically distinct "pointer states" $\{|a_n\rangle\}$. Why macroscopically distinct states? Any suitable measurement apparatus must comprise of these, otherwise we will not perceive distinct outcomes for the measurement. Of course, this is not an explanation of how such macroscopically distinct states arise - that is the subject of the next section - merely the statement that they must arise (somehow) in order for the word "measurement" to have any meaning.

Hence a suitable measurement apparatus $|A\rangle$ comprises some basis of pointer states $\{|a_n\rangle\}$ which "mirror" the set of eigenstates of the system $\{|s_n\rangle\}$. This one–to–one correspondence between system and pointer states implies a system-apparatus state of the following special form (as introduced by Von Neumann [85])

$$|\Psi_{SA}\rangle = \sum_n \mathcal{C}_n |s_n\rangle|a_n\rangle \tag{5.8}$$

Here is a very famous example of such a state, as introduced by Schrodinger [86, 87]:

$$|\Psi_{SA}\rangle = |+\rangle|\text{live cat}\rangle + |-\rangle|\text{dead cat}\rangle \tag{5.9}$$

The cat above makes a good "pointer", because an alive cat corresponds to a particular quantum state (say a spin-up atom $|+\rangle$) whereas a dead cat corresponds to

an orthogonal quantum state (say a spin-down atom $|-\rangle$). Why don't we see a superposition of live and dead cats though? This is resolved by consistently taking into account the role of the environment state $|E\rangle$ in suppressing such superposition states. This is discussed in the next section on decoherence, which explains what makes an "observable" - a distinct macroscopic configuration with definite properties - observable.

A "faithful" measurement of $|S\rangle$ by $|A\rangle$ is one for which $|S\rangle$ is **unaffected by the influence of the environment** that $|A\rangle$ and $|S\rangle$ are embedded within. A formal way of stating this requirement is the notion of **envariance** ("environmentally assisted invariance") as introduced by Zurek [88–91]. If we define two operators as

$$\begin{aligned} \hat{U}_S &\equiv \hat{u}_S \otimes I_E \\ \hat{U}_E &\equiv I_S \otimes \hat{u}_E \end{aligned} \tag{5.10}$$

then a state $|\Psi_{SE}\rangle$ is **envariant** under the operator $\hat{U}_S$ if

$$\hat{U}_S \left(\hat{U}_E |\Psi_{SE}\rangle \right) = |\Psi_{SE}\rangle \tag{5.11}$$

is satisfied. If $\hat{U}_S$ is an envariant operator then its eigenvalues can be "faithfully" measured through subsequent entanglement with a distinct pointer state $|a_n\rangle$ of $|A\rangle$. All "faithful" measurements hence emerge as the macroscopically distinct direct products of three states: the system $|S\rangle$ its environment $|E\rangle$ and an apparatus $|A\rangle$

$$|\Psi_{SEA}\rangle = |S\rangle\,|E\rangle\,|A\rangle \tag{5.12}$$

The above 3-product state has a unique basis due to the tri–decompositional uniqueness theorem. This solves the preferred basis problem - the environment state $|E\rangle$ becomes entangled with states of $|S\rangle$ and $|A\rangle$, thereby selecting a preferred basis for these. The outcomes of measurements - "observables" - are then just the eigenvalues of $|S\rangle$ in the basis where $|S\rangle$ satisfies the "envariance" property.

Hence "observables" are observable by virtue of the fact that other remaining properties of $|S\rangle|A\rangle$ are dissipated through entanglements with $|E\rangle$. The mechanism

for this "dissipation" (known as decoherence) is now explored.

5.2 Decoherence - A Toy Model

The following two-state "toy model" was proposed by Zurek [92] to illustrate the concept of decoherence. For the state $|\Psi_{SE}\rangle \equiv |S\rangle\,|E\rangle$ we are to imagine the "system" as a single atom prepared in the coherent state

$$|S\rangle = a|+\rangle + b|-\rangle \tag{5.13}$$

and the "environment" as a bath of N atoms in a box with either spin up ($|+\rangle = (1,0)^T$) or spin down ($|-\rangle = (0,1)^T$) and with the state vector

$$|E\rangle = \prod_{k=1}^{N} [\alpha_k|+\rangle + \beta_k|-\rangle] \tag{5.14}$$

The Hamiltonian of this system is given by $\mathcal{H} = \mathcal{H}_0 + \mathcal{H}_{int}$, where

$$\mathcal{H}_{int} = \hat{\sigma}_3 \sum_{k=1}^{N} \left[\left(\bigotimes_{j=1}^{k-1} \hat{I} \right) \otimes \hbar\, g_k\, \hat{\sigma}_3 \bigotimes_{j=k+1}^{N} \hat{I} \right] \tag{5.15}$$

This interaction describes the coupling between system (S) and environment (E). If an atom of $|S\rangle$ has the same (opposite) spin as an atom of $|E\rangle$ it couples to with strength $\hbar g_k$ then the energy of the system will be raised (lowered) by an amount $\Delta E_k = +\hbar g_k$, given that $\hat{\sigma}_3\,|\pm\rangle = \pm|\pm\rangle$. I have retained $\hbar$ (and not set $\hbar = 1$) above in order to make it clear that this system-environment coupling alters the energy of the system by some minimum discrete amount, determined by a fundamental constant of nature and hence impossible to arbitrarily reduce to zero (as would be the case in the classical limit $\hbar \to 0$).

Since S is initially prepared in a coherent state we have

$$|\Psi_{SE}^{in}\rangle = [a|+\rangle + b|-\rangle] \bigotimes_{k=1}^{N} [\alpha_k|+\rangle + \beta_k|-\rangle] \tag{5.16}$$

At time t this becomes

$$|\Psi_{SE}(t)\rangle = e^{i\mathcal{H}_{int}t}\,|\Psi_{SE}^{in}\rangle \;=\; a|+\rangle\bigotimes_{k=1}^{N}\left[\alpha_k e^{+i\hbar g_k t}|+\rangle + \beta_k e^{-i\hbar g_k t}|-\rangle\right] + \; b|-\rangle\bigotimes_{k=1}^{N}\left[\alpha_k e^{-i\hbar g_k t}|+\rangle + \beta_k e^{+i\hbar g_k t}|-\rangle\right] \quad (5.17)$$

The state $|\Psi_{SE}(t)\rangle$ above will have a density matrix $\rho_{SE} \equiv |\Psi_{SE}(t)\rangle\langle\Psi_{SE}(t)|$. From this we can calculate the **reduced density matrix** $\rho_S \equiv Tr_E\left[\rho_{SE}\right]$ as:

$$\rho_S = |a|^2|+\rangle\langle+| + |b|^2|-\rangle\langle-| + z(t)ab^\star|+\rangle\langle-| + z^\star(t)a^\star b|-\rangle\langle+| \quad (5.18)$$

where

$$z(t) = \prod_{k=1}^{N}\left[\cos 2g_k t + i(|\alpha_k|^2 - |\beta_k|^2)\sin 2g_k t\right] \quad (5.19)$$

The co-efficients α_k and β_k will satisfy $|\alpha_k|^2 + |\beta_k|^2 = 1$ and have a random distribution of values within the unit circle on the complex plane. This results in the expectation

$$\langle|z(t \gg t_D)|^2\rangle = 2^{-N}\prod_{k=1}^{N}\left[1 + (|\alpha_k|^2 - |\beta_k|^2)^2\right] \sim 2^{\frac{N}{2}} \quad (5.20)$$

where

$$t_D \sim \frac{1}{N}\sum_{k=1}^{N} g_k \quad (5.21)$$

is the 'Decoherence time' - the characteristic time over which the system S becomes entangled with the environment E, such that $\psi(t > t_D) \neq \psi(t = 0)\rangle_E$.

Decoherence is closely analogous to entropy - for example a ball ("the system") is observed to stop bouncing not because its motion is absolutely "lost", but because this is dissipated throughout the many atoms of the floor ("the environment") in a process that is, for all practical purposes, irreversible. A ball in motion is somewhat like a quantum coherent state - it must be carefully prepared and becomes unstable and impermanent once any coupling to the environment is introduced. And so, perhaps the resolution to Schrodinger's cat is that asking: "why don't we see a cat that is both alive and dead?" is the same as asking: "why don't we see a ball

spontaneously bouncing higher and higher?". The answer to both questions being that such states are practically impossible to prepare, given that the environment consists of many unknown degrees of freedom which interact with (and hence over time will randomise or "de–cohere") the component parts of the systems we wish to study.

5.3 Decoherence and Leptogenesis

The rest of this chapter is based upon the paper [7], in which we considered decoherence in leptogenesis scenarios. Decoherence will occur during the production of a Δ_{B-L} asymmetry via leptogenesis, in a manner precisely analogous to the "toy model" of the previous section. The various correspondences between the relevant quantities in leptogenesis and the "toy model" of the previous section are given in the table below:

Table 5.1: Decoherence: toy model vs leptogenesis

quantity	toy model	leptogenesis
system (S)	coherent spin state: $a\|+\rangle + b\|-\rangle$	coherent flavour state: $\|l_i\rangle = \sum_\alpha \langle l_\alpha \| l_i\rangle \| l_\alpha\rangle$
environment (E)	N incoherent atoms	a thermal bath of SM particles
S-E coupling	coupling to kth atom: $\hbar g_k$	Higgs-$\|l_\alpha\rangle$ coupling: $h_{\alpha i}$
decoherence time	$t_D \sim \frac{1}{N}\sum_{k=1}^{N} g_k$	$t_D \sim \frac{1}{\Gamma_{l_\alpha \to e_\alpha + \phi}}$

To describe decoherence we extend the flavour number densities of section 3.2 to flavoured density matrices. Recall that the lepton and anti-lepton number densities evolved according to

$$\frac{dN_\ell}{dz} = \frac{\Gamma_1}{H\,z}\,N_{N_1} - \frac{\Gamma_1^{ID}}{H\,z}\,N_{\ell_1} \qquad \frac{dN_{\bar{\ell}}}{dz} = \frac{\bar{\Gamma}_1}{H\,z}\,N_{N_1} - \frac{\bar{\Gamma}_1^{ID}}{H\,z}\,N_{\bar{\ell}_1} \tag{5.22}$$

We now define a lepton number density matrix $\rho^l_{ij} \equiv |l_i\rangle\langle l_j|$ in the basis $\{l_1,\, l_1^\perp\}$ and an anti-lepton number density matrix $\rho^{\bar{l}}_{ij} \equiv |l_i\rangle\langle l_j|$ in the basis $\{\bar{l}_1,\, \bar{l}_1^\perp\}$. These will

be given explicitly by

$$\rho^l = \begin{pmatrix} 1 & 0 \\ 0 & 0 \end{pmatrix} \qquad\qquad \rho^{\bar{l}} = \begin{pmatrix} 1 & 0 \\ 0 & 0 \end{pmatrix} \tag{5.23}$$

given that the N_1s always decay initially into into $|l_1\rangle$, $|\bar{l}_1\rangle$ states and never into $|l_1^\perp\rangle$, $|\bar{l}_1^\perp\rangle$ states, by definition. If we now define the lepton and anti-lepton number density matrices as $N^l_{ij} \equiv N_{l_1}\,\rho^l_{ij}$ and $N^{\bar{l}}_{ij} \equiv N_{\bar{l}_1}\,\rho^{\bar{l}}_{ij}$ then eq. (5.22) can be recast as a density matrix equation

$$\frac{dN^\ell_{ij}}{dz} = \left(\frac{\Gamma_1}{H\,z}\,N_{N_1} - \frac{\Gamma_1^{ID}}{H\,z}\,N_{\ell_1}\right)\rho^\ell_{ij}\,, \qquad \frac{dN^{\bar{\ell}}_{ij}}{dz} = \left(\frac{\bar{\Gamma}_1}{H\,z}\,N_{N_1} - \frac{\bar{\Gamma}_1^{ID}}{H\,z}\,N_{\bar{\ell}_1}\right)\rho^{\bar{\ell}}_{ij} \tag{5.24}$$

The above equation is only valid in a limit where interactions modifying the lepton number density matrix - the gauge and charge lepton interactions - are negligible. We begin, in the next section, with the case where both these interactions are negligible, before generalising eq. (5.24) to incorporate charged lepton interactions in section 5.3.2 and also gauge interactions in section 5.3.3

5.3.1 Neglecting Both Charged Lepton and Gauge Interactions

In this section we shall simply take eqs. (5.24) for granted. In order to obtain from these an equation for the total $B-L$ asymmetry matrix $N_{B-L} \equiv N^{\bar{\ell}} - N^\ell$, we have first to write the two equations in the same flavour basis, for convenience the lepton flavour basis τ–$\tau_1^\perp$, and then subtract them. The matrix rotating between the unflavoured $\{i,\,j\}$ and flavoured $\{\alpha,\,\beta\}$ lepton basis will be defined by

$$R^{(1)} = \begin{pmatrix} \mathcal{C}_{1\tau} & -\mathcal{C}^\star_{1\tau_1^\perp} \\ \mathcal{C}_{1\tau_1^\perp} & \mathcal{C}^\star_{1\tau} \end{pmatrix} \qquad \bar{R}^{(1)} = \begin{pmatrix} \bar{\mathcal{C}}_{1\tau} & -\bar{\mathcal{C}}^\star_{1\tau_1^\perp} \\ \bar{\mathcal{C}}_{1\tau_1^\perp} & \bar{\mathcal{C}}^\star_{1\tau} \end{pmatrix} \tag{5.25}$$

where the second equalities follow from substituting $|l_i\rangle \equiv \sum_\alpha \mathcal{C}_{i\alpha}|l_\alpha\rangle$ and $|\bar{l}_i\rangle \equiv \sum_\alpha \bar{\mathcal{C}}_{i\alpha}|\bar{l}_\alpha\rangle$ for $\alpha = \tau,\,\tau_1^\perp$. Hence an equation for the $B-L$ asymmetry matrix is given as

$$\frac{dN^{B-L}_{\alpha\beta}}{dz} = \bar{R}^{(1)}_{\alpha i}\,\frac{dN^{\bar{\ell}}_{ij}}{dz}\,\bar{R}^{\dagger\,(1)}_{j\beta} - R^{(1)}_{\alpha i}\,\frac{dN^\ell_{ij}}{dz}\,R^{\dagger\,(1)}_{j\beta} \tag{5.26}$$

whose trace gives the $B-L$ asymmetry N_{B-L}. We can also define a flavoured projection matrix $\mathcal{P}^{(1)}_{\alpha\beta}$ as

$$\mathcal{P}^{(1)} \equiv R^{(1)}\,\rho^{l}\,R^{\dagger\,(1)} = \begin{pmatrix} p_{1\tau} & \mathcal{C}_{1\tau_1^{\perp}}\,\mathcal{C}^{\star}_{1\tau} \\ \mathcal{C}_{1\tau}\,\mathcal{C}^{\star}_{1\tau_1^{\perp}} & p_{1\tau_1^{\perp}} \end{pmatrix} \tag{5.27}$$

$$\overline{\mathcal{P}}^{(1)} \equiv \overline{R}^{(1)}\,\rho^{\bar{l}}\,\overline{R}^{\dagger\,(1)} = \begin{pmatrix} \bar{p}_{1\tau} & \bar{\mathcal{C}}_{1\tau_1^{\perp}}\,\bar{\mathcal{C}}^{\star}_{1\tau} \\ \bar{\mathcal{C}}_{1\tau}\,\bar{\mathcal{C}}^{\star}_{1\tau_1^{\perp}} & \bar{p}_{1\tau_1^{\perp}} \end{pmatrix} \tag{5.28}$$

and a flavoured lepton number density matrix $N^{l}_{\alpha\beta}$ in terms of $R^{(1)}$ above as

$$\begin{aligned} N^{l}_{\alpha\beta} &\equiv R^{(1)}_{\alpha i}\,N^{l}_{ij}\,R^{\dagger\,(1)}_{j\beta} \equiv \mathcal{P}^{(1)}_{\alpha\beta}\,N_{l} \\ N^{\bar{l}}_{\alpha\beta} &\equiv \bar{R}^{(1)}_{\alpha i}\,N^{\bar{l}}_{ij}\,\bar{R}^{\dagger\,(1)}_{j\beta} \equiv \bar{\mathcal{P}}^{(1)}_{\alpha\beta}\,N_{\bar{l}} \end{aligned} \tag{5.29}$$

In terms of these matrices then, eq. 5.26 can be recast, first as

$$\frac{dN^{B-L}_{\alpha\beta}}{dz} = \varepsilon^{(1)}_{\alpha\beta}\,D_1\,\left(N_{N_1} - N^{\rm eq}_{N_1}\right) - W_1\,N_{B-L}\,\left[\frac{\mathcal{P}^{(1)}_{\alpha\beta}\,\Gamma_1 + \overline{\mathcal{P}}^{(1)}_{\alpha\beta}\,\bar{\Gamma}_1}{\Gamma_1 + \bar{\Gamma}_1}\right] \tag{5.30}$$

and then, neglecting terms $\mathcal{O}(\varepsilon_1\,N_{B-L})$ and $\mathcal{O}(\Delta p\,N_{B-L})$, as

$$\frac{dN^{B-L}_{\alpha\beta}}{dz} = \varepsilon^{(1)}_{\alpha\beta}\,D_1\,(N_{N_1} - N^{\rm eq}_{N_1}) - W_1\,N_{B-L}\,\mathcal{P}^{(1)0}_{\alpha\beta} \tag{5.31}$$

where recall that this result has been obtained assuming that there are only ℓ_1 leptons and $\bar{\ell}_1$ anti-leptons. Notice that we defined the *CP* asymmetry matrix for the lightest RH neutrino N_1 as

$$\varepsilon^{(1)} = \frac{\overline{\mathcal{P}}^{(1)}\,\overline{\Gamma}_1 - \mathcal{P}^{(1)}\,\Gamma_1}{\Gamma_1 + \overline{\Gamma}_1} = \varepsilon_1\,\frac{\overline{\mathcal{P}}^{(1)} + \mathcal{P}^{(1)}}{2} - \frac{\Delta\mathcal{P}^{(1)}}{2} \tag{5.32}$$

where $\Delta\mathcal{P}^{(1)} \equiv \overline{\mathcal{P}}^{(1)} - \mathcal{P}^{(1)}$. This expression [93] generalises the eq. (3.43) of section 3.2 that is obtained for the diagonal terms in the charged lepton flavour basis where the diagonal terms simply correspond to the flavoured *CP* asymmetries, $\varepsilon^{(1)}_{\alpha\alpha} = \varepsilon_{1\alpha}$, while the off-diagonal terms obey $\varepsilon^{(1)}_{\alpha\beta} = (\varepsilon^{(1)}_{\beta\alpha})^{\star}$ and are not necessarily real. This expression can be generalised to the *CP* asymmetry matrix $\varepsilon^{(i)}_{\alpha\beta}$, of any RH neutrino species N_i

that in terms of the Yukawa couplings can be written as

$$\varepsilon^{(i)}_{\alpha\beta} = \frac{3}{32\pi(h^\dagger h)_{ii}}\sum_{j\neq i}\{\mathrm{i}\left[h_{\alpha i}h^\star_{\beta j}(h^\dagger h)_{ji} - h^\star_{\beta i}h_{\alpha j}(h^\dagger h)_{ij}\right]\frac{\xi(x_j/x_i)}{\sqrt{x_j/x_i}} + \mathrm{i}\,\frac{2}{3(x_j/x_i-1)}\left[h_{\alpha i}h^\star_{\beta j}(h^\dagger h)_{ij} - h^\star_{\beta i}h_{\alpha j}(h^\dagger h)_{ji}\right]\} \quad (5.33)$$

where the ξ function was defined underneath eq. (3.43). This expression slightly differs from that one in [73, 94] (simply the first term there is minus the imaginary part of the first term written here, so that the off-diagonal terms are real) while it agrees with the expression given in [97].

5.3.2 Including Charged Lepton Interactions

The result eq. (5.31) is valid only in the absence of charged (and gauge) lepton interactions - for $T \gg 10^{12}GeV$. We consider next what happens when tau lepton interactions "turn on" at $T \sim 10^{12}GeV$. Eq. (5.22) then generalises to [73, 95–97]

$$\begin{aligned}\frac{dN^\ell}{dz} &= \frac{\Gamma_1}{H\,z}N_{N_1}\begin{pmatrix}1&0\\0&0\end{pmatrix} - \frac{1}{2}\frac{\Gamma_1^{ID}}{H\,z}\left\{\begin{pmatrix}1&0\\0&0\end{pmatrix}, N^\ell\right\} + \Lambda + G \\ \frac{dN^{\bar\ell}}{dz} &= \frac{\bar\Gamma_1}{H\,z}N_{N_1}\begin{pmatrix}1&0\\0&0\end{pmatrix} - \frac{1}{2}\frac{\bar\Gamma_1^{ID}}{H\,z}\left\{\begin{pmatrix}1&0\\0&0\end{pmatrix}, N^{\bar\ell}\right\} + \bar\Lambda + \bar G \end{aligned} \quad (5.34)$$

where the matrix Λ contains the charged lepton interactions that induce decoherence through and the matrix G contains the gauge interaction which thermalise the leptons to their chemical equilibrium abundances. Using eq. (5.27) the eq. (5.34) may be recast in the flavoured basis as

$$\begin{aligned}\frac{dN^\ell_{\alpha\beta}}{dz} &= \frac{\Gamma_1}{H\,z}N_{N_1}\mathcal{P}^{(1)}_{\alpha\beta} - \frac{1}{2}\frac{\Gamma_1^{ID}}{H\,z}\left\{\mathcal{P}^{(1)}, N^\ell\right\}_{\alpha\beta} + \Lambda_{\alpha\beta} + G_{\alpha\beta} \\ \frac{dN^{\bar\ell}_{\alpha\beta}}{dz} &= \frac{\bar\Gamma_1}{H\,z}N_{N_1}\overline{\mathcal{P}}^{(1)}_{\alpha\beta} - \frac{1}{2}\frac{\bar\Gamma_1^{ID}}{H\,z}\left\{\overline{\mathcal{P}}^{(1)}, N^{\bar\ell}\right\}_{\alpha\beta} + \bar\Lambda_{\alpha\beta} + \bar G_{\alpha\beta}\end{aligned} \quad (5.35)$$

where the $\Lambda_{\alpha\beta}$ and $\bar{\Lambda}_{\alpha\beta}$ matrices are given explicitly in this $\{\tau, \tau_1^{\perp}\}$ basis as

$$\begin{aligned}
\Lambda &= -i\,\frac{\mathrm{Re}(\Lambda_\tau)}{Hz}\begin{pmatrix} 0 & N^l_{\tau\ \tau_1^{\perp}} \\ -N^l_{\tau_1^{\perp}\tau} & 0 \end{pmatrix} - \frac{\mathrm{Im}(\Lambda_\tau)}{Hz}\begin{pmatrix} 0 & N^l_{\tau\ \tau_1^{\perp}} \\ N^l_{\tau_1^{\perp}\tau} & 0 \end{pmatrix} \\
\bar{\Lambda} &= +i\,\frac{\mathrm{Re}(\Lambda_\tau)}{Hz}\begin{pmatrix} 0 & N^{\bar{l}}_{\tau\ \tau_1^{\perp}} \\ -N^{\bar{l}}_{\tau_1^{\perp}\tau} & 0 \end{pmatrix} - \frac{\mathrm{Im}(\Lambda_\tau)}{Hz}\begin{pmatrix} 0 & N^{\bar{l}}_{\tau\ \tau_1^{\perp}} \\ N^{\bar{l}}_{\tau_1^{\perp}\tau} & 0 \end{pmatrix}
\end{aligned} \tag{5.36}$$

The first terms describe flavour oscillations, which precess in opposite senses for particles, with sign $-i$, and anti-particles, with sign $+i$. The second terms describes decoherence via the damping of off-diagonal terms in the N^l matrix. Explicitly the real and imaginary parts of Λ_τ, the tau lepton self-energy, are given by [98, 99]

$$\mathrm{Re}(\Lambda_\tau) \approx \frac{f_\tau^2}{64} T \qquad\qquad \mathrm{Im}(\Lambda_\tau) \approx 8 \times 10^{-3}\, f_\tau^2\, T \tag{5.37}$$

Decoherence - implying here the transition from an un-flavoured to a two-flavoured regime - will start to kick in when its effective "rate" $\mathrm{Im}(\Lambda_\tau)(T)$ is similar to the Hubble rate $H(T) = \sqrt{8\pi^3 g_\star/90}\, T^2/M_{pl}$. This gives an approximate decoherence temperature T_{12} of

$$T_{12} \sim 8 \times 10^{-3}\, f_\tau^2 \sqrt{\frac{90}{8\pi^3 g_\star}}\, M_{pl} \sim 10^{12}\mathrm{GeV} \tag{5.38}$$

given that $f_\tau \sim 10^{-2}$, $g_\star \sim 10^2$ and $M_{pl} \sim 10^{19}$GeV.

This result justifies our earlier treatment in section 3.2, where we regarded the temperature $T_{12} \sim 10^{12} GeV$ as a transition temperature between unflavoured and two-flavoured regimes. Taking $T \gg 10^{12} GeV$ we would expect to recover the set of unflavoured Boltzmann equations from eq. (5.35), since decoherence effects in the Λ-matrix term are then negligible. Conversely, taking $T \ll 10^{12} GeV$ we would expect to recover the two-flavoured Boltzmann equations from eq. (5.35), since decoherence effects from the Λ-matrix term are then strong.

5.3.3 Including Both Charged Lepton and Gauge Interactions

If we now take into account the effect of gauge interactions, these will thermalise not only the abundances of the leptons ℓ_1 and of the anti-leptons $\bar{\ell}_1$, independently of the strength of the Yukawa interactions and of the RH neutrino abundance, but also the abundances of their orthogonal states $\ell_{1^\perp}$ and $\bar{\ell}_{1^\perp}$. Since they are flavour blind and *CP* conserving, their presence is described by an additional unflavoured term in the lepton and anti-lepton abundance matrices that in this way get generalised as

$$\begin{aligned} N^{\ell} &= N^{\ell}_{\rm eq}\, I + N_{\ell_1}\, \mathcal{P}^{(1)} - \frac{N_{\ell_1} + N_{\bar{\ell}_1}}{2}\, \mathcal{P}^{(1)0} \\ N^{\bar{\ell}} &= N^{\ell}_{\rm eq}\, I + N_{\bar{\ell}_1}\, \overline{\mathcal{P}}^{(1)} - \frac{N_{\ell_1} + N_{\bar{\ell}_1}}{2}\, \mathcal{P}^{(1)0} \end{aligned} \tag{5.39}$$

The third terms in the right-hand side describe how annihilation's mediated by gauge interactions drag out of the ℓ_1 and $\bar{\ell}_1$ their tree-level components, *CP* conjugated of each other, that are thermalised [1]. In this way the gauge interactions annihilations act as a sort of detector of the differences of flavour compositions of leptons and anti-leptons, though they cannot measure the flavour compositions themselves, as implied by the term $N^{\rm eq}_{\ell}\, I$ that is invariant under rotations in flavour space. One could wonder whether instead of the tree level components $\propto \mathcal{P}^{(1)0}$ one should subtract, for example, the average components $\propto \left(\overline{\mathcal{P}}^{(1)} + \mathcal{P}^{(1)}\right)/2$. However one can verify that the same result is obtained unless $\mathcal{O}(\Delta P^2)$ terms. If we now write N_{ℓ_1} and $N_{\bar{\ell}_1}$ in terms of their symmetric and anti-symmetric parts as

$$N_{\ell_1} = \left(\frac{N_{\ell_1} + N_{\bar{\ell}_1}}{2}\right) - \frac{1}{2} N_{\Delta_{B-L}}\,, \qquad N_{\bar{\ell}_1} = \left(\frac{N_{\ell_1} + N_{\bar{\ell}_1}}{2}\right) + \frac{1}{2} N_{\Delta_{B-L}} \tag{5.40}$$

[1] The third term cancels the CP–even part of the second term (as can be seen substituting eq. 5.40) given that the gauge bosons re–equilibrate the CP–even part of eq. 5.39, but cannot touch the CP–odd part.

then eqs. (5.39) can be recast as [2]

$$\begin{aligned} N^{\ell} &= N^{\ell}_{\rm eq}\, I + \left(\frac{N_{\ell_1} + N_{\bar{\ell}_1}}{2}\right) (\mathcal{P}^{(1)} - \mathcal{P}^{(1)0}) - \frac{1}{2}\, N_{\Delta_{B-L}}\, \mathcal{P}^{(1)} \\ N^{\bar{\ell}} &= N^{\ell}_{\rm eq}\, I + \left(\frac{N_{\ell_1} + N_{\bar{\ell}_1}}{2}\right) (\overline{\mathcal{P}}^{(1)} - \mathcal{P}^{(1)0}) + \frac{1}{2}\, N_{\Delta_{B-L}}\, \overline{\mathcal{P}}^{(1)} \end{aligned} \tag{5.41}$$

From these equations one can find an expression for the asymmetry matrix,

$$N^{B-L} = \frac{N_{\ell_1} + N_{\bar{\ell}_1}}{2}\, \left(\overline{\mathcal{P}}^{(1)} - \mathcal{P}^{(1)}\right) + \frac{N_{\Delta_{B-L}}}{2}\, \left(\mathcal{P}^{(1)} + \overline{\mathcal{P}}^{(1)}\right) \tag{5.42}$$

that has to be compared with the eq. (5.32) for the *CP* asymmetry matrix: the first term gives the contribution to the flavour asymmetries from the difference in flavour compositions, the phantom terms, while the second term is the usual contributions proportional to the total asymmetry. Notice that the quantity $(N_{\ell_1} + N_{\bar{\ell}_1})/2$ has to be regarded as a dynamical quantity, like the total asymmetry $N_{\Delta_{B-L}}$. We can also write an expression for the sum

$$N^{\ell+\bar{\ell}} \equiv N^{\ell} + N^{\bar{\ell}} = 2\, N^{\ell}_{\rm eq}\, I + \frac{N_{\ell_1} + N_{\bar{\ell}_1}}{2}\, \left(\delta\mathcal{P}^{(1)} + \delta\overline{\mathcal{P}}^{(1)}\right) + \frac{N_{\Delta_{B-L}}}{2}\, \left(\overline{\mathcal{P}}^{(1)} - \mathcal{P}^{(1)}\right) \tag{5.43}$$

where we defined $\delta\mathcal{P}^{(1)} \equiv \mathcal{P}^{(1)} - \mathcal{P}^{(1)0}$ and $\delta\overline{\mathcal{P}}^{(1)} \equiv \overline{\mathcal{P}}^{(1)} - \mathcal{P}^{(1)0}$. Considering that in the tree level basis one has $(i_0, j_0 = 1_0, 1_0^{\perp})$

$$\delta\mathcal{P}^{(1)}_{i_0 j_0} = \begin{pmatrix} 0 & \delta p \\ \delta p^{\star} & 0 \end{pmatrix} \tag{5.44}$$

with $\delta p = \mathcal{C}^0_{1\tau_1^{\perp}}\, \delta\mathcal{C}_{1\tau} - \mathcal{C}^0_{1\tau}\, \delta\mathcal{C}_{1\tau_1^{\perp}}$ and $\delta\mathcal{C}_{1\alpha} \equiv \mathcal{C}_{1\alpha} - \mathcal{C}^0_{1\alpha}$, one obtains the equalities

$$\left\{\mathcal{P}^{(1)}, \delta\mathcal{P}^{(1)}\right\} = \delta\mathcal{P}^{(1)} + \mathcal{O}(\delta\mathcal{P}^2)\,, \quad \left\{\overline{\mathcal{P}}^{(1)}, \delta\overline{\mathcal{P}}^{(1)}\right\} = \delta\overline{\mathcal{P}}^{(1)} + \mathcal{O}(\delta\overline{\mathcal{P}}^2) \tag{5.45}$$

[2] Notice that now these equations also describe consistently the case of vanishing initial RH neutrino abundance that yields seemingly unphysical negative values of $N_{\ell_1} + N_{\bar{\ell}_1}$ since now these correspond to the production of the orthogonal states $\ell_{1^{\perp}}$ and $\bar{\ell}_{1^{\perp}}$, considering that $\mathcal{P}^{(1)} = I - \mathcal{P}^{(1)}_{\perp}$, $\mathcal{P}^{(1)0} = I - \mathcal{P}^{(1)0}_{\perp}$ and analogously for the anti-leptons.

and neglecting terms $\mathcal{O}(\varepsilon\,\Delta P)$ and $\mathcal{O}(\delta\mathcal{P}^2)$, one arrives at the following equation

$$\begin{aligned}\frac{dN^{B-L}}{dz} = \varepsilon^{(1)}\,D_1\,(N_{N_1} - N_{N_1}^{\rm eq}) \;&-\; \frac{1}{2}\,W_1\,\frac{N_{\ell_1} + N_{\bar{\ell}_1}}{2}\,\left(\overline{\mathcal{P}}^{(1)} - \mathcal{P}^{(1)}\right) \\ &-\; W_1\,\frac{N_{\Delta_{B-L}}}{2}\,\left(\mathcal{P}^{(1)} + \overline{\mathcal{P}}^{(1)}\right) \end{aligned} \tag{5.46}$$

Using the eqs. (5.45), it can be also recast more compactly as [3]

$$\frac{dN^{B-L}}{dz} = \varepsilon^{(1)}\,D_1\,(N_{N_1} - N_{N_1}^{\rm eq}) - \frac{1}{2}\,W_1\,\left\{\mathcal{P}^{0(1)}, N^{B-L}\right\} \tag{5.47}$$

The eq. (5.46) implies that, having accounted for the unflavoured thermal bath from gauge interactions, phantom terms are washed out - contrarily to the calculation in section 4 from chapter 3, where the effects of gauge interactions were not taken into account. However, non trivially, the wash-out term acting on phantom terms is **half** compared to that one acting on the total asymmetry. Let us show this result explicitly, finding the solutions for the diagonal components in the charged lepton flavour basis, $N^{B-L}_{\tau\tau}$ and $N^{B-L}_{\tau_1^\perp\tau_1^\perp}$. If one first considers the eq. (5.47) in the tree level basis, in this basis the decomposition of $\varepsilon^{(1)}$ in the right-hand side of eq. (5.32) specialises into

$$\varepsilon^{(1)}_{i_0 j_0} = \begin{pmatrix} \varepsilon_1 & 0 \\ 0 & 0 \end{pmatrix} + \begin{pmatrix} 0 & \delta\varepsilon \\ \delta\varepsilon^\star & 0 \end{pmatrix} \tag{5.48}$$

where $\delta\varepsilon = (\delta\bar{p} - \delta p)/2 = \Delta p/2$. In this way in this basis the $1_0 1_0$ term is just the total asymmetry $N_{\Delta_{B-L}}$ that gets washed out by W_1. Instead the off-diagonal terms, upon rotation to the charged lepton flavour basis, give the phantom terms that are washed by $W_1/2$. In this way, in the charged lepton flavour basis, one finds

$$\begin{aligned} N^{B-L,{\rm f}}_{\tau\tau} &\simeq p^0_{1\tau}\,N^{\rm f}_{\Delta_{B-L}} + \frac{\Delta p_{1\tau}}{2}\,\kappa(K_1/2) \\ N^{B-L,{\rm f}}_{\tau_1^\perp\tau_1^\perp} &\simeq p^0_{1\tau_1^\perp}\,N^{\rm f}_{\Delta_{B-L}} - \frac{\Delta p_{1\tau}}{2}\,\kappa(K_1/2) \end{aligned} \tag{5.49}$$

This result confirms the presence of phantom terms but it also clearly shows how the effect of the gauge interactions annihilations in detecting the differences between

[3] We wish to thank M. Herranen and B. Garbrecht for pointing out that the eq. (5.47) implies some wash-out of the phantom terms and that, therefore, is not equivalent to the eq. (5.31) taking into account the differences of lepton and anti-lepton flavour compositions.

lepton and anti-lepton flavour compositions, results into a wash-out of the phantom terms, though with a wash-out rate that is halved compared to the wash-out rate acting on the total asymmetry. If we next consider a generic three RHN mass patterns with masses $M_i \gg 10^6\,\mathrm{GeV}$, the set of density matrix equations eqs. (5.35) further generalises. It can be written explicitly in the $\{e,\,\mu,\,\tau\}$ basis (in which the charged lepton matrices Λ of eqs. (5.35) take a simple definite form) as [7]

$$\begin{aligned}
\frac{dN^{B-L}_{\alpha\beta}}{dz} &= \varepsilon^{(1)}_{\alpha\beta}\, D_1\,(N_{N_1} - N^{\rm eq}_{N_1}) - \frac{1}{2}\, W_1\, \left\{\mathcal{P}^{(1)0}, N^{B-L}\right\}_{\alpha\beta} \\
&+ \varepsilon^{(2)}_{\alpha\beta}\, D_2\,(N_{N_2} - N^{\rm eq}_{N_2}) - \frac{1}{2}\, W_2\, \left\{\mathcal{P}^{(2)0}, N^{B-L}\right\}_{\alpha\beta} \\
&+ \varepsilon^{(3)}_{\alpha\beta}\, D_3\,(N_{N_3} - N^{\rm eq}_{N_3}) - \frac{1}{2}\, W_3\, \left\{\mathcal{P}^{(3)0}, N^{B-L}\right\}_{\alpha\beta} \\
&- {\rm Im}(\Lambda_\tau) \left[\left(\begin{array}{ccc} 1 & 0 & 0 \\ 0 & 0 & 0 \\ 0 & 0 & 0 \end{array}\right), \left[\left(\begin{array}{ccc} 1 & 0 & 0 \\ 0 & 0 & 0 \\ 0 & 0 & 0 \end{array}\right), N^{B-L}\right]\right]_{\alpha\beta} \\
&- {\rm Im}(\Lambda_\mu) \left[\left(\begin{array}{ccc} 0 & 0 & 0 \\ 0 & 1 & 0 \\ 0 & 0 & 0 \end{array}\right), \left[\left(\begin{array}{ccc} 0 & 0 & 0 \\ 0 & 1 & 0 \\ 0 & 0 & 0 \end{array}\right), N^{B-L}\right]\right]_{\alpha\beta}
\end{aligned} \tag{5.50}$$

for $\alpha, \beta = \tau, \mu, e$. The effect of gauge interactions is implicit in the above: they set a condition of thermal equilibrium on the abundances of the leptons and anti-leptons, leading to the anti-commutator structure of the washout terms (and the resulting "half-washout" of the phantom terms). If one of the three masses is lower than $\sim 10^6\,\mathrm{GeV}$, electron flavour interactions terms have to be included as well, though they have no real impact, within this framework, on the final asymmetry. This is because the electron asymmetry is in any case already measured as a 'neither-muon-nor-tauon' asymmetry.

This "master equation" can now be used to calculate the final asymmetry not only for all the ten mass patterns shown in fig. 3.4 of section 3.4, but also when the M_i's fall in one of the flavour transition regimes. Note that although in this thesis I am only considering hierarchical RH neutrino mass patterns, the eqs. (5.50) can also be used to calculate the asymmetry beyond the hierarchical limit [100]

and even in the resonant case [101]. In this latter case, however, many different effects can become important and should be included [102]. Solutions of this set of equations are particularly difficult when at least two of the five kinds of interactions are simultaneously effective, something that goes beyond our objectives. The aim of the subsequent sections of this chapter are more modest: to recover some of the results already derived in previous chapters in the limits where we expect the Boltzmann equations to be a good approximation to the full density matrix equations above.

5.4 From Density Matrix to Boltzmann Equations

As a consistency check that the "master equation" eq. (5.50) we derived at the end of the last section is correct, we can now rederive the more familiar basis-dependant Boltzmann equations of the previous two chapters as limiting cases of it. We first consider an unflavoured case with two RHNs at $T \gg 10^{12} GeV$. This is the "heavy flavoured scenario" we considered in section 3.5 of chapter 4. We shall also confirm that the "phantom terms" found in that section can also emerge in the density matrix formalism, but are partially washed out when gauge bosons interactions are consistently taken into account.

We shall consider two cases: first we revisit the heavy flavoured scenario of section 3.5 only this time in the density matrix formalism. We show how to rederive eq. 3.75 this time with phantom terms modified by a factor of $\kappa(\frac{K_2}{2})$ due to the "half-washout" by gauge bosons. Next we shall consider a new case - the two-flavoured two right-handed neutrino model. The equations we derive, including phantom terms, shall be extensively studied in chapter 6.

5.4.1 Density Matrix Equations for the Heavy Flavoured Scenario

The heavy flavoured scenario involved the mass spectrum $M_2 \gtrsim 3\, M_1 \gg 10^{12}\,\mathrm{GeV}$, where $M_2 \gtrsim 3\, M_1$ recovers the hierarchical limit [100] and we can assume for simplicity that $M_3 \gg 10^{14} GeV$ and so N_3 decouples. Note also that tauon flavoured interactions are out of equilibrium for $T \gg 10^{12} GeV$ during leptogenesis, so the Λ_τ

term (and of course then the Λ_μ term also) of the previous section can be "thrown away" as negligible. Hence eq. (5.50) simplifies down to the set of equations below

$$\begin{aligned}\frac{dN^{B-L}}{dz} &= \varepsilon^{(1)} D_1 \left(N_{N_1} - N_{N_1}^{\rm eq}\right) - \frac{1}{2} W_1 \left\{\mathcal{P}^{(1)0}, N^{B-L}\right\} \\ &+ \varepsilon^{(2)} D_2 \left(N_{N_2} - N_{N_2}^{\rm eq}\right) - \frac{1}{2} W_2 \left\{\mathcal{P}^{(2)0}, N^{B-L}\right\} \end{aligned} \tag{5.51}$$

where we have kept the above basis independent, rather than choosing to project into the $\{e, \mu, \tau\}$ basis of eqs. (5.50). There is now a potential ambiguity upon choosing a new flavour basis $\{\alpha, \beta\}$ into which the basis independant eqs. (5.51) above are to be projected. In general, the basis $\ell_1 - \ell_1^\perp$ does not coincide with $CP(\bar{\ell}_1 - \bar{\ell}_1^\perp)$ because the anti-lepton states that the N_1 decay into are in general **not** CP conjugates of the lepton states - that is why there are differences between lepton and anti-lepton flavour compositions (and hence "phantom terms") in the first place! However the states $|1\rangle$ and $CP|\bar{1}\rangle$ **do** coincide at tree level and so if we project into the tree level basis $1^0 - 1^{0\perp}$ then eq (5.51) can consistently describe both N_2 and N_1 processes. In this basis then

$$|2\rangle = \langle 1^0|2\rangle\,|1^0\rangle + \langle 1^{0\perp}|2\rangle\,|1^{0\perp}\rangle \quad \text{and} \quad |\bar{2}\rangle = \langle \bar{1}^0|\bar{2}\rangle\,|\bar{1}^0\rangle + \langle \bar{1}^{0\perp}|\bar{2}\rangle\,|\bar{1}^{0\perp}\rangle \tag{5.52}$$

and therefore, writing eq. (5.51) in this basis, we have at the production ($i_1^0, j_1^0 = 1^0, 1^{0\perp}$)

$$\frac{dN^{B-L}_{i_1^0 j_1^0}}{dz} = \varepsilon^{(2)}_{i_1^0 j_1^0} D_2 \left(N_{N_2} - N_{N_2}^{\rm eq}\right) - \frac{1}{2} W_2 \left\{\mathcal{P}^{(2)0}, N^{B-L}\right\}_{i_1^0 j_1^0} \tag{5.53}$$

where as usual the superscript "0" indicates the tree level quantities that can be approximately fully employed in the calculation of the washout term. The projection matrices $\mathcal{P}^{(2)}_{i_1^0 j_1^0}$ and $\bar{\mathcal{P}}^{(2)}_{i_1^0 j_1^0}$ are given explicitly by

$$\begin{aligned}\mathcal{P}^{(2)}_{i_1^0 j_1^0} &= \begin{pmatrix} p_{1^0 2} & \langle 1^0|2\rangle\langle 2|1^{0\perp}\rangle \\ \langle 1^{0\perp}|2\rangle\langle 2|1^0\rangle & 1 - p_{1^0 2} \end{pmatrix} \\ \bar{\mathcal{P}}^{(2)}_{i_1^0 j_1^0} &= \begin{pmatrix} \bar{p}_{1^0 2} & \langle \bar{1}^0|\bar{2}\rangle\langle \bar{2}|\bar{1}^{0\perp}\rangle \\ \langle \bar{1}^{0\perp}|\bar{2}\rangle\langle \bar{2}|\bar{1}^0\rangle & 1 - \bar{p}_{1^0 2} \end{pmatrix} \end{aligned} \tag{5.54}$$

where $p_{1^0 2} \equiv |\langle 1^0|2\rangle|^2$ and $\bar{p}_{1^0 2} \equiv |\langle \bar{1}^0|\bar{2}\rangle|^2$. What about $\varepsilon^{(2)}_{i^0_1 j^0_1}$ in eq. (5.53) ? Recalling the general, basis independent eq. (5.53) for $\varepsilon^{(i)}$ one finds for the diagonal components in the $\{1^0,\, 1^0_\perp\}$ basis

$$\varepsilon^{(2)}_{1^0 1^0} = p^0_{1^0 2}\varepsilon_2 + \frac{\Delta p_{1^0 2}}{2} \quad \text{and} \quad \varepsilon^{(2)}_{1^0 1^0} = (1 - p^0_{1^0 2})\varepsilon_2 - \frac{\Delta p_{1^0 2}}{2} \tag{5.55}$$

and hence integrating eqs. (5.53) one obtains the diagonal components of the $B - L$ asymmetry matrix after N_2 decay, but prior to N_1 washout, as

$$\begin{aligned} N^{B-L}_{1^0 1^0}(T \simeq T_{B2}) &\simeq p^0_{12}\,\varepsilon_2\,\kappa(K_2) - \frac{\Delta p_{21^0}}{2}\,\kappa(K_2/2) \\ N^{B-L}_{1^0_\perp 1^0_\perp}(T \simeq T_{B2}) &\simeq (1 - p^0_{12})\,\varepsilon_2\,\kappa(K_2) + \frac{\Delta p_{21^0}}{2}\,\kappa(K_2/2) \end{aligned} \tag{5.56}$$

where notice that having identified $\Delta p_{21^0} \equiv |\langle 1^0|2\rangle|^2 - |\langle \bar{1}^0|\bar{2}\rangle|^2$ we have recovered the "phantom terms" derived in section 3.5, but modified by washouts of $\kappa\left(\frac{K_2}{2}\right)$ due to taking into account the gauge bosons. Finally, taking into account the lightest RH neutrino washout and asymmetry production, we obtain for the final asymmetry

$$\begin{aligned} N^{\rm f}_{B-L} = \varepsilon_1\,\kappa(K_1) &+ \left[p^0_{12}\, e^{-\frac{3\pi}{8} K_1} + (1 - p^0_{12})\right]\,\varepsilon_2\,\kappa(K_2) \\ &+ \left(1 - e^{-\frac{3\pi}{8} K_1}\right)\,\frac{\Delta p_{21^0}}{2}\,\kappa(K_2/2) \end{aligned} \tag{5.57}$$

Therefore, the phantom terms give an additional contribution to both components and in particular to the orthogonal component. If $K_1 \ll 1$, both the parallel and the orthogonal components are unwashed and the phantom terms cancel with each other. On the other hand, in the opposite case, for $K_1 \gg 1$, the parallel component is completely washed out so that only the orthogonal one survives (together with the additional N_1-unwashed phantom term contribution). Finally, it should be clear that an account of the different flavour compositions of the ℓ_1 and $\bar{\ell}_1$ quantum states at the production from N_1, would lead to additional phantom terms. These, however, cancel with each other and do not contribute to the final asymmetry.

5.4.2 Density Matrix Equations for Two-Flavoured 2RHN Model

We consider a two RHN model [103] corresponding to a situation where M_3 is sufficiently large ($M_3 \gg 10^{14}\,\mathrm{GeV}$) to decouple in the seesaw formula for the calculation of the neutrino masses [104]. In order to reproduce the observed baryon asymmetry one has to impose $M_1 \gtrsim 10^9\,\mathrm{GeV}$ so that the muon interactions can be neglected in the Eqs. (5.50) On the other hand, in order to have M_1 and M_2 as low as possible, it is interesting to consider the case $10^{12}\,\mathrm{GeV} \gg M_2 \gtrsim 3\,M_1 \gg 3\times 10^9\,\mathrm{GeV}$ in a way to obtain a RHN mass spectrum corresponding to the third panel (from upper left) in Fig. 3.4.

This model has been recently revisited in [8]. We want here to re-derive, starting from the density matrix equations eqs. (5.50), the Boltzmann kinetic equations and the consequent formula for the final asymmetry that in [8] has been used to calculate the value of M_1 necessary to reproduce the observed baryon asymmetry [4].

Thanks to the hierarchical limit, we can again introduce different simplifications. First of all we can impose the complete damping of the $\tau\alpha$ and $\alpha\tau$ ($\alpha \neq \tau$) off-diagonal terms in the asymmetry matrix.

Second, we can consider the N_2 production at $T \simeq T_{B2}$. With these assumptions, only the N_2-terms can be considered in the Eq. (5.50) and the asymmetry matrix can be treated as a 2×2 matrix in τ–$\tau_2^\perp$ flavour space. In this way the density matrix equations reduce to a set of two Boltzmann equations in an effective two fully flavoured regime,

$$\frac{dN^{B-L}_{\tau\tau}}{dz} = \varepsilon^{(2)}_{\tau\tau}\, D_2\,(N_{N_2} - N^{\mathrm{eq}}_{N_2}) - p^0_{2\tau}\, W_2\, N^{B-L}_{\tau\tau} \tag{5.58}$$

$$\frac{dN^{B-L}_{\tau_2^\perp\tau_2^\perp}}{dz} = \varepsilon^{(2)}_{\tau_2^\perp\tau_2^\perp}\, D_2\,(N_{N_2} - N^{\mathrm{eq}}_{N_2}) - p^0_{2\tau_2^\perp}\, W_2\, N^{B-L}_{\tau_2^\perp\tau_2^\perp} \tag{5.59}$$

Integrating the above, one finds after the N_2 production stage

$$N^{B-L}_{\tau\tau}(T \simeq T_{B2}) = \varepsilon_{2\tau}\,\kappa(K_{2\tau}) \quad \text{and} \quad N^{B-L}_{\tau_2^\perp\tau_2^\perp}(T \simeq T_{B2}) = \varepsilon_{2\tau_2^\perp}\,\kappa(K_{2\tau^\perp}) \tag{5.60}$$

[4] It has been shown in [8] that even the N_2 production depends just on M_1 and not on M_2, provided that this is much smaller than $10^{12}\,\mathrm{GeV}$.

The $\tau_2^\perp$ component of the asymmetry at the end of the N_2 production has now to be decomposed into a $\tau_1^\perp$ parallel component and into a $\tau_1^\perp$ orthogonal component that we indicate with the symbol $\tau_{1^\perp}^\perp$. In this way one finds that the final asymmetry is the sum of three flavour components (cf. fig. 5.1),

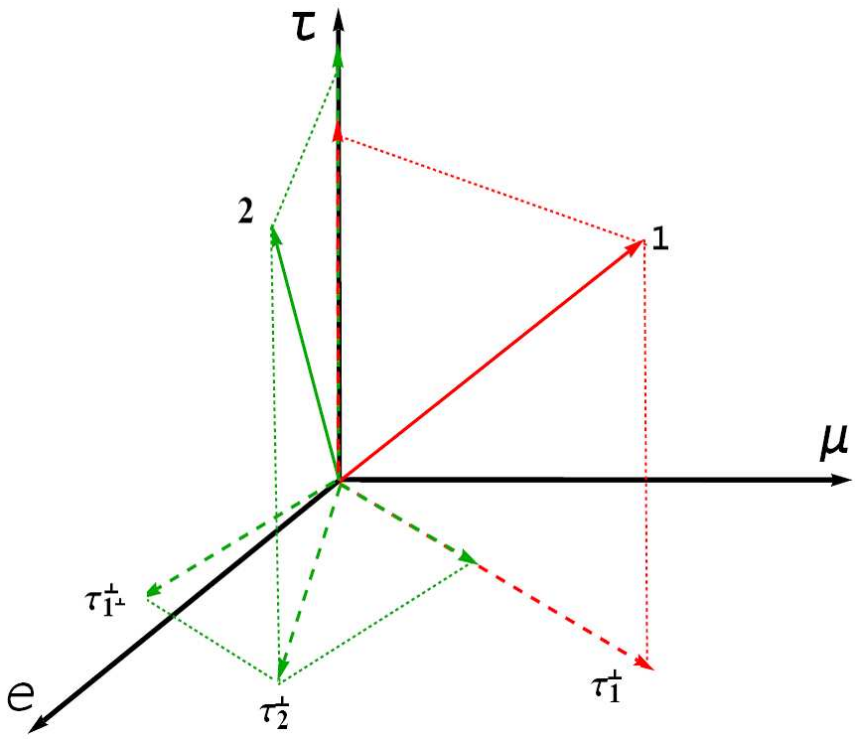

Figure 5.1: Relevant lepton flavours in the two RHN model.

$$N_{B-L}^{\rm f} = N_{\tau\tau}^{B-L}(T \simeq T_{B1}) + N_{\tau_1^\perp\tau_1^\perp}^{B-L}(T \simeq T_{B1}) + N_{\tau_{1^\perp}^\perp\tau_{1^\perp}^\perp}^{B-L}(T \simeq T_{B1}) \tag{5.61}$$

where following the same steps as lead to eq. (5.57) one finds

$$\begin{aligned} N_{B-L}^{\rm f} &= \varepsilon_{1\tau}\,\kappa(K_{1\tau}) + \varepsilon_{2\tau}\,\kappa(K_{2\tau})\,e^{-\frac{3\pi}{8}K_{1\tau}} \\ &+ \varepsilon_{1\tau_1^\perp}\,\kappa(K_{1\tau_1^\perp}) + \left(p^0_{\tau_1^\perp\tau_2^\perp}\varepsilon_{2\tau_2^\perp}\,\kappa(K_{2\tau_2^\perp}) - \frac{\Delta p_{\tau_2^\perp\tau_{1^0}^\perp}}{2}\,\kappa(K_{2\tau_2^\perp}/2)\right) e^{-\frac{3\pi}{8}K_{1\tau_1^\perp}} \\ &+ \left(1 - p^0_{\tau_1^\perp\tau_2^\perp}\right)\varepsilon_{2\tau_2^\perp}\,\kappa(K_{2\tau_2^\perp}) + \frac{\Delta p_{\tau_2^\perp\tau_{1^0}^\perp}}{2}\,\kappa(K_{2\tau_2^\perp}/2) \end{aligned} \tag{5.62}$$

where each of the three lines corresponds respectively to the τ, $\tau_1^\perp$ and $\tau_{1^\perp}^\perp$ components and where now $\Delta p_{\tau_2^\perp\tau_{1^0}^\perp} \equiv |\langle\tau_{1^0}^\perp|\tau_2^\perp\rangle|^2 - |\langle\bar\tau_{1^0}^\perp|\bar\tau_2^\perp\rangle|^2$. This last example shows, once more, how phantom terms are present whenever the production occurs either in one or in a two flavour regime, though only those generated by the heavier RHNs

can be afterwards asymmetrically washed out by the lighter RHNs and contribute to the final asymmetry without canceling with each other. The eq. (5.62) is therefore a second example where "phantom terms" appear and one can check that the general comments made at the end of section 3.5 - then motivated by the heavy flavoured scenario - also apply to the 2-flavoured 2RHN model. We shall use eq. (5.62) extensively in the next chapter "revisit" the 2RHN model, studying it in greater generality by including for the first time the role of N_2 dynamics and finally phantom terms.

Chapter 6

The Two Right Handed Neutrino Model

6.1 Two or Three Right Handed Neutrinos?

What is the two right-handed neutrino model? Back in section 1.2 I discussed the experimental data taken from neutrino oscillation experiments. That data was summarised in table 1.3 which gave **two** mass splittings measured in neutrino oscillation experiments. Since neutrino oscillations are sensitive to mass **differences** only, we do not yet know the mass of the lightest neutrino. Recall also that in section 1.4 we discussed the seesaw mechanism, which obtains the new light neutrino scales as an effective field theory low-energy limit of new heavy mass scales, arising from RHN Majorana mass terms. If there are only two new RHNs at high energy then two new light scales emerge in the low energy effective field theory limit. This is the 2RHN model [105, 106]. The 2RHN model can account for the data provided that the mass of the lightest neutrino is exactly zero and hence the splittings measured in neutrino experiments are equal to the two non-zero masses of the next-to-lightest and heaviest light neutrinos.

The key point in favour of the 2RHN model vs a 3RHN model is its increased predictiveness, due to fewer high energy (free) parameters - leading for example to testable relations between lepton flavour violating decay rates [107]. Of course, this

predictiveness comes at the price of losing the flexibility to describe three non-zero light neutrino masses. As such the 2RHN model may be ruled out by experiments such as KATRIN in the coming years [40]. One might also object on theoretical grounds - for example in the context of Grand Unification (see chapter VII of [48] for an introduction) it can be noticed that the 15 SM matter representations (cf. table 1.2) + 1 additional gauge singlet - the RHN - fit neatly into three 16s of $SO(10)$ - one for each generation. But this is no longer works if there are only two RHNs. However the 2RHN model can also be regarded as a limiting case of a 3RHN model in which one of the RHNs decouples, as occurs upon making the sequential dominance ansatz described back in section 1.5. In this chapter, based largely upon the paper [8], we shall consider case where the heaviest RHN decouples entirely, as happens for $M_3 \gg 10^{14}$GeV and corresponding to light sequential dominance. But first, a convenient parametrisation of the seesaw mechanism is developed.

6.2 The Orthogonal Parametrisation

For this section I will consider a general case of 3 lots ν_L and N lots of N_R in the seesaw Lagrangian, given below

$$\mathcal{L}_{Seesaw} = \mathcal{L}_{SM} - Y^{\nu}_{i\alpha}\,\bar{N}_i\,\phi\,L_\alpha - \frac{1}{2}M_{ij}\bar{N}_i\bar{N}_j + \text{h.c.} \quad i = 1,\,2,\,...,\,N \quad \alpha = e,\,\mu,\,\tau \tag{6.1}$$

Our aim here is to find a parametrisation of the seesaw mechanism that identifies which of the various parameters of $Y^{\nu}_{\alpha i}$ become relevant in the low energy effective field theory limit of $\mathcal{L}_{seesaw}$ above and which do not. This is exactly what the **orthogonal parametrisation**, as developed by Casas and Ibarra [108], does. Our first step is to define a 3×3 matrix U and an $N \times N$ U_M according to

$$|\nu_\alpha\rangle \equiv \sum_{j=1}^{3}\langle\nu_j|\nu_\alpha\rangle\,|\nu_j\rangle \equiv \sum_{j=1}^{3}U^{\star}_{\alpha j}\,|\nu_j\rangle \tag{6.2}$$

$$|N_\alpha\rangle \equiv \sum_{j=1}^{N}\langle N_j|N_\alpha\rangle\,|N_j\rangle \equiv \sum_{j=1}^{N}(U_M)^{\star}_{\alpha j}\,|N_j\rangle \tag{6.3}$$

such that U and U_M rotate between the mass and flavour basis of ν_L and N_R respectively. U and U_M diagonalise the ν_L and N_R Majorana mass matrices

$$\begin{aligned} U^\dagger m_\nu U^\star &\equiv D_k \\ U_M^\dagger M U_M^\star &\equiv D_M \end{aligned} \tag{6.4}$$

where we have defined the diagonal matrices $D_k = \text{diag}(m_1, m_2, m_3)$ and $D_M = \text{diag}(M_1, M_2, ..., M_N)$. In the basis where Y^e is diagonal we may identify U with U_{PMNS}. The effective (3×3) light neutrino mass matrix m_ν is given as

$$m_\nu = m_D M^{-1} m_D^T \tag{6.5}$$

From the above, one obtains

$$U^\dagger m_D M^{-1} m_D^T U^\star = D_k \,. \tag{6.6}$$

Substituting $U_M^\dagger M U_M^\star = D_M$ in the above equation we get

$$U^\dagger \, m_D \, U_M^\star \, D_M^{-1} \, U_M^\dagger \, m_D^T \, U^\star = D_k \,. \tag{6.7}$$

We now introduce a very useful parametrisation known as the R-matrix. The R matrix is defined as [108] [1]

$$R = D_{\sqrt{M}}^{-1} U_M^\dagger m_D^T U^\star D_{\sqrt{k}}^{-1} \tag{6.8}$$

where R is a $3 \times N$ complex orthogonal matrix $R^T R = I$. Substituting the above into eq. (6.7) and rearranging, one gets the following equation relating R directly to m_D

$$m_D = U D_{\sqrt{k}} R^T D_{\sqrt{M}} \tag{6.9}$$

The point of the R-matrix parametrisation is to divide the Dirac mass matrix, as above, into the "low energy" parameters present in $\mathcal{L}_{eff}$ (contained within U and D_k) and the "high energy" parameters "integrated out" of $\mathcal{L}_{eff}$ to first order (contained

[1] In terms of PMNS mixing matrix $R = D_{\sqrt{M}}^{-1} U_M^\dagger m_D^T U_l^\star U_{PMNS}^\star D_{\sqrt{k}}^{-1}$ where $U_{PMNS} = U_l^\dagger U$.

within R and D_M). In general m_D above is a complex $N \times 3$ matrix with $6N - 3$ physical parameters ($3N$ lots of complex numbers, minus 3 non-physical phases that can be eliminated by rephasing the three l_α fields the seesaw Lagrangian (cf. eq. (1.35)). Of these $6N - 3$ parameters in eq. (6.9) U contains the ν_L mixings and phases, D_k contains the ν_L masses and D_M contains the N_R masses. Any remaining parameters of m_D are contained within the R-matrix.

We first discuss the $N = 2$ case. Since m_D in general contains $6N - 3$ physical parameters it contains 9 for the $N = 2$ case, of which 5 are contained in U (3 ν_L mixings and 2 phases), 2 in D_k (2 ν_L masses) and 2 in D_M (2 N_R masses). This leaves just **two** remaining m_D parameters contained within the R-matrix (one modulus and one phase). Given that the R-matrix is (by definition) orthogonal this information can be put into the complex angle $z \equiv x + iy$ and from eq. 6.8 we obtain

$$R^{(NH)} = \begin{pmatrix} 0 & \cos z & \zeta \sin z \\ 0 & -\sin z & \zeta \cos z \end{pmatrix} \tag{6.10}$$

$$R^{(IH)} = \begin{pmatrix} \cos z & \zeta \sin z & 0 \\ -\sin z & \zeta \cos z & 0 \end{pmatrix} \tag{6.11}$$

where $\zeta = \pm 1$ accounts for the possibility of two different choices ('branches'). These "branches" are analogous to choosing either a left-handed or a right-handed co-ordinate system to parametrise a space - seesaw physics is unaffected by the choice (this is shown later, in section 6.5).

We next consider the $N = 3$ case. For all cases $N \geq 3$ there are a total of 9 parameters contained in D_k and U (3 masses, 3 mixing angles, 3 phases). Hence of the $6N - 3$ parameters in a general m_D a $3 \times N$ R-matrix contains the remaining $6N - 12$ real parameters ($3N - 6$ moduli and $3N - 6$ phases). This implies a general R-matrix has $3N - 6$ complex angles. Hence the 3×3 R-matrix for the $N = 3$ case will have $3N - 6 = 3$ complex angles and may be parametrised as a combination of three complex Euler rotations as

$$R(z_{23}, z_{13}, z_{12}) = \pm R_{23}(z_{23})\ R_{13}(z_{13})\ R_{12}(z_{12})\ , \tag{6.12}$$

where the overall sign accounts for a possible change of parity (choice between left-handed and right-handed co-ordinate systems) and the R_{ij} are defined by

$$R_{23} = \begin{pmatrix} 1 & 0 & 0 \\ 0 & \cos z_{23} & \sin z_{23} \\ 0 & -\sin z_{23} & \cos z_{23} \end{pmatrix} , \; R_{13} = \begin{pmatrix} \cos z_{13} & 0 & \sin z_{13} \\ 0 & 1 & 0 \\ -\sin z_{13} & 0 & \cos z_{13} \end{pmatrix} , \; R_{12} = \begin{pmatrix} \cos z_{12} & \sin z_{12} & 0 \\ -\sin z_{12} & \cos z_{12} & 0 \\ 0 & 0 & 1 \end{pmatrix} \tag{6.13}$$

We can also obtain the $N = 2$ case as a limit of the $N = 3$ case when $M_3 \gg 10^{14} GeV$, which also implies that $m_1 \ll m_2$ for normal hierarchy (NH), or $m_3 \ll m_1$ for inverted hierarchy (IH). Taking these limits in eq. (6.8) for the R-matrix we obtain for NH

$$R^{(NH)} = \begin{pmatrix} 0 & \cos z & \zeta \sin z \\ 0 & -\sin z & \zeta \cos z \\ 1 & 0 & 0 \end{pmatrix} \tag{6.14}$$

and for IH

$$R^{(IH)} = \begin{pmatrix} \cos z & \zeta \sin z & 0 \\ -\sin z & \zeta \cos z & 0 \\ 0 & 0 & 1 \end{pmatrix} . \tag{6.15}$$

where we can identify $z_{13} = z$ and $z_{12} = z_{23} = 0$ in eq. (6.13).

The results of this section for 2, 3 and $N \geq 3$ RHN models are summarised in table 6.1.

Table 6.1: Seesaw parameter space (sources of **CP violation** in bold)

# of N_R	"low energy" parameters	"high energy" parameters	totals
2	2 ν_L masses	2 N_R masses	
	3 ν_L mixing angles		
	1 Dirac phase	**1 complex angle**	
	1 Majorana phase		11
3	3 ν_L masses	3 N_R masses	
	3 ν_L mixing angles		
	1 Dirac phase	**3 complex angles**	
	2 Majorana phases		18
$N \geq 3$	3 ν_L masses	N N_R masses	
	3 ν_L mixing angles		
	1 Dirac phase	$3N-6$ **complex angles**	
	2 Majorana phases		$7N-3$

6.3 Leptogenesis in a Two-Flavoured 2RHN Model

We now consider leptogenesis in a two-flavoured 2RHN model, which is the limit of a 3RHN model, with $M_3 \mapsto \infty$. Such a 2RHN model has the mass spectrum $10^9 GeV \ll M_1 \leq \frac{1}{3} M_2 \ll 10^{12} GeV$, for which N_2 and N_1 both decay in a two-flavoured regime. The constraint $M_1 \leq \frac{1}{3} M_2$ serves to recover the hierarchical limit $M_1 \ll M_2$ [100] such that all equations valid in this limit - those for $\varepsilon_{i\alpha}$ for example, can be applied. The leptogenesis happens in two stages:

1. First, the N_2s decay at temperature $T \sim M_2$, producing flavoured asymmetries $N^{N_2}_{\Delta_\alpha}$ in a flavour basis $\alpha = \{\tau_2^\perp, \tau\}$.

2. Next, the N_1s decay at temperature $T \sim M_1$ partially washing out the N_2 generated asymmetry and producing some of their own asymmetry $N^{N_1}_{\Delta_\alpha}$ in a basis $\alpha = \{\tau_1^\perp, \tau\}$)

The general flavour space alignments of $|l_1\rangle$ and $|l_2\rangle$ were also illustrated in fig. 5.1 of the previous chapter, in which I also derived an equation for the final asymmetry produced by both N_2 and N_1 processes as (cf. eq. (5.62)

$$\begin{aligned} N^{\rm f}_{\Delta_{B-L}} &= \varepsilon_{1\tau}\,\kappa(K_{1\tau}) + \varepsilon_{2\tau}\,\kappa(K_{2\tau})\,e^{-\frac{3\pi}{8}K_{1\tau}} \\ &+ \varepsilon_{1\gamma_1}\,\kappa(K_{1\gamma_1}) + \left(p^0_{\gamma_1^0\gamma_2}\varepsilon_{2\gamma_2}\,\kappa(K_{2\gamma_2}) - \frac{\Delta p_{\gamma_2\gamma_1^0}}{2}\,\kappa(K_{2\gamma_2}/2)\right)\,e^{-\frac{3\pi}{8}K_{1\gamma_1}} \\ &+ \left(1 - p^0_{\gamma_1^0\gamma_2}\right)\,\varepsilon_{2\gamma_2}\,\kappa(K_{2\gamma_2}) + \frac{\Delta p_{\gamma_2\gamma_1^0}}{2}\,\kappa(K_{2\gamma_2}/2) \end{aligned} \tag{6.16}$$

where I have identified $\tau_2^\perp \equiv \gamma_2$ and $\tau_1^\perp \equiv \gamma_1$, $\tau_{1^\perp}^\perp \equiv \gamma_1^\perp$ in order to simplify the notation of the previous chapter somewhat. To make use of eq. (6.16) it is necessary to evaluate the projectors $p^0_{\gamma_1^0\gamma_2} \equiv \frac{1}{2}\left(|\langle\gamma_1^0|\gamma_2\rangle|^2 + |\langle\bar{\gamma}_1^0|\bar{\gamma}_2\rangle|^2\right)$ and $p^0_{\gamma_1^0\gamma_2} \equiv |\langle\gamma_1^0|\gamma_2\rangle|^2 - |\langle\bar{\gamma}_1^0|\bar{\gamma}_2\rangle|^2$ explicitly in terms of the neutrino Yukawa matrix components The tree-level projector is evaluated in section 6.4.2 and the loop-level projector in section 6.6.

Eq. (6.16) is the sum of three flavoured components

$$N^f_{\Delta_{B-L}} = N^f_{\Delta_{\gamma_1}} + N^f_{\Delta_{\gamma_1^\perp}} + N^f_{\Delta_\tau} \tag{6.17}$$

It is also useful to split $N^f_{\Delta_{B-L}}$ into an N_2 generated part and an N_1 generated part, according to

$$N^{\rm f}_{\Delta_{B-L}} = N^{\rm f(1)}_{\Delta_{B-L}} + N^{\rm f(2)}_{\Delta_{B-L}} \tag{6.18}$$

where

$$N^{\rm f(1)}_{\Delta_{B-L}} = \varepsilon_{1\gamma}\,\kappa(K_{1\gamma_1}) + \varepsilon_{1\tau}\,\kappa(K_{1\tau}) \tag{6.19}$$

and

$$\begin{aligned} N^{\rm f(2)}_{\Delta_{B-L}} &= \left(p^0_{\gamma_1\gamma_2}\varepsilon_{2\gamma}\kappa(K_{2\gamma_2}) \,+\, \Delta p_{\gamma_1\gamma_2}\,\kappa(K_{2\gamma}/2)\right) e^{-\frac{3\pi}{8}K_{1\gamma}} \\ &+ \;(1-p^0_{\gamma_1\gamma_2})\varepsilon_{2\gamma}\kappa(K_{2\gamma_2}) \,-\, \Delta p_{\gamma_1^0\gamma_2}\,\kappa(K_{2\gamma}/2) \\ &+ \;\varepsilon_{2\tau}\,\kappa(K_{2\tau})\,e^{-\frac{3\pi}{8}\,K_{1\tau}} \end{aligned} \tag{6.20}$$

The baryon-to-photon number ratio at recombination is then given by

$$\eta_B = a_{\rm sph}\,\frac{N^{\rm f}_{\Delta_{B-L}}}{N^{\rm rec}_\gamma} \simeq 0.96\times 10^{-2}\,\left(N^{\rm f(1)}_{\Delta_{B-L}} + N^{\rm f(2)}_{\Delta_{B-L}}\right) \tag{6.21}$$

to be compared with the value measured from the CMB anisotropies observations [39]. In [8] the 2RHN model was "revisited" and the impact of the $N^{\rm f(2)}_{\Delta_{B-L}}$ term upon η_B above (which had been neglected in previous studies) was incorporated and compared to the pure N_1 contribution from the $N^{\rm f(1)}_{\Delta_{B-L}}$ term. The results of that comparison is the subject of the next section.

6.4 The 2RHN Model Revisited

We shall ignore the impact of phantom terms for the time being, by artificially setting $\Delta p_{\gamma_1^0\gamma_2} = 0$. However we shall return to consider their impact in section 6.6, where I calculate $\Delta p_{\gamma_1^0\gamma_2} \neq 0$ explicitly and consider its impact upon the final asymmetry. Setting $\Delta p_{\gamma_1^0\gamma_2} = 0$ the components of eq. (6.17) are given by

$$\begin{aligned} N^f_{\Delta_{\gamma_1}} &= \varepsilon_{\gamma_1}\kappa^f_{1\gamma} + p^0_{\gamma_1\gamma_2}\varepsilon_{2\gamma}\kappa^f_{2\gamma}\,e^{-\frac{3\pi}{8}K_{1\gamma}} \\ N^f_{\Delta_{\gamma_1^\perp}} &= (1-p^0_{\gamma_1\gamma_2})\varepsilon_{2\gamma}\kappa^f_{2\gamma} \\ N^f_{\Delta_\tau} &= \varepsilon_1\kappa^f_{1\tau} + \varepsilon_2\kappa^f_{2\tau}e^{-\frac{3\pi}{8}K_{1\tau}} \end{aligned} \tag{6.22}$$

We shall consider vanishing initial abundances, for which the efficiency factor is lower, thus giving a more stringent upper bound on the RHN masses - if leptogenesis succeeds for vanishing initial abundance it will also succeed for thermal initial abundance, but the converse is not true. In the case of vanishing initial abundances, the final efficiency factors $\kappa^f_{i\alpha}$ above are the sum of two different contributions, a negative and a positive one, explicitly [71]

$$\kappa^f_{i\alpha} \simeq \kappa_-(K_i, P^0_{i\alpha}) + \kappa_+(K_i, P^0_{i\alpha}) \tag{6.23}$$

The negative contribution arises from a first stage where $N_{N_i} \leq N^{\rm eq}_{N_i}$, for $z_i \leq z_i^{\rm eq}$, and is given approximately by

$$\kappa_-(K_i, P^0_{i\alpha}) \equiv -\frac{2}{P^0_{i\alpha}}\, e^{-\frac{3\,\pi\, K_{i\alpha}}{8}} \left(e^{\frac{P^0_{i\alpha}}{2}\, N_{N_i}(z_{\rm eq})} - 1 \right) \tag{6.24}$$

The positive contribution arises from a second stage where $N_{N_i} \geq N^{\rm eq}_{N_i}$, for $z_i \geq z_i^{\rm eq}$, and is approximately given by

$$\kappa_+(K_i, P^0_{i\alpha}) \equiv \frac{2}{z_B(K_{i\alpha})\, K_{i\alpha}} \left(1 - e^{-\frac{K_{i\alpha}\, z_B(K_{i\alpha})\, N_{N_i}(z_{\rm eq})}{2}} \right) \tag{6.25}$$

The N_i abundance at $z_i^{\rm eq}$ is well approximated by the expression

$$N_{N_i}(z_i^{\rm eq}) \simeq \frac{N(K_i)}{\left(1 + \sqrt{N(K_i)}\right)^2} \tag{6.26}$$

that interpolates between the limit $K_i \gg 1$, where $z_i^{\rm eq} \ll 1$ and $N_{\rm N_i}(z_i^{\rm eq}) = 1$, and the limit $K_i \ll 1$, where $z_i^{\rm eq} \gg 1$ and $N_{N_i}(z_i^{\rm eq}) = N(K_i) \equiv 3\pi K_i/4$.

Everything is now given in terms of washouts $K_{i\alpha}$, CP asymmetries $\varepsilon_{i\alpha}$ and a projector $p^0_{\gamma_1\gamma_2}$. We would like to express all three quantities explicitly in terms of the orthogonal parametrisation, such that scans over the complex angle $z \equiv x + iy$ can be made to find the allowed regions of the model. As we will see, there will be some sensitivity to the low energy neutrino parameters, in particular to the value of θ_{13}, of the Dirac phase and of the Majorana phase. We will therefore perform the

scans with the following 4 benchmark U_{PMNS} choices A,B,C and D:

$$A: \quad \theta_{13} = 0,\, \delta = 0,\, \frac{\alpha_{21}}{2} = 0 \tag{6.27}$$

$$B: \quad \theta_{13} = 11.5^\circ,\, \delta = 0,\, \frac{\alpha_{21}}{2} = 0 \tag{6.28}$$

$$C: \quad \theta_{13} = 11.5^\circ,\, \delta = \frac{\pi}{2},\, \frac{\alpha_{21}}{2} = 0 \tag{6.29}$$

$$D: \quad \theta_{13} = 11.5^\circ,\, \delta = 0,\, \frac{\alpha_{21}}{2} = \frac{\pi}{2}, \tag{6.30}$$

where for all benchmarks the solar mixing angle and the atmospheric mixing angle are fixed to $\theta_{12} = 34^\circ$ and $\theta_{23} = 45^\circ$ which are chosen to be close to their best fit values. Notice that benchmark A is close to tri–bimaximal (TB) mixing [109], with no low energy CP violation in the Dirac or Majorana sectors, while the remaining benchmarks all feature the highest allowed reactor angle consistent with the recent T2K electron appearance results [110] [2]. On the other hand, varying the atmospheric and solar angles within their experimentally allowed ranges has little effect on the results, so all benchmarks have the fixed atmospheric and solar angles above. Benchmark B involves no CP violation in the low energy Dirac or Majorana sectors, with any CP violation arising from the high energy see-saw mechanism parametrized by the complex angle z. Benchmark C involves maximal low energy CP violation via the Dirac phase, corresponding to the oscillation phase $\delta = \pi/2$, but has zero low energy CP violation via the Majorana phase, with $\alpha_{21}/2 = 0$. Benchmark D involves maximal CP violation from the Majorana sector, $\alpha_{21}/2 = \pi/2$, but zero CP violation in the Dirac sector, $\delta = 0$. These benchmark points are thus chosen to span the relevant parameter space and to illustrate the effect of the different sources of CP violation.

6.4.1 Washouts in 2RHN Model

In order to start performing scans fixing the various "benchmark" PMNS matrix choices of the previous secion, we begin by considering how to express washout param-

[2] The paper [8] was completed prior to the latest results from the RENO [37] and Daya Bay [36] experiments, which now rule out $\theta_{13} = 0$ for benchmarks A,B.

eters in the orthogonal parametrisation. First recall from section 3.2 that flavoured washout parameters are defined in terms of the Dirac mass matrix m_D as

$$K_{i\alpha} \equiv \frac{\tilde{\Gamma}_{i\alpha}}{H(T=M_i)} = \frac{|m_{D\alpha i}|^2}{M_i\, m_\star} \tag{6.31}$$

where $m_\star$ is the (SM) equilibrium neutrino mass defined by [71, 111]

$$m_\star \equiv \frac{16\,\pi^{5/2}\,\sqrt{g^\star_{SM}}}{3\,\sqrt{45}}\,\frac{v^2}{M_{\rm Pl}} \simeq 1.08\times 10^{-3}\,{\rm eV}\,. \tag{6.32}$$

Also recall from section 6.2 that $m_D = U D_k R^T D_M$ in the orthogonal parametrisation, or, in terms of its components

$$m_{D_{\alpha i}} = \sqrt{M_i}\,\sum_k \sqrt{m_k}\,U_{\alpha k} R_{ik} \tag{6.33}$$

Substituting the above into eq. (6.31) one obtains for the washouts in the orthogonal parametrisation

$$K_{i\alpha} = \frac{1}{m_\star}\left|\sum_k \sqrt{m_k}\,U_{\alpha k}\,R_{ik}\right|^2 \tag{6.34}$$

$$K_i = \sum_\alpha K_{i\alpha} = \frac{1}{m_\star}\sum_k m_k\,|R_{ik}|^2 \tag{6.35}$$

With two RH neutrinos, we may express all quantities explicitly in terms of complex angle z for NH ($m_1 = 0$) as

$$K_1 = K_{\rm sol}\,|\cos z|^2 + K_{\rm atm}\,|\sin z|^2 \tag{6.36}$$

$$K_2 = K_{\rm sol}\,|\sin z|^2 + K_{\rm atm}\,|\cos z|^2 \tag{6.37}$$

$$K_{1\alpha} = \frac{1}{m_\star}\,|\sqrt{m_{\rm sol}}\,U_{\alpha 2}\,\cos z + \zeta\,\sqrt{m_{\rm atm}}\,U_{\alpha 3}\,\sin z|^2 \tag{6.38}$$

$$K_{2\alpha} = \frac{1}{m_\star}\,|\zeta\,\sqrt{m_{\rm atm}}\,U_{\alpha 3}\,\cos z - \sqrt{m_{\rm sol}}\,U_{\alpha 2}\,\sin z|^2 \tag{6.39}$$

where we defined $K_{\rm sol} \equiv m_{\rm sol}/m_\star \sim 10$ and $K_{\rm atm} \equiv m_{\rm atm}/m_\star \sim 50$.

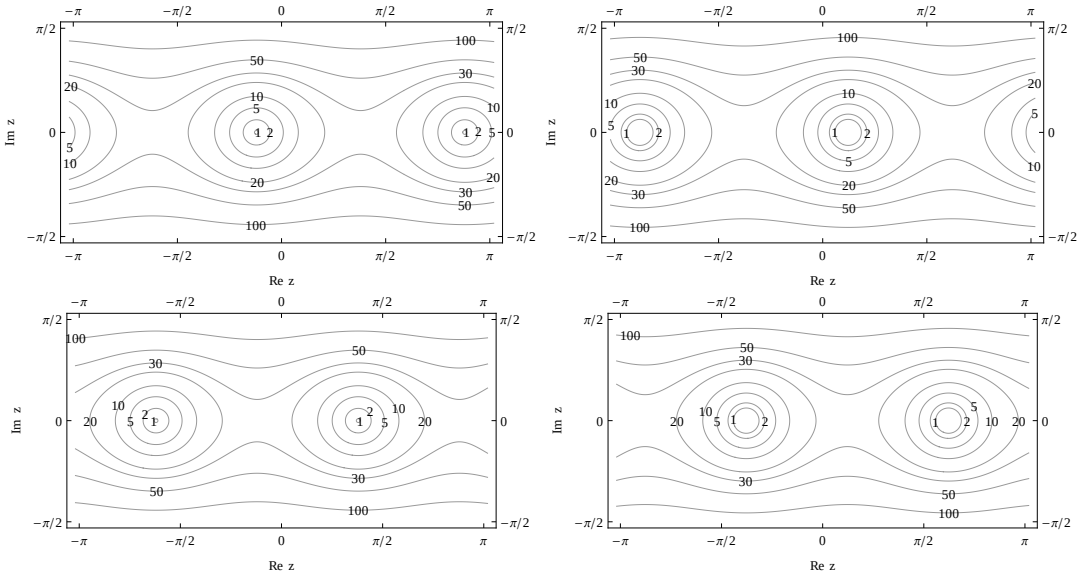

Figure 6.1: Contour plots showing $K_{1\gamma} = \sum_{\alpha=e,\mu} K_{1\alpha}$ (upper left panel), $K_{1\tau}$ (upper right panel), $K_{2\gamma} = \sum_{\alpha=e,\mu} K_{2\alpha}$ (lower left panel) and $K_{2\tau}$ (lower right panel) dependence on complex angle z for benchmark B (cf. eq. (6.28)), $\zeta = +1$, and NH.

For IH, $(m_3 = 0)$, we can approximate $m_1 \simeq m_2 = m_{\rm atm}$ and simplify further

$$K_1 \simeq K_2 \simeq K_{\rm atm}\, \left(|\cos z|^2 + |\sin z|^2\right) = K_{\rm atm}\, \cosh[2{\rm Im}z] \tag{6.40}$$

$$K_{1\alpha} \simeq K_{\rm atm}\, |U_{\alpha 1}\, \cos z + \zeta\, U_{\alpha 2}\, \sin z|^2$$

$$K_{2\alpha} \simeq K_{\rm atm}\, |\zeta\, U_{\alpha 2}\, \cos z - U_{\alpha 1}\, \sin z|^2 \tag{6.41}$$

In Fig. 6.1 we show contour plots of the flavoured decay parameters $K_{1\gamma}, K_{1\tau}$ and $K_{2\gamma}, K_{2\tau}$ in the relevant region of the z complex plane for NH and for the benchmark case B, since this will prove the case maximizing the effect of the N_2 asymmetry production. Notice that Fig. 6.1 is periodic in π along the Rez axis as can be also inferred analytically from eqs. (6.38) and (6.39) using double angle identities. The most significant feature to be noticed at this stage is that for most of the parameter space $K_{i\alpha} \gg 1$ holds. In these regions a strong wash-out regime is realized and this implies that the dependence of the results on the initial conditions is negligible and corrections due to the effects that we have listed earlier, after the kinetic equations, are at most $\mathcal{O}(1)$ factors. On the other hand, as we will discuss in sections 6.4.4 and 6.5, there are two interesting new flavoured regions for leptogenesis around $z\pm \sim \pi/2$ for NH, where the decay asymmetry from N_2 decays dominates

over the one from N_1 decays ('N_2-dominated regions'). Fig. 6.1 shows that in this region $K_{2\alpha}$ is between 2 and 5. We are therefore in a 'optimal washout' region where thermal leptogenesis works most efficiently but still the dependence on the initial conditions amounts not more than $\sim 50\%$. Very similar results are obtained for the other benchmark cases as well.

6.4.2 Projector in 2RHN Model

The tree-level projector $p^0_{\gamma_1\gamma_2}$ is straightforward to calculate. First we may express the states $l_1\rangle$ and $|l_2\rangle$ in terms of the $\mathcal{C}$ and $\bar{\mathcal{C}}$ of section 3.2 as

$$|\ell_{\gamma_2}\rangle = \frac{\mathcal{C}_{2e}}{\sqrt{|\mathcal{C}_{2e}|^2 + |\mathcal{C}_{2\mu}|^2}}\,|\ell_e\rangle \;+\; \frac{\mathcal{C}_{2\mu}}{\sqrt{|\mathcal{C}_{2e}|^2 + |\mathcal{C}_{2\mu}|^2}}\,|\ell_\mu\rangle \tag{6.42}$$

The tree-level projector is then given as

$$p^0_{\gamma_1\gamma_2} = \frac{\left|\sum_{\alpha=e,\mu}\mathcal{C}^0_{1\alpha}\mathcal{C}^{0\star}_{2\alpha}\right|^2}{\left(|\mathcal{C}^0_{1e}|^2 + |\mathcal{C}^0_{1\mu}|^2\right)\,\left(|\mathcal{C}^0_{2e}|^2 + |\mathcal{C}^0_{2\mu}|^2\right)} \tag{6.43}$$

where $\mathcal{C}^0_{i\alpha}$ is the tree-level part of $\mathcal{C}_{i\alpha}$, which we may recall from section 3.2 is given in terms of $Y^\nu_{\alpha i}$ as

$$\mathcal{C}^0_{i\alpha} = \frac{Y^\nu_{\alpha i}}{\sqrt{(Y^{\nu\dagger}\,Y^\nu)_{ii}}} \qquad \text{and} \qquad \bar{\mathcal{C}}^0_{i\alpha} = \frac{Y^{\nu\star}_{\alpha i}}{\sqrt{(Y^{\nu\dagger}\,Y^\nu)_{ii}}} \tag{6.44}$$

and so substituting the above back into eq. (6.43) one obtains

$$p^0_{\gamma_1\gamma_2} = \frac{\left|\sum_{\alpha=e,\,\mu}Y^{\nu\star}_{\alpha1}\,Y^\nu_{\alpha2}\right|^2}{(Y^{\nu\dagger}\,Y^\nu)_{11}\;(Y^{\nu\dagger}\,Y^\nu)_{22}} \tag{6.45}$$

having identified $p^0_{1\gamma} \equiv |\mathcal{C}^0_{1e}|^2 + |\mathcal{C}^0_{1\mu}|^2$ and $p^0_{2\gamma} \equiv |\mathcal{C}^0_{2e}|^2 + |\mathcal{C}^0_{2\mu}|^2$. Now substituting eq. (6.9) for $Y^\nu = m_D/v$ we obtain $p^0_{\gamma^0_1\gamma_2}$ in the orthogonal parametrisation as

$$p^0_{\gamma_1\gamma_2} = \frac{1}{p^0_{1\gamma}\,p^0_{2\gamma}\,\widetilde{m}_1\,\widetilde{m}_2}\left|\sum_{k,k'}\sum_{\alpha=e,\mu}\sqrt{m_k\,m_{k'}}\,U^\star_{\alpha k}\,U_{\alpha k'}\,R^\star_{1k}\,R_{2k'}\right|^2 \tag{6.46}$$

where I have defined the $\widetilde{m}_i$ above as

$$\widetilde{m}_i \equiv \sum_k m_k |R_{ik}|^2 \tag{6.47}$$

and γ-flavoured branching ratios as $p_{i\gamma} = p_{ie} + p_{i\mu}$. Fig. 6.2 gives the contour plot of eq. (6.46) which indicates that the quantity significantly differs from unity in general. For NH $p^0_{\gamma_1\gamma_2}$ is periodic in π along the Rez axis and is approximately periodic in $\pi/2$. One can already see that in the new flavoured regions around $z \sim \pm\pi/2$ the quantity $1-p^0_{\gamma_1\gamma_2}$ is maximal. We thus find good conditions for leptogenesis regarding washout from N_2 as well as from N_1 processes.

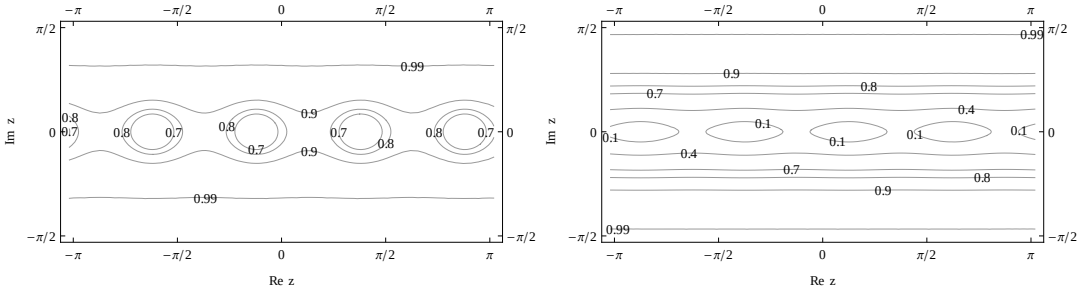

Figure 6.2: Contour plots of $p^0_{\gamma_1\gamma_2}$ for NH (left) and IH (right) (benchmark B, $\zeta = 1$).

6.4.3 CP Asymmetry in the 2RHN Model

Let us now re-express the *CP* asymmetries in the orthogonal parametrization. The expression (3.43) for the *CP* asymmetries can be recast as

$$\begin{aligned} \varepsilon_{i\alpha} &= -\frac{3}{16\,\pi v^2}\,\frac{1}{(m_D^\dagger\, m_D)_{ii}} \sum_{j\neq i}\left(\mathcal{I}^\alpha_{ij}\,\frac{\xi(M_j^2/M_i^2)}{M_j/M_i} + \mathcal{J}^\alpha_{ij}\,\frac{2}{3\,(M_j^2/M_i^2-1)}\right) \\ &\equiv \varepsilon^{\mathcal{I}}_{i\alpha} + \varepsilon^{\mathcal{J}}_{i\alpha} \end{aligned} \tag{6.48}$$

in an obvious notation where we have defined

$$\mathcal{I}^\alpha_{ij} \equiv \mathrm{Im}\Big[\big(m_D^\dagger\big)_{i\alpha}\big(m_D\big)_{\alpha j}\big(m_D^\dagger m_D\big)_{ij}\Big]\ ,\ \mathcal{J}^\alpha_{ij} \equiv \mathrm{Im}\Big[\big(m_D^\dagger\big)_{i\alpha}\big(m_D\big)_{\alpha j}\big(m_D^\dagger m_D\big)_{ji}\Big] \tag{6.49}$$

Substituting eq. (6.9) for m_D in the orthogonal parametrisation into the above, we find

$$\mathcal{I}^{\alpha}_{ij} = M_i\, M_j\, \mathrm{Im}\Big[\sum_{k,k',k''} (m_k m_{k'})^{1/2} m_{k''} U^*_{\alpha k} U_{\alpha k'}\, R^*_{ik}\, R_{jk'} R^*_{ik''}\, R_{jk''}\Big] \tag{6.50}$$

$$\mathcal{J}^{\alpha}_{ij} = M_i\, M_j\, \mathrm{Im}\Big[\sum_{k,k',k''} (m_k m_{k'})^{1/2} m_{k''} U^*_{\alpha k} U_{\alpha k'}\, R^*_{ik}\, R_{jk'} R^*_{jk''}\, R_{ik''}\Big] \tag{6.51}$$

In order to simply the notation, it will prove convenient to introduce the ratios

$$r_{i\alpha} \equiv \frac{\varepsilon_{i\alpha}}{\bar{\varepsilon}(M_1)}\,, \;\; r^{\mathcal{I}}_{i\alpha} \equiv \frac{\varepsilon^{\mathcal{I}}_{i\alpha}}{\bar{\varepsilon}(M_1)} \;\; r^{\mathcal{J}}_{i\alpha} \equiv \frac{\varepsilon^{\mathcal{J}}_{i\alpha}}{\bar{\varepsilon}(M_1)} \tag{6.52}$$

where

$$\bar{\varepsilon}(M_1) \equiv \frac{3}{16\,\pi}\,\frac{M_1\, m_{\rm atm}}{v^2} \simeq 10^{-6}\,\left(\frac{M_1}{10^{10}\,\mathrm{GeV}}\right) \tag{6.53}$$

is the upper bound for the total *CP* asymmetries [69] that is therefore used as a reference value.

For the lightest right handed neutrino CP asymmetry we set $j = 1$ in eq. (6.50) and obtain

$$r^{\mathcal{I}}_{1\alpha} = \sum_{k,k'} \frac{m_{k'}\,\sqrt{m_{k'}\, m_k}}{\widetilde{m}_1\, m_{\rm atm}}\, \mathrm{Im}[U_{\alpha k}\, U^{\star}_{\alpha k'}\, R_{1k}\, R_{1k'}] \tag{6.54}$$

having used $R^T R = I$ and $\xi(M_j^2/M_1^2) \simeq 1$ (as is the case in the hierarchical limit, when $M_2 \gtrsim 3\, M_1$) to simplify the result. Recall that $\widetilde{m}_1$ was defined in eq. (6.47). This term is bounded by [72, 73, 112]

$$\left|r^{\mathcal{I}}_{1\alpha}\right| < \sqrt{p^0_{1\alpha}}\,\frac{\mathrm{max}_i[m_i]}{m_{\rm atm}}\,\mathrm{max}_k\,[|U_{\alpha k}|] \tag{6.55}$$

and it is the only term that has been considered in all previous analyses of leptogenesis in the two RH neutrino model so far. It is useful to give a derivation of this upper bound. One can first write

$$\left|r^{\mathcal{I}}_{1\alpha}\right| \;\leq\; \frac{1}{\widetilde{m}_1\, m_{\rm atm}}\,\left|\sum_k \sqrt{m_k}\, U_{\alpha k}\, R_{1k}\right|\,\left|\sum_{k'} (m_{k'})^{\frac{3}{2}}\, U^{\star}_{\alpha k'}\, R_{1k'}\right| \tag{6.56}$$

$$\;=\; \sqrt{p^0_{1\alpha}}\,\frac{\mathrm{max}_i[m_i]}{m_{\rm atm}}\,\sqrt{\widetilde{p}^0_{1\alpha}} \tag{6.57}$$

where in the second line we defined the quantity

$$\widetilde{p}^0_{1\alpha} \equiv \frac{\left|\sum_{k'} (m_{k'})^{\frac{3}{2}}\, U^\star_{\alpha k'}\, R_{1k'}\right|^2}{(\max_i[m_i])^2\, \widetilde{m}_1} \tag{6.58}$$

Considering the definition eq. (6.47) for $\tilde{m}_i$, this can then be maximised writing

$$\widetilde{p}^0_{1\alpha} \leq \frac{\sum_{k'} m_{k'}\, |\, U^\star_{\alpha k'}\, R_{1k'}|^2}{\widetilde{m}_1} \leq \max_k\, [|U_{\alpha k}|^2] \tag{6.59}$$

In this way one obtains the upper bound eq. (6.55).

The second term containing $\mathcal{J}_{1j}$ cannot be simplified using the R orthogonality and one obtains [76]

$$r^{\mathcal{J}}_{1\alpha} = -\frac{2}{3} \sum_{j,k,k',k''} \frac{M_1}{M_j}\ \frac{m_{k''}\sqrt{m_k\, m_{k'}}}{\widetilde{m}_1\, m_{\rm atm}}\, \mathrm{Im}[U^\star_{\alpha k}\, U_{\alpha k'}\, R^\star_{1k}\, R_{jk'}\, R^\star_{jk''}\, R_{1k''}] \tag{6.60}$$

In our case of the 2RHN model as the limit of a 3RHN model, we can substitute in eqs. (6.14) and (6.15) for the R-matrix to obtain for NH

$$\begin{aligned} r^{\mathcal{I}}_{1\alpha} &= \frac{m_{\rm atm}}{\widetilde{m}_1}\, \mathrm{Im}[\sin^2 z]\, \left(|U_{\alpha 3}|^2 - \frac{m^2_{\rm sol}}{m^2_{\rm atm}}\, |U_{\alpha 2}|^2\right) \\ &+ \zeta\, \frac{\sqrt{m_{\rm sol}\, m_{\rm atm}}}{\widetilde{m}_1\, m_{\rm atm}}\, \{(m_{\rm atm} - m_{\rm sol})\, \mathrm{Im}[U_{\alpha 2}\, U^\star_{\alpha 3}]\, \mathrm{Re}[\sin z\, \cos z] \\ &+ (m_{\rm atm} + m_{\rm sol})\, \mathrm{Re}[U_{\alpha 2}\, U^\star_{\alpha 3}]\, \mathrm{Im}[\sin z\, \cos z]\} \end{aligned} \tag{6.61}$$

$$\begin{aligned} -r^{\mathcal{J}}_{1\alpha} &= \frac{2}{3}\, \frac{M_1}{M_2} \left\{ \frac{m_{\rm sol}}{\widetilde{m}_1}\, \mathrm{Im}[\sin^2 z]\, \left(|U_{\alpha 3}|^2 - |U_{\alpha 2}|^2\right) \right. \\ &+ \zeta\, \frac{\sqrt{m_{\rm atm}\, m_{\rm sol}}}{\widetilde{m}_1\, m_{\rm atm}}\, \left[(m_{\rm atm} - m_{\rm sol})\, \mathrm{Im}[U^\star_{\alpha 2}\, U_{\alpha 3}]\, \mathrm{Re}[\sin z\, \cos^\star z]\, (|\cos z|^2 + |\sin z|^2)\right. \\ &+ \left.\left. (m_{\rm atm} + m_{\rm sol})\, \mathrm{Re}[U^\star_{\alpha 2}\, U_{\alpha 3}]\, \mathrm{Im}[\sin z\, \cos^\star z]\, (|\cos z|^2 - |\sin z|^2)\right] \right\} \end{aligned}$$

and for IH (approximating $m_1 \simeq m_2 \simeq m_{\rm atm}$) one obtains

$$r^{\mathcal{I}}_{1\alpha} = \frac{m_{\rm atm}}{\widetilde{m}_1}\, \left\{\mathrm{Im}[\sin^2 z]\, (|U_{\alpha 1}|^2\, - |U_{\alpha 2}|^2) - 2\, \zeta\, \mathrm{Re}[U_{\alpha 1}\, U^\star_{\alpha 2}]\, \mathrm{Im}[\sin z\, \cos z]\right\} \tag{6.62}$$

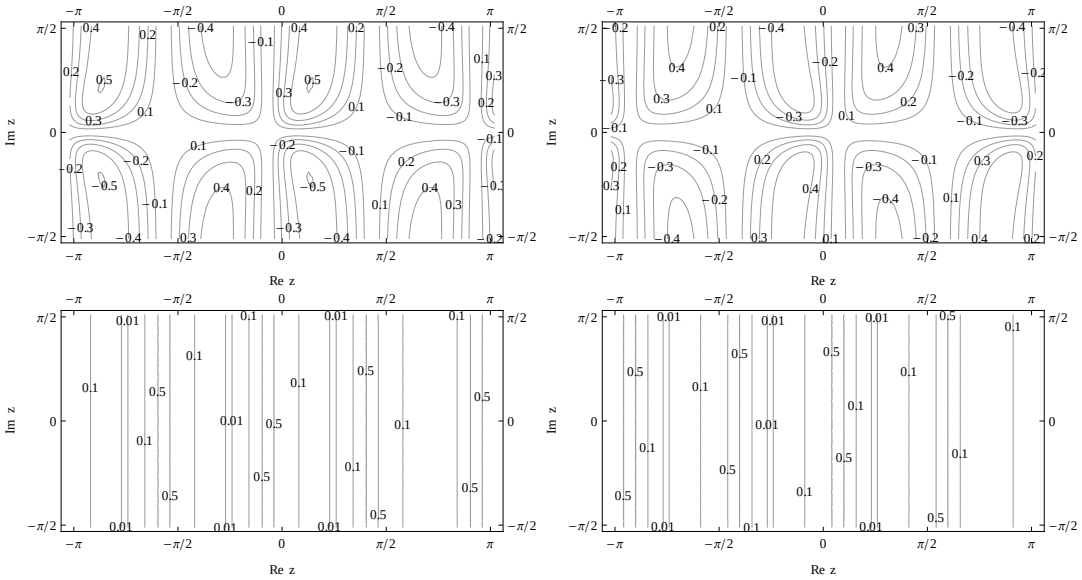

Figure 6.3: Contour plots of $r^{\mathcal{I}}_{1\gamma}$ (upper left panel) , $r^{\mathcal{I}}_{1\tau}$ (upper right panel), $|r^{\mathcal{J}}_{1\gamma}/r^{\mathcal{I}}_{1\gamma}| = |\varepsilon^{\mathcal{J}}_{1\gamma}/\varepsilon^{\mathcal{I}}_{1\gamma}|$ (lower left panel) and $|r^{\mathcal{J}}_{1\tau}/r^{\mathcal{I}}_{1\tau}| = |\varepsilon^{\mathcal{J}}_{1\tau}/\varepsilon^{\mathcal{I}}_{1\tau}|$ (lower right panel) for NH, benchmark B eq. (6.27), $\zeta = +1$ and $M_2/M_1 = 3$.

$$
\begin{aligned}
r^{\mathcal{J}}_{1\alpha} \;\simeq\; & \frac{2}{3}\,\frac{M_1}{M_2}\,\frac{m_{\rm atm}}{\widetilde{m}_1}\,\Big\{\mathrm{Im}[\sin^2 z]\,(|U_{\alpha 1}|^2 - |U_{\alpha 2}|^2) \\
+ \;& 2\,\zeta\,\left(|\sin z|^2 - |\cos z|^2\right)\,\mathrm{Re}[U_{\alpha 1}\,U^{\star}_{\alpha 2}]\,\mathrm{Im}[\sin z\,\cos^{\star} z]\Big\}
\end{aligned}
\tag{6.63}
$$

Notice that while the terms $r^{\mathcal{J}}_{1\alpha}$ are proportional to M_1/M_2, the terms $r^{\mathcal{I}}_{1\alpha}$ are not. Hence the former terms are somewhat suppressed with respect to the latter.

In Figure 6.3 we have plotted the quantities $r^{\mathcal{I}}_{1\alpha}$ and $|r^{\mathcal{J}}_{1\alpha}/r^{\mathcal{I}}_{1\alpha}| = |\varepsilon^{\mathcal{J}}_{1\alpha}/\varepsilon^{\mathcal{I}}_{1\alpha}|$ for the benchmark B U_{PMNS} choice eq. (6.28), $\zeta = +1$ and $M_2/M_1 = 3$. Once again there is periodicity in π along Rez, for the same reasons as with Figs. 6.1,6.2. One can notice how $|r^{\mathcal{J}}_{1\alpha}/r^{\mathcal{I}}_{1\alpha}| \ll 1$ both for $\alpha = \gamma$ and $\alpha = \tau$. Only in a very fine tuned region this ratio gets up to about 0.5. Therefore, it will prove out the term $r^{\mathcal{J}}_{1\alpha}$ can be safely neglected in the regions of interest for this study. Also, one can notice that $r^{\mathcal{I}}_{1\alpha}$, the dominant contribution to the baryon asymmetry from N_1 decays, is suppressed in the region $z \sim \pi/2$, hence this region is potentially dominated by N_2 decays.

We now repeat the same steps for the next-to-lightest NR, setting $j = 2$ in

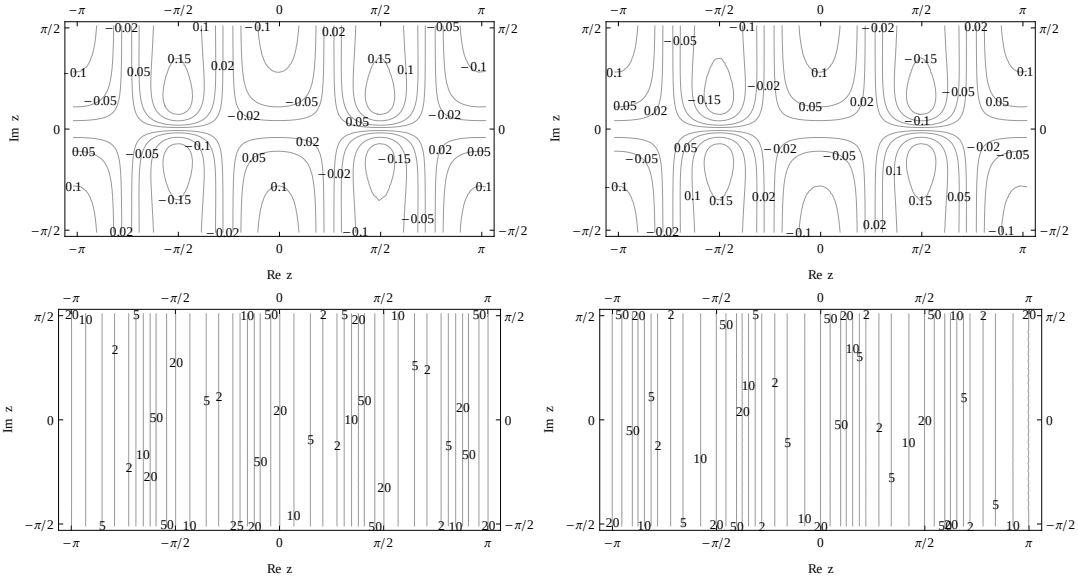

Figure 6.4: Contour plots of $r^{\mathcal{J}}_{2\gamma}$ (upper left panel), $r^{\mathcal{J}}_{2\tau}$ (upper right panel), $|r^{\mathcal{J}}_{2\gamma}/r^{\mathcal{J}}_{2\gamma}| = |\epsilon^{\mathcal{J}}_{2\gamma}/\epsilon^{\mathcal{J}}_{2\gamma}|$ (lower left panel) and $|r^{\mathcal{J}}_{2\tau}/r^{\mathcal{J}}_{2\tau}| = |\varepsilon^{\mathcal{J}}_{2\tau}/\varepsilon^{\mathcal{J}}_{2\tau}|$ (lower right panel) for benchmark B, eq. (6.28), $\zeta = +1$, $M_2/M_1 = 3$ and NH.

eq. (6.50) and (6.51). In the hierarchical limit $M_2 \gtrsim 3\, M_1$ we first obtain

$$
\begin{aligned}
r^{\mathcal{J}}_{2\alpha} \simeq \quad & -\frac{4}{3}\left(\frac{M_1}{M_2}\right)\left[\ln\left(\frac{M_2}{M_1}\right) - 1\right] \\
& \times \sum_{k,k',k''} \frac{m_{k''}\sqrt{m_k\, m_{k'}}}{\tilde{m}_2\, m_{atm}}\, \mathrm{Im}[U^*_{\alpha k} U_{\alpha k'}\, R^*_{2k}\, R_{1k'}\, R^*_{2k''}\, R_{1k''}]
\end{aligned}
\tag{6.64}
$$

$$
r^{\mathcal{J}}_{2\alpha} \simeq \frac{2}{3} \sum_{k,k',k''} \frac{m_{k''}\sqrt{m_{k'}\, m_k}}{\tilde{m}_2\, m_{atm}}\, \mathrm{Im}[U^*_{\alpha k}\, U_{\alpha k'}\, R^*_{2k}\, R_{1k'}\, R^*_{1k''}\, R_{2k''}]
\tag{6.65}
$$

Specialising to the R-matrix of eqs. (6.14) and (6.15) the above imply for NH

$$
\begin{aligned}
r^{\mathcal{J}}_{2\alpha} \;=\; & -\frac{4}{3}\frac{M_1}{M_2}\left[\ln\left(\frac{M_2}{M_1}\right) - 1\right]\left\{\frac{m_{\rm atm}}{\widetilde{m}_1}\,\mathrm{Im}[\sin^2 z]\,\left[|U_{\alpha 3}|^2 - \frac{m^2_{\rm sol}}{m^2_{\rm atm}}\,|U_{\alpha 2}|^2\right]\right. \\
& + \zeta\,\frac{\sqrt{m_{\rm atm}\, m_{\rm sol}}}{\widetilde{m}_2\, m_{\rm atm}}\,(m_{\rm atm} - m_{\rm sol})\,\mathrm{Im}[U_{\alpha 2}\, U^\star_{\alpha 3}]\,\mathrm{Re}[\sin z\,\cos^\star z]\,[|\cos z|^2 + |\sin z|^2] \\
& \left. + \zeta\,\frac{\sqrt{m_{\rm atm}\, m_{\rm sol}}}{\widetilde{m}_2\, m_{\rm atm}}\,(m_{\rm atm} + m_{\rm sol})\,\mathrm{Re}[U_{\alpha 2}\, U^\star_{\alpha 3}]\,\mathrm{Im}[\sin z\,\cos^\star z]\,[|\cos z|^2 - |\sin z|^2]\right\}
\end{aligned}
\tag{6.66}
$$

$$
\begin{aligned}
r^{\mathcal{J}}_{2\alpha} \;=\; & \frac{2}{3}\,\frac{m_{\rm sol}}{\widetilde{m}_2}\,\mathrm{Im}[\sin^2 z]\,\left[|U_{\alpha 2}|^2 - |U_{\alpha 3}|^2\right] \\
& + \frac{2}{3}\,\zeta\,\frac{\sqrt{m_{\rm atm}\, m_{\rm sol}}}{\widetilde{m}_2\, m_{\rm atm}}\,(m_{\rm atm} - m_{\rm sol})\,\mathrm{Im}[U^\star_{\alpha 2}\, U_{\alpha 3}]\,\mathrm{Re}[\sin z\,\cos^\star z]\,[|\cos z|^2 + |\sin z|^2] \\
& + \frac{2}{3}\,\zeta\,\frac{\sqrt{m_{\rm atm}\, m_{\rm sol}}}{\widetilde{m}_2\, m_{\rm atm}}\,(m_{\rm atm} + m_{\rm sol})\,\mathrm{Re}[U^\star_{\alpha 2}\, U_{\alpha 3}]\,\mathrm{Im}[\sin z\,\cos^\star z]\,[|\cos z|^2 - |\sin z|^2]
\end{aligned}
\tag{6.67}
$$

and similarly, for IH

$$\begin{aligned} r_{2\alpha}^{\mathcal{I}} &= \frac{m_{\rm atm}}{\widetilde{m}_1}\,\left\{{\rm Im}[\sin^2 z]\,\left(|U_{\alpha 1}|^2-|U_{\alpha 2}|^2\right)\right. \\ &+ 2\,\zeta\,\left(|\sin z|^2\,{\rm Im}[U_{\alpha 1}^{\star}\,U_{\alpha 2}]\,{\rm Re}[\sin z\,\cos^{\star} z]\right. \\ &+ \left.\left.|\cos z|^2\,{\rm Re}[U_{\alpha 1}^{\star}\,U_{\alpha 2}]\,{\rm Im}[\sin z\,\cos^{\star} z]\right)\right. \end{aligned} \tag{6.68}$$

$$\begin{aligned} r_{2\alpha}^{\mathcal{J}} &= \frac{m_{\rm atm}}{\widetilde{m}_2}\,\left\{{\rm Im}[\sin^2 z]\,\left(|U_{\alpha 1}|^2-|U_{\alpha 2}|^2\right)\right. \\ &+ \left.2\,\zeta\,{\rm Re}[U_{\alpha 1}\,U_{\alpha 2}^{\star}]\,{\rm Im}[\sin z\,\cos^{\star} z]\,[|\sin z|^2-|\cos z|^2]\right\} \end{aligned} \tag{6.69}$$

In fig. 6.4 we have plotted $r_{2\alpha}^{\mathcal{I}}$ and $|r_{2\alpha}^{\mathcal{J}}/r_{2\alpha}^{\mathcal{I}}|$ for $\zeta=+1$, $M_2/M_1=3$, benchmark U_{PMNS} choice B (cf. eq. (6.28)) and NH. This time, as one can see from the figures, one has $|r_{2\alpha}^{\mathcal{J}}/r_{2\alpha}^{\mathcal{I}}|\gg 1$ for all values of z and M_1/M_2 (since $|r_{2\alpha}^{\mathcal{J}}/r_{2\alpha}^{\mathcal{I}}|$ gets even larger if $M_2/M_1>3$), implying that the term $r_{2\alpha}^{\mathcal{J}}$ dominates and that $r_{2\alpha}^{\mathcal{I}}$ can be safely neglected. It can again be seen in fig. 6.4 that $r_{2\alpha}^{\mathcal{J}}/r_{2\alpha}^{\mathcal{I}}$ depends only on Rez for the same reasons as with $|r_{1\alpha}^{\mathcal{J}}/r_{1\alpha}^{\mathcal{I}}|$. Once again there is periodicity in π along Rez, for the same reasons as with figs. 6.1,6.2,6.3.

Crucially, we find that $r_{2\alpha}^{\mathcal{J}}$, the dominant contribution to the baryon asymmetry from N_2 decays, is maximised in the regions $z\sim\pm\pi/2$ (just above and below the Im$z=0$ line), in contrast to $r_{1\alpha}^{\mathcal{I}}$, the dominant contribution from N_1 decays, which is minimised in this region (see fig 6.3). Given this result and the favourable values of $K_{2\gamma}$ and p_{12}, shown in fig 6.1 and fig 6.2 respectively, one expect the $z\sim\pm\pi/2$ regions will be N_2 dominated.

6.4.4 Final Baryon Asymmetry in 2RHN Model

We can now finally go back to the expression for the final asymmetry (cf. eqs. (6.18), (6.19) and (6.20)) and recast it within the orthogonal parametrization. This can be written as the sum of four terms,

$$N_{\Delta_{B-L}}^{\rm f}=N_{\Delta_{B-L}}^{\rm f(1,\mathcal{I})}+N_{\Delta_{B-L}}^{\rm f(1,\mathcal{J})}+N_{\Delta_{B-L}}^{\rm f(2,\mathcal{I})}+N_{\Delta_{B-L}}^{\rm f(2,\mathcal{J})} \tag{6.70}$$

The sum of the first two terms is the contribution $N^{\rm f(1)}_{\Delta_{B-L}}$ from the lightest RH neutrinos,

$$\begin{aligned} N^{\rm f(1,\mathcal{I})}_{\Delta_{B-L}}(z,U,M_1) &= \bar{\varepsilon}(M_1)\sum_{\alpha=\tau,\gamma} r^{\mathcal{I}}_{1\alpha}(z,U)\,\kappa_{1\alpha} \\ N^{\rm f(1,\mathcal{J})}_{\Delta_{B-L}}(z,U,M_1,M_1/M_2) &= \bar{\varepsilon}(M_1)\sum_{\alpha=\tau,\gamma} r^{\mathcal{J}}_{1\alpha}(z,U,M_1/M_2)\,\kappa_{1\alpha} \end{aligned} \tag{6.71}$$

and it should be noticed that only the second one depends on M_2.

Analogously the sum of the last two terms in eq. (6.70) is the contribution $N^{\rm f(2)}_{\Delta_{B-L}}$ from the next-to-lightest RH neutrinos,

$$\begin{aligned} N^{\rm f(2,\mathcal{I})}_{\Delta_{B-L}}(z,U,M_1,M_1/M_2) &= \bar{\varepsilon}(M_1)\,\frac{M_1}{M_2}\left[\ln\left(\frac{M_2}{M_1}\right)-1\right] f^{\mathcal{I}}(z,U) \\ N^{\rm f(2,\mathcal{J})}_{\Delta_{B-L}}(z,U,M_1) &= \bar{\varepsilon}(M_1)\, f^{\mathcal{J}}(z,U) \end{aligned} \tag{6.72}$$

where

$$\begin{aligned} \frac{M_1}{M_2}\left[\ln\left(\frac{M_2}{M_1}\right)-1\right] f^{\mathcal{I}}(z,U) &= p^0_{\gamma_1\gamma_2}\, r^{\mathcal{I}}_{2\gamma}\,\kappa^f_{2\gamma}\, e^{-\frac{3\pi}{8}K_{1\gamma}} \\ &+ (1-p^0_{\gamma_1\gamma_2})\, r^{\mathcal{I}}_{2\gamma}\,\kappa^f_{2\gamma} + r^{\mathcal{I}}_{2\tau}\,\kappa^f_{2\tau}\, e^{-\frac{3\pi}{8}K_{1\tau}} \end{aligned} \tag{6.73}$$

and

$$f^{\mathcal{J}}(z,U) = p^0_{\gamma_1\gamma_2}\, r^{\mathcal{J}}_{2\gamma}\,\kappa^f_{2\gamma}\, e^{-\frac{3\pi}{8}K_{1\gamma}} + (1-p^0_{\gamma_1\gamma_2})\, r^{\mathcal{J}}_{2\gamma}\,\kappa^f_{2\gamma} + r^{\mathcal{J}}_{2\tau}\,\kappa^f_{2\tau}\, e^{-\frac{3\pi}{8}\,K_{1\tau}} \tag{6.74}$$

Notice that this time the first term depends on M_2 while the second does not. We can then write the total asymmetry as

$$N^{\rm f}_{\Delta_{B-L}} = [N^{\rm f(1,\mathcal{I})}_{\Delta_{B-L}} + N^{\rm f(2,\mathcal{J})}_{\Delta_{B-L}}](z,U,M_1)\,[1+\delta_1+\delta_2](z,U,M_1,M_1/M_2) \tag{6.75}$$

where we defined $\delta_1 \equiv N^{\rm f(1,\mathcal{J})}_{\Delta_{B-L}}/[N^{\rm f(1,\mathcal{I})}_{\Delta_{B-L}} + N^{\rm f(2,\mathcal{J})}_{\Delta_{B-L}}]$ and $\delta_2 \equiv N^{\rm f(2,\mathcal{I})}_{\Delta_{B-L}}/[N^{\rm f(1,\mathcal{I})}_{\Delta_{B-L}} + N^{\rm f(2,\mathcal{J})}_{\Delta_{B-L}}]$. We found that $\delta_1, \delta_2 \lesssim 0.05$ for any choice of $M_1/M_2, z, U$. Therefore, one can conclude that the total final asymmetry is independent of M_2 with very good accuracy [3] . It should be however remembered that our calculation of $N^{\rm f(2)}_{\Delta_{B-L}}$ holds for $M_2 \lesssim$

[3]Notice that all *CP* asymmetries, and consequently the final asymmetry, are $\propto M_1$. Therefore, there will be still a lower bound on M_1 contrarily to the 3 RH neutrino scenarios considered in [6].

10^{12} GeV and $M_2/M_1 \gtrsim 3$, implying $M_1 \lesssim (100\,/\,3)\times 10^{10}$ GeV. As such, when N_2 decays are included the largest value of M_1 we will allow is $M_1 = 30\times 10^{10}$GeV, whereas when N_2 decays are neglected, we will consider values as large as $M_1 = 100\times 10^{10}$GeV.

In fig. 6.5 we show the contours plots for M_1 obtained imposing successful leptogenesis, i.e. $\eta = \eta_B^{\rm CMB}$ (we used the 2σ lower value $\eta_B^{CMB} = 5.9 \times 10^{-10}$), for $\zeta = +1$ and for initial thermal abundance. The four panels correspond to the four benchmark cases A, B, C and D in the NH case. The solid lines are obtained including the contribution $N^{\rm f(2)}_{\Delta_{B-L}}$ in the final asymmetry and therefore represent the main result of the paper [8]. These have to be compared with the dashed lines where this contribution is neglected. In Fig. 6.5 and indeed in all subsequent figures, one can notice again a periodicity in π along Rez. This is because final asymmetries are given from eq. (6.70), for which all terms are dependant upon quantities periodic in π along Rez (these quantities being the washouts, $p^0_{\gamma_1\gamma_2}$ and the CP asymmetries). As one can see, on most of the regions leptogenesis is N_1-dominated as one would expect [4]. However, there are two regions, around $z \sim \pm\pi/2$, where the asymmetry is N_2-dominated. If $N^{\rm f(2)}_{\Delta_{B-L}}$ is neglected, this region would be only partially accessible and in any case only for quite large values $M_1 \gtrsim 30 \times 10^{10}\,$GeV [5].

When the contribution $N^{\rm f(2)}_{\Delta_{B-L}}$ is taken into account one can have successful leptogenesis for M_1 values as low as $1.3 \times 10^{11}\,$GeV for benchmark case B and vanishing initial N_2-abundance. The existence of these 'N_2-dominated regions' is the result of a combination of different effects: i) the value of $(1 - p^0_{\gamma_1\gamma_2})$, setting the size of the contribution from N_2 decays that survives the N_1 washout, is maximal in these regions as one can see from Fig. 6.2; ii) the wash-out at the production is in these region minimum as one can see from the plots of $K_{2\tau}$ and $K_{2\gamma}$ (cf. Fig. 6.1); iii) the N_2-flavoured CP asymmetries are not suppressed in these regions contrarily

[4] The N_1-dominated regions are approximately invariant for $z \to -z$, implying $N^{\rm f(1,\mathfrak{I})}_{\Delta_{B-L}}(z) \simeq N^{\rm f(1,\mathfrak{I})}_{\Delta_{B-L}}(-z)$. This is because $r^{\mathfrak{I}}_{1\alpha}$ is dominated by the first term in the eq. (6.61), exactly invariant for $z \to -z$, and because the $K_{1\alpha}$ are also approximately invariant for $z \to -z$ (see upper panels in Fig. 1).

[5] Notice that this time there is no invariance with respect to $z \to -z$ since $r^{\mathfrak{J}}_{2\alpha}$ is dominated either by the third term (for cases A, B, C,) or by the second term (for case D) in eq. (6.67) that are not invariant for $z \to -z$. On the other hand the second term is invariant for $\mathrm{Re}\, z \to -\mathrm{Re}\, z$ and therefore one could naively expect a specular region at $z \sim -\pi/2$. However, notice that $K_{2\gamma}$ is not invariant for $\mathrm{Re}\, z \to -\mathrm{Re}\, z$. In this way, for negative $\mathrm{Re}\, z$ and same values of $|z|$, the wash-out is strong and prevents the existence of this specular region.

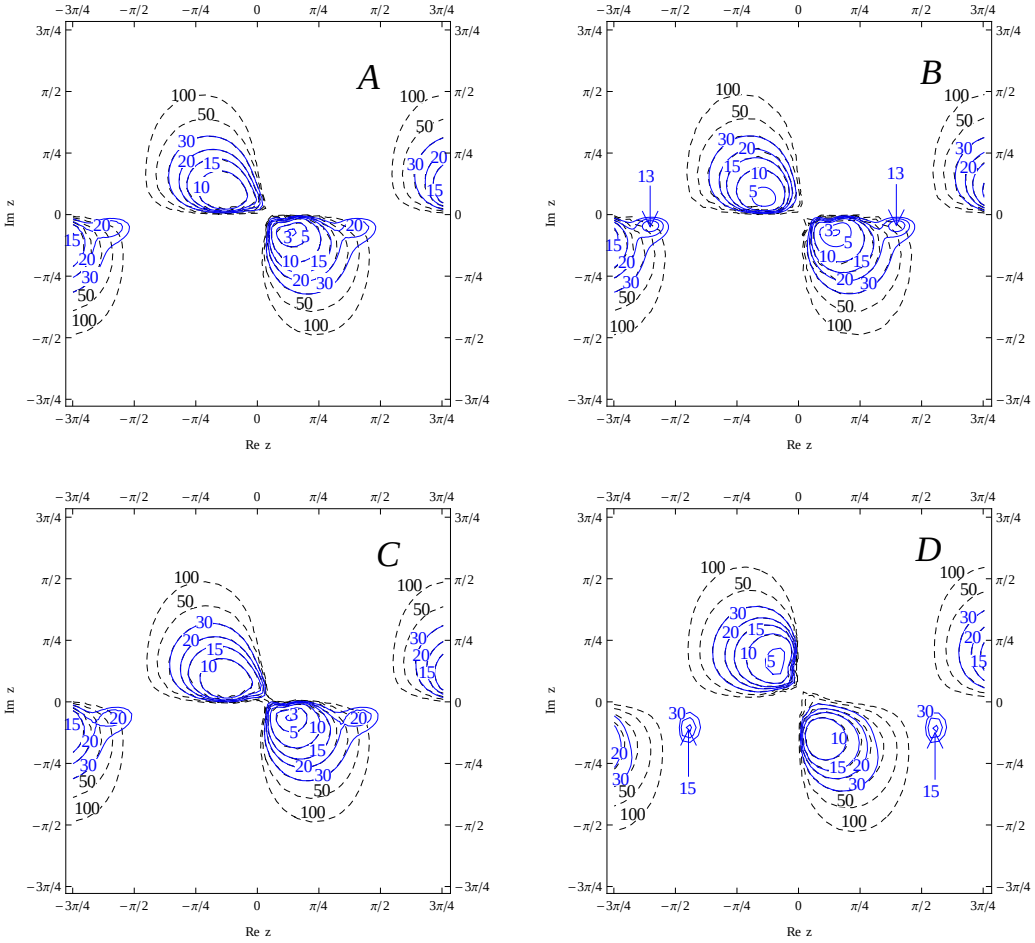

Figure 6.5: Contours plots in the z-plane of the M_1 values obtained imposing successful leptogenesis ($\eta_B = \eta_B^{CMB}$) for the NH case, $\zeta = +1$ and benchmarks A (top left), B (top right), C (bottom left) and D (bottom right) fixing U. The solid lines are obtained taking into account the contribution $N^{\mathrm{f}(2)}_{\Delta_{B-L}}$ to the final asymmetry while the dashed lines are obtained neglecting this contribution. Contours are labeled with the value of M_1 in units of 10^{10}GeV.

to the N_1 flavoured CP asymmetries (cf. figs. 6.3,6.4). It is interesting to compare the results obtained for the 4 different benchmark cases. A comparison between the case A (upper left panel) and the case B (upper right panel) shows that large values of θ_{13} and no Dirac phase enhance $N^{\mathrm{f}(2)}_{\Delta_{B-L}}$ so that the N_2-dominated regions get enlarged. On the other hand a comparison between B and C shows that a Dirac phase seems to suppress $N^{\mathrm{f}(2)}_{\Delta_{B-L}}$. A comparison between B and D shows that a Majorana phase seems just to change the position of the N_2-dominated regions without consistently modify their size differently from the N_1-dominated regions that are instead maximised by the presence of non-vanishing Majorana phase as known [112, 113]. Notice that, though this effect is shown only for $\theta_{13} = 11.5°$, it actually occurs for any choice of θ_{13}, in particular for $\theta_{13} = 0$. Interestingly, for non-zero Majorana

phase the new region where leptogenesis is favoured now overlaps with the $\mathrm{Im}(z) = 0$ axis. This means that CP violation for N_2-dominated leptogenesis can be successfully induced just by the Majorana phase. We have also checked that varying the low energy parameters within the ranges of values set by the 4 benchmark cases, one has a continuous variation of the allowed regions.

On the other hand if we consider the IH case, the situation is very different as one can see from fig. 6.6. The much stronger wash-out acting both on the N_1 and on the N_2 contributions (cf. eqs. (6.40,6.41) suppresses the final asymmetry in a way that large fraction of the allowed regions disappear, including the N_2-dominated regions. The surviving allowed regions are therefore strongly reduced and strictly N_1-dominated. Analogous results are obtained for the branch $\zeta = -1$, shown in fig. 6.7. A comparison between the plots obtained for the two branches shows that the the finally asymmetry is invariant for $(\xi, z) \to (-\xi, -z)$ and this is confirmed by the analytical expressions both for the flavoured decay parameters determining the wash-out and for the *CP* asymmetries.

6.5 Light Sequential Dominance and the 2RHN Model

In section 6.4.4 we have seen that two new favoured region for leptogenesis have appeared where $z \sim \pm\pi/2$, for $\zeta = \pm 1$, and for NH. Compared to previous studies where the production of the baryon asymmetry in this region of parameters was thought to be very suppressed, we found that, due to effects from N_2 decays, leptogenesis is quite efficient and can be realised with comparatively low $M_1 \sim 10^{11}$ GeV. This result is particularly interesting since $z \sim \pm\pi/2$ corresponds to the class of neutrino mass models with Light Sequential Dominance (LSD) [50], as we will now discuss. The dictionary between the parameter z and the Sequential Dominance (SD) parameters will be given explicitly in section 6.5.1. Finally, in 6.5.2 we will discuss the decay asymmetries in an explicit example scenario of LSD and show the enhancement of the asymmetry from N_2 decays analytically in terms of SD parameters and the deviation from TB mixing.

Recall from section 1.5 that for the parametrisation of the neutrino Yukawa

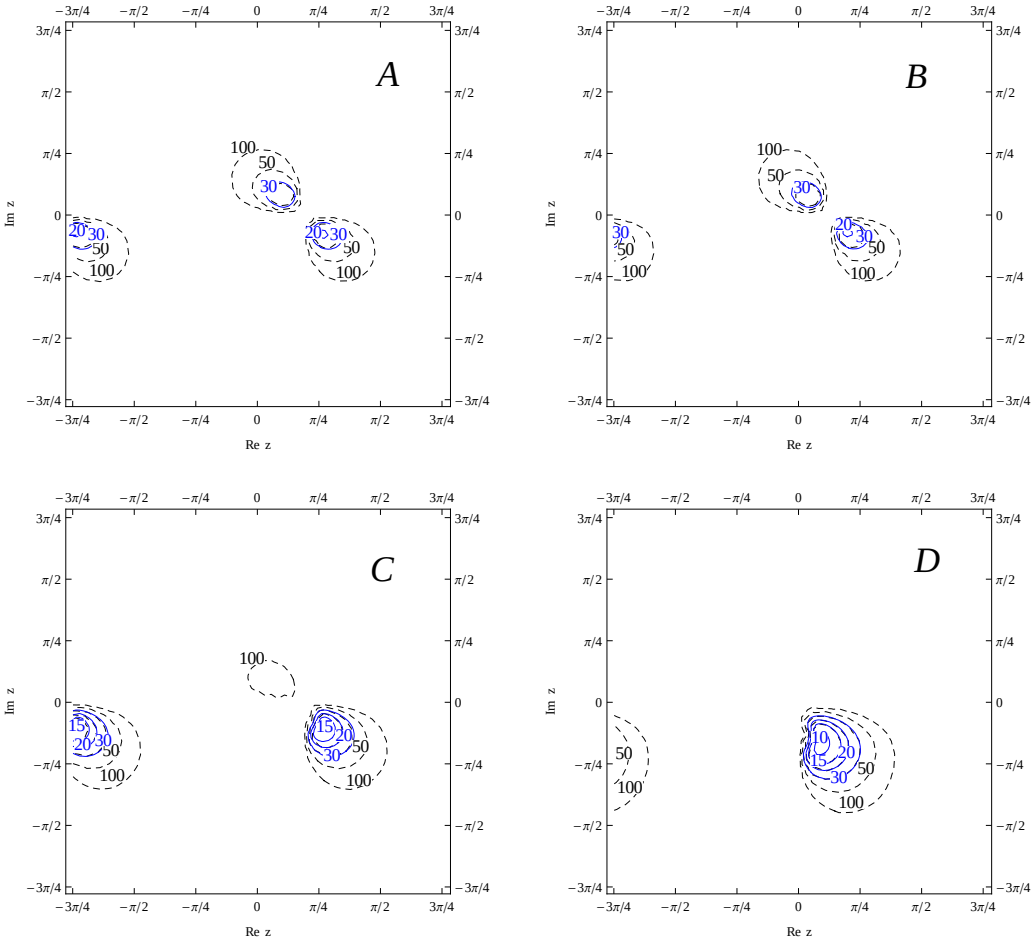

Figure 6.6: Contours plots in the z-plane of the M_1 values obtained imposing successful leptogenesis ($\eta_B = \eta_B^{CMB}$) for the IH case, $\zeta = +1$ and benchmarks A (top left), B (top right), C (bottom left) and D (bottom right) fixing U. The solid lines are obtained taking into account the contribution $N_{\Delta_{B-L}}^{\mathrm{f}(2)}$ to the final asymmetry while the dashed lines are obtained neglecting this contribution. Contours are labelled with the value of M_1 in units of 10^{10} GeV.

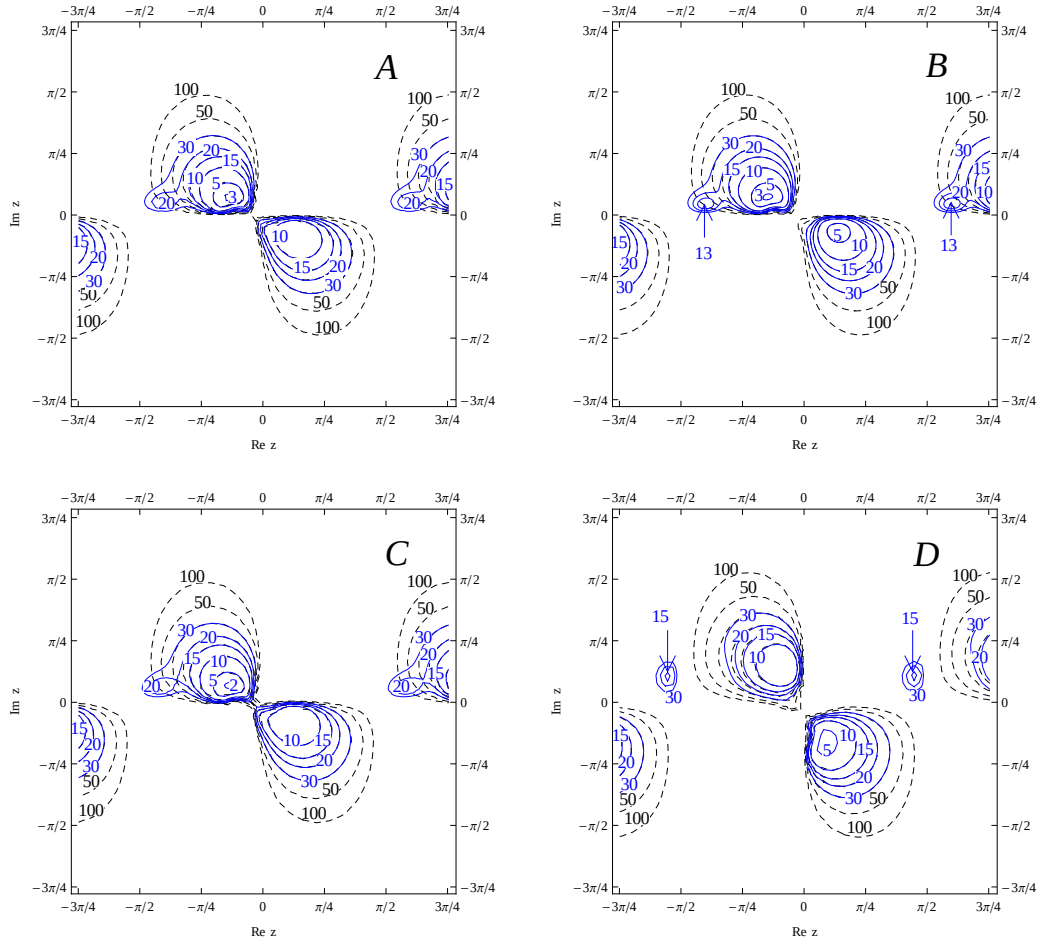

Figure 6.7: Contours plots in the z-plane of the M_1 values obtained imposing successful leptogenesis ($\eta_B = \eta_B^{CMB}$) for the NH case, $\zeta = -1$ and benchmarks A (top left), B (top right), C (bottom left) and D (bottom right) fixing U. The solid lines are obtained taking into account the contribution $N_{\Delta_{B-L}}^{f(2)}$ to the final asymmetry while the dashed lines are obtained neglecting this contribution. Contours are labeled with the value of M_1 in units of 10^{10}GeV.

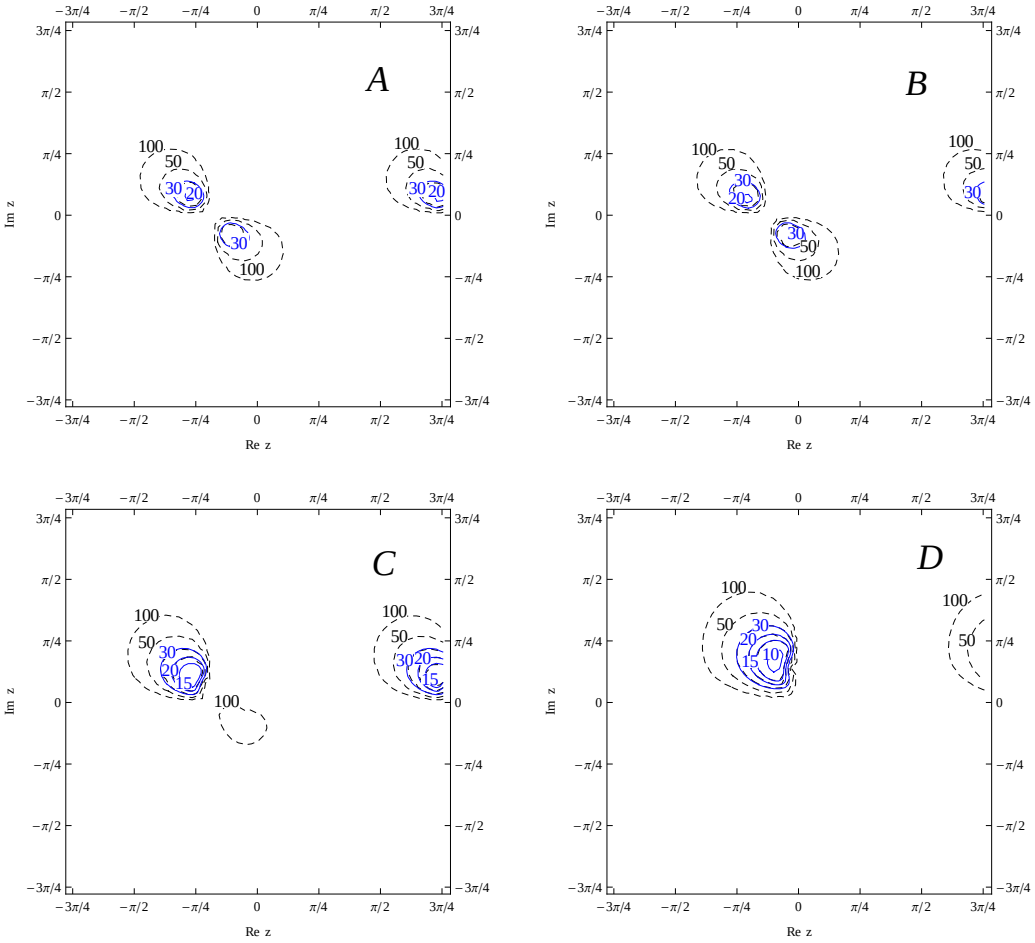

Figure 6.8: Contours plots in the z-plane of the M_1 values obtained imposing successful leptogenesis ($\eta_B = \eta_B^{CMB}$)for the IH case, $\zeta = -1$ and benchmarks A (top left), B (top right), C (bottom left) and D (bottom right) fixing U. The solid lines are obtained taking into account the contribution $N_{\Delta_{B-L}}^{\mathrm{f}(2)}$ to the final asymmetry while the dashed lines are obtained neglecting this contribution. Contours are labeled with the value of M_1 in units of 10^{10}GeV.

matrix below

$$Y_\nu = \begin{pmatrix} A_1 & B_1 & C_1 \\ A_2 & B_2 & C_2 \\ A_3 & B_3 & C_3 \end{pmatrix} \tag{6.76}$$

light sequential dominance (LSD) involves making the ansatz

$$\frac{A_i A_j}{M_1} \gg \frac{B_i B_j}{M_2} \gg \frac{C_i C_j}{M_3} \tag{6.77}$$

Constrained Sequential Dominance (CSD) is defined as [114]:

$$|A_1| = 0 \tag{6.78}$$

$$|A_2| = |A_3| \tag{6.79}$$

$$|B_1| = |B_2| = |B_3| \tag{6.80}$$

$$A^\dagger B = 0 \tag{6.81}$$

CSD implies TB mixing [114] and vanishing leptogenesis if $M_3 >> M_1, M_2$ [115,116].

6.5.1 An R matrix dictionary for LSD

According to LSD, the "dominant" N_1, i.e. its mass and Yukawa couplings, governs the largest light neutrino mass m_3, whereas the "subdominant" N_2 governs the lighter neutrino mass m_2, while the decoupled N_3 is associated with $m_1 \to 0$. Ignoring m_2/m_3 corrections, the R-matrix for LSD then takes the approximate form [117]:

$$R^{LSD} \approx \text{diag}(\pm 1, \pm 1, 1) \begin{pmatrix} 0 & 0 & 1 \\ 0 & 1 & 0 \\ 1 & 0 & 0 \end{pmatrix} \tag{6.82}$$

where the four different combinations of the signs correspond physically to the four different combinations of signs of the Dirac matrix columns associated with the lightest two RH neutrinos of mass M_1 and M_2. The sign of the third column associated with $M_3 \to \infty$ is irrelevant and has been dropped since it would in any case just redefine the overall sign of the Dirac mass matrix. These choices of signs are of course

irrelevant for the light neutrino phenomenology, since the effect of the orthogonal R matrix cancels in the see-saw mechanism (by definition). The four choices of sign are also irrelevant for type I leptogenesis, since each column enters quadratically in both the asymmetry and the washout formulas of section 6.4, independently of flavour or whether N_1 or N_2 is contributing. Comparing eq. (6.82) to the parametrisation of $R^{(NH)}$ for the 2 RHN models in eq. (6.14), we see that LSD just corresponds to $z \sim \pm\pi/2$ which correspond to the new regions opened up by N_2 leptogenesis that were observed numerically in the previous section. To be precise the dictionary for the sign choices in eq. (6.82) are as follows: for the $\zeta = 1$ branch, $z \approx \pi/2$, corresponds to diag$(1, -1, 1)$, while $z \approx -\pi/2$, corresponds to diag$(-1, 1, 1)$; for the $\zeta = -1$ branch, $z \approx \pi/2$, corresponds to diag$(-1, -1, 1)$, while $z \approx -\pi/2$, corresponds to diag$(1, 1, 1)$. According to the above observation, all four of these regions will contribute identically to leptogenesis, as observed earlier in the numerical and analytical results (i.e. giving identical results for $\zeta = \pm 1$ and $z \approx \pm\pi/2$).

We may expand eq. (6.14) for LSD for any one of these identical regions to leading order in m_2/m_3. For example consider the case $\zeta = -1$ and $z \approx -\pi/2$ corresponding to the case where all the Dirac columns have the same relative sign, diag$(1, 1, 1)$. Then expanding eq. (6.14) around $z \approx -\pi/2$, defining $\Delta \approx z + \frac{\pi}{2}$, we may write,

$$R^{LSD} \approx \begin{pmatrix} 0 & \Delta & 1 \\ 0 & 1 & -\Delta \\ 1 & 0 & 0 \end{pmatrix}. \tag{6.83}$$

Using the results in [118] we find useful analytic expressions which relate the R-matrix angle to the Yukawa matrix elements near the CSD limit of LSD corresponding to small Δ,

$$\begin{aligned} \mathrm{Re}(\Delta) &\approx \frac{\mathrm{Re}(A^\dagger B)v^2}{(m_3 - m_2)M_3^{1/2}M_2^{1/2}} \\ \mathrm{Im}(\Delta) &\approx \frac{\mathrm{Im}(A^\dagger B)v^2}{(m_3 + m_2)M_3^{1/2}M_2^{1/2}}. \end{aligned} \tag{6.84}$$

Notice that $\Delta \to 0$ when $A^\dagger B \to 0$ to all orders in m_2/m_3. This is just the

case in CSD due to eq. (6.81). Thus in the CSD limit of LSD eq. (6.82) becomes exact [117] to all orders in m_2/m_3. Clearly, leptogenesis vanishes in CSD which can be understood from the fact that the R-matrix in CSD is real and diagonal (up to a permutation) [116] or from the fact that A is orthogonal to B [115]. However in the next section we consider a perturbation of CSD, allowing leptogenesis but preserving TB mixing.

6.5.2 Example: perturbing the CSD limit of LSD

Using eq. (6.48), we obtain, making the usual hierarchical RH neutrino mass assumption the N_1 contribution to the leptogenesis asymmetry parameter is given by:

$$\varepsilon_{1\alpha} \approx -\frac{3}{16\pi}\frac{M_1}{M_2}\frac{1}{A^\dagger A}\mathrm{Im}\left[A_\alpha^*(A^\dagger B)B_\alpha\right] \tag{6.85}$$

Clearly the asymmetry vanishes in the case of CSD due to eq. (6.81). In this subsection we consider an example which violates CSD, but maintains TB mixing and stays close to LSD.

Before we turn to an explicit example, let us state the expectation for the size of the decay asymmetries. We expect that, typically,

$$\varepsilon_{1\mu,\tau} \approx -\frac{3}{16\pi}\frac{m_2 M_1}{v^2}\,, \qquad \varepsilon_{1e} \approx \frac{A_1}{A_2}\varepsilon_{1\mu,\tau} \tag{6.86}$$

The N_2 contribution to the leptogenesis asymmetry parameter is given by the interference with the lighter RH neutrino in the loop via the second term in eq. (6.48), which is indeed often ignored in the literature:

$$\varepsilon_{2\alpha} \approx -\frac{2}{16\pi}\frac{1}{B^\dagger B}\mathrm{Im}\left[B_\alpha^*(A^\dagger B)A_\alpha\right] \tag{6.87}$$

This leads to typically,

$$\varepsilon_{2\mu,\tau} \approx -\frac{1}{16\pi}\frac{m_3 M_1}{v^2}\,, \qquad \varepsilon_{2e} \approx \frac{A_1}{A_2}\varepsilon_{2\mu,\tau} \tag{6.88}$$

which should be compared to eq. (6.86). The N_2 contribution to the decay asymme-

tries looks larger than the N_1 contribution.

To compare the two asymmetries and the produced baryon asymmetry explicitly, let us now calculate the final asymmetries in a specific perturbation of the Light CSD form. As an example, we may consider

$$\begin{aligned}(A_1, A_2, A_3) &= (0, a, a) \\ (B_1, B_2, B_3) &= (b, b+q, -b+q)\end{aligned} \tag{6.89}$$

such that

$$Y_\nu = \begin{pmatrix} 0 & b & C_1 \\ a & b+q & C_2 \\ a & -b+q & C_3 \end{pmatrix} \tag{6.90}$$

Providing $|q| \ll |b|$, this perturbation of CSD stays close to LSD and allows non-zero leptogenesis. Interestingly this perturbation of CSD also preserves TB mixing as discussed in [118], where more details can be found. Note that z is given by eq. (6.84) and therefore depends on a, b and q.

For our example, we now obtain (assuming real a and neglecting q in $B^\dagger B$):

$$\varepsilon_{1\gamma} \approx -\frac{3}{16\pi}\frac{m_2 M_1}{v^2}\frac{\mathrm{Im}[q\,b + q^2]}{B^\dagger B}, \quad \varepsilon_{1\tau} \approx -\frac{3}{16\pi}\frac{m_2 M_1}{v^2}\frac{\mathrm{Im}[-q\,b + q^2]}{B^\dagger B} \tag{6.91}$$

The N_2 contribution to the leptogenesis asymmetry parameter is given by the interference with the lighter RH neutrino in the loop via the second term in eq. (6.48):

$$\varepsilon_{2\gamma} \approx -\frac{2}{16\pi}\frac{m_3 M_1}{v^2}\frac{\mathrm{Im}[q\,b^*]}{B^\dagger B}\,, \qquad \varepsilon_{2\tau} \approx -\varepsilon_{2\gamma} \tag{6.92}$$

For the washout parameters, we obtain:

$$K_{1\gamma} = K_{1\tau} \approx \frac{m_3}{m_*} \qquad \text{and} \qquad K_{2\gamma} \sim K_{2\tau} \approx \frac{m_2}{m_*} \tag{6.93}$$

The parameter p_{12} is given by (neglecting q in the last step)

$$p_{12} \approx -\frac{|A_1 B_2 + A_2 B_1|^2}{(|A_1|^2 + |A_2|^2)(|B_1|^2 + |B_2|^2)} \approx \frac{1}{2} \tag{6.94}$$

For the final asymmetries from N_1 decay this means

$$N_{B-L}^{f(1)} \approx -(\varepsilon_{1\gamma} + \varepsilon_{1\tau})\,\kappa_{1\gamma} \approx 2\frac{3}{16\pi}\frac{m_2 M_1}{v^2}\frac{\mathrm{Im}[q^2]}{B^\dagger B}\kappa(m_3/m^*) \tag{6.95}$$

whereas

$$N_{B-L}^{f(2)} \approx -(1-p_{12})\varepsilon_{2\gamma}\,\kappa_{2\gamma} \approx \frac{1}{2}\frac{2}{16\pi}\frac{m_3 M_1}{v^2}\frac{\mathrm{Im}[q\,b^*]}{B^\dagger B}\kappa(m_2/m^*) \tag{6.96}$$

So we can estimate:

$$\frac{N_{B-L}^{f(2)}}{N_{B-L}^{f(1)}} \approx \frac{m_3}{m_2}\frac{\kappa(m_2/m^*)}{\kappa(m_3/m^*)}\frac{\mathrm{Im}[q\,b^*]}{\mathrm{Im}[6\,q^2]} \tag{6.97}$$

We see that, as already anticipated in the beginning of this subsection, there is an enhancement of the asymmetry from the N_2 decay by a factor of $\frac{m_3}{m_2}$ (from the decay asymmetries). Furthermore, there is another enhancement factor from the efficiency factor κ given by $\frac{\kappa(m_2/m^*)}{\kappa(m_3/m^*)}$. Both terms imply an enhancement of a factor of 5 each. Finally, the factor $\frac{\mathrm{Im}[q\,b^*]}{\mathrm{Im}[6\,q^2]}$ can get large for small q, i.e. close to the CSD case. However, of course, closer to the CSD case the decay asymmetries get more and more suppressed.

In summary, in models with Light Sequential Dominance (LSD) the asymmetry from the N_2 decays is generically larger than the asymmetry from N_1 decays, in agreement with the results obtained in the previous sections in the R matrix parametrisation. We like to emphasise that in order to calculate the prospects for leptogenesis in models with LSD (in the two flavour regime), it is thus crucial to include the N_2 decays (which have previously been neglected).

6.6 Phantom Leptogenesis in the 2RHN Model

In section 6.4.2 I gave the symmetric part of the projector $p_{\gamma_1^0\gamma_2}$ as

$$p^0_{\gamma_1\gamma_2} = \frac{\left|\sum_{\alpha=e,\mu} \mathcal{C}^0_{1\alpha}\mathcal{C}^{0\star}_{2\alpha}\right|^2}{\left(|\mathcal{C}^0_{1e}|^2 + |\mathcal{C}^0_{1\mu}|^2\right)\left(|\mathcal{C}^0_{2e}|^2 + |\mathcal{C}^0_{2\mu}|^2\right)} \tag{6.98}$$

for $\mathcal{C}_{i\alpha} \equiv \langle l_i | l_\alpha \rangle$ and $\mathcal{C}^0_{i\alpha} = \frac{m_{D_{\alpha i}}}{\sqrt{\left(m_D^\dagger m_D\right)_{ii}}}$ as the tree-level part of $\mathcal{C}_{i\alpha}$. Similarly the anti-symmetric part of $p_{\gamma_1^0\gamma_2}$, upon which the two-flavour 2RHN model phantom terms [7] depend, is given as

$$\Delta p_{\gamma_1^0\gamma_2} = \frac{\left|\sum_{\alpha=e,\mu}\left(\mathcal{C}^0_{1\alpha}\mathcal{C}^\star_{2\alpha} - \mathcal{C}^0_{1\alpha}\bar{\mathcal{C}}^\star_{2\alpha}\right)\right|^2}{\left(|\mathcal{C}^0_{1e}|^2 + |\mathcal{C}^0_{1\mu}|^2\right)\left(|\mathcal{C}^0_{2e}|^2 + |\mathcal{C}^0_{2\mu}|^2\right)} \tag{6.99}$$

Expanding the sum over flavours explicitly, one finds

$$\begin{aligned}\Delta p_{\gamma_1^0\gamma_2} &= \frac{1}{p^0_{1\gamma}p^0_{2\gamma}}|\mathcal{C}^0_{1e}|^2\left(|\mathcal{C}_{2e}|^2 - |\bar{\mathcal{C}}_{2e}|^2\right) + \frac{1}{p^0_{1\gamma}p^0_{2\gamma}}|\mathcal{C}^0_{1\mu}|^2\left(|\mathcal{C}_{2\mu}|^2 - |\bar{\mathcal{C}}_{2\mu}|^2\right) \\ &+ \frac{1}{p^0_{1\gamma}p^0_{2\gamma}}\left(\mathcal{C}^{0\star}_{1e}\,\mathcal{C}_{2e}\,\mathcal{C}^0_{1\mu}\,\mathcal{C}^\star_{2\mu} - \mathcal{C}^0_{1e}\,\bar{\mathcal{C}}_{2e}\,\mathcal{C}^{0\star}_{1\mu}\,\bar{\mathcal{C}}^\star_{2\mu}\right) + \{e \leftrightarrow \mu\}\end{aligned} \tag{6.100}$$

having identified γ-flavoured branching ratios $p^0_{1\gamma} \equiv |\mathcal{C}^0_{1e}|^2 + |\mathcal{C}^0_{1\mu}|^2$ and $p^0_{2\gamma} \equiv |\mathcal{C}^0_{2e}|^2 + |\mathcal{C}^0_{2\mu}|^2$. We can immediately identify $p^0_{i\alpha} \equiv |\mathcal{C}^0_{i\alpha}|^2$ and $\Delta p_{i\alpha} \equiv |\mathcal{C}_{i\alpha}|^2 - |\bar{\mathcal{C}}_{i\alpha}|^2$ and so first term may be related straightforwardly to tree-level branching ratios and the CP asymmetry as

$$\text{1st} \times p^0_{1\gamma}p^0_{2\gamma} = p^0_{1e}\Delta p_{2e} + p^0_{1\mu}\Delta p_{2\mu} \tag{6.101}$$

where the $\Delta p_{i\alpha}$ were calculated explicitly back in section 3.2. The second term is a little more tricky to calculate - we require explicit expressions for the $\mathcal{C}_{2\alpha}$ and $\bar{\mathcal{C}}_{2\alpha}$ to 1-loop level. In section 3.2 these were given as

$$\mathcal{C}_{2\alpha} = \frac{1}{\sqrt{(Y^{\nu\dagger}Y^\nu)_{22} - 2\,\mathrm{Re}(Y^{\nu\dagger}Y^\nu\,\xi_u)_{22}}}\left(Y^\nu_{\alpha 2} - (Y^\nu\,\xi_u)_{\alpha 2}\right) \tag{6.102}$$

$$\bar{\mathcal{C}}_{\bar{2}\bar{\alpha}} = \frac{1}{\sqrt{(Y^{\nu\dagger}Y^\nu)_{22} - 2\,\mathrm{Re}(Y^{\nu\dagger}Y^\nu\,\xi_v^\star)_{22}}}\left(Y^{\nu\star}_{\alpha 2} - (Y^{\nu\star}\,\xi_v)_{\alpha 2}\right) \tag{6.103}$$

where ξ_u and ξ_v are loop-level kinematic functions of $\mathcal{O}(Y^2)$, given explicitly in section 3.2. Substituting the eqs. (6.102) one may then express the second line (up to $\mathcal{O}(Y^2)$

terms) in eq. (6.100) as

$$\begin{aligned}
\text{2nd} \times p^0_{1\gamma} p^0_{2\gamma} &= -\frac{Y^{\nu\star}_{e1}\,(Y^\nu\,\xi_u)_{e2}\,Y^\nu_{\mu1}\,Y^{\nu\star}_{\mu2}}{(Y^{\nu\dagger}\,Y^\nu)_{11}\,(Y^{\nu\dagger}\,Y)_{22}} - \frac{Y^{\nu\star}_{e1}\,Y^\nu_{e2}\,Y^\nu_{\mu1}\,(Y^\nu\,\xi_u)^\star_{\mu2}}{(Y^{\nu\dagger}\,Y^\nu)_{11}\,(Y^{\nu\dagger}\,Y)_{22}} \\
&+ \frac{Y^\nu_{e1}\,(Y^{\nu\star}\,\xi_v)_{e2}\,Y^{\nu\star}_{\mu1}\,Y^\nu_{\mu2}}{(Y^{\nu\dagger}\,Y^\nu)_{11}\,(Y^{\nu\dagger}\,Y)_{22}} + \frac{Y^\nu_{e1}\,Y^{\nu\star}_{e2}\,Y^{\nu\star}_{\mu1}\,(Y^{\nu\star}\,\xi_v)^\star_{\mu2}}{(Y^{\nu\dagger}\,Y^\nu)_{11}\,(Y^{\nu\dagger}\,Y)_{22}} \\
&+ \frac{Y^{\star\nu}_{1e}\,Y^\nu_{2e}\,Y^\nu_{1\mu}\,Y^{\nu\star}_{2\mu}}{(Y^{\nu\dagger}\,Y^\nu)_{11}\,(Y^{\nu\dagger}\,Y^\nu)_{22}}\left[1+\frac{2\,\mathrm{Re}\left(Y^{\nu\dagger}\,Y^\nu\,\xi_u\right)_{22}}{(Y^{\nu\dagger}\,Y^\nu)_{22}}\right] \\
&- \frac{Y^\nu_{1e}\,Y^{\nu\star}_{2e}\,Y^{\nu\star}_{1\mu}\,Y^\nu_{2\mu}}{(Y^{\nu\dagger}\,Y^\nu)_{11}\,(Y^{\nu\dagger}\,Y^\nu)_{22}}\left[1+\frac{2\,\mathrm{Re}\left(Y^{\nu\dagger}\,Y^\nu\,\xi^\star_v\right)_{22}}{(Y^{\nu\dagger}\,Y^\nu)_{22}}\right] \qquad (6.104)
\end{aligned}$$

and similarly for the $\{e \leftrightarrow \mu\}$ term, where the first two lines above come from the numerator of eq. (6.102) and the final two lines from binomially expanding the denominator. Adding the $\{e \leftrightarrow \mu\}$ term of eq. (6.100) also, one obtains after some algebra an equation for the total projector as

$$\begin{aligned}
p^0_{1\gamma} p^0_{2\gamma}\,\Delta p_{\gamma^0_1\gamma_2} &= p^0_{1e}\Delta p_{2e} + p^0_{1\mu}\Delta p_{2\mu} \qquad (6.105)\\
&- \frac{|Y^\nu_{e1}|^2}{(Y^{\nu\dagger}\,Y^\nu)_{11}}\,2\,\mathrm{Re}\left[\frac{Y^\nu_{\mu1}\,Y^{\nu\star}_{\mu2}}{(Y^{\nu\dagger}\,Y^\nu)_{22}}\,(\xi_u-\xi^\star_v)_{12}\right] \\
&- \frac{\left|Y^\nu_{\mu1}\right|^2}{(Y^{\nu\dagger}\,Y^\nu)_{11}}\,2\,\mathrm{Re}\left[\frac{Y^\nu_{e1}\,Y^{\nu\star}_{e2}}{(Y^{\nu\dagger}\,Y^\nu)_{22}}\,(\xi_u-\xi^\star_v)_{12}\right] \\
&+ 4\,\mathrm{Re}\left[\frac{Y^{\star\nu}_{e1}\,Y^\nu_{e2}\,Y^\nu_{1\mu}\,Y^{\nu\star}_{\mu2}}{(Y^{\nu\dagger}\,Y^\nu)_{11}\,(Y^{\nu\dagger}\,Y^\nu)_{22}}\right]\mathrm{Re}\left[\frac{(Y^{\nu\dagger}\,Y^\nu)_{21}}{(Y^{\nu\dagger}\,Y^\nu)_{22}}\,(\xi_u-\xi^\star_v)_{12}\right]
\end{aligned}$$

In section 3.2 during the calculation of $\Delta p_{i\alpha}$ I identified

$$\varepsilon_{i\alpha} = \sum_{k\neq i}\mathrm{Re}\left[\frac{Y^{\nu\star}_{\alpha i}\,Y^\nu_{\alpha k}}{(Y^{\nu\dagger}\,Y^\nu)_{ii}}\,(\xi_u-\xi^\star_v)_{ki}\right] \qquad (6.106)$$

$$\varepsilon_i = \sum_{k\neq i}\mathrm{Re}\left[\frac{(Y^{\nu\dagger}\,Y^\nu)_{ik}}{(Y^{\nu\dagger}\,Y^\nu)_{ii}}\,(\xi_u-\xi^\star_v)_{ki}\right] = \sum_\alpha \varepsilon_{i\alpha} \qquad (6.107)$$

and hence substituting the above into eq. (6.105) with $i=2$, $k=1$ (and a decoupled third RHN) obtains

$$\begin{aligned}
\Delta p_{\gamma^0_1\gamma_2} &= \frac{p^0_{1e}\Delta p_{2e}}{p^0_{1\gamma}p^0_{2\gamma}} + \frac{p^0_{1\mu}\Delta p_{2\mu}}{p^0_{1\gamma}p^0_{2\gamma}} - \frac{2\,\left(p^0_{1e}\,\varepsilon_{2\mu}+p^0_{1\mu}\,\varepsilon_{2e}\right)}{p^0_{1\gamma}\,p^0_{2\gamma}} \\
&+ \frac{4\,\varepsilon_2}{p^0_{1\gamma}\,p^0_{2\gamma}}\,\mathrm{Re}\left[\frac{Y^{\star\nu}_{e1}\,Y^\nu_{e2}\,Y^\nu_{\mu1}\,Y^{\nu\star}_{\mu2}}{(Y^{\nu\dagger}\,Y^\nu)_{11}\,(Y^{\nu\dagger}\,Y^\nu)_{22}}\right] + \mathcal{O}(Y^4) \qquad (6.108)
\end{aligned}$$

having also identified $p^0_{i\alpha} \equiv |Y^\nu_{\alpha i}|^2/(Y^{\nu\dagger}\,Y^\nu)_{ii}$. Using the identities $\varepsilon_{2\alpha} \equiv p^0_{2\alpha}\,\varepsilon_2 - \frac{\Delta p_{2\alpha}}{2}$, $p^0_{1\gamma} \equiv p^0_{1e} + p^0_{1\mu}$ and $\varepsilon_{2\gamma} \equiv \varepsilon_{2e} + \varepsilon_{2\mu}$ this result may be further simplified, yielding

$$\Delta p_{\gamma^0_1\gamma_2} \,=\, -\frac{2\,\varepsilon_{2\gamma}}{p^0_{2\gamma}} \,+\, \frac{2\,\varepsilon_2}{p^0_{1\gamma}\,p^0_{2\gamma}}\,\left(2\,\mathrm{Re}\left[\frac{Y^{\star\nu}_{e1}\,Y^\nu_{e2}\,Y^\nu_{\mu 1}\,Y^{\nu\star}_{\mu 2}}{(Y^{\nu\dagger}\,Y^\nu)_{11}\,(Y^{\nu\dagger}\,Y^\nu)_{22}}\right] + p^0_{1e}\,p^0_{2e} \,+\, p^0_{1\mu}\,p^0_{2\mu}\right)$$

In section 6.4.3 I showed that $\varepsilon_2 \ll \varepsilon_{2\alpha}$ in the 2RHN model and so neglecting the second term in ε_2 we can approximate the final projector as

$$\Delta p_{\gamma^0_1\gamma_2} \,\approx\, -\,\frac{2\,\varepsilon_{2\gamma}}{p^0_{2\gamma}} \tag{6.109}$$

In fig. 6.9 the above equation is plotted in the z-plane, having used eq. (6.65) for $\varepsilon_{2\gamma} = \varepsilon_{2e} + \varepsilon_{2\mu}$ in the orthogonal parametrisation.

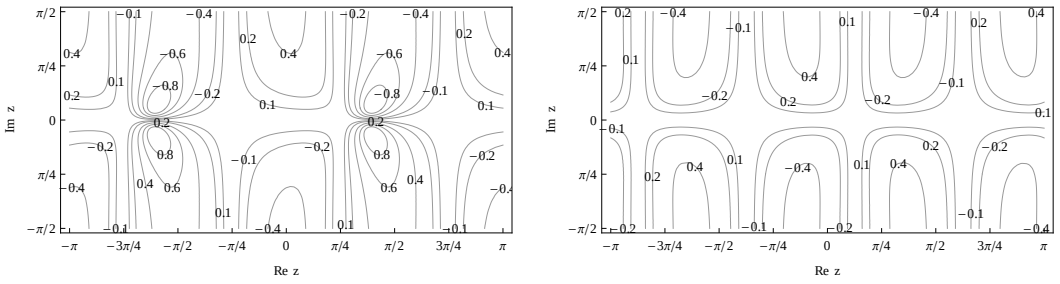

Figure 6.9: Contour plots of $\Delta p_{\gamma^0_1\gamma_2}\,/\,\bar{\varepsilon}_1$ for NH (left) and IH (right) (benchmark B, $\zeta = 1$).

Since $|\Delta p_{\gamma^0_1\gamma_2}| \gtrsim \varepsilon_{2\gamma}$ and the "phantom term" containing it is washed out only half as much as the standard γ-flavoured terms (cf. eq. 6.16), one expects that upon inclusion of the phantom terms the N_2 dominated regions found in [8] and described in section 6.4.4 get **enhanced**. This is indeed what happens - in fig. 6.10 I have plotted the final asymmetry for vanishing initial abundance with phantom terms included. Comparing with fig. 6.5 of section 6.4.4 one can see that the N_2-dominated regions around $z \sim \frac{\pi}{2}$ get enlarged upon inclusion of the phantom terms, lowering the bound on M_1 by about an order of magnitude.

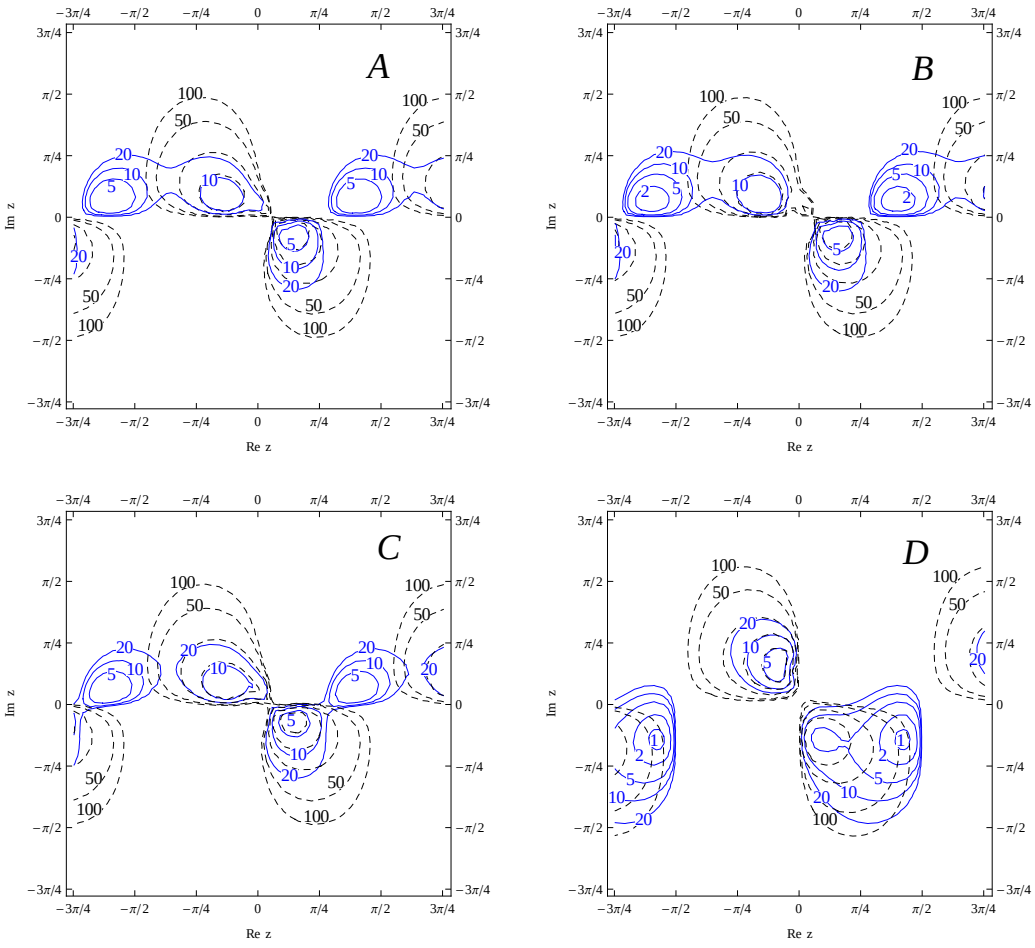

Figure 6.10: Final Baryon Asymmetry in the SM with vanishing initial abundance and $\zeta = +1$, for NH and with phantom terms included. Blue solid lines (black dashed lines) are with (without) N_2 decays included.

Chapter 7

Supersymmetric Leptogenesis

7.1 Supersymmetry - The Rough Idea

Supersymmetry (SUSY) is an extended space-time symmetry. The Poincare algebra in section 1.1 is extended to include anti-commuting generators. Altogether this Super-Poincare algebra (for $N = 1$ SUSY) is given by [119]

$$\begin{aligned}
[M_{\mu\nu}, M_{\rho\sigma}] &= i\left(M_{\mu\nu}\eta_{\rho\sigma} + M_{\mu\rho}\eta_{\rho\sigma} - M_{\nu\rho}\eta_{\nu\sigma} - M_{\nu\sigma}\eta_{\mu\rho}\right) \\
[P_\mu,\, P_\nu] &= 0 \\
[M_{\mu\nu},\, P_\sigma] &= i\left(P_\mu\eta_{\nu\sigma} - P_\nu\eta + \mu\sigma\right) \\
[Q_\alpha,\, M_{\mu\nu}] &= (\sigma_{\mu\nu})_\alpha^\beta\, Q_\beta \\
\left[\bar{Q}^{\dot{\alpha}},\, M_{\mu\nu}\right] &= (\bar{\sigma}_{\mu\nu})_{\dot{\beta}}^{\dot{\alpha}}\, \bar{Q}^{\dot{\beta}} \\
[Q_\alpha,\, P_\mu] &= \left[\bar{Q}_{\dot{\alpha}},\, P_\mu\right] = 0 \\
\{Q_\alpha, Q_\beta\} &= \left\{\bar{Q}_{\dot{\alpha}}, \bar{Q}_{\dot{\beta}}\right\} = 0 \\
\left\{Q_\alpha, \bar{Q}_{\dot{\beta}}\right\} &= 2\left(\sigma^\mu\right)_{\alpha\dot{\beta}} P_\mu
\end{aligned} \tag{7.1}$$

where undotted indices α, β denote components of the $(\frac{1}{2}, 0)$ generator Q and dotted indices $\dot{\alpha}$, $\dot{\beta}$ denote components of the $(0, \frac{1}{2})$ generator $\bar{Q}$. The generators Q and $\bar{Q}$ mix the representations of the Lorentz group, changing particle spin by a half unit whilst preserving charges under gauge groups. They mix spin 1 vector bosons with spin $\frac{1}{2}$ fermions and spin $\frac{1}{2}$ fermions with spin 0 scalar bosons. We can write

schematically [120]

$$\begin{aligned} Q\,|\text{fermion}\,\rangle &= |\,\text{boson}\rangle & \bar{Q}\,|\text{fermion}\,\rangle &= |\,\text{boson}\,\rangle \\ Q\,|\text{boson}\,\rangle &= |\,\text{fermion}\,\rangle & \bar{Q}\,|\text{boson}\,\rangle &= |\,\text{fermion}\,\rangle \end{aligned} \tag{7.2}$$

In this thesis I will consider only the MSSM. The MSSM field content [120] is specified in the table below, which extends table 1.2 to include the SUSY partners of the SM fields in section 1.1. We can also include a RH neutrino $\bar{N}$ (spin $\frac{1}{2}$) and sneutrino $\widetilde{N}^\star$ (spin 0) both "charged" as (1, 1, 0) under the SM gauge group, since we intend to look at leptogenesis in the MSSM.

Table 7.1: MSSM partners of table 1.2s SM fields

field	gauge rep	Lorentz rep	B	L
$\begin{pmatrix}\widetilde{u}\\ \widetilde{d}\end{pmatrix}$ $\begin{pmatrix}\widetilde{c}\\ \widetilde{s}\end{pmatrix}$ $\begin{pmatrix}\widetilde{t}\\ \widetilde{b}\end{pmatrix}$	$\left(3,\, 2,\, \frac{1}{3}\right)$	(0, 0)	$\frac{1}{3}$	0
$\widetilde{u}^\star$ $\widetilde{c}^\star$ $\widetilde{t}^\star$	$\left(\bar{3},\, 1, -\frac{4}{3}\right)$	(0, 0)	$-\frac{1}{3}$	0
$\widetilde{d}^\star$ $\widetilde{s}^\star$ $\widetilde{b}^\star$	$\left(\bar{3},\, 1,\, \frac{2}{3}\right)$	(0, 0)	$-\frac{1}{3}$	0
$\begin{pmatrix}\widetilde{\nu}_e\\ \widetilde{e}\end{pmatrix}$ $\begin{pmatrix}\widetilde{\nu}_\mu\\ \widetilde{\mu}\end{pmatrix}$ $\begin{pmatrix}\widetilde{\nu}_\tau\\ \widetilde{\tau}\end{pmatrix}$	(1, 2, 1)	(0, 0)	0	1
$\widetilde{e}^\star$ $\widetilde{\mu}^\star$ $\widetilde{\tau}^\star$	(1, 1, 2)	(0, 0)	0	-1
$\widetilde{g}$ (gluinos)	$(8, 1, 0)$	$(\frac{1}{2}, 0)$	0	0
$\widetilde{W}$ (winos)	(1, 3, 0)	$(\frac{1}{2}, 0)$	0	0
$\widetilde{B}$ (bino)	(1, 1, 0)	$(\frac{1}{2}, 0)$	0	0
$\begin{pmatrix}\widetilde{\phi}_u^+\\ \widetilde{\phi}_u^0\end{pmatrix}$ (up Higgsino)	(1, 2, 1)	$\left(\frac{1}{2}, 0\right)$	0	0
$\begin{pmatrix}\widetilde{\phi}_d^0\\ \widetilde{\phi}_d^-\end{pmatrix}$ (down Higgsinos)	(1, 2, −1)	$\left(\frac{1}{2}, 0\right)$	0	0

7.2 The Impact of $\tan\beta$ on Leptogenesis

In SM leptogenesis a lepton asymmetry can be produced via the decays of RH neutrinos into leptons. In the MSSM case both RH neutrinos and sneutrinos may decay into both leptons and sleptons. The MSSM seesaw mechanism is defined by the superpotential below [96]

$$W_{seesaw} = W_{MSSM} + Y^{\nu}_{\alpha i}\, L_\alpha\, H_u\, N_i \;+\; \frac{1}{2}\, M_i\, N_i\, N_i \tag{7.3}$$

where the fields L, H, N above are **chiral superfields** containting spin 0 and spin $\frac{1}{2}$ components, given explicitly by [121]

$$\chi(x,\,\theta) = \phi(x) + \sqrt{2}\theta^\alpha\,\psi_\alpha(x) + \theta^\alpha\theta^\beta\epsilon_{\alpha\beta}F(x) \tag{7.4}$$

where ϕ is the spin 0 component and ψ is the spin $\frac{1}{2}$ component (and F is a spin 0 "auxiliary" field required to close the algebra of eqs. (7.1)). The various Feynman diagrams obtained from unpacking the components of the $Y_{\alpha i}\, L_\alpha\, H_u\, N_i$ term in eq. (7.3) are shown in fig. 7.1 , with the top left diagram common to both SM and MSSM leptogenesis.

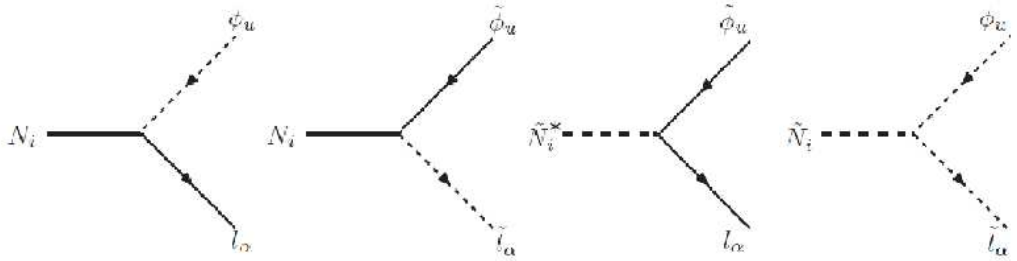

Figure 7.1: Supersymmetric Feynman diagrams for tree level neutrino decays

In MSSM models the Higgs sector works a little differently. In the SM only one Higgs doublet ϕ may give masses to all the SM fermions, by acquiring a vev, v. In the MSSM case one Higgs doublet ϕ_u - with a vev v_u - is needed to give mass to the upper halves of (s)fermion doublets, and a second Higgs doublet ϕ_d - with a vev v_d - is needed to give masses to the lower halves [120]. These vevs must satisfy

$v_u^2 + v_d^2 \equiv v^2$ and so we can define a parameter β as

$$\tan\beta \equiv \frac{v_u}{v_d} \tag{7.5}$$

such that $v_u \equiv v\sin\beta$ and $v_d \equiv v\cos\beta$ satisfy $v_u^2 + v_d^2 \equiv v^2$. Because the masses of the fermions are fixed by experiment, if MSSM Higgs vevs are rescaled by factors of $\cos\beta$ and $\sin\beta$ then MSSM Yukawa couplings must be rescaled by factors of $\frac{1}{\cos\beta}$ and $\frac{1}{\sin\beta}$, such that all combination of vev $\times$ Yukawa remain invariant.

This rescaling has particular relevance for SS leptogenesis, which is directly sensitive to the (s)neutrino and charged (s)lepton Yukawa couplings. For a lepton doublet $l_\alpha = (\nu_L,\, e_L)^T$ the neutrino belongs to the upper half of the doublet - hence gets its mass from $v_u \equiv v\sin\beta$ - and the charged lepton to the lower half - hence gets its mass from $v_d \equiv v\cos\beta$. So the neutrino Yukawa Y^ν and charged lepton Yukawa Y^e should be rescaled according to

$$Y^\nu \mapsto \frac{1}{\sin\beta}\, Y^\nu\,, \qquad\qquad Y^e \mapsto \frac{1}{\cos\beta}\, Y^e \tag{7.6}$$

The leptogenesis Boltzmann equations are then sensitive to $\tan\beta$ in two key ways:

1. Through $Y^\nu_{\alpha i}$: this determines the decay rates for $N_i \mapsto l_\alpha + \phi_u$ and hence the CP violating and washout parameters. Rescaling $Y^\nu_{\alpha i}$ rescales $K_{i\alpha}$ and $\varepsilon_{i\alpha}$

2. Through $Y^e_{\alpha i}$: the Boltzmann equations' flavour basis depends upon which flavours have decohered at $T \sim T_L$, the leptogenesis temperature, which in turn depends upon the rate of $l_\alpha \rightleftharpoons \alpha_R + \phi_d$, as set by $Y^e_{\alpha i}$. Hence rescaling $Y^e_{\alpha i}$ can completely alter the leptogenesis flavour dynamics.

How strong is the impact of $\tan\beta$? Since we observe that the up type quarks are more massive than the down type quarks, it is also a general requirement for MSSM models that $v_u > v_d$, or equivalently $\tan\beta > 1$. In cases where $\tan\beta \sim 1$ not very much changes - the rescalings to Y^ν and Y^e introduce only $\mathcal{O}(1)$ corrections. However, in many phenomenologically viable models we have that $\tan\beta \gg 1$. For such cases $cos\beta \ll 1$ meaning that Y^e gets significantly enhanced. This ensures transitions between flavour regimes happen at a much higher temperature, because

if $\Gamma_{l_\alpha \mapsto \alpha_R + \phi_d} \propto T$ is enhanced by a factor $\frac{1}{\cos^2\beta} \equiv \left(1 + \tan^2\beta\right) \gg 1$ it first becomes $\mathcal{O}(1)$ relative to $H(T) \propto T^2$ at a higher temperatures than without this factor. Hence the $1 \mapsto 2$ flavour regime transition temperature T_{12} and the $2 \mapsto 3$ flavour regime transition temperature T_{23} are both shifted up according to

$$T_{12} \sim 10^{12} GeV \mapsto \left(1 + \tan^2\beta\right) 10^{12} GeV \tag{7.7}$$

$$T_{23} \sim 10^{9} GeV \mapsto \left(1 + \tan^2\beta\right) 10^{9} GeV \tag{7.8}$$

In section 7.5.2 we will consider an example where $\tan\beta \gg 1$ changes a SM two-flavour regime at $T \sim 10^{10} GeV$ into a MSSM three–flavour regime through the rescaling $Y^e_{1\mu} \mapsto \frac{1}{\cos\beta} Y^e_{1\mu}$ shifting $T_{23} \sim 10^9 GeV \mapsto \left(1 + \tan^2\beta\right) 10^9 GeV \sim 10^{12} GeV$ for $\tan\beta \sim 30$.

7.3 Supersymmetric Leptogenesis

Supersymmetric leptogenesis proceeds on more or less the same manner as in the SM, with the modification that there are now both neutrino and sneutrino process active, producing both a total lepton and slepton asymmetry. In the MSSM the effect is to basically double the "x-abundance" of the heavy particles decaying t produce the asymmetry [122]. In analogy with the standard model quantities, one may define

$$\hat{N}^f_{\Delta_\alpha} = \hat{\varepsilon}_{i\alpha}\, \kappa(\hat{K}_{i\alpha}) \tag{7.9}$$

where $\hat{N}_{\Delta_\alpha}$ denotes a total lepton slepton asymmetry $\hat{\varepsilon}_{i\alpha}$ denotes a CP asymmetry with both internal lepton and slepton contributions included and $\hat{K}_{i\alpha}$ denotes a total washout parameter for inverse decays into both neutrinos and sneutrinos. In the MSSM the decay rates satisfy [115]

$$\Gamma_{N_i\, l_\alpha} + \Gamma_{N_i \bar{l}_\alpha} = \Gamma_{N_i \widetilde{l}_\alpha} + \Gamma_{N_i \widetilde{l}^\star_\alpha} = \Gamma_{\widetilde{N}^\star_i l_\alpha} = \Gamma_{\widetilde{N}_i \bar{l}_\alpha} = \Gamma_{\widetilde{N}_i \widetilde{l}_\alpha} = \Gamma_{\widetilde{N}^\star_i \widetilde{l}^\star_\alpha} \tag{7.10}$$

where for example $\Gamma_{\widetilde{N}_i^\star l_\alpha}$ denotes the rate of the decay $\widetilde{N}_i^\star \to l_\alpha + \widetilde{\phi}_u$. From this, one obtains from the definition of the washout parameter $K_{i\alpha} \equiv \frac{\Gamma_{i\alpha}}{H(z=1)}$ that

$$\hat{K}_{i\alpha} = \frac{2K_{i\alpha}}{\sin^2\beta}\sqrt{\frac{g^\star_{SM}}{g^\star_{MSSM}}} \approx \sqrt{2}\,K_{i\alpha} \tag{7.11}$$

for $g^\star_{SM} = 106.75$ and $g^\star_{MSSM} = 228.75$ [122] and where $K_{i\alpha}$ denotes the SM washout. The factor two relative to the SM comes from the doubling of "x-abundance" already mentioned, the factor of $\sqrt{\frac{g^\star_{SM}}{g^\star_{MSSM}}}$ from an increased expansion of the universe in the MSSM due to the approximate doubling of radiative degrees of freedom and the factor of $\frac{1}{\sin^2\beta}$ comes from the difference between SM and MSSM Yukawa couplings, already discussed in section 7.2. Next the CP violating parameter: in general one has

$$\varepsilon_{i\alpha} \quad = \quad \frac{1}{8\,\pi}\,\frac{1}{(Y^{\nu\dagger}\,Y^{\nu})_{ii}}\sum_{j\neq i}\left(\mathcal{I}^\alpha_{ij}\,f\left(\frac{M_j^2}{M_i^2}\right) + \mathcal{J}^\alpha_{ij}\,g\left(\frac{M_j^2}{M_i^2}\right)\right) \tag{7.12}$$

where I have defined

$$\mathcal{I}^\alpha_{ij} \equiv \mathrm{Im}\Big[\big(Y^{\nu\dagger}\big)_{i\alpha}\big(Y^{\nu}\big)_{\alpha j}\big(Y^{\nu\dagger}Y^{\nu}\big)_{ij}\Big]\ ,\ \mathcal{J}^\alpha_{ij} \equiv \mathrm{Im}\Big[\big(Y^{\nu\dagger}\big)_{i\alpha}\big(Y^{\nu}\big)_{\alpha j}\big(Y^{\nu\dagger}Y^{\nu}\big)_{ji}\Big] \tag{7.13}$$

For the SM the functions $f(x_i)$, $g(x_i)$ are given by [68]

$$f^{SM}(x_i) = \sqrt{x_i}\left[\frac{2-x_i}{1-x_i} - (1+x_i)ln\left(\frac{1+x_i}{x_i}\right)\right]$$

$$g^{SM}(x_i) = \frac{1}{1-x_i} \tag{7.14}$$

while for the MSSM the functions $f(x_i)$, $g(x_i)$ are given by [68]

$$f^{MSSM}(x_i) = \sqrt{x_i}\left[\frac{2}{1-x_i} - ln\left(\frac{1+x_i}{x_i}\right)\right]$$

$$g^{MSSM}(x_i) = \frac{2}{1-x_i} \tag{7.15}$$

In the hierarchical limit $x_i \gg 1$ it can be shown from the above that $f^{MSSM}(x_i \gg 1) = 2f^{SM}(x_i \gg 1)$. The factor of 2 can be understood given that in the MSSM

there is a second loop–level diagram (one with an internal slepton) for $N_i \to l_\alpha + \phi_u$ at one loop versus the SM (cf. fig. 2.7). Recalling from section 7.2 that $Y^\nu \mapsto \frac{Y^\nu}{\sin\beta}$ for $SM \mapsto MSSM$ one obtains

$$\hat{\varepsilon}_{i\alpha} = \frac{2}{\sin^2\beta}\,\varepsilon_{i\alpha} \tag{7.16}$$

where $\varepsilon_{i\alpha}$ denotes the SM CP violating parameter, given explicitly by eq. (3.43). Substituting eqs. (7.11) and (7.16) into eq. (7.9) one obtains

$$\hat{N}^f_{\Delta_{B-L}} = \sum_\alpha \hat{N}^f_{\Delta_\alpha} = \frac{2}{\sin^2\beta}\sum_\alpha \varepsilon_{i\alpha}\,\kappa(\frac{\sqrt{2}}{\sin^2\beta}\,K_{i\alpha}) \tag{7.17}$$

for the final MSSM $B-L$ asymmetry in terms of known SM quantities The MSSM baryon to photon ratio is calculated by the same method as lead to eq. (3.23) in section 3.1 and is hence given by

$$\hat{N}^{rec}_\gamma = \frac{4}{3}\frac{g^{\star s}_{MSSM}}{g^{\star s}_{rec}} = \frac{4}{3}\times\frac{228.75}{2+\frac{7}{8}\times 2\times 3\times\left(\frac{4}{11}\right)} \approx 78 \tag{7.18}$$

Hence the final baryon to photon ratio is

$$\eta_B \equiv \frac{\hat{N}^f_{\Delta_B}}{\hat{N}^{\rm rec}_\gamma} = a_{\rm sph}\,\frac{\hat{N}^{\rm f}_{\Delta_{B-L}}}{\hat{N}^{\rm rec}_\gamma} \simeq 0.89\times 10^{-2}\,\hat{N}^{\rm f}_{B-L} \tag{7.19}$$

having used $a_{\rm sph} = \frac{8}{23}$ in the MSSM [122] and where $\hat{N}^{\rm f}_{B-L}$ was already given by eq. (7.17). The above equation may also be expressed in terms of $\tan\beta \geq 1$ as

$$\eta^{MSSM}_B \approx 0.89\times 10^{-2}\times 2\left(\frac{1+\tan^2\beta}{\tan^2\beta}\right)\sum_\alpha \varepsilon^{SM}_{i\alpha}\,\kappa\left(\sqrt{2}\left(\frac{1+\tan^2\beta}{\tan^2\beta}\right)K^{SM}_{i\alpha}\right) \tag{7.20}$$

7.4 The Gravitino Problem

In supersymmetric leptogenesis there is a potential conflict between the high reheat temperature thermal leptogenesis requires to produce RHNs satisfying the Davidson–Ibarra bound (cf. eq. (2.69)) and the overproduction of gravitinos. This is referred to in the literature as "the gravitino problem". The problem is that gravitinos are

very weakly interacting and so can still be decaying (if they are not the lightest supersymmetric particle (LSP)) or being decayed into (if they are the LSP) during big bang nucleosynthesis (BBN). If enough gravitinos are produced in the early universe these extra decays will spoil agreement with the light element abundances observed today. How many gravitinos get produced? For massive gravitinos with $m_{3/2} \sim$ GeV the abundance is given by [123–125]

$$\Omega_{3/2}\, h^2 \approx 0.3 \left(\frac{1\text{GeV}}{m_{3/2}}\right) \left(\frac{T_R}{10^{10}\text{GeV}}\right) \sum_i c_i \left(\frac{M_i}{100\text{GeV}}\right)^2 \tag{7.21}$$

where M_i are the masses of the SUSY partners coupling to the gravitino with strength c_i and h parametrises the uncertainty of the Hubble parameter
(cf. eq. (2.24)) according to $H(t_0) = 100\, h\, km\, s^{-1}\,\text{MPc}^{-1}$ (such that $h \sim 0.7$). Gravitinos of mass $m_{3/2}$ have a lifetime of

$$\tau_{3/2} = 6 \times 10^7 s \left(\frac{m_{3/2}}{100\text{GeV}}\right)^{-3} \tag{7.22}$$

and thus lighter gravitinos lead to more stringent bounds on the reheat temperature T_{RH} - BBN, occurring over a timescale $\tau_{BBN} \sim 3\,\text{mins}$, is only "safe" for $m_{3/2} \gtrsim$ 40TeV. There is also an absolute bound of $\Omega_{3/2} \leq 1$ so as not to overclose the universe, which translates into an absolute bound of $T_{RH} \lesssim 10^{10}$GeV, as well as bounds from the abundances of light nuclei after BBN. These various bounds are summarised in fig. 7.2.

7.5 Supersymmetric 2RHN Model

7.5.1 Small $\tan\beta$ case

As discussed in section 7.2, in the $\tan\beta \gtrsim 1$ case supersymmetric leptogenesis occurs in the same flavour regime as for the SM. In section 6.4.4 we found the final baryon-to-photon ratio for a SM leptogenesis in the 2RHN model, occurring at a temperature of $10^9 GeV \ll T \ll 10^{12} GeV$ - the two-flavour regime for the SM. Using the results of the previous section, the final baryon-to-photon ratio for MSSM leptogenesis, also

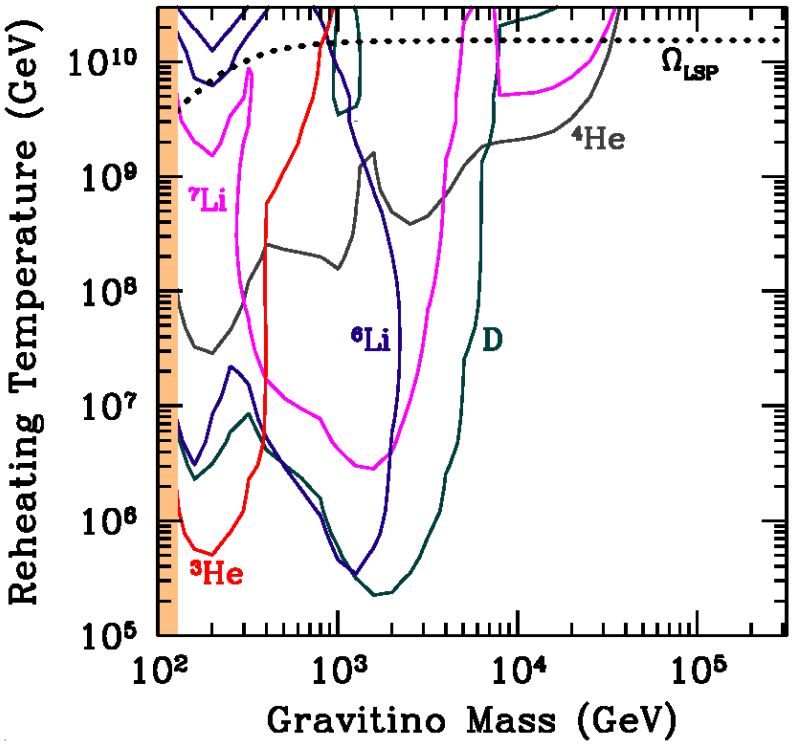

Figure 7.2: Upper bounds on reheat temperature, from BBN and flatness constraints on gravitinos. Plot taken from [126].

occurring in the two-flavour regime (provided $\tan\beta \gtrsim 1$) is given by

$$\eta_B = 0.89 \times 10^{-2} \left(\hat{N}^{\mathrm{f}(1)}_{\Delta_{B-L}} + \hat{N}^{\mathrm{f}(2)}_{\Delta_{B-L}} \right) \tag{7.23}$$

where

$$\hat{N}^{\mathrm{f}(1)}_{\Delta_{B-L}} = \varepsilon_{1\gamma}\, \kappa(K_{1\gamma}) + \varepsilon_{1\tau}\, \kappa(K_{1\tau}) \tag{7.24}$$

and

$$\begin{aligned} \hat{N}^{\mathrm{f}(2)}_{\Delta_{B-L}} &= \left(p^0_{\gamma_1\gamma_2} \varepsilon_{2\gamma} \kappa(K_{2\gamma}) + \Delta p_{\gamma_1^0\gamma_2} \kappa(K_{2\gamma}/2) \right) e^{-\frac{3\pi}{8} K_{1\gamma}} \\ &+ (1 - p^0_{\gamma_1\gamma_2})\, \varepsilon_{2\gamma} \kappa(K_{2\gamma}) + \Delta p_{\gamma_1^0\gamma_2} \kappa(K_{2\gamma}/2) \\ &+ \varepsilon_{2\tau}\, \kappa(K_{2\tau})\, e^{-\frac{3\pi}{8} K_{1\tau}} \end{aligned} \tag{7.25}$$

where $K_{i\alpha}$, $\varepsilon_{i\alpha}$, $p^0_{\gamma_1^0\gamma_2}$ and $\Delta p_{\gamma_1^0\gamma_2}$ refer now to supersymmetric quantities, given in terms of the SM quantities for $SM \mapsto MSSM$ as $K_{i\alpha} \mapsto \frac{\sqrt{2}}{\sin^2\beta} K_{i\alpha}$, $\varepsilon_{i\alpha} \mapsto \frac{2}{\sin^2\beta}\varepsilon_{i\alpha}$, $p^0_{\gamma_1\gamma_2} \mapsto p^0_{\gamma_1\gamma_2}$ and $\Delta p_{\gamma_1^0\gamma_2} \mapsto \frac{2}{\sin^2\beta}\Delta p_{\gamma_1^0\gamma_2}$ [1]. In figs. 7.3 and 7.4 this final asymmetry is

[1] where the final relation for $\Delta p_{\gamma_1^0\gamma_2}$ follows from applying $Y^\nu_{\alpha i} \mapsto \frac{1}{\sin\beta} Y^\nu_{\alpha i}$ and $\varepsilon_{i\alpha} \mapsto \frac{2}{\sin^2\beta}\varepsilon_{i\alpha}$ to eq. 6.109 of section 6.6

given in the MSSM for $\tan\beta = 2$. All plots are given for vanishing initial abundances. The results are quite similar to the SM case considered in chapter 6 since for $\tan\beta \gtrsim 1$ MSSM leptogenesis occurs in the same flavour regime as for the SM (cf. section 7.2) and so there are only order one corrections introduced. Notice again that inclusion of the "phantom terms" for fig. 7.4 enlarges the N_2-dominated regions around $z \sim \pi/2$. Notice that this lowers the bound on M_1 below 10^{10}GeV and so, recalling the discussion of section 7.4, upon consistently taking into account phantom terms one may circumvent the "gravitino problem" in the process - although this statement is dependent upon the gravitino mass being larger than $\sim 40\,\text{TeV}$, as fig. 7.2 shows. All figures are for vanishing initial RHN abundance so as to give the most stringent bounds - for thermal initial abundance the lower bound on M_1 can be further relaxed by a factor $\sim 1/3$.

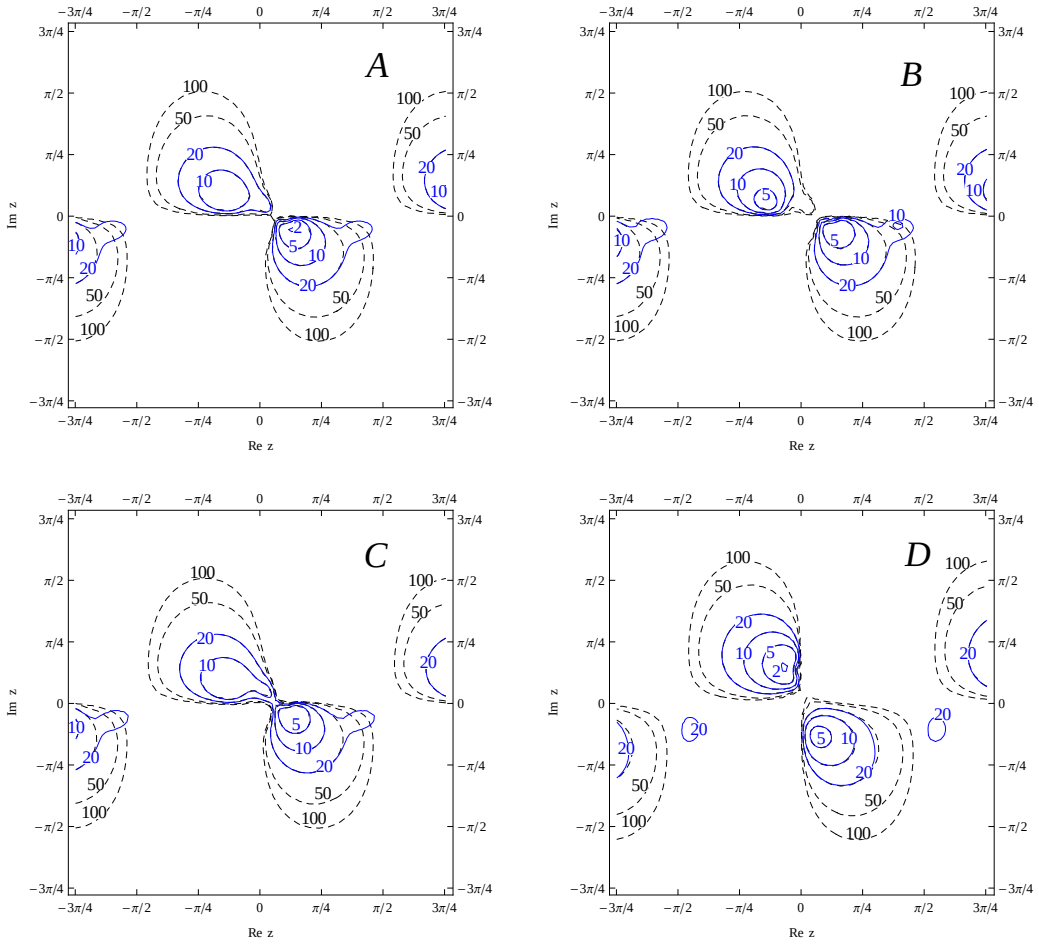

Figure 7.3: Final Baryon Asymmetry in the MSSM with $\tan\beta = 2$ for a normal hierarchy and neglecting "phantom terms". Blue solid lines (black dashed lines) are with (without) N_2 decays included.

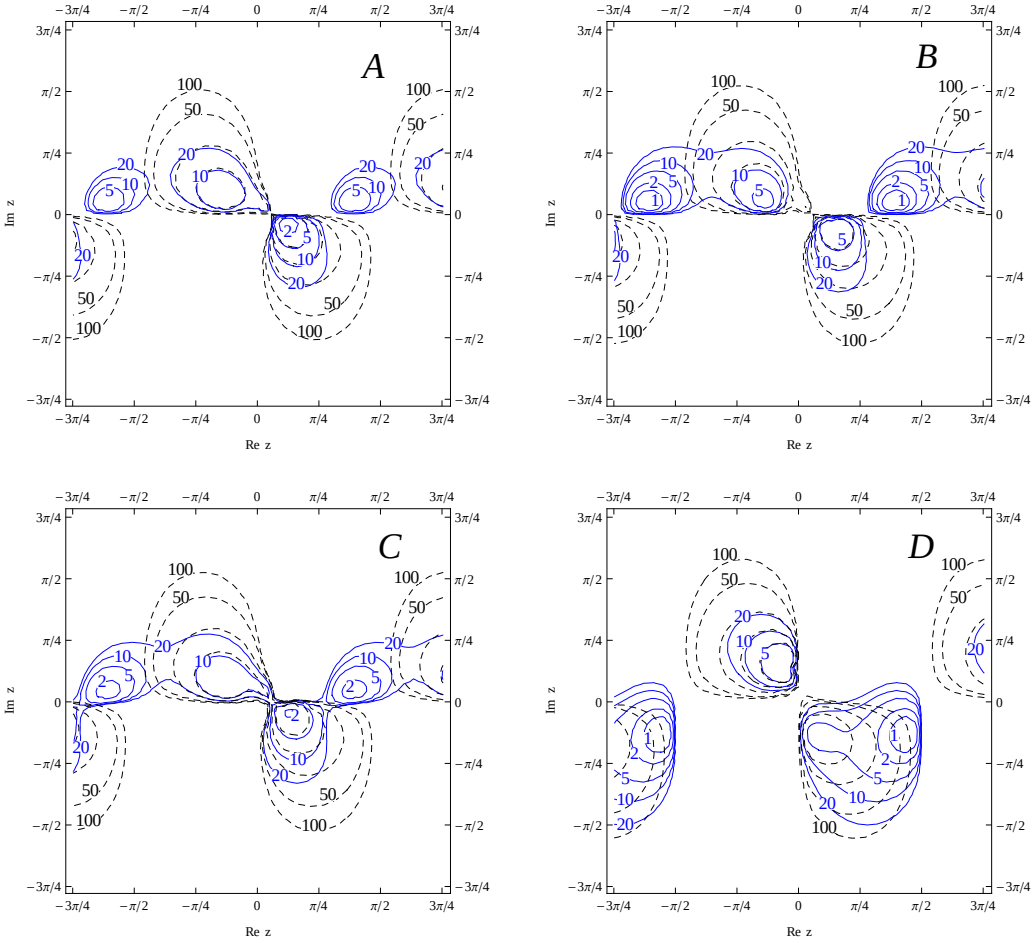

Figure 7.4: Final baryon asymmetry in the MSSM with $\tan\beta = 2$ for a normal hierarchy and including "phantom terms". Solid lines (dashed lines) are with (without) N_2 decays included.

7.5.2 Large $\tan\beta$ case

When $\tan\beta >> 1$ the flavour regime shifts from two–flavoured to three flavoured, given that the three-flavoured regime occurs for $T \ll (1+\tan^2\beta)10^9 GeV$, which for $\tan^2\beta \sim 10^3$ shifts the bound on the three–flavour regime to $T \ll 10^{12}$GeV. The final baryon-to-photon ratio for a supersymmetric leptogenesis in the three–flavour regime is then given by

$$\eta_B = 0.89 \times 10^{-2} \left(\hat{N}^{\mathrm{f}(1)}_{\Delta_{B-L}} + \hat{N}^{\mathrm{f}(2)}_{\Delta_{B-L}} \right) \tag{7.26}$$

where

$$\hat{N}^{\mathrm{f}(1)}_{\Delta_{B-L}} = 2\varepsilon_{1e}\,\kappa(K_{1e}) + 2\varepsilon_{1\mu}\,\kappa(K_{1\mu}) + 2\varepsilon_{1\tau}\,\kappa(K_{1\tau}) \tag{7.27}$$

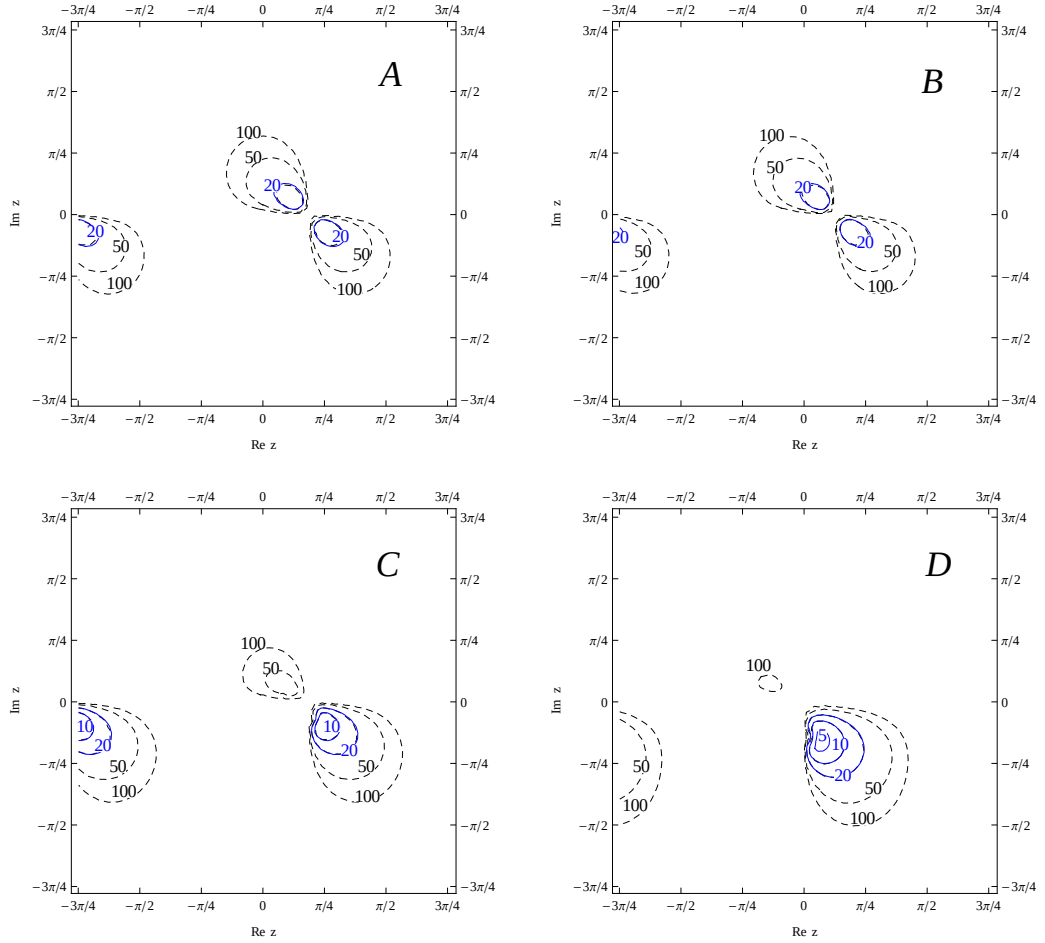

Figure 7.5: Final Baryon Asymmetry in the MSSM with $\tan\beta = 2$ for an inverted hierarchy. Blue solid lines (black dashed lines) are with (without) N_2 decays included.

and

$$\hat{N}^{\mathrm{f}(2)}_{\Delta_{B-L}} = 2\varepsilon_{2e}\,\kappa(K_{2e}) + 2\varepsilon_{2\mu}\,\kappa(K_{2\mu}) + 2\varepsilon_{2\tau}\,\kappa(K_{2\tau}) \tag{7.28}$$

where $K_{i\alpha}$ and $\varepsilon_{i\alpha}$ above refer to the supersymmetric quantities, given in terms of the SM quantities for $SM \mapsto MSSM$ as $K_{i\alpha} \mapsto \frac{\sqrt{2}}{\sin^2\beta}\,K_{i\alpha}$, $\varepsilon_{i\alpha} \mapsto \frac{2}{\sin^2\beta}\varepsilon_{i\alpha}$. In figs. 7.6 and 7.7 this final asymmetry is given in the MSSM for $\tan\beta = 30$. Unlike figs. 7.3–7.5 I have not distinguished an $N_1 + N_2$ produced asymmetry from the N_1 produced asymmetry – it turns out that for the large $\tan\beta$ case the asymmetry is N_1–dominated.

Notice the new allowed regions compared to the two-flavour case, particularly in fig. 7.7 for the case of an inverted hierarchy, where the electron part of the asymmetry becomes well separated from the muon and tauon part and so a separate colour has

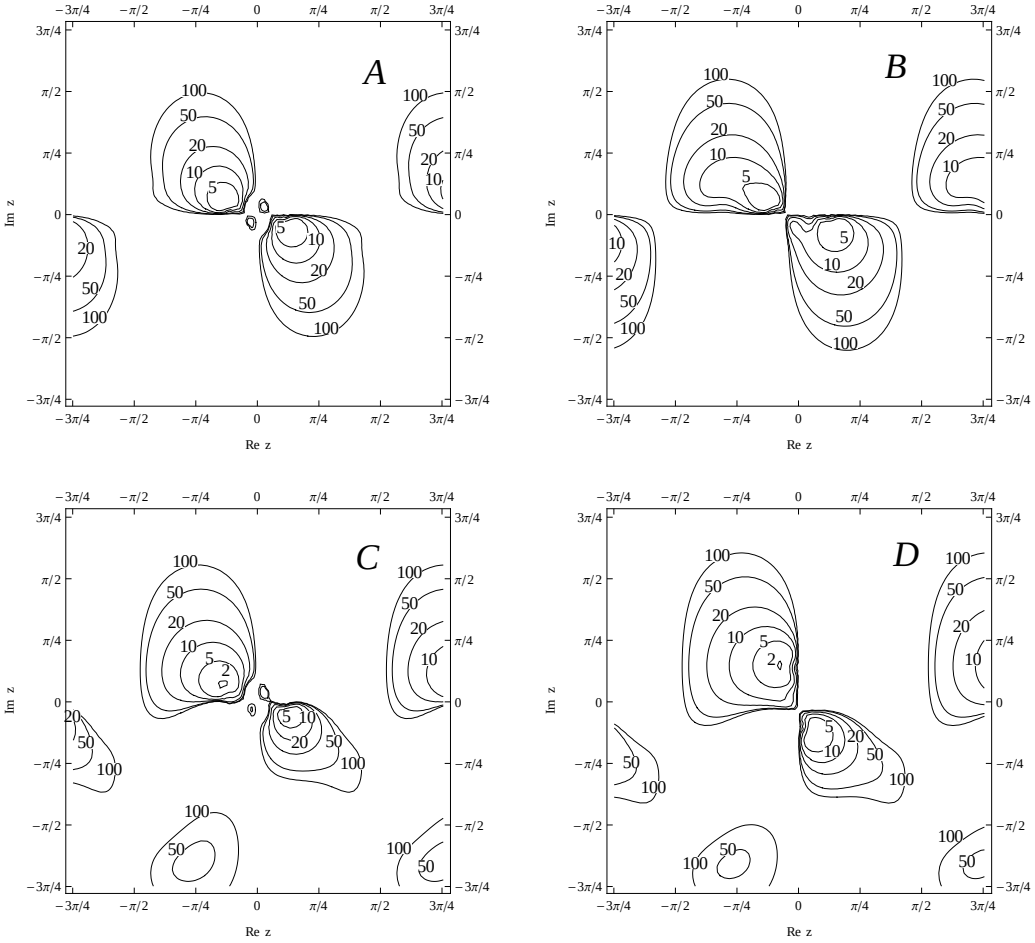

Figure 7.6: Final N_1–dominated Baryon Asymmetry in the MSSM, for NH with vanishing initial abundance and $\tan\beta = 30$.

been used to indicate it in fig. 7.7. These new allowed regions appear due to a small electron flavour washout in a particular region of the z-plane preserving a final $B-L$ asymmetry stored in the electron flavour. Fig. 7.8 compares the (small) electron washout acting in the large $\tan\beta$ case, when the electron flavour is "measured", with the (large) electron plus muon washout acting in the small $\tan\beta$ case, where the electron flavour is not "measured". In this latter case a separate electron part of the asymmetry is not preserved and comparing fig. 7.7 with fig. 7.5 one sees that the red regions of fig. 7.7 vanish from fig. 7.5.

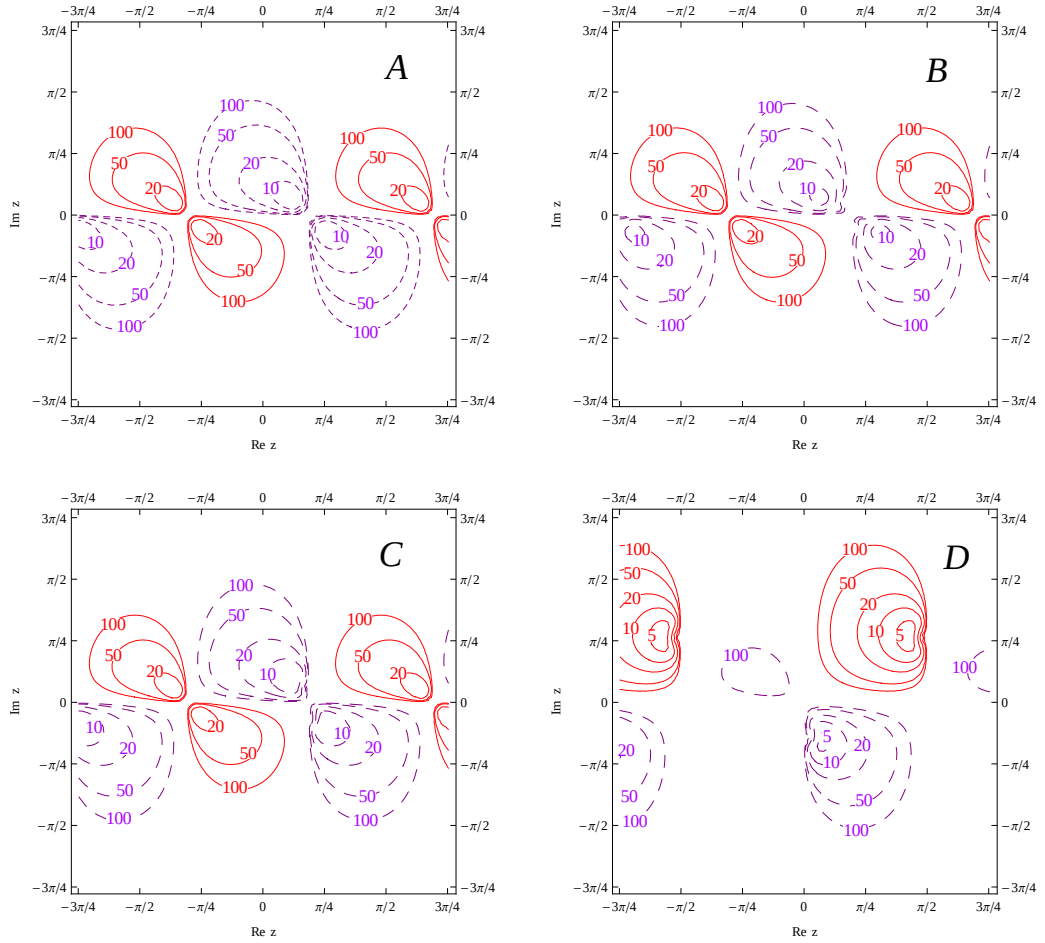

Figure 7.7: Final Baryon Asymmetry in the MSSM, for IH with vanishing initial abundance and $\tan\beta = 30$. Red solid lines are the electron part of the asymmetry, purple dashed lines the muon plus tauon part.

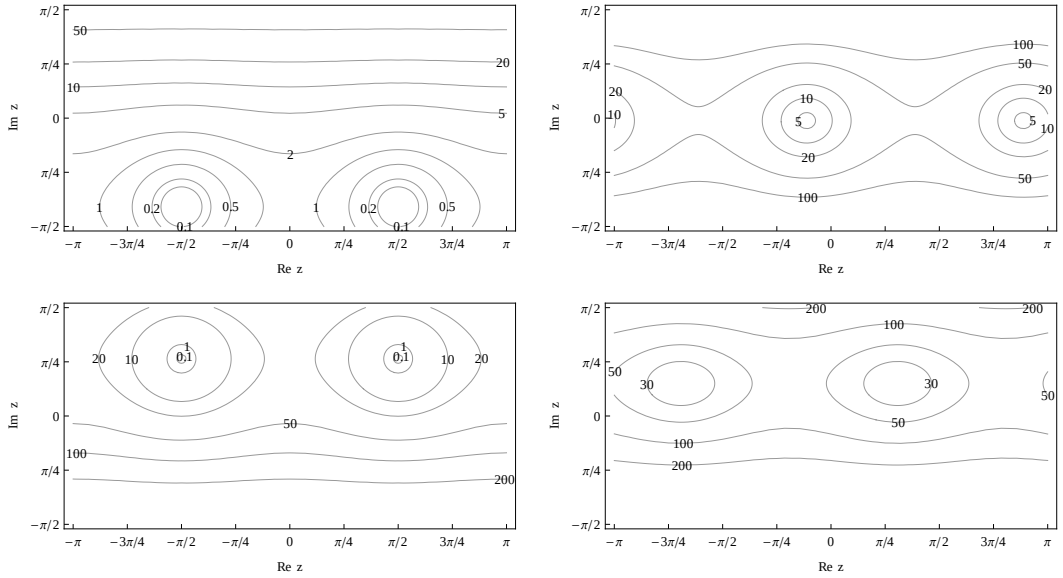

Figure 7.8: Washouts of e (left panel) and e+μ (right panel) asymmetries for benchmark D. Upper (lower) panels are for NH (IH).

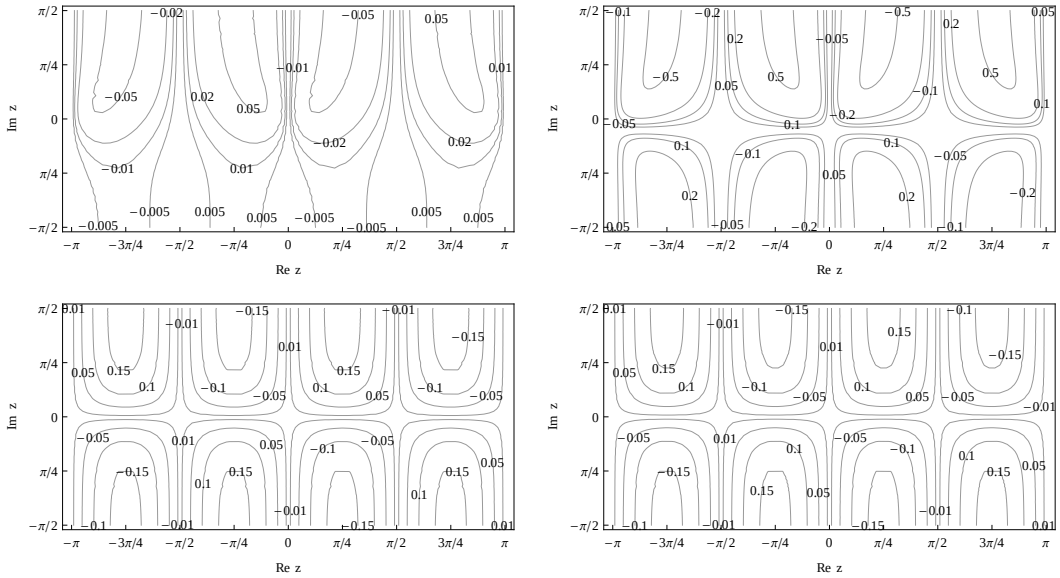

Figure 7.9: Normalised CP asymmetries $\varepsilon_{2e} \,/\, \bar{\varepsilon}_1$ (left panel) and $\varepsilon_{2\gamma} \,/\, \bar{\varepsilon}_1$ (right panel) for benchmark D. Upper (lower) panels are for NH (IH).

Discussion

I now review the key results of this work. As discussed back in the Introduction, the origin of neutrino mass and the baryon asymmetry of the universe (BAU) are two major outstanding problems for the Standard Model of particle physics and the "standard cosmological model" of ΛCDM. These problems were each considered, in chapters 1 and 2 respectively. Then, in chapter 3, I discussed the hypothesis that these problems have a common solution through the physics of the seesaw mechanism - an idea known as leptogenesis - and developed in detail the theoretical machinery needed to account for the many relevant lepton flavour effects impacting the predicted final baryon asymmetry.

This theoretical machinery was subsequently put to work, first during chapter 4 based upon the paper [6], which considered leptogenesis in the N_2–dominated scenario. Two novel lepton flavour effects were identified – the "flavour swap scenario" and "phantom leptogenesis" – each of which was shown to be both unique to leptogenesis scenarios with more than one active right handed neutrino (RHN) and able to enhance the final baryon asymmetry order–of–magnitude–wise in relevant regions of the parameter space. It was shown that both generically (cf. figs. 4.2 and 4.3) and for realistic models with heavy and light sequential dominance (cf. section 4.6) that both phantom terms and flavour coupling can give relevant, and in some cases even order–of–magnitude, local corrections to the theoretical predictions on the BAU within an N_2–dominated scenario.

In chapter 5, based upon the paper [7], I developed a more sophisticated description of leptogenesis using the density matrix formalism. The density matrix formalism allows one to extend the description given by Boltzmann equations, which

require that lepton flavours are projected into a definite flavour basis, into regions of the parameter space for which a transition between two flavoured bases is induced via decoherence effects. I showed how to take into account both the effect of damping of lepton flavour oscillations induced via leptonic Yukawa interactions and the thermalisation of gauge bosons. The latter was shown to modify the previous chapter's expression for "phantom terms" (cf. section 4.3), with the gauge bosons introducing some washout to these terms, but non-trivially only half the amount of washout the ordinary flavoured terms receive. A "master equation" (cf. eq. (5.50)) was given, able to account for flavoured dynamics at all temperatures and which for specific temperatures can reproduce the set of ten flavoured Boltzmann equations (cf. fig. 3.4) whilst also describing the transitional regimes in which the aforementioned are invalid. I then gave two examples of this, first rederiving the Boltzmann equations describing the heavy flavoured scenario (cf. section 3.4) and then deriving the Boltzmann equations (including phantom terms) describing the 2RHN model in a two-flavoured regime.

In chapter 6, based upon the paper [8], I "revisited" the 2RHN model, this time taking into account fully the impact of the decays of the next-to–lightest RHN N_2 upon the BAU. It was shown (cf. section 6.4.4) that for regions of the parameter space $z \sim \pi/2$ (where z is a complex angle in the orthogonal parametrisation (cf. section 6.2) the BAU is produced via these N_2 decays. These regions were shown to correspond to models with light sequential dominance (cf. section 6.5). I also extended the results of the paper [8] by including the phantom terms not considered in that paper (cf. section 6.6), showing that upon including phantom terms the N_2 dominated regions become enlarged, lowering the bound on M_1 in these N_2–dominated regions by about one order of magnitude, from $M_1 \lesssim 10^{11}$GeV down to $M_1 \lesssim 10^{10}$GeV.

Finally, in chapter 7 I considered the supersymmetric version of the 2RHN models discussed in the previous chapter. I described (cf. section 7.2) an interesting sensitivity leptogenesis has to $\tan\beta$, which in principle provides a means to distinguish between various supersymmetric models, by using the production of the BAU via leptogenesis as a relevant constraint on the supersymmetric seesaw parameter

space. A striking illustration of this was shown for leptogenesis in the 2RHN model with an inverted hierarchy, where entirely new allowed regions of parameter space successfully realising the observed BAU become accessible when $\tan\beta$ gets large (cf. section 7.5.2). I also briefly discussed the "gravitino problem" (cf. section 7.4) and showed how it might be possible to just avoid this problem in cases of normal hierarchy where $\tan\beta$ is small (cf. section 7.5.1). It is also shown for such cases that upon inclusion of phantom terms, one can relax the lower bound upon M_1 in the N_2–dominated regions to just below the "danger zone" of $M_1 \sim 10^{10}$GeV, where otherwise the requirement of sufficient N_2 production would lead to the problem of overproducing gravitinos (and thus over–closing the universe).

One can see that there are quite a diversity of interesting new lepton flavour effects present, particularly in cases where more than one RHN are relevant during the production of the BAU via leptogenesis. Certainly there is much more to be understood before a "precision era" of leptogenesis is reached, but it seems we are beginning to get a handle upon which of the lepton flavour effects are important and which may be safely neglected within various regions of the seesaw mechanism's extensive unconstrained parameter space. Sometimes it is said that leptogenesis is hard to test and perhaps "not even wrong" but I feel this is somewhat unfair – it is the seesaw mechanism itself that is hard to test and leptogenesis may yet deliver us a relevant and non-trivial constraint upon its allowed parameter space. In conjunction with other constraints, such as for example "$SO(10)$ inspired" constraints upon the neutrino Yukawa matrix, non-trivial predictions on the low-energy physics can emerge [127, 128] and so leptogenesis may yet serve as a "bridge" connecting speculative GUT / Planck scale particle theories and cosmologies to testable low–energy phenomenology. Making this "bridge" more solid for fellow travelers will be an ongoing task, requiring the work of many hands; but a task to which I hope the present work can provide some modest assistance.

Appendix on A–matrix and C–matrix Calculations

Recall from section 3.3 that with all SM spectator process in equilibrium one obtains the set of chemical potential constraints below

$$0 = \mu_{l_i} + \mu_{\phi_d} - \mu_{\alpha_R} \quad \text{(A-1)}$$

$$0 = \mu_{q_i} + \mu_{\phi_u} - \mu_{\beta_R} \quad \text{(A-2)}$$

$$0 = \mu_{q_i} + \mu_{\phi_d} - \mu_{\gamma_R} \quad \text{(A-3)}$$

$$0 = \sum_i \mu_{l_i} + 3\sum_i \mu_{q_i} \quad \text{(A-4)}$$

$$2\mu_{Q_3} + \mu_{t_R} + \mu_{b_R} = 2\mu_{Q_2} + \mu_{c_R} + \mu_{s_R} = 2\mu_{Q_1} + \mu_{u_R} + \mu_{d_R} \quad \text{(A-5)}$$

$$0 = 2\sum_i \mu_{q_i} - \sum_\beta \mu_{\beta_R} - \sum_\gamma \mu_{\gamma_R} \quad \text{(A-6)}$$

$$0 = \sum_i \mu_{q_i} + 2\sum_\beta \mu_{\beta_R} - \sum_\gamma \mu_{\gamma_R} - \sum_i \mu_{l_i} - \sum_\alpha \mu_{\alpha_R} + \mu_{\phi_u} + \mu_{\phi_d} \quad \text{(A-7)}$$

$$0 = \mu_{\phi_u} + \mu_{\phi_d} \quad \text{(A-8)}$$

where $i = 1, 2, 3$, $\alpha = e, \mu, \tau$, $\beta = u, c, t$ and $\gamma = d, s, b$.

In total there are 14 constraints on 17 SM particle abundances [2] (15 matter fields plus the ϕ_u and ϕ_d fields). A simple code can be written to eliminate 14 of the 17 variables and express everything in terms of $17 - 14 = 3$ remaining variables $\Delta_\alpha \equiv \frac{\Delta_B}{3} - \Delta_{L_\alpha}$ (for $\alpha = e, \mu, \tau$). In particular $N_{\Delta_{l_\alpha}} + N_{\Delta_\phi}$ written in the $\{\Delta_{\alpha'}\}$ basis gives the $C_{\alpha\alpha'}$. For example the Mathematica code Solve[...] returns the output {{ ... }} – see the screenshots overleaf, for which C1, C2, C3 label the three rows of

[2] If you count them there are actually 15 constraints, but a combination of them is redundant.

the C–matrix obtained in a temperature where all constraints apply and D1, D2, D3 label the basis Δ_e, Δ_μ, Δ_τ. Also, "a" labels a_{sph}, the fraction of $B-L$ asymmetry transferred into B by sphalerons, as was given in eq. (3.68).

```
Solve[{l3 - h - tau == 0, l2 - h - m == 0, l1 - h - e == 0,
  q3 + h - t == 0, q2 + h - c == 0, q1 + h - u == 0,
  q3 - h - b == 0, q2 - h - s == 0, q1 - h - d == 0,
  3 * (q1 + q2 + q3) + l1 + l2 + l3 == 0,
  2 * (q1 + q2 + q3) - u - c - t - d - s - b == 0,
  2 q1 + u + d == 2 q2 + c + s,
  2 q2 + c + s == 2 q3 + t + b,
  q1 + q2 + q3 + 2 * (t + c + u) - d - s - b - l1 - l2 - l3 - e - m - tau + 2 h == 0,
  -C1 == h + l1, -C2 == h + l2, -C3 == h + l3,
  a == (2 q1 + 2 q2 + 2 q3 + u + d + s + c + t + b) /
    (2 q1 + 2 q2 + 2 q3 + u + d + s + c + t + b - 2 l1 - e - 2 l2 - m - 2 l3 - tau),
  D1 == 1 / 6 * (2 q1 + 2 q2 + 2 q3 + u + d + s + c + t + b) - l1 - e / 2,
  D2 == 1 / 6 * (2 q1 + 2 q2 + 2 q3 + u + d + s + c + t + b) - l2 - m / 2,
  D3 == 1 / 6 * (2 q1 + 2 q2 + 2 q3 + u + d + s + c + t + b) - l3 - tau / 2},
 {u, d, s, c, t, b, q1, q2, q3, e, m, tau, h, l1, l2, l3, C1, C2, C3, a}]
```

$$\left\{\left\{C1 \to \frac{2}{711}(257\,D1 + 20\,D2 + 20\,D3),\ C2 \to \frac{2}{711}(20\,D1 + 257\,D2 + 20\,D3),\right.\right.$$
$$C3 \to \frac{2}{711}(20\,D1 + 20\,D2 + 257\,D3),\ e \to -\frac{2}{711}(185\,D1 - 52\,D2 - 52\,D3),$$
$$m \to \frac{2}{711}(52\,D1 - 185\,D2 + 52\,D3),\ tau \to \frac{2}{711}(52\,D1 + 52\,D2 - 185\,D3),$$
$$l1 \to -\frac{2}{711}(221\,D1 - 16\,D2 - 16\,D3),\ l2 \to \frac{2}{711}(16\,D1 - 221\,D2 + 16\,D3),$$
$$l3 \to \frac{2}{711}(16\,D1 + 16\,D2 - 221\,D3),\ u \to -\frac{10}{237}(D1 + D2 + D3),$$
$$d \to \frac{38}{237}(D1 + D2 + D3),\ t \to -\frac{10}{237}(D1 + D2 + D3),$$
$$b \to \frac{38}{237}(D1 + D2 + D3),\ h \to -\frac{8}{79}(D1 + D2 + D3),\ s \to \frac{38}{237}(D1 + D2 + D3),$$
$$c \to -\frac{10}{237}(D1 + D2 + D3),\ q1 \to \frac{14}{237}(D1 + D2 + D3),$$
$$\left.\left.q3 \to \frac{14}{237}(D1 + D2 + D3),\ q2 \to \frac{14}{237}(D1 + D2 + D3),\ a \to \frac{28}{79}\right\}\right\}$$

Recalling now the definitions of the "A–matrix" and "C-matrix"

$$\begin{aligned} N_{\Delta_{l_\alpha}} &\equiv -\sum_{\alpha'} A_{\alpha\alpha'}\, N_{\Delta_{\alpha'}} \\ N_{\Delta_{l_\alpha}} + N_{\Delta_\phi} &\equiv -\sum_{\alpha'} C_{\alpha\alpha'}\, N_{\Delta_{\alpha'}} \end{aligned} \tag{A-9}$$

where $\Delta_\alpha \equiv \frac{\Delta_B}{3} - L_\alpha$, one obtains

$$\begin{aligned} A^{(T\ll 10^8\mathrm{GeV})} &= \begin{pmatrix} 442/711 & -32/711 & -32/711 \\ -32/711 & 442/711 & -32/711 \\ -32/711 & -32/711 & 442/711 \end{pmatrix} \\ C^{(T\ll 10^8\mathrm{GeV})} &= \begin{pmatrix} 514/711 & 40/711 & 40/711 \\ 40/711 & 514/711 & 40/711 \\ 40/711 & 40/711 & 514/711 \end{pmatrix}, \quad a_{sph} = \frac{28}{79} \end{aligned} \tag{A-10}$$

We now consider in more detail what happens as the temperature increases and some of the above constraint cease to apply. For convenience I repeat here table 3.3, showing the temperatures at which various processes are in equilibrium.

Processes in equilibrium at various temperatures

T [GeV]	processes in equilibrium
$\gg 10^{13}$GeV	top Yukawa
$\sim 10^{13}$GeV	+ QCD sphalerons
$10^{12,13}$	+ bottom, tau Yukawas
$10^{11,12}$	+ EW sphalerons, charm Yukawa
$10^{8,9,10}$	+ strange, mu Yukawas
$\ll 10^8 GeV$	+ all remaining Yukawas

Thus the first constraints to become redundant are eq. (A-1) (with $\alpha = e$) for the electron Yukawa coupling and eqs. (A-2, A-3) (with $\beta = u$ and $\gamma = d$ respectively) for the up and down quark Yukawas. The electron constraint can be simply replaced by the condition $\mu_e = 0$ given that there is no active interaction to transfer any asymmetry into the lepton flavour [3]. The replacemet for the u, d constraints is a bit

[3] Strictly speaking it is g_e, the radiative degrees of freedom of the electron, rather than its chemical

more subtle: we replace these by $\mu_u = \mu_d$ given that there **is** an active process transferring asymmetry into these RH quarks, namely QCD sphalerons, which put equal asymmetry into up and down type quarks. By making these simple replacements to the Mathematica code shown previously, one obtains

$$\begin{aligned} A^{(T\sim 10^8\mathrm{GeV})} &= \begin{pmatrix} 151/179 & -20/179 & -20/179 \\ -25/358 & 344/527 & -14/537 \\ -25/358 & -14/537 & 344/527 \end{pmatrix} \\ C^{(T\sim 10^8\mathrm{GeV})} &= \begin{pmatrix} 339/358 & 6/179 & 6/179 \\ 6/179 & 422/537 & 64/537 \\ 6/179 & 64/537 & 422/537 \end{pmatrix} \end{aligned} \tag{A-11}$$

The above C–matrix is the 3×3 matrix $C^{(3)}$ (cf. eq (3.67)) used throughtout the thesis.

The next set of constraints will apply for $10^9\mathrm{GeV} \ll T \ll 10^{12}\mathrm{GeV}$, where the strange and mu Yukawa interactions go out of equilibrium and so their coupling constraints eq. (A-3) (for $\gamma = s$) and eq. (A-1) (for $\alpha = \mu$) must be modified to $\mu_s = \mu_d\,(= \mu_u)$ (given that the strange quark asymmetry must equal the other quark asymmetries only populated via sphalerons – the up and down quarks) and $\mu_\mu = 0$ respectively. Making these simple changes to the code yields

$$\begin{aligned} A^{(10^9\mathrm{GeV}\ll T\ll 10^{12}\mathrm{GeV})} &= \begin{pmatrix} 503/589 & -86/589 & -60/589 \\ -86/589 & 503/589 & -60/589 \\ -30/589 & -30/589 & 390/589 \end{pmatrix} \mapsto \begin{pmatrix} 417/589 & -120/589 \\ -30/589 & 390/589 \end{pmatrix} \\ C^{(10^9\mathrm{GeV}\ll T\ll 10^{12}\mathrm{GeV})} &= \begin{pmatrix} 585/589 & -4/589 & 52/589 \\ -4/589 & 585/589 & 52/589 \\ 52/589 & 52/589 & 502/589 \end{pmatrix} \mapsto \begin{pmatrix} 581/589 & 104/589 \\ 52/589 & 502/589 \end{pmatrix} \end{aligned} \tag{A-12}$$

where the mappings $3 \times 3 \mapsto 2 \times 2$ (recall we are in the "two–flavoured" regime

potential μ_e, which become zero, since the electron decouples from the thermal bath for $T \ll 10^8\mathrm{GeV}$. But since the effect on $n_{\Delta_e} \propto g_e\,\mu_e$ is the same by setting either μ_e or g_e to zero, I choose to do the latter for simplicity. A related point is that in reality g_e would go from zero to two not instantly (at $T \sim 10^8\mathrm{GeV}$, cf. the table above) but transition gradually, as a function of temperature. This is also ignored, again for simplicity, by treating the transition as a step change at $T = 10^8\mathrm{GeV}$.

when $10^9\text{GeV} \ll T \ll 10^{12}\text{GeV}$) are made by averaging across rows and summing down columns. The above C–matrix is the 2×2 matrix $C^{(2)}$ (cf. eq (3.66)) used throughtout the thesis.

If one wants to go the even higher temperatures, where first the electroweak sphalerons drop out of equilibrium, the constraints eq. (A-4) and eq. (A-5) can be replaced by

$$2\mu_{Q_3} + \mu_t + \mu_b = 2\mu_{Q_2} + \mu_c + \mu_s = 2\mu_{Q_1} + \mu_u + \mu_d = 0 \tag{A-13}$$

given that there is no longer any mechanism to transfer asymmetry from leptons to baryons and so $\Delta_B = 0$ for all three generations. The bottom and tau Yukawas dropping out of equilibrium is handled in an exactly analagous way to the strange and mu Yukawas. Making these further modifications to the constraints, one obtains

$$\begin{aligned} A^{(T\sim 10^{13}\text{GeV})} &= \begin{pmatrix} 1 & 0 & 0 \\ 0 & 1 & 0 \\ 0 & 0 & 1 \end{pmatrix} \mapsto 1 \\ C^{(T\sim 10^{13}\text{GeV})} &= \begin{pmatrix} 30/23 & 7/23 & 7/23 \\ 7/23 & 30/23 & 7/23 \\ 7/23 & 7/23 & 30/23 \end{pmatrix} \mapsto 44/23 \end{aligned} \tag{A-14}$$

where the mapping $3 \times 3 \mapsto 1 \times 1$ (given we are in the "un–flavoured" regime for $T \gg 10^{12}\text{GeV}$) is again obtained by averaging across rows and summing down columns.

Finally, when the QCD sphalerons drop out of equilibrium we replace constraint eq. (A-6) by the initial conditions

$$\mu_u = \mu_d = \mu_s = \mu_c = \mu_b = 0 \tag{A-15}$$

given that there is no longer any mechanism to transfer asymmetry to the RH quark states (apart from the top quark, which still has the top Yukawa coupling at $T \sim$

10^{13}GeV). Making this final modification to the constraints, one obtains

$$
\begin{aligned}
A^{(T\gg 10^{13}\mathrm{GeV})} &= \begin{pmatrix} 1 & 0 & 0 \\ 0 & 1 & 0 \\ 0 & 0 & 1 \end{pmatrix} \mapsto 1 \\
C^{(T\gg 10^{13}\mathrm{GeV})} &= \begin{pmatrix} 4/3 & 1/3 & 1/3 \\ 1/3 & 4/3 & 1/3 \\ 1/3 & 1/3 & 4/3 \end{pmatrix} \mapsto 2
\end{aligned}
\tag{A-16}
$$

The above "un–flavoured" C–matrix can be identified as the $C^{(1)}$–matrix of section 3.3 (cf. eq. (3.65)). Thus we see that consistently taking into account the Higgs asymmetry appears to **double** the washout in the un–flavoured regime [4].

[4] If the top Yukawa is also taken out of equilibrium by setting $\mu_t = 0$ one further obtains $A \mapsto 1$ and $C \mapsto 5/2$ and so the lepton plus Higgs washout becomes even stronger.

Bibliography

[1] A. A. Michelson, speech at the dedication of Ryerson Physics Lab, U. of Chicago, 1894

[2] Lightman, Alan P. (2005). *The discoveries: great breakthroughs in twentieth-century science, including the original papers.* Toronto: Alfred A. Knopf Canada. p. 8. ISBN 0-676-97789-8.

[3] M. Fukugita and T. Yanagida, *Baryogenesis Without Grand Unification*, Phys. Lett. B174 (1986) 45.

[4] P. Minkowski, Phys. Lett. B **67** (1977) 421; T. Yanagida, in *Workshop on Unified Theories*, KEK report 79-18 (1979) p. 95; M. Gell-Mann, P. Ramond, R. Slansky, in *Supergravity* (North Holland, Amsterdam, 1979) eds. P. van Nieuwenhuizen, D. Freedman, p. 315; S.L. Glashow, in *1979 Cargese Summer Institute on Quarks and Leptons* (Plenum Press, New York, 1980) p. 687; R. Barbieri, D. V. Nanopoulos, G. Morchio and F. Strocchi, Phys. Lett. B **90** (1980) 91; R. N. Mohapatra and G. Senjanovic, Phys. Rev. Lett. **44** (1980) 912.

[5] A. D. Sakharov, Pisma Zh. Eksp. Teor. Fiz. 5, 32 (1967) [JETP Lett. 5, 24 (1967 SOPUA,34,392- 393.1991 UFNAA,161,61-64.1991)].

[6] S. Antusch, P. Di Bari, D. A. Jones, S. F. King, Nucl.Phys. B856 (2012) 180-209 [arXiv:1003.5132].

[7] S. Blanchet, D. A. Jones, P. Di Bari, L. Marzola, arXiv:1112.4528

[8] S. Antusch, P. Di Bari, D. A. Jones, S. F. King, Phys.Rev. **D86** (2012) 023516 [arXiv:1107.6002].

[9] *Leptogenesis in the Two Right-Handed Neutrino Model Revisited* - talk given at: Baryogenesis and First Order Phase Transitions in the Early Universe Workshop, Leiden (2011) [see: *http://www.lorentzcenter.nl/lc/web/2011/455/info.php3?wsid=455*]

[10] *Leptogenesis in Your Face* - talk given at: ITN Invisibles pre–meeting, Madrid (2012) [see: *http://www.ft.uam.es/workshops/InvisiblesITNpre-meeting/*]

[11] P. A. M. Dirac (1928). *The Quantum Theory of the Electron*. Proceedings of the Royal Society A: Mathematical, Physical and Engineering Sciences 117 (778): 610. doi:10.1098/rspa.1928.0023.

[12] P. A. M. Dirac (1930). *A Theory of Electrons and Protons*. Proceedings of the Royal Society A: Mathematical, Physical and Engineering Sciences 126 (801): 360. doi:10.1098/rspa.1930.0013. JSTOR 95359.

[13] P. A. M. Dirac (1931). *Quantised Singularities in the Quantum Field*. Proc. R. Soc. Lond. A 133 (821): 23. Bibcode 1931RSPSA.133...60D. doi:10.1098/rspa.1931.0130.

[14] C. D. Anderson (1933). *The Positive Electron*. Physical Review 43 (6): 491494. Bibcode 1933PhRv...43..491A. doi:10.1103/PhysRev.43.491

[15] A. S. Beach et. al., Phys. Rev. Lett. 87 (2001) 271101, [arXiv:astro-ph/0111094].

[16] A. G. Cohen, A. D. Rujula, S. L. Glashow. Astrophys.J. 495 (1998) 539-549 [arXiv:astro-ph/9707087]

[17] J. Beringer et al. (PDG), PR D86, 010001 (2012) (http://pdg.lbl.gov)

[18] A. Strumia and F. Vissani, arXiv:hep-ph/0606054.

[19] N. Jarosik et al., Astrophys. J. Supp. 192, 14 (2011); D. Larson et al., Astrophys. J. Supp. 192, 16 (2011); E. Komatsu et al., Astrophys. J. Supp. 192, 18 (2011).

[20] H. Georgi and S. L. Glashow (1974). *Unity of All Elementary Particle Forces*. Physical Review Letters 32: 438441. Bibcode 1974PhRvL..32..438G. doi:10.1103/PhysRevLett.32.438.

[21] V. A. Kuzmin, V. A. Rubakov, and M. E. Shaposhnikov, Phys. Lett. B **155**, 36 (1985).

[22] M. B. Gavela, P. Hernandez, J. Orloff and O. P'ene, Mod. Phys. Lett. A **9** (1994) 795 [arXiv:hep-ph/9312215].

[23] M. Trodden, Rev. Mod. Phys. 71 (1999) 1463-1500 [arxiv:hep-ph/9803479].

[24] M. Dine and A. Kusenko, Rev. Mod. Phys. 76 (2003) 1 [arXiv:hep-ph/0303065]

[25] S. Davisdon, E. Nardi, Y. Nir, Phys. Rept. 466 (2008) 105-177 [arXiv:0802.2962].

[26] *The Strangest Man: the Hidden Life of Paul Dirac, Quantum Genius*; Faber & Faber, 2009, ISBN 978-0-571-22286-5, p. 430.

[27] S. Weinberg, *The Quantum Theory of Fields, Vol I*, Cambridge University Press (1995).

[28] F. Tanedo, http://www.lepp.cornell.edu/ pt267/files/notes/FlipSUSY.pdf

[29] S. Willenbrock, arXiv:hep-ph/0410370.

[30] C. L Cowan Jr., F. Reines, F.B. Harrison, H.W. Kruse, A.D McGuire (1956), Science **124** (3212): 1034.

[31] J. N. Bahcall, arXiv:physics/0406040.

[32] B. Pontecorvo, Sov. Phys. JETP 7 (1958) 172 [Zh. Eksp. Teor. Fiz. 34 (1957) 247]; B. Pontecorvo, Sov. Phys. JETP 26 (1968) 984 [Zh. Eksp. Teor. Fiz. 53 (1967) 1717].

[33] L. Wolfenstein, Phys. Rev. D17 (1978) 2369; S. Mikheyev and A. Yu. Smirnov, Sov. J. Nucl. Phys. 42 (1985) 913.

[34] Y. Fukuda et al. [Super-Kamiokande Collaboration], Phys. Rev. Lett. 81, 1562 (1998).

[35] S. N. Ahmed et al. [SNO Collaboration], Phys. Rev. Lett. 92 (2004) 181301 [arXiv:nucl-ex/0309004].

[36] Daya-Bay Collaboration, F. P. An et al, Phys. Rev. Lett.**108**, 171803 (2012).

[37] RENO Collaboration, J. K. Ahn et al. Phys. Rev. Lett.**108**, 191802 (2012).

[38] D. V. Forero et al, arXiv 1205.4018.

[39] E. Komatsu *et al.* [WMAP Collaboration], Astrophys. J. Suppl. **192** (2011) 18. [arXiv:1001.4538 [astro-ph.CO]].

[40] KATRIN Collaboration, A. Osipowicz et. al., arXiv:hep-ex/0109033.

[41] S. F. King, arXiv 0712.1750

[42] F. T. Avignone, S. R. Elliot, J. Engel, Rev. Mod. Phys. 80 (2008) 481-516 [arXiv:0708.1033 [nucl-ex]].

[43] B. Kayser, Phys. Rev. D **24**, 110116 (1981)

[44] G. Lazarides, Q. Shafi and C. Wetterich, 1981 Nucl. Phys. B **181** 287; R. N. Mohapatra and G. Senjanovic, 1981 Phys. Rev. D **23** 165; C. Wetterich, 1981 Nucl. Phys. B **187** 343.

[45] R. Foot, H. Lew, X.-G. He and G. C. Joshi, Z. Phys. C44 (1989) 441.

[46] J. Kersten, A. Smirnov, Phys. Rev. D **76**, 073005

[47] S. Blanchet et al, Phys. Rev. D **82**, 076008

[48] A. Zee, *Quantum Field Theory in a Nutshell*, Princeton University Press (2003)

[49] S. F. King, Phys. Lett. B **439** (1998) 350 [arXiv:hep-ph/9806440].

[50] S. F. King, Nucl. Phys. **B576** (2000), 85–105, [arXiv:hep-ph/9912492].

[51] S. F. King, JHEP **0209** (2002) 011 [arXiv:hep-ph/0204360].

[52] For a review of sequential dominance, see: S. Antusch and S. F. King, New J. Phys. **6** (2004) 110 [arXiv:hep-ph/0405272].

[53] S. F. King, C. Luhn, Journal of High Energy Physics, 2009, (JHEP10), 093-093 [arxiv:0908.1897].

[54] A. A. Penzias and R. W. Wilson, Astrophys. J. **142**, 419 (1965). DOI 10.1086/148307.

[55] G. F. Smoot et al., Ap. J. 396, L1 (1992).

[56] E. W. Kolb and M. S. Turner, *The Early Universe*, Perseus Publishing (1994), ISBN 0-201-62674-8.

[57] F. Hahn–Woernle, M. Plumacher, Y. Y. Y. Wong, JCAP 0908 (2009) 028 [arXix:0907.0205].

[58] M. Beneke et al, Nucl.Phys. B843 (2011) 177-212 [arXiv:1007.4783].

[59] A. Basboll, S. Hannestad, JCAP 0701 (2007) 003 [arXiv:hep-ph/0609025].

[60] L. Kadanov and G. Baym, *Quantum Statistical Mechan- ics* (Benjamin, New York, 1962).

[61] A. Anisimov et al, Annals Phys. 326 (2011) 1998-2038 [arXiv:1012.5821].

[62] S. Weinberg, *The Quantum Theory of Fields, Vol II*, Cambridge University Press (1995)

[63] Y. Aharonov, D. Bohm, Phys. Rev. 115 (1959) 485-491; Also in *Wilczek, F. (ed.): Fractional statistics and anyon superconductivity* 125-131 ; In *Thouless, D.J.: Topological quantum numbers in nonrelativistic physics* 167-173 ; In *Taylor, J.C. (ed.): Gauge theories in the twentieth century* 95-101.

[64] A. A. Belavin et al, Phys. Lett. **59B**, 85 (1975).

[65] F. R. Klinkhamer and N. S. Manton, Phys. Rev. D30 (1984) 2212.

[66] C. Jarlskog, Z. Phys. C **29** (1985) 491; J. Bernabu, G. C. Branco and M. Gronau, Phys. Lett. B **169** (1986) 243.

[67] W. Buchmuller, P. Di Bari, M. Plumachercar, New J. Phys. 6 (2004) 105 [arXiv:hep-ph/0406014].

[68] L. Covi, E. Roulet, F. Vissani, Phys.Lett. B **384** (1996) 169-174 [arXiv:hep-ph/9605319].

[69] S. Davidson and A. Ibarra, Phys. Lett. B **535**, 25 [arXiv:hep-ph/0202239].

[70] K. Kajantie, M. Laine, K. Rummukainen and M. Shaposhnikov, Phys. Rev. Lett. **77** (1996) 2887, [hep-ph/9605288].

[71] W. Buchmuller, P. Di Bari and M. Plumacher, Annals Phys. **315** (2005) 305 [arXiv:hep-ph/0401240].

[72] E. Nardi, Y. Nir, E. Roulet, and J. Racker, JHEP **01** (2006) 164, [arXiv:hep-ph/0601084].

[73] A. Abada, S. Davidson, F.-X. Josse-Michaux, M. Losada, and A. Riotto, JCAP **0604** (2006) 004, [arXiv:hep-ph/0601083].

[74] W. Buchmuller, M. Plumacher, Phys. Lett. **B431**, 354-362 (1998). [arXiv:hep-ph/9710460].

[75] R. Barbieri et al, Nucl. Phys. **B575** (2000) 61-77 [arXiv:hep-ph/9911315].

[76] S. Blanchet, P. Di Bari, Nucl.Phys. **B807** (2009) 155-187 [arXiv:0807.0743].

[77] Chee Sheng Fong, M. C. Gonzalez-Garcia, Enrico Nardi, J. Racker, JCAP 1012 (2010) 013 [arXiv:arXiv:1009.0003].

[78] J. A. Harvey, M. S. Turner, Phys. Rev. **D42** (1990) 3344-3349.

[79] F. X. Josse–Michaux, A. Abada, JCAP 0710 (2007) 009 [arXiv:hep-ph/0703084].

[80] G. Engelhard et al, Phys. Rev. Lett. 99 (2007) 081802 [arXiv:hep-ph/0612187].

[81] E. Bertuzzo, P. Di Bari, L. Marzola, Nucl. Phys. **B849** (2011) 521-548 [arXiv:1007.1641].

[82] S. F. King, Phys. Lett. **B675** (2009) 347-351, arXiv:0903.3199 [hep-ph].

[83] R. P. Feynman, *Statistical Mechanics: A Set of Lectures*, Westview Press; 2 edition (March 26, 1998).

[84] M. Schlosshauer, Rev. Mod. Phys. 76 (2004) 1267-1305 [arXiv:quant-ph/0312059].

[85] J. von Neumann, 1932, Mathematische Grundlagen der Quantenmechanik (Springer, Berlin).

[86] E. Schrdinger, (November 1935). *"Die gegenwrtige Situation in der Quantenmechanik (The present situation in quantum mechanics)"*. Naturwissenschaften.

[87] For a translation see: *http://www.tu-harburg.de/rzt/rzt/it/QM/cat.html* (section 5).

[88] Zurek, W. H., 2003b, Rev. Mod. Phys. 75, 715.

[89] Zurek, W. H., 2003c, Phys. Rev. Lett. 90, 120404.

[90] Zurek, W. H., 2004a, eprint quant-ph/0405161.

[91] Zurek, W. H., 2004b, in Science and Ultimate Reality, edited by J. D. Barrow, P. C. W. Davies, and C. H. Harper (Cambridge University, Cambridge, England), pp. 121137.

[92] Zurek, W. H., 1982, Phys. Rev. D 26, 1862.

[93] R. Barbieri, P. Creminelli, A. Strumia, N. Tetradis, Nucl. Phys. **B575** (2000) 61-77.

[94] A. De Simone, A. Riotto, JCAP **0702** (2007) 005. [hep-ph/0611357].

[95] G. Sigl and G. Raffelt, Nucl. Phys. B **406** (1993) 423.

[96] S. Blanchet, *A New Era of Leptogenesis*, Ph.D thesis, [arXiv:0807.1408 [hep-ph]].

[97] M. Beneke, B. Garbrecht, C. Fidler, M. Herranen, P. Schwaller, Nucl. Phys. **B843** (2011) 177-212. [arXiv:1007.4783 [hep-ph]].

[98] H. A. Weldon, Phys. Rev. **D26**, 2789 (1982).

[99] J. M. Cline, K. Kainulainen, K. A. Olive, Phys. Rev. **D49**, 6394-6409 (1994).

[100] S. Blanchet, P. Di Bari, JCAP **0606** (2006) 023.

[101] A. Pilaftsis and T. E. J. Underwood, Nucl. Phys. B **692** (2004) 303 [hep-ph/0309342].

[102] A. De Simone and A. Riotto, JCAP **0708** (2007) 013 [arXiv:0705.2183 [hep-ph]].

[103] S. F. King, Nucl. Phys. B **576** (2000) 85; P. H. Frampton, S. L. Glashow and T. Yanagida, Phys. Lett. B **548** (2002) 119.

[104] S. F. King, Phys. Rev. D **67** (2003) 113010 [arXiv:hep-ph/0211228]; P. H. Chankowski and K. Turzynski, Phys. Lett. B **570** (2003) 198 [arXiv:hep-ph/0306059]; A. Ibarra and G. G. Ross, Phys. Lett. B **591** (2004) 285 [arXiv:hep-ph/0312138].

[105] A. Kleppe, "Extending The Standard Model With Two Right-Handed Neutrinos", in *Lohusalu 1995, Neutrino physics*, 118-125; A. Kleppe, "Extending The Standard Model By Including Right-Handed Neutrinos". Prepared for Workshop on What Comes Beyond the Standard Model, Bled, Slovenia, 29 Jun - 9 Jul 1998;. E. Ma, D. P. Roy and U. Sarkar, Phys. Lett. B 444 (1998) 391; P. H. Frampton, S. L. Glashow and T. Yanagida, Phys. Lett. B 548 (2002) 119. M. Raidal and A. Strumia, Phys. Lett. B 553, 72 (2003). V. Barger, D. A. Dicus, H. J. He and T. j. Li, Phys. Lett. B 583 (2004) 173 W. l. Guo and Z. z. Xing, Phys. Lett. B 583 (2004) 163 R. Gonzalez Felipe, F. R. Joaquim and B. M. Nobre, Phys. Rev. D 70, 085009 (2004) S. Raby, Phys. Lett. B 561 (2003) 119; B. Dutta and R. N. Mohapatra, Phys. Rev. D 68 (2003) 056006; R. Kuchimanchi and R. N. Mohapatra, Phys. Lett. B 552 (2003) 198; T. Appelquist and R. Shrock, Phys. Lett. B 548 (2002) 204, Phys. Rev. Lett. 90 (2003) 201801; T. Endoh, S. Kaneko, S. K. Kang, T. Morozumi and M. Tanimoto, Phys. Rev. Lett. 89 (2002) 231601. S. Chang, S. K. Kang and K. Siyeon, Phys. Lett. B 597 (2004) 78.

[106] A. Y. Smirnov, Phys. Rev. D 48 (1993) 3264; M. Jezabek and Y. Sumino, Phys. Lett. B 440 (1998) 327; S. F. King, Nucl. Phys. B 562 (1999) 57, Nucl. Phys. B 576 (2000) 85, JHEP 0209 (2002) 011; S. F. King and G. G. Ross, Phys. Lett. B 574 (2003) 239. W. Rodejohann, Eur. Phys. J. C 32 (2004) 235; H. K. Dreiner, H. Murayama and M. Thormeier, Nucl. Phys. B 729 (2005) 278.

[107] A. Ibarra, JHEP 0601 (2006) 064 [arXiv:hep-ph/0511136]

[108] J. A. Casas and A. Ibarra, Nucl. Phys. B **618** (2001) 171 [arXiv:hep–ph/0103065].

[109] P. F. Harrison, D. H. Perkins and W. G. Scott, Phys. Lett. B **530** (2002) 167 [arXiv:hep-ph/0202074].

[110] T2K Collaboration, Phys.Rev.Lett. 107 (2011) 041801 [arXiv:1106.2822].

[111] E. Nezri and J. Orloff, JHEP **0304** (2003) 020 [arXiv:hep-ph/0004227].

[112] S. Blanchet and P. Di Bari, JCAP 0703 (2007) 018 [arXiv:hep-ph/0607330].

[113] E. Molinaro and S. T. Petcov, Phys. Lett. B **671** (2009) 60 [arXiv:0808.3534 [hep-ph]].

[114] S. F. King, JHEP **0508** (2005) 105 [arXiv:hep-ph/0506297].

[115] S. Antusch, S. F. King and A. Riotto, JCAP **0611** (2006) 011 [arXiv:hep-ph/0609038].

[116] S. Choubey, S. F. King and M. Mitra, Phys. Rev. D **82** (2010) 033002 [arXiv:1004.3756 [hep-ph]].

[117] S. F. King, Nucl. Phys. B **786** (2007) 52 [arXiv:hep-ph/0610239].

[118] S. F. King, JHEP **1101** (2011) 115 [arXiv:1011.6167 [hep-ph]].

[119] J. D. Lykken, Talk given at Conference: C96-06-02, p.85-153 [arXiv:hep-th/9612114].

[120] S. P. Martin, Published in in *Kane, G.L. (ed.): Perspectives on supersymmetry II 1-153 [arXiv:hep-ph/9709356].

[121] M. Drees, Lectures given at Conference: C96-06-04.1 [arXiv:hep-ph/9611409].

[122] P. Di Bari, Submitted to Conference: C04-03-21 [arXiv:hep-ph/0406115].

[123] M. Bolz, A. Brandenburg, W. Buchmuller, Nucl. Phys. **B606** (2001) 518-544, Erratum-ibid. B790 (2008) 336-337 [arXiv:hep-ph/0012052].

[124] J. Pradler, F. D. Steffen, Phys. Lett. **B648** (2007) 224-235 [arXiv:hep-ph/0612291].

[125] V. S. Rychkov, A. Strumia, Phys. Rev. **D75** (2007) 075011 [arXiv:hep-ph/0701104].

[126] M. Kawasaki, K. Kohri, T. Moroi, A. Yotsuyanagi, Phys. Rev. **D78** (2008) 065011 [arXiv:0804.3745].

[127] P. Di Bari, A. Riotto, Phys.Lett. **B671** (2009) 462-469 [arXiv:0809.2285].

[128] P. Di Bari, A. Riotto, JCAP **1104** (2011) 037 [arXiv:1012.2343].